**Univerzita Karlova / Charles University**

**Lékařská fakulta v Plzni / Faculty of Medicine in Pilsen**

Studijní program: Anatomie, histologie a embryologie

Ph.D. study program: Anatomy, Histology and Embryology

Studijní obor / Branch of study: D4AH5112

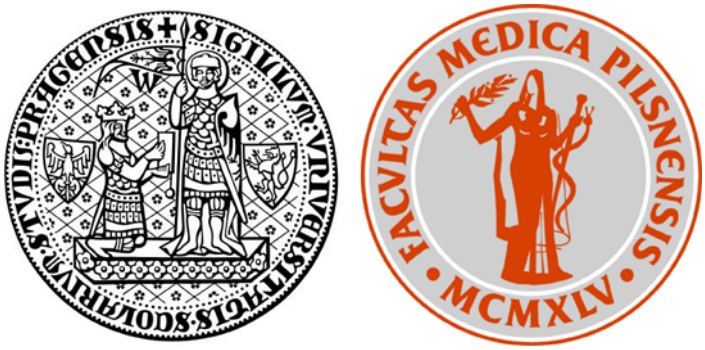


**Mgr. Pavla Sauerová**

# STUDIUM INTERAKCE BUNĚK S BIOMIMETICKÝM MATERIÁLEM A JEHO VYUŽITÍ V BIOMEDICÍNĚ

# STUDY OF CELL INTERACTIONS WITH BIOMIMETIC MATERIAL AND ITS APPLICATION IN BIOMEDICINE

Dizertační práce / Ph.D. Thesis

Školitel / Supervisor: Doc. RNDr. Marie Hubálek Kalbáčová, Ph.D.

Školitel-specialista / Supervisor-specialist: Ing. Tomáš Suchý, Ph.D.

Plzeň / Pilsen, 2017

**Prohlášení:**

Prohlašuji, že jsem závěrečnou práci zpracovala samostatně a že jsem uvedla všechny použité informační zdroje a literaturu. Tato práce ani její podstatná část nebyla předložena k získání jiného nebo stejného akademického titulu.

**Statement of authorship:**

I declare that I prepared the PhD thesis independently and that I stated all the information sources and literature. This work or a substantial portion thereof has not been submitted to obtain another academic degree or equivalent.

V Plzni / In Pilsen Podpis / Signature

Firstly, I would like to express my sincere gratitude to my supervisor Doc. Marie Hubálek Kalbáčová, Ph.D. for the support of my Ph.D. study and related research, for her patience, motivation, and immense knowledge. Her guidance helped me in research and writing of this thesis. My sincere thanks also goes to Ing. Tomáš Suchý, Ph.D. who provided me an opportunity to cooperate with him and his „biomaterial dream team“. I thank Tomáš and his team for preparation and mechanical expertise of developed biomaterials and for enrichment of science by their great sense of humour. I am also grateful to Prof. Miloslav Pekař and his team for preparation of surfactant-HyA complexes, Tereza and Doc. MUDr. Mgr. Zbyněk Tonar, Ph.D. for histology analyses and Petr Vyleťal and other colleagues from Prague or Pilsen for laboratory advice and help. Special thanks belong to my great lab colleagues and friends Martina, Blanka, Lucka, Tonda, Tereza and Shahin. I thank them for their help, support and friendly atmosphere in our lab.

Last but not the least, I would like to thank my beloved parents, sister, Petr and my grandfather for their care, love, support and patience.

**Abstract**

Biomaterials are considered as very promising tools for regenerative medicine. They have compensatory or supporting function in organism and they are often developed to support specific conventional medical procedures. So-called biomimetic materials are developed to imitate natural environment of organism and to induce positive innate responses of organism. An essential part of biomaterial development is *in vitro* biological evaluation, which characterizes (often for the first time) the potential of developed material for its clinical application. This Ph.D. thesis deals with *in vitro* biological evaluation of three different biomimetic materials. In all three cases, the comprehensive evaluation was an integral part of the material development and optimization processes. Each material was *in vitro* characterised at the level of cell-material interactions with respect to its intended specific application.. In the first part, cell response to potential drug delivery system based on colloidal complexes of cationic surfactants with hyaluronic acid (HyA) was characterized. HyA protection ability and its limits were described; also the role of fetal bovine serum (FBS) in cell response to the stress stimuli was confirmed. Results considered surfactant-HyA complexes as promising system for drug delivery. In the second part, cell carriers (scaffolds) based on collagen with application potential for bone surgery were evaluated. We proved the impact of crosslinking process of scaffold on adhesion of human cells and benefits and potential of dynamic cultivation for cell culturing on biodegradable scaffolds. Moreover, we selected the optimal biodegradable scaffold suitable for cell cultivation In the third part, local drug delivery system based on collagen/hydroxyapatite nano-/micro-structured resorbable layers with controlled elution of antibiotics was evaluated *in vitro*. The positive effect of hydroxyapatite content on cells and its limits in relation to the tested antibiotic type were emphasized. Layers were recommended for clinical application as bioactive interfaces that can not only support new formation of bone but also can serve as local drug delivery system. The last part of this thesis focuses on general description of cell adhesion process as a fundamental point of cell-surface interaction. For the first time, the difference in the early cell adhesion in the presence and absence of serum proteins was described in detail. Expression and localization of various proteins involved in cell adhesion and signaling were evaluated as being dependent on the presence or absence of serum proteins. Taken together, results of this thesis helped to evaluate the developed biomaterials under *in vitro* conditions. It was shown that every tested material has potential to support established medical procedures or to become the new alternative of treatment in the regenerative medicine. Our results also demonstrated the importance of *in vitro* biological evaluation in biomaterial development.

**Table of Contents**

# 1 INTRODUCTION

## 1.1 Biomaterials, Composite Materials, Biomimetic Materials and Biocompatibility

Nowadays, biomaterials science represents a very dynamic field of medicine. Besides materials science, this interdisciplinary field comprises medicine, biology, chemistry, mechanical engineering and tissue engineering. Currently, compensation or support of specific functions of biological system are common reasons of development of various biomaterials. Over the years, many definitions of biomaterials were presented. One of the first one was presented by Williams in 1987: "A biomaterial is a non-viable material used in a medical device, intended to interact with biological systems." (Williams, 1987). Thus, with respect to substantial progress of biomaterial science in recent years, biomaterial can be now defined as "a substance which has been designated and developed to interact with living (biological) system with primarily emphasis to clinical applicability or medicinal procedures improvement".

Biomaterial can be derived from nature or products of living system (e.g. biopolymers) or it can be also derived from various synthetic components (e.g. synthetic polymers such as poly(glycolic acid) and poly(lactic acid)). With the respect to complexity and wide range of requirements of living system, biomaterials are often designated on principle of composite material (Wang, 2003). The key advantage of biomaterial in a form of composite is that it is compounded of more specific components with unique features that result in one final structure which combine advantages of all specific and particular components but simultaneously all components remain in separate state (Gay, 2014). Biomaterials in form of composite material are widely developed in bone tissue engineering because of composite character of bones (Wang, 2003).

Regardless of whether the biomaterial is a composite or not, it can be designed by means of biomimetic approach. Especially tissue engineering is often based on principle of „biomimetic materials". The specific sign of these materials is an ability to induce specific cellular responses and direct new tissue formation mediated by biomolecular recognition, which can be manipulated by altering different parameters of the biomaterial. Biomolecular recognition of materials by cells is then achieved by surface and bulk modification of biomaterials via chemical or physical methods with bioactive molecules (e.g. native long chain of extracellular matrix (ECM) proteins or short peptide sequences derived from intact ECM proteins that can induce specific interactions with cell receptors) (Shin et al., 2003). Biomimetic materials imitate the function or structure, properties of natural materials, or are developed in the same way as is common in nature.

The crucial phenomenon of biomaterial science is "biocompatibility" which terms function and interactions of biomaterial with living system (Williams, 2003). As it was outlined, biomaterials are not products of biological system (those are not "a biological materials"). It means that every developed biomaterial must be controlled and well defined. This defining includes evaluation of biomaterial compatibility with the organism. Beside evaluation of mechanical and further physio-chemical properties, biological evaluation, as a fundamental step of biomaterials compatibility evaluation, is ordinarily determined firstly on the level of cells under *in vitro* conditions and secondly it is determined at the level of tissues and organisms under *in vivo* conditions.

## 1.2 Application of Biomimetic Materials

Application of biomimetic materials interferes with a wide range of medical areas with various requirements. Based on these more and less specific requirements, biomimetic materials are developed and thus specified with the respect to their specific application. For example, from the perspective of development of biomimetic material for tissue engineering, there are some practical requirements such as adhesivity or anti-adhesivity of material, suitability of material for specific cell type and a way of cell cultivation or degradability of material with the respect to its preventive or therapeutic role. Taken together, composition of biomimetic material must allow specific structural desing to ensure maximal imitation of specific and various roles of ECM of typical tissue (Anselme et al., 2012; Shin et al., 2003). Great example from medical field is bone surgery where application of biomimetic materials is successfully performed and poses great future therapeutic potential. In addition, two parts of this thesis focuse on evaluation of biomimetic materials for bone surgery. Therapeutic repair of skeletal tissues by tissue engineering has raised the interest. Bone tissue engineering seems to be a way with promising results how to support common surgical intervention and thus help to significantly reduce the considerable morbidity associated with frequently occurring loss or dysfunction of skeletal tissue (mechanical or degenerative damages, trauma, tumors or with surgery-associated infections etc.) (Black et al., 2015; Cancedda et al., 2003).

With the respect to wide range of medical areas, various biomimetic materials have been developed and thus, there are various ways how to divide biomimetic materials according to their application. Nevertheless, based on focus of this thesis, we can divide biomaterials to two groups according to purpose of material-induced imitation: i) the imitation of specific mechanism (e.g. drug delivery systems or depots of therapeutic substances) and ii) the imitation of specific structure (e.g. scaffold as cell carrier or structural substitution) respectively.

Three sections of this thesis are based on three different systems of biomimetic materials and two of them are directly connected with bone tissue engineering.

### 1.2.1 Drug Delivery System as Imitation of Specific Mechanism

Drug delivery systems are generally developed to maximize a therapeutic effect of delivered agents (e.g. drugs, genes, various contrast agents etc) or to maximize target tissue concentration of delivered agents while minimizing the risk of negative effects (e.g. the risk of systemic toxicity). Those systems are often nanostructured and dispose of high surface-area-to-volume ratio, which predicts nanostructures as efficient drug delivery agents. Additionally, in case of local drug delivery systems, the effectivity of drug delivery is often elevated by structures based on nano- or microfibers which provide to system high porosities and three-dimensional (3D) open porous structures (Rogina, 2014). Nanostructures are also well combined and well organized into larger structures, moreover those allow the control of the system at the molecular level. Setting of delivery system must take into account the type of drug (or other "cargo"), drug-loading method, its release in organism and its final localization. Drug-loading method and the drug-release are often based on chemical composition or various physical factors of delivery system, such as hydrophobic or charge interactions, covalent conjugation and other intermolecular interactions (He et al., 2007; Jie et al., 2005). The way and the level of transport mechanism of delivery systems often come from naturally occurring transport mechanisms of organism (via inter- to intracelular transport level) (Torchilin, 2001).

Drug delivery systems typically work on a glaze of micelles, polymers, nanoparticles or nanotubes (Cheung et al., 2012; Prestwich, 2011; Safari and Zarnegar, 2014). Delivery systems based primarily on principle of "particles" predominantly predict more "systemic" effects within organism. As various research reports show, these delivery systems are very variable. Besides polymeric micelles based on hyaluronic acid and phospoholipids (Saadat et al., 2014), hyaluronic acid-coated chitosan or lipid nanoparticles (Almalik et al., 2013; Mizrahy et al., 2011a) or carbone nanotubes (Flahaut et al., 2006) were showed as potential delivery systems. However, there were performed also more specified and more characterized systems such as zinc oxide nanoparticles developed with the aim of selective destruction of cells (Rasmussen et al., 2010), self-assembled pH-responsive hyaluronic acid–g-poly(L-histidine) copolymer micelles for targeted intracellular delivery of doxorubicin (Qiu et al., 2014) or anticancer drug delivery surfactant-templated mesoporous silica nanoparticles (He et al., 2010). Interestingly, we can see frequent use of hyaluronic acid (HyA) in mentioned examples of delivery systems. HyA is often used in developed systems as a tool providing either bicompatibility or controlled

cell entrance. For these reasons, HyA was also used in development of potential drug delivery system based on surfactant micelles evaluated by Halasová et al. (Halasová et al., 2011) and evaluated in this thesis (see 4.2.).

A it was mentioned, systems organised to larger forms such as various layers or hydrogels were also developed with the great potential for local drug delivery systems (Jang et al., 2015; Waeiss et al., 2014; Zhang et al., 2015). These systems are often based on principle of nano- or microfibers with mentioned role of efficient drug delivery agents (Rogina, 2014). Many local drug delivery systems are applied in bone surgery. The drug delivery systems appear to be very effective and promising way of supporting therapy in common treatment procedures. Specifically, local antibiotic treatment is the most perspective treatment of implant-associated infections and osteomyelitidis induced by implantation of endoprostheses or various bone trauma. In addition, there are increasing number of age-related disseases and loss of skeletal tissue leading to trauma or injury. Thus, several commercially available products and systems were developed in combination with various antibiotics (especially gentamicin and vancomycin are the most frequently used ones) (Bertazzoni Minelli et al., 2004; Chen et al., 2012)) and in various forms (fibres, powders, solutions, hydrogels). Wide spectrum of materials for controlled release of antibiotics is used – e.g. polymethylmethacrylate, collagen-polylactide-coglycolide, polylactide, polycaprolactone, chitosan and tricalcium phosphate (Alt et al., 2015; Bertazzoni Minelli et al., 2004; Busscher et al., 2012; Chen et al., 2012; Chou et al., 2016; Fang et al., 2012; Hong et al., 2013; Nair et al., 2011; Noel et al., 2010; Schlapp and Friess, 2003; Simchi et al., 2011; Subbiahdoss et al., 2009).

### 1.2.2 Scaffolds as Imitation of Specific Structure

With the respect to structural substitution, biomimetic materials can be primarily designed to imitate structural units of tissues or as carries of cells. These artificial substitues, so called scaffolds, are often developed to compensate lost or irreversibily damaged tissues caused by trauma, inflammation or tumor occurence etc. In principle, these materials need to maximally mimic natural composition and structural organization of native ECM of substituted tissue. Appropriate scaffold has assumption of enough cell-ECM interactions and thus subsequent supporting of tissue renewal. Therapeutic potential of scaffolds can be significantly elevated by combination with cell therapy. Nowadays, it seems that effectivity of combination of scaffold with cell therapy can be further enhanced by application of stem cells (because of their self-renewal, differentiation capacity and production of various bioactive molecules that provide regenerative environment (Anselme et al., 2012; Caplan and Dennis, 2006; Uccelli et al., 2008)).

However, despite the required imitation of native tissue ECM, some of ECM naturally occurring components are significantly instable in artificial environment. These instable components must be either modified or supported by additional components or methods. Typical example of an unstable component under non-native conditions is collagen, a key component of ECM. It needs to be specifically modified (e.g. crosslinking) for induction of its native features and advantages (Ma et al., 2004a; Rýglová et al., 2017; Wollensak and Spoerl, 2004) (see 1.3.3.). The example of additional components are syntetic or natural biodegradable polymers (e.g. polylactide, polycaprolactone, collagen, chitosan, hyaluronic acid) (see 1.3.3.) with high potential to provide several important features of native ECM as porosity, biocompatibility and directed degradability. Composition and structure requirements of biomimetic materials are described in detail below (see 1.3.3. and 1.3.4).

In general, ideal scaffold should allow infiltration and colonization of cells (artificially added or naturally occurred), for good tissue regeneration and recovery. As various results show, design of the ideal scaffold should respect many parameters, thus its development is still a high challenge. Permeability, 3D interconnectivity of pores, elasticity, stiffness, stability, surface topography, pore size etc. are crutial scaffold parameters playing important role for cell ingrowth, migration and scaffold colonization (Karp et al., 2003; Kemppainen and Hollister, 2010; Li et al., 2002; O'Brien et al., 2005). For example, permeability significantly affects nutrient and oxygen diffusion, and waste removal in scaffold volume (Dalby et al., 2014, 2003; Deligianni et al., 2001; Engler et al., 2006; Jungreuthmayer et al., 2009; Wen et al., 2014). However, besides mechanical parameters, the way of cell cultivation also crutially affects successful application of scaffolds. Especially, dynamic cultivation (see1.5.3) is now considered as the most effective way for sufficient collonization of cells before scaffold implantation (Zhang et al., 2010).

Scaffolds are highly perspective in bone surgery as supporting therapy of various bone trauma or diseases or they can serve as a supplement of implantations as well. Thus, a wide spectrum of variously modified or chemicaly treated scaffolds with special features or properties that respect native bone ECM is extensively studied and developed. Various combinations of collagen and hydroxyapatite with polylactide or polycaprolactone fibres, also various glycosaminoglycans or bone growth factors are frequently used aiming at development of an ideal bone graft (Black et al., 2015; Cheng et al., 2014; Hempel et al., 2014; Jungreuthmayer et al., 2009, 2008; Kasten et al., 2005; Kuboki et al., 1998; Laurencin et al., 2001; Novotna et al., 2014; Rampichová et al., 2013; Yao et al., 2004).

## 1.3 Native and Artificial Extracellular Matrix

Apart from soluble factors provided by environment, cells are also fundamentally affected by chemical and physical interactions with non-soluble components of their environment. Such non-soluble components are provided by ECM, thus composition and structure of ECM are essential factors for determination of cell survival and behaviour. Accordingly, composition and structure are key points in development of articifial ECM such as biomimetic material.

### 1.3.1 Native Extracellular Matrix

Native ECM is a complex and highly dynamic network of macromolecules, which presents in all tissues. It is three-dimensional non-cellular structure which is unique substrate for every tissue and which is continually (not only at the stage of organism development) modified and remodelled (Bonnans et al., 2014; Gattazzo et al., 2014). Despite that, ECM provides structural support, strenght and elasticity of tissues. Moreover, ECM and cells are significantly affected by each other. While cells establish or change surrounding ECM by remodelling due to various adaptive or repair processes, ECM affects cell survival, migration, proliferation and differentiation (Bissell and Aggeler, 1987). In general, composition and structural organization of tissues together with cell-matrix interactions direct tissue integrity, functions and natural mechanical properties and thus participate in tissue homeostasis (Humphrey et al., 2014).

#### 1.3.1.1 Native Extracellular Matrix Composition and Remodeling

Native ECM is composed of over 300 proteins, 200 glycoproteins, and 30 proteoglycans. However, major components of ECM are fibrous proteins (collagens and elastin), glycoproteins (fibronectin (FN), vitronectin (VN), laminin and fibrilin), glykosaminoglycans (GAGs) (e.g. hyaluronic acid (HyA)) and proteoglycans (PGs) (heparan, chondroitin and keratin sulfates) (Hynes and Naba, 2012; Walters and Gentleman, 2015).

**Collagen** is the main structural protein of most of ECMs (hard and soft tissues) of mammals. It represents 30 % of all proteins in organism. Collagen is produced by connective tissue cells. At first, collagen polypeptide chains are transported from ribosomes to the endoplasmic reticulum in a form of procollagen. There post-translational modification (hyroxylation) and formation of three-helical structure of procollagen takes place. Procollagen is then released into the ECM by exocytosis, where it is subsequently cleaved to final form of collagen (Gelse et al., 2003; Gordon and Hahn, 2010; Rýglová et al., 2017). Approxiamtely 30 collagen types were identified up to present. The most abundant collagens are collagen I

(mainly in bones, tendons and skin), collagen II (mainly in cartilage) and collagen III (mainly in skin). Collagen types are consistent in composition of three chain–helix structure and differ in amino acid composition and characteristic strength (Dong and Lv, 2016; Gelse et al., 2003; Rýglová et al., 2017). In addition, three-dimensional architecture of collagen in tissue (including its density and spatial alignment) directs its stiffness, strenght, distensibility and porosity. All of these parametres play a role in maintaining of structural and biological integrity, in extracelular scaffolding and also participate on immune and regenerative responses of organism via collagen-mediated regulation of cell behaviour (migration, proliferation, differentiation) (Bonnans et al., 2014; Engler et al., 2006; Wolf et al., 2009). Collagen secures extracellular scaffolding and stiffness also by binding of inorganic compounds, proteoglycans, glycoproteins or growth factors to ECM network (Dong and Lv, 2016; Salasznyk et al., 2004b). The dependence of collagen on interaction with various components of ECM or cells was showed in past. For example, Huang et al. demonstated the participation of hydroxyapatite (HA) (and thus calcium phosphate which the major inorganic component of bone) on collagen I self-assembly via coordinate bonds generated between collagen I and calcium. This cooperation contributes to better and more compact appearance of collagen I (Huang et al., 2012). Furthermore, it was also demonstrated that collagen matrix assembly needs active fibronectin (FN) fibrillogenesis provided by cells. Interestingly, it seems that the collagen I-FN interaction is reciprocal - while relaxed FN fibrils induce collagen assembly, the assembled collagen then creates a shield for fibronectin fibres from being stretched by cellular traction forces. Moreover, it nicely reflects the regulation of interactions among different ECM components at the level of mechanical forces (Kubow et al., 2015). Interestingly, water is also important component of collagen architecture, it is located within the colagen fibrils and between them. In general, with respect to bone ECM, collagen fibrils are deposited in a sheetlike manner and with a parallel fiber alignment (with the exception of woven bone) into the free space, created by resorbing osteoclasts during bone remodeling. These lamellae form osteons (functional units of cortical/compact bone) bone) and trabeculae (functional units of trabecular/ spongy bone) that are responsible for the outstanding mechanical properties of the bone tissue and its perfect adaptation to the local force distribution (Makhlouf and Scharnweber, 2015); see 1.3.2.1 for scheme of hierarchical organization of bone.

**Glycoproteins** (FN, VN, laminin and fibrilin) participate on ECM architecture, on interactions with cells (bind to cell intergrins - see 1.4.1) and on binding of growth factors (Allain et al., 2002; Klim et al., 2010). For example, FN and VN fundamentally participate in cell adhesion process. FN is adhesion-stimulating protein; it binds to integrins and also

associates with large number of other cell adhesion receptors, ECM components (e.g. collagen I) and various growth factors. Thus, besides the adhesion, migration and cell growth, it naturally participates in cell differentiation and in would healing process (Lenselink, 2015; Pankov and Yamada, 2002; Williams et al., 2008; Zollinger and Smith, 2016). VN also interacts with integrins, thus it promotes cell adhesion as well. It is preferentially present in blood serum and, in addition, it specifically regulates complement action (Preissner, 1991). Key sign of both FN and VN is the presence of RGD sequence in their structure, which is recognized and subsequently bound by many different integrins (Ruoslahti, 1996).

**PGs** (heparan, chondroitin and keratin sulfates) and **GAGs** (HyA) fill interstitial matrix space, secure matrix hydration by binding of water molecules and some of them bind growth factors and release them to matrix environment (Naka et al., 2005; Ruoslahti and Yamaguchi, 1991). Extremely widely distributed GAG is HyA. HyA is connected with a wide spectrum of functions at various organism levels. It is a fundamental component of ECM and participates in maintaining of tissue homeostasis, hydration and wound healing. HyA also plays a role in cell migration, proliferation and signalization (Dicker et al., 2014). Many HyA functions are directly affected by interaction with HyA-binding proteins, which are specified by certain HyA activity and its localization. The most typical HyA-binding proteins are CD44 receptor (the main HyA receptor; playing a role in ECM interactions, migration etc.) (Aruffo et al., 1990; Knudson, 2003; Ponta et al., 2003) and RHAMM receptor (playing a role in HyA-mediated motility; triggering of cellular signalization by interaction with HyA and CD44) (Cheung et al., 1999). HyA natural polymer is synthesized inside of cell membrane by membrane proteins - HyA synthetases. Its degradation is performed by hyaluronidases (Dicker et al., 2014; Harada and Takahashi, 2007; Hofinger et al., 2008).

Not only organic compounds but also inorganic compounds play important role in ECM. The unique component is **calcium phosphate** (CaP) in bone ECM. The bone mineral, a calcium phosphate is often incorrectly described as HA ($Ca_{10}(PO_4)_6(OH)_2$). However, bone mineral is not chemically pure HA, it is associated with further minor groups and elements (mainly $CO_3^{2-}$) and trace elements (e.g., $Na^+$, $Mg^{2+}$, $Fe^{2+}$, $Cl^-$, F), some of them at the ppm level (Šupová and Suchý, 2015). CaP interacts with collagen and provides rigidity, roughness of matrix surface and protein availability for cells. As it was shown, all of these factors significantly participate on cell adhesion and differentiation (Mygind et al., 2007; Novotna et al., 2014; Song et al., 2013). Additionally, CaP mineral formation is mainly secured by alkaline phosphatase (enzyme expressed by osteoblasts) (Makhlouf and Scharnweber, 2015).

ECM composition is closely related to fundamentall process of ECM-remodeling that contributes to maintaining of structure and function of tissues (e.g. dysfunctional bone tissue remodelling results in osteoporosis or osteosclerosis (Alford et al., 2015). The major enzymes of physiological turnover of ECM are matrix-degrading enzymes, metalloproteinases (MMPs). This zinc-dependent endopeptidases are variously regulated by organism (growth factors, hormones, oncogenes) to digest on one hand specific components of ECM (collagen, elastin, laminin, fibronectin etc.), but also non-matrix proteins as well (cytokines, adhesion molecules etc.). Thus, beside the primary matrix remodelling effect, MMPs affect cell-cell or cell-matrix interaction and regulate growth factor release via cleaving of ECM components and various cell surface receptors. In general, MMPs regulate cell proliferation, migration, apoptosis, cancer progression or immune system response (Bourboulia and Stetler-Stevenson, 2010; Koshikawa et al., 2000; Nagase et al., 2006; Nagase and Woessner, 1999; Vandenbroucke and Libert, 2014). In organism, MMPs' activity is physiologically low and controlled by various molecules via feedback pathways (cytokines, growth factors, hormones, etc). However, it is also regulated by specific inhibitors (tissue inhibitors of MMPs ;TIMs) (Bourboulia and Stetler-Stevenson, 2010). As we can see, environment of ECM is complex matter, which consists of a large number of partial processes and interactions. Thus, it clearly shows difficulties connected with the development of artificial ECM to maximally imitate innate structures.

### 1.3.2 Surface Necessities for Cell Interactions

Every type of ECM exhibits a combination of properties that have individual and overall impact on cell behaviour and final cell interactions. Besides chemical surface properties, there is the complex of specific physical surface features that participates on resulting nano- and microtopography. These features express specific needs of specific tissue and cell types. As it follows, the goal of tissue engineering is also to mimic these innate surface necessities for biomaterial designing. The key properties seems to be roughness, surface topography, stiffness, porosity and pore dimensions (Dohan Ehrenfest et al., 2010).

#### 1.3.2.1 Influence of Surface Topography and Roughness on Cell Behaviour

Not only ECM composition is important but also its spatial organization. Amount and parameters of individual compounds, their conformation and orientation state give rise a matrix surface nano- and microscaled topography. As it has been presented many times until now, topography is essential point for cell interactions. This essentiality is nicely performed in native bone ECM. High amount of collagen fibrils is assembled in triple-helix form (300 nm length,

1.5 nm diameter) and organised in parallels with specific overlapping and holes. This structure is additionally combined with high content of CaP crystals of nanoscale size. Subsequently created collagen /CaP structural units then interact with other ECM compounds and form basic structural unit of bone. CaP (HA) content determines a total roughness of interacting surface which clearly affects cell adhesion and spreading on the surface – these subsequently affect such phenomena as cell proliferation or differentiation (Feng et al., 2002; Novotna et al., 2014; Song et al., 2013; Walters and Gentleman, 2015; Weiner and Wagner, 1998). Example of bone ECM also nicely represents an overall hierarchical organization of different hierarchical levels that affects short and also long term cell interactions. Nowaday it seems, there are different hierarchical patterns or scheme (Fig. 1) in various bone tissues that combine well-ordered mineralized collagen fibrils and disordered collagen fibrils (Reznikov et al., 2014).

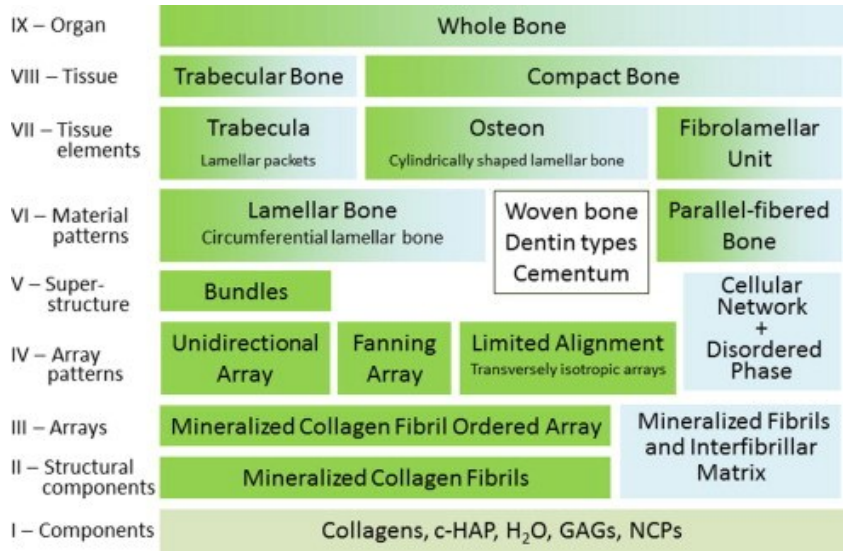


**Figure 1: Scheme of hierarchical organization of bone.** Up to level V the hierarchical levels can be divided into the ordered material (green) and the disordered material (blue). At level VI, these two materials combine in lamellar bone and parallel fibered bone (other members of the bone family are not investigated (without color). Level VII depicts the lamellar packets that make up trabecular bone material and the cylindrically shaped lamellar bone that makes up osteonal bone. The fibrolamellar unit comprises the primary hypercalcified layer, parallel fibered bone and lamellar bone. c-HAP: carbonated hydroxyapatite; GAGs: glycosaminoglycans; NCPs: non-collagenous proteins. Adopted from (Reznikov et al., 2014).

Apart from roughness, flatness is also important factor of surface topography. As it has been repeatedly shown by Dalby et al., cell morphology, growth, spreading and differentiation are highly affected depending on whether the flatness of surface or unevenness of surface defined by protrusions ("islands of 95 nm height") is present. Lack of cell spreading and low recruitment of cell numbers on the protrusions was observed (Dalby et al., 2003). Similar effect

was observed on various ridges and other patterned or flat substrates. More specifically, it seems that specific topographic pattern can interferre with growth of focal adhesions (FAs; see 1.4.1) and thus makes adhesions unstable. It results in changes in polarisation and migration of cell (Ventre et al., 2014). Also cell differentiation can be stimulated only by specific topography without differentiation specific media (Dalby et al., 2007, 2006). It means, just changes of the cell shape (often induced by combination of specific symmetry and degree of disorder) are sufficient for driving of cell fate. Efficiency of this topographically induced differentiation is similarly strong as efficiency as that driven by specific supplements of differentiation (McBeath et al., 2004). Effects of topography on cells is connected to availability of ligands that participate on the process of cell adhesion. Cells can be specifically sensitive to patterns of ligands and their position. The universal ligand interspacing range seems to be between 58-73 nm. This range supports enough cell attachment, spreading and formation of focal adhesions (it induces appropriate integrin clustering and activation) (Arnold et al., 2004).

In general, topography substantially influences cell morphology and behaviour by induction of changes in cell transduction at the level of cell adhesion. High efficiency of controlled topography was also shown in *in vivo* experiments, where it was proved as an effective tool of osseointegration process of implants (Karazisis et al., 2017).

### 1.3.2.2 Influence of Surface Stiffness, Porosity and Pore-Size on Cell Behaviour

Material stiffness participates on generation of cell traction forces (Fig.2) that subsequently affect changes in cell morphology, movement and differentiation. As it was discovered by Engler et al., material rigidity determines stem cell fate and its differentiation (Engler et al., 2006). While soft material acts as neurogenic inducer, stiffer and rigid ones act as myogenic and osteogenic inducers, repsectively. Surprisingly, in the long-run, effects of stiffness can predominate effects of treatment by differentiation supplements (Engler et al., 2006; Evans and Gentleman, 2014; Kasten et al., 2008a). Interestingly, Wu et al. demonstrated on the example of cartilage, that stiffness (softer or stiffer surface) combined with substrate nanotopography (pillar or nano-grating substrate) can give rise to cartilage of different phenotypes (Wu et al., 2016). As we can see, the level of material rigidity has potential to direct stem cell fate, thus it is important parameter for tissue engineering.

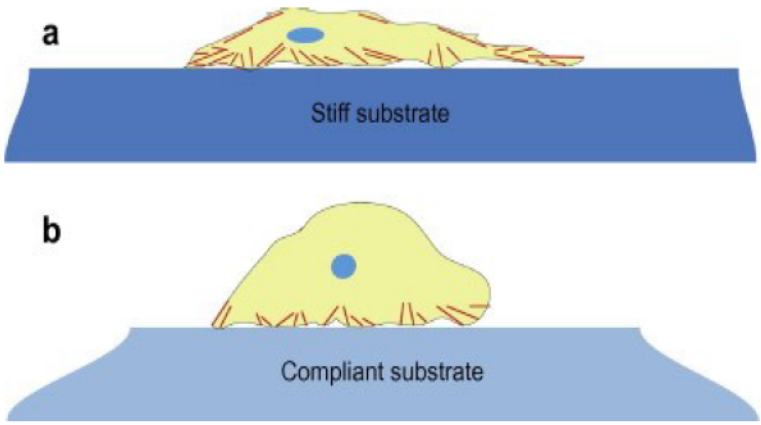


**Figure 2: Substrate stiffness influences cell morphology and differentiation.** (a) Adherent cells (yellow) are unable to generate sufficient traction force to deform stiff hydrogel substrates (dark blue). As a result, they develop spread morphologies with many well-defined actin fibres (red). (b) By contrast, cells cultured on compliant substrates (pale blue) deform the matrix, and assume a more rounded morphology with fewer and less defined stress fibres. The distorted shapes of the hydrogel substrates of varying stiffness represent the deformation induced by the cell.Adopted from (Walters and Gentleman, 2015).

Pore-size and porosity are next important surface parameters with impact on cell interactions. In native state, both parameters depend on ECM and tissue specifity and on cellular needs such as nutrition and migration. Moreover, both parameters can differ on the level of one specific tissue and the fine example is a native bone. While cortical bone is characterized by low porosity (3–12 %) and pore-size diameter around 100–200 µm, trabecular bone is characterized by relative high porosity (50–90 %) and pore-size diameter to 1 mm (Cooper et al., 2004; Keaveny et al., 2001). Thus, pore-size and porosity reflect differences in native function of both types of bone – while cortical bone represents primarily mechanical features, the trabecular bone represents (besides mechanical features important for bone remodelation) a larger surface with high metabolic activity. Surprisingly, we can find no clear results about ideal pore-size or level of porosity with the respect of development of artificial ECM. There is high variability among results describing ideal pore-size (the range 0.5 – 600 µm ). Results in porosity are also markedly variable (in average 25-75%) for cells (Akin et al., 2001; Grier et al., 2017; Kasten et al., 2008a; Murphy et al., 2010; Mygind et al., 2007; Zhang et al., 2015). Despite of variability, it seems, both paramers (especially pore-size) together with the surface structure might play an important role for cell differentiation *in vivo*, however, the exact mechanisms have not been still determined (Kasten et al., 2008a). Thus, it seems that identification of other parameters will explain the the role of pore-size and porostity on cell behaviour and describes the mechanism of their function.

### 1.3.3 Composition of Biomimetic Materials (Artificial ECM)

ECM is complex network composed of many components that differ according to tissue type. Every type of ECM exhibits specific composition which participates on its specific topography, roughness, strength, stiffness, elasticity and other mechanical properties. These properties of ECM promote cytoskeletal tension, cell penetration, proliferation or differentiation (Walters and Gentleman, 2015) (Grier et al., 2017; O'Brien et al., 2005; van der Smissen et al., 2015). Thus with the respect to process of regeneration, the biomimetic material should achieve above mentioned ECM properties and simultaneously it should allow to be the gradually naturally remodelled in the body for satisfactory integration to organism (Jungreuthmayer et al., 2009; Swinehart and Badylak, 2016; Vago et al., 2002).

As mentioned above, collagen is the common dominant structural component of ECM. The most abundant collagen type I creates the architecture of ECM, influences ECM mechanical properties (tensile strength, torsional stiffness), binds and thus integrates other components to ECM network (e.g. inorganic coumpounds, proteoglycans, glycoproteins). However while native collagen possesses to tissue significant strength (due to physiological crosslinking during post-translational modification), non-native collagen products can lost these features in dependence on its processing. Under non-physiological conditions, it shows poor dimensional stability, low *in vivo* mechanical strength and considerably limited degree of elasticity. This insufficiency can be reduced or overcome by a way of isolation and associated handling, a processing by electrospinning method with suitable parameters (mentioned below) and chemically or physically secured crosslinking (Dong and Lv, 2016; Lewis et al., 2010; Ma et al., 2004a; Rýglová et al., 2017; Wollensak and Spoerl, 2004). Crosslinking methods can be based on e.g. physical crosslinking (combined riboflavin/ultraviolet A and rose bengal/white-light irradiation (Raiskup and Spoerl, 2013; Walters and Stegemann, 2014; Wollensak and Spoerl, 2004) and chemical crosslinking. For the chemical crosslinking several agents have been widely used, namely glutaraldehyde, glyceraldehyde (reduces immunogenicity but also the level of long-term stability) and *N*-(3-Dimethylaminopropyl)-*N*′-ethylcarbodiimide hydrochloride (EDC) / N-hydroxysuccinimide (NHS) (McDade et al., 2013) in aqueous or ethanol solutions (Park et al., 2002; Prosecká et al., 2015; Sell et al., 2008). Another common crosslinking reagent is genipin, an iridoid glycoside. It is one of the main components of gardenia fruit (*Gardenia jasminoides ELLIS*) and generates crosslinks spontaneously with protein, collagen, gelatin, chitosan, etc. (X. Zhang et al., 2014).

Next components of native ECM are GAGs. The frequently used GAG in tissue engineering and in development of artificial ECM is HyA. HyA is the most widely spread

naturally-occurring polymer that participates in such essential processes as cell migration, proliferation and signalisation, tissue homeostasis and hydration. It also participates in cell adhesion (Zimmerman et al., 2002). Besides biocompatibility, its application can provide to material specific targeting via CD44 (it is frequently used absorbed on particles in drug delivery system (Halasová et al., 2011; Mizrahy et al., 2011a, 2014)), it could also extend potential of developed material via its great mechanical properties and high level of modifiability (Dicker et al., 2014; Grishko et al., 2009; Prestwich, 2011).

With the respect to focus of this thesis on bone tissue engineering, CaP need to be mentioned in this capture as well. CaP is the critical component of native bone ECM: it is the main inorganic compound of bones with key osteoinductive effects. It interacts with colagen and directly influences its interations with other ECM proteins and also binds molecules of water. It fundamentally participates on resulting texture of matrix, thus in biomaterials it affects important parameter for cell interaction called roughness. The elevation of CaP (HA) content leads to the elevation of material roughness which supports cell adhesion and spreading area of adhered cells (Deligianni et al., 2001). In addition, HA (CaP) can elevate protein availability from environment to cells by protein binding via its calcium and phosphate. And it is well known that proteins on the surface belong to main players in cell adhesion process (Anselme et al., 2012; Feng et al., 2002; Novotna et al., 2014; Song et al., 2013; Walters and Gentleman, 2015). HA is most frequently used in bone tissue engineering to mimic the natural minerals in bone (CaP). Bioapatite (bCaP) is its variant which can be used due to its biocompatibility (BaoLin and MA, 2014; Zhang and Ma, 1999). In general, it was found that HA-based composite scaffolds well mimic the nanosized features of natural-bone mineral (Ngiam et al., 2009) and support protein adsorption capacity, suppresses apoptotic cell death, and provides a more favorable microenvironment (Chou et al., 2005). In addition to mimicking the inorganic-organic nature of the natural bone, nano-HA-polymer composite scaffolds have been developed too (Šupová and Suchý, 2015) (for more details see next paragraph).

Besides the maximal structure imitation based on compounds of native ECM (such as collagen, HA, HyA, GAGs), artificial conditions often need alternative compounds for perfect imitation of the native state (BaoLin and MA, 2014). Such compounds are biodegradable polymers - syntetic or natural biodegradable polymers (e.g. polylactide, polycaprolactone, collagen, chitosan, hyaluronic acid). Using of biodegradable polymers in tissue engineering arises from knowledges about native ECM which perform the chemical composition, physical structure, and biologically functional moieties as important features of tissue (Chen et al., 2002). Polymers can help to provide all these features and additionally those can provide

biocompatibility and biodegradability without release of nontoxic degradation products. Biodegradable polymers are the most perspective materials in tissue engineering because they can provide porous biodegradable scaffolds (Nair and Laurencin, 2007). Naturally derived polymers have the potential advantage of supporting cell adhesion and function. Collagen, gelatin, silk, and alginate are commonly used natural polymers for scaffolds development (Van Vlierberghe et al., 2011). However, immunogenicity and pathogen transmission connected to natural polymers, have been supported the development of synthetic polymers as possible scaffolding materials. In addition, synthetic polymers usually have controlled structure, a higher degree of processing flexibility, and no immunological concerns (Magnusson et al., 2011). In result, synthetic biodegradable polymers (polylactide (PLA), polyglycolide (PGA), their copolymers poly(lactide-*co*-glycolide) (PLGA) or poly(ε-caprolactone) (PCL)) associated with naturally derived polymers are widely used (Li et al., 2002; Raiskup and Spoerl, 2013; Rampichová et al., 2013; Venugopal and Ramakrishna, 2005; Wollensak and Spoerl, 2004). Interestingly, mentioned PLA is ferquently used due to its high hydrophobicity which prevents the loss of mechanical integrity of material under *in vitro* or *in vivo* conditions for a long time (Gupta et al., 2007).

Next advantage for development of artificial ECM is that all of mentioned components (collagen, HyA, HA and polymers) can be modified to enhance the structural features of material or to promote the selected cell skills (Collins and Birkinshaw, 2013; Hempel et al., 2014; Kuo and Yeh, 2011; Wang et al., 2003).

In summary this capture help to clarify why biomaterials are often developed in a form of composite material. Besides „composite“ character of native tissues, one-component material is often insufficient for regeneration requirements of cells and organism. Fine example of this „composite“ character in native state is represented again by bone ECM which is composed of organic (collagen) and inorganic (apatite) compounds. Importance of this „composite“ character is supported by various biomimetic composite scaffolds for bone tissue engineering which demonstrate advantages of HA enrichment (Delabarde et al., 2012; Deligianni et al., 2001; Prosecká et al., 2015; Zhang and Ma, 1999). With the respect to mentioned benefits of syntetic polymers in biomimetic material development, also various PLA/HA or PLGA/HA composite scaffolds are widely designed for bone regeneration (Chen et al., 2006; Delabarde et al., 2012; Sonseca et al., 2012).

### 1.3.4 Structure of Biomimetic Material (Artificial ECM)

Native structure of ECM reflects that composition is not sufficient factor to achieve perspective biomimetic material (Walters and Stegemann, 2014). Thus, the structure is the key factor in design of artificial tissue templates that should support cell attachment, proliferation, differentiation and new tissue formation. As it was performed, 3D and porous structure with pore interconectivity together with surface topography positively interacts with cells, facilitates nutrient transport to cells and supports proces of regeneration (Holzwarth and Ma, 2011). Because many ECM proteins possess a fibrous structure (e.g. widely represented collagens) with diameters on the nanometer or sub-micrometer scales, thus the nano and micro features of a structure play important roles in development of succesfull scaffold for tissue-engineering (Wei and Ma, 2009)

The simple and cheap method to produce novel fibers (fibrous polymer mats) with micro- and nano-character ranging from several microns down to 100 nm or less is electrospinning. It is a fabrication process that uses an electric field to control the deposition of polymer fibers (polymer solutions, suspensions of solid particles and emulsions) onto a target substrate (the electrostatic force results in an electrically charged jet of polymer solution flowing out from a pendant or sessile droplet) (Matthews et al., 2002) (Reneker et al., 2007). The electrospinning process makes possible to fabricate complex, and seamless, 3D shapes. For example, the importance of „three-dimensionality“and its efficiency (with the respect imitation of native structures) is well represented by electrospun collagen. It was demonstrated that it promotes cell growth and the penetration of cells into the engineered matrix. The structural, material, and biological properties of electrospun collagen suggest that this material may represent a nearly ideal tissue engineering scaffold (Matthews et al., 2002). Besides natural polymers, there are widely used electrospun biodegradable syntetic polymers (PLA, PGA, PLGA or PCL; (BaoLin and MA, 2014; Li et al., 2002; Novotna et al., 2014; Rampichová et al., 2013; Venugopal and Ramakrishna, 2005) that have potential to change mechanical properties and degradation kinetics to suit various applications or design of desired pore morphologic features.

In general, electrospinning together with various combinantions of natural polymers, synthetic polymers and their derivates are currently the dominant and the most perspective scaffolding methods and materials in tissue engineering (Tian et al., 2008) (Li et al., 2002; Raiskup and Spoerl, 2013; Rampichová et al., 2013; Venugopal and Ramakrishna, 2005; Wollensak and Spoerl, 2004).

## 1.4 Cell - Extracellular Matrix Interactions

Tissue engineering is based on knowledge of the ECM. All cell types are in contact with ECM which differ in biochemical and physical properties according to the position in organism (Özbek et al., 2010). Cells are not only controlled by various soluble factors (such as signalling molecules), but also by structure of their environment. Thus, cell-ECM interaction essentialy contributes to the cellular behaviour (adhesion, migration, differentiation etc). Interactions between cell and ECM are bidirectional and take place in highly specific microenvironment. A key intermediator in cell-ECM interaction is cellular cytoskelet and its rearrangement. Interactions are based on mechanotransduction process which works on a principle of physical forces, deformation and remodelling (Grier et al., 2017; Murphy et al., 2014; Walters and Gentleman, 2015; Wang et al., 1993). Taken together, knowledges about cell-ECM dynamics, its microenvironment, ECM architecture and cell adhesion process, its mechanisms and variability is crutial for successful biomaterial development and its utilization in tissue engineering.

### 1.4.1 Cell adhesion

Cell adhesion and its regulation is a crutial point of mechanisms and processes in organism such as embryonegensis including tissue formation, immune system function, regulation of homeostasis and reparation mechanisms. Also many diseases are associated with just dysfunction at the level of cell adhesion as well (immune system disorders, process of cancer metastasis, etc.). That is also, why cell adhesion is still in a centre of scientific research. Cell adhesion is a process which allow to cells to interact with each other and with ECM or other surrounding. It reflects condition of cell and cell environment resulting in direction of cell fate (proliferation, differentiation or migration). Cell adhesion is based on bidirectional communication, which can dynamically react on specific situation - it can be adapted by surrounding requirements and simultaneously it can adapt its own surrounding as well (e.g. bidirectionality via remodelation). For anchorage-dependent cells, cell adhesion is a matter of survival and growth. Attachment of these cells to ECM or cell to one another initiates cell signals for their survival. Loss of cell-ECM or cell-cell interactions causes programmed cell death, so called anoikis (Chiarugi and Giannoni, 2008). As it was mentioned above, composition and organization of ECM varies according to tissue function and needs of tissue cells. Therefore, the cell adhesion is dependent on context of the specific ECM (Frisch and Francis, 1994; Geiger and Yamada, 2011).

Integrity of tissues is executed by cell junction that is classified to several structures: adherence junctions, focal adhesions, desmosomes and hemidesmosomes. In addition, there are tight and gap junctions special structures for epithelium and endothelium. In general, cell-cell or cell-ECM junctions are mediated by cell adhesion molecules (CAMs). CAMs bind to cell cytoskeleton via specific protein adaptors. As it follows, CAMs participate on input and output signalization. The main CAMs for cell-cell interactions are cadherines ($Ca^{2+}$ dependent), selectins (sugar enriched) or special types of immunoglobulins. The main CAMs for cell-ECM interactions are integrins ($Ca^{2+}$ and $Mg^{2+}$ dependent proteins) which can also participate on cell-cell interaction as well. Adhesion structures can be highly specialized with specialized cell contacts due to securing of specific physiological function of tissues. Typical representatives of specialized contacts are focal adhesions (FAs) of migrating cells and immune and neuronal synapses (Sergé, 2016).

Cell adhesion is hierarchically ordered. The basic prerequisite of FA formation is protein adsorption to surface and formation of a layer. Under native conditions, the layer is organized by dynamics of body fluids. Under *in vitro* conditions the layer is formed by proteins contained in fetal bovine serum (FBS), which is a supplement of cultivation medium. The first step of cell adhesion process is the contact of cells with the adsorbed proteins via intermolecular and ionic forces taking seconds. In some cell types, as Zimmermann et al. showed, this first contact can be strengthen and foregone by formed cell-surface HyA coat (Zimmerman et al., 2002). Second step, minutes lasting process, is cell attachment to the surface followed by its spreading. During this phase integrin receptors bind to ligans and form clusters. Third step is the cytoskeleton reorganization, which includes next active cell spreading, which is executed within hours. During the last step, cells synthesize their own ECM over hours to days and thus remodelate their own ECM microenvironment (Anselme et al., 2012; Bonnans et al., 2014; Kubow et al., 2015; Zaidel-Bar et al., 2004). Based on variability of ECM topography pattern or integrin specificity, there can be distinguished three basic types of adhesions and one additional: 1) dot-like and short-lived adhesions with occurrence along lamellipodia protrusions (this type has also potential of transformation to focal adhesions); 2) classical focal adhesions generated by flat and rigid surface and with occurrence at the ends of actin fibres; 3) elongated fibrilar adhesions with occurrence under center of cells and along matrix fibrils such as fibronectin; 4) podosomes or invadopodia with occurrence around actin fibres for anchoring of actin to membrane (Geiger and Yamada, 2011).

It is considered that focal adhesions (FAs) play a central role in adhesion process (Zaidel-Bar et al., 2003). They are large and dynamic protein complexes, which are situated

close to plasma membrane. FAs serve as linkages and simultaneously as adhesive signalling centres for cells. Dynamics and turnover of FAs are key points of FAs role – it directs cell-ECM interactions, adhesion signalization and cell migration. 3D architecture of FAs is closely related to the dynamics of FAs molecule degradation. Interestingly, just the degradation process secures important FAs turnover which is executed by proteolysis and disassembly that are dependent on $Ca^{2+}$ influx (Chang et al., 2017). FAs formation and final cell spreading can be affected only by type of ECM substrate, as demonstrating in figure 3. Variability in the quantity of only one component participating in FAs formation (e.g. FN or VN) leads to FAs molecular differences and distribution in cell volume and thus it results in change of morphology of same cell type (Geiger and Yamada, 2011). In addition, matrix flexibility (rigidity together with filaments orientation) can also affect FAs morphology, which results in intracellular contractility changes. The stiffer matrix, the greater the focal adhesions in cell of normal morphology occur. In addition, more regular shape and increased intracellular contractility are generated. Cells spontaneously migrate in the direction of increasing stiffness (so called durotaxis). It seems, the stiffness is preferred by cells due to easier FAs formation (Pelham and Wang, 1997). It also seems that FA dynamic is mechanosensitive process due to its interplay and coordination with cytoskeleton or extracellular matrix generated forces (Oakes and Gardel, 2014).

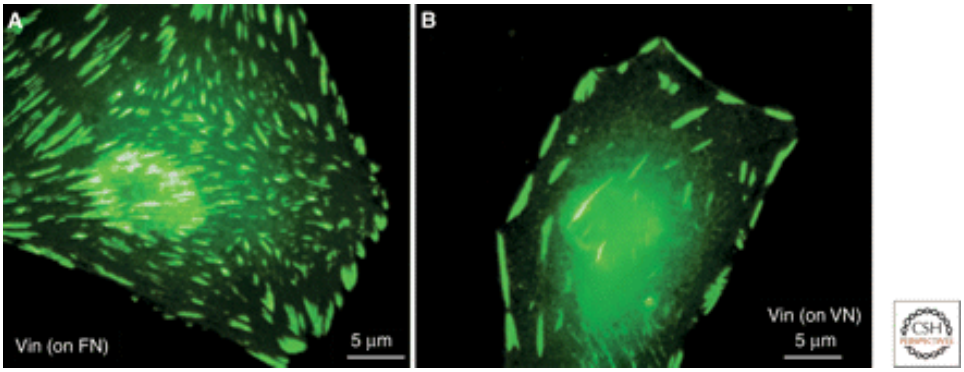


**Figure 3: Differential effects of different matrices on fibroblast spreading and FAs formation.** Differences between integrin adhesions induced by fibronectin (FN) or vitronectin (VN). Adopted by (Geiger and Yammada 2011)

FAs is a network of integrins and other cytoplasmic proteins, which interconnect actin cytoskeleton of cell to ECM. Kanchanawong et al. were first who described molecular architecture of FAs (see figure 4; (Kanchanawong et al., 2010)). FA can be divided to three spatial and functional compartments which are interdependent. These compartments are an

integrin signalling layer, a force transduction layer, and an actin regulatory layer. The first compartment, integrin signalling layer, can be divided to external and internal part due to integrin transmembrane heterodimeric composition. External part is composed of extracellular domain of integrin which is a key linker of cell with ECM. Typical ligands of extracellular domain of integrin are FN, collagen, laminin or VN; their interactions are carried out via major recognition sequence for cell adhesion, so called RGD (arginine-glycine-aspartic acid) peptide (Kim et al., 1992; Ruoslahti, 1996). Internal part of integrin signalling layer is composed of intracellular integrin domain, focal adhesion kinase (FAK) and paxilin – it directs adhesion dynamic and transcription via signalling control (Giancotti, 2000; Liu et al., 1999; Sieg et al., 2000). The second compartment of FA architecture is a force tranduction layer composed for example of talin and vinculin, that directly link integrin to actin and it also regulates force transmission between integrins and actin (Humphries et al., 2007). The last compartment is an actin regulatory layer composed of VASP (vasodilator-stimulated phosphoprotein), zyxin and actin filament terminy. VASP and zyxin are involved in FA strengthening. The structure continues in formation of actin network - actin stress fibres cross-linked by α-actinin (Kanchanawong et al., 2010; Reinhard et al., 1995).

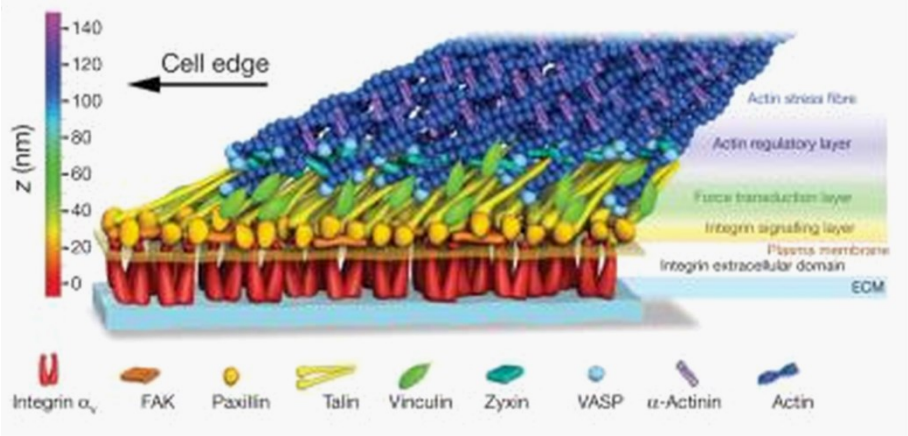


**Figure 4: Nanoscale architecture of focal adhesions.** Adopted from (Kanchanawong et al., 2010)

Adhesion is mediated not only by integrins but also by other nonintergin molecules. Widespread glycosaminoglycans of ECM, which can be in a close contact with cell, can participate on early stages of adhesion as well. In the past, there was observed a role of HyA as a possible mediator and a modulator of the first interaction between cell surface and its substrate. Interestingly, it occured only when HyA was present on either cell surface or on

substrate, when it occurred on both sufaces then adhesion was blocked (Zimmerman et al., 2002).

#### 1.4.1.1 Signalling in Adhesion

**FAK** is a focal adhesion-associated protein kinase that is concentrated in FAs. It plays a crutial role in integrin signalling layer of FAs and participates on cell survival, spreading and migration. FAK is activated by phosphorylation of its specific sites (predominantly on Tyr-397). Phosphotyrosine of activated FAK provides a docking site for various adaptor proteins with SH2 or SH3 domains (paxilin, Src kinase, phospholipase C, GRAF or Grb2 with SOS complex) which transduce signal to downstream pathways. In result, it leads to cytoskeletal reorganization, adhesion and migration, controlling of cell cycle and cell growth (Mitra et al., 2005; Parsons, 2003). Interestingly, FAK activity is closely connected to ERK1/2 kinases (extracellular signal-regulated kinases 1 and 2) (Chaturvedi et al., 2007). Thus it seems that FAK signaling plays an important role in regulating ECM-induced osteogenic differentiation of hMSC (Salasznyk et al., 2007).

**ERK1/2** are protein-serine/threonine kinases that participate in Ras-Raf-MEK-ERK signal transduction cascade. They regulate cell survival, adhesion, cell cycle progression, proliferation, migration or differentiation. ERK1/2 dispose of wide substrate specifity for quantum of cytosolic and nucelar proteins. ERK1/2 are activated by phosphorylation via MEK1/2 (mitogen-activated protein kinase (MAP)/ERK kinase) and are inactivated by protein-tyrosine specific phosphatases via dephosphorylation. Activated ERK1/2 phosporylate important nuclear transciption fators such as c-Fos and Elk that participate on early gene response connected with adhesion, migration, differentiation, survival etc. (Murphy et al., 2002; Roskoski Jr., 2012). Interestingly, it was shown that only contact of cell with ECM proteins activates ERK1/2 dependent pathway which induces osteogenic differentiation of hMSC (it seems that FAK participates in this process as well) (Salasznyk et al., 2007, 2004a).

**p38 kinase** is mitogen-activated protein kinase that participates in stress stimuli response, cell death and also in cell differentiation. It integrates environmental signals and participates in cell adaptive responses and in regeneration process (Segalés et al., 2016; Xu et al., 2014).

### 1.4.2 Fetal Bovine Serum

Fetal bovine serum (FBS) is the blood fraction after clotting, free of blood cell elements. In general, FBS is the standard supplement of *in vitro* cultured medium. It mimics chemical

environment of *in vivo* conditions via wide variety of proteins and factors important for cell survival, adhesion and proliferation (growth factors, adhesion-mediating factors such as FN, VN, hormones and transport factors (e.g. albumin, transferrin)). It also provides vitamins, various cofactors and nutrients such as nucleosides, amino and fatty acids and lipids (Krebs, 1950).

In general, it is used *in vitro* culturing because it importantly supports cell interactions with surface. After addition to cell culture, FBS proteins immediately cover surfaces and form a protein layer on them. This protein layer plays a key role in the initial adhesion step (see 1.4.1). This ability to cover free surfaces can basically affect initial reactions of cells or organism on various materials. As it follows, resulting pattern of protein layer can significantly change surface properties of material (Wilson et al., 2005). FBS promotes cell adhesion because it contains main mediators of cell adhesions - fibronectin a vitronectin - glycoproteins naturally occurring in blood serum and ECM. As it was mentioned above (see 1.3.1.1.) both are important players in process of cell adhesion, following migration and differentiation. However, the most abundant protein of FBS is bovine serum albumin (BSA). The protein makes up more than one half of FBS protein content. BSA negatively affects cell adhesion and as it was shown, it is the main player in so-called protein competitive adsorption to surface. In other words, resulting cell adhesion rate and its quality are directed by ratio of adhesion-promoting (*e.g.* FN) and adhesion-inhibiting (*e.g.* BSA) proteins in protein layer originated from FBS (Carré and Lacarrière, 2010; Wei et al., 2009).

Besides various advantages of FBS application in basic research, it has some limitations in medical practise. FBS cannot be used for clinical applications due to its many potential health risks, especially four viral contaminants are often detected in commercial lots of FBS: bacteriophage, infectious bovine rhinotracheitis, parainfluenza-3 and bovine viral diarrhea virus. Additionally, there is the possibility of anti-FBS antibody production (Ga et al., 1991; Sundin et al., 2007). It can also distort results of specific molecular methods or it can make impossible some specific applications (Gstraunthaler Gerhard, 2003; Lesniak et al., 2010). The next disadvantage is that FBS is the supplement of unknown and variable composition and also the way of its production is in conflict with ethical principles. Therefore, there is lot of effort for development of chemically defined supplements free of animal derived components (van der Valk et al., 2004). Despite the fact that some alternative media supplements are already commercially available for some cell types (e.g. widely used human platelet lysate because of high growth factors content), many of them are not still completely defined. Thus, completelly defined serum-fee media are still in intensive development phase (Hemeda et al., 2014; van der

Valk et al., 2010). Next disadvantage of FBS under *in vitro* conditions is already mentioned BSA presence. BSA can interact with various molecules via wide variety of binding sites for both hydrophobic and negatively charged hydrophilic moieties. Thus, this is the reason why some experimental systems (nanoparticles, gene delivery systems, methods based on transfection principles etc.) should use FBS alternatives (Fasano et al., 2005; Little et al., 2009). Therefore, all novel specific systems should be tested not only under FBS presence but also under FBS absence conditions for exclusion of FBS negative effects.

## 1.5 Stem Cells and Stemness

In organism two different types of stem cells exist - embryonic and adult stem cells. While embryonic stem cells direct development of whole organism with specialized cells and tissues, adult stem cells repair and renew tissues with the aim of maintenance and restoration of organism. Typical deposites of stem cells in organism are bone marrow, blood or adipose tissue, but can be found also elsewhere.

Stem cells are cells that exhibit two main properties together: 1) self- renewal ability that secures undifferentiated state of cell and thus maintains the stemness in organism; 2) differentiation ability that specialized cell types (tissue cells). Replication of stem cells is intentionally slow to minimize mutation risk. Currently it seems that stem cells divide by two mechanisms that are able to maintain stem cell population and at the same time to produce differentiated cells for tissue maintaining. The first mechanism of division is based on asymmetric replication that gives rise to two different daughter cells with different cell fate – one cell is identical to the mother stem cell and the second cell is differentiated. The second mechanism of division is based on symmetric replication (or stochastic) that produces two daughter cells with similar properties – i.e. while one stem cell is divided to two differentiated cells, other stem cell is divided to two undifferentiated stem cells. Interestingly, because symmetric division supports stem cell to expand, it seems that the cancer development is closely connected to specific mutations that alter probability of symmetric and asymmetric division (Dingli et al., 2007; McCulloch and Till, 2005; Morrison and Kimble, 2006).

Stem cells are classified to five groups according to their differentiation capacity (differentiation potential): totipotent-, pluripotent-, multipotent-, oligo- and unipotent cells. Totipotent cells are on the top of differentiation capacity. These cells are able to differentiate into all embryonic and extraembryonic cell types and tissues. Thus, one totipotent cell has potential to give rise to whole organism. Totipotent cells are produced by fusion of egg and sperm, forming zygote. In addition, few division stages of zygote are composed of totipotent

cells. The lower level of differentiation capacity is connected to pluripotent cells. Those cells have potential to differentiate to any fetal or adult cell type (i.e. any cell of entoderm, ectoderm or mesoderm layer) and can be derived from adult tissues. Potency that is more limited is provided by multipotent cells that can differentiate to number of related cell types (e.g. bone marrow, neural or hematopoetic somatic stem cells). Oligopotent stem cells differentiate into only a few cell types, and unipotent cells can produce only one cell type (Mitalipov and Wolf, 2009). The most of stem cells in adult organism (e.g. mesenchymal stem cells, hematopoetic stem cells, adipose-derived stem cells) are multipotent and they can be derived from various tissues (e.g. bone marrow, blood, adipose etc.). Interestingly it was shown that these cells have a tendency to differentiate to cells of tissue of their origin (Polo et al., 2010).

Stem cells have great potential for regenerative medicine and tissue engineering including cell therapy. There is still challenge to expand undifferentiated stem cells for clinical applications because it means to maintain full self-renewal ability and differentiation potential without feeder layer and non-defined supplements in media. Additionaly, *in vitro* differentiation often gives rise a mixed population of variously differentiated cells and it generally provides relative low yield of differentiated cell (Uccelli et al., 2008; Ulloa-Montoya et al., 2005). However, *in vitro* effort to expand undifferentiated stem cells and keep them in stemness state is more complicated the higher differentiation capacity stem cells provide (Tabar and Studer, 2014). It seems, that knowledge of specifity of stem cell environment (stem cell "niches") is key point for their amplification and specific differentiation under *in vitro* conditions and also for regenerative medicine (Barrilleaux et al., 2006; Engler et al., 2006; Jhala and Vasita, 2015; Murphy et al., 2014).

One of crutial points of stem cell differentiation is various combinations of growth factors that ensure correct differentiation, survival and sufficient expansion of cell (see 1.5.2.). Next crutial points of stem cell differentiation are combination of 3D environment and dynamic cultivation conditions (see 1.5.3.), surface topography and other mechanical features (see 1.3.2.). It was shown, that these mentioned factors can induce (stem) cell differentiation even without chemical supplements of differentiation. Additionally, it was shown that stem cells can spontaneously produce growth factors or cytokines (see 1.5.2.) with paracrine and autocine effects that induce specific differentiation state (Caplan and Dennis, 2006; Dalby et al., 2014, 2007, 2006; McCoy et al., 2012; Mitalipov and Wolf, 2009; Ulloa-Montoya et al., 2005).

### 1.5.1 Mesenchymal Stem Cells and Their Differentiation Capacity

Mesenchymal stem cells (MSC) were firstly described by Caplan (Caplan, 1991). He connected MSC function not only to embryonic bone and cartilage formation but also to adult repair and turnover of skeletal tissues. He postulated the different lineages derived from MSC, which are given by combination of extrinsic (environment) and intrinsic factors (genomic potential). Nowaday, MSCs can be described as a specific group of stromal cells (connective tissue cells of organs) with multipotent differentiation ability at the level of mesodermal lineage (they can differentiate to osteocytes, adipocytes and chondrocytes), but it was reported they also have endodermic and neuroectodermic differentiation potential (Fig.5). Under *in vitro* conditions, these are plastic-adherent cells of fibroblast-like morphology (Uccelli et al., 2008).

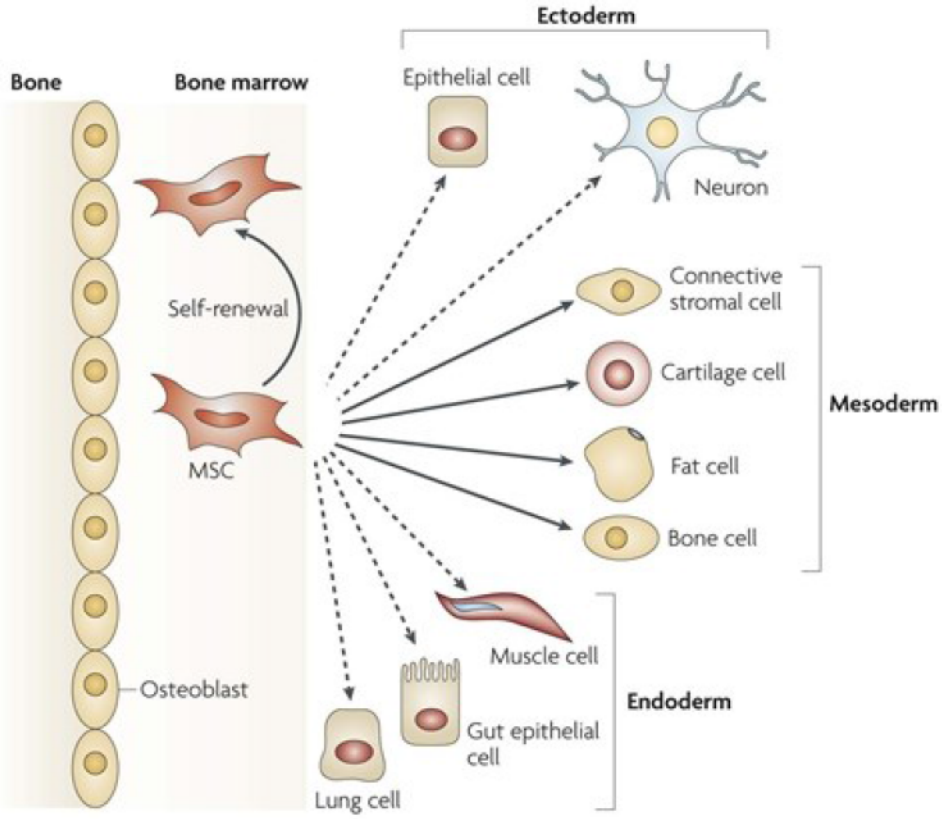


**Figure 5: Multipotentiality of MSC.** Adopted from (Uccelli et al., 2008)

Interestingly, phenotype and differentiation potential of MSC derived from various organs or tissues seems to be still related to tissue of their origin (Meirelles et al., 2006; Meirelles and Nardi, 2009).

MSC are widely used for tissue engineering and development of cell therapy because those have been shown as cells of high plasticity in culture and ability to migrate to sites of

injury. Other essencial feature of MSCs is production of bioactive molecules that support regenerative environment and repair (see 1.5.2). Just these findings predict MSC as an efficient tool with high potential for future therapy (Camassola et al., 2012; Meirelles and Nardi, 2009). In addition to human MSCs (hMSCs) application in practise, cells of larger animal models are also preffered in tissue engineering and in *in vitro* and *in vivo* evaluation of biomaterials. Especially porcine MSCs (pMSCs) seems to be very suitable and perspective due to their high similarity to hMSCs based on mutual similarity of both organisms in anatomy, physiology, development or disease occurrence (Cancedda et al., 2007; Juhásová et al., 2011; Vodička et al., 2005; Wang et al., 2007).

### 1.5.2 Regulators of Differentiation

Cell differentiation includes a number of essential changes in cell size and shape, metabolic activity, cell signal transduction activity, membrane potential etc. It depends on number of external factors such as growth factors, hormones or various signal molecules. Beside epigenetics mechanisms (such as histone remodelation etc.), it is also closely connected to gene expression. With respect to **gene expression**, there seems to be critical a pool of three specific transcription factors and their accessibility – those are Oct4, Sox2 or Nanog which are known as factors of the stemness maintenance (Christophersen and Helin, 2010). Their expression leads to undifferentiated state of cell, pluripotency and supports stemness maintenance. On the other hand, disbalance in their expression leads to differentiatiated state. It seems, that differentiation specifity is given by level of their expression together with specific balance among all of three transcription factors (Mitalipov and Wolf, 2009; Yu et al., 2007). Interestingly, high impact of these factors on cell differentiated or undifferentiated state was demonstrated by induction (by artificial reprogramming) of pluripotent stem cells from mouse embryonic and adult fibroblast cultures by regulation of these factors (Takahashi and Yamanaka, 2006).

Differentiation into different lineages is directed by other transcriptional factors (Figure 6). Osteoblasts differentiation is regulated by Runx2, Osterix and β-catenin (their cooperation directs immature osteoblasts to produce bone ECM) (Komori, 2006; Nishio et al., 2006). Adipocyte differentiation is regulated by C/EBP family and PPARγ (Hu et al., 1995) and chondrocyte differentiation is regulated by SOX family of transcription factors (Ikeda et al., 2005).

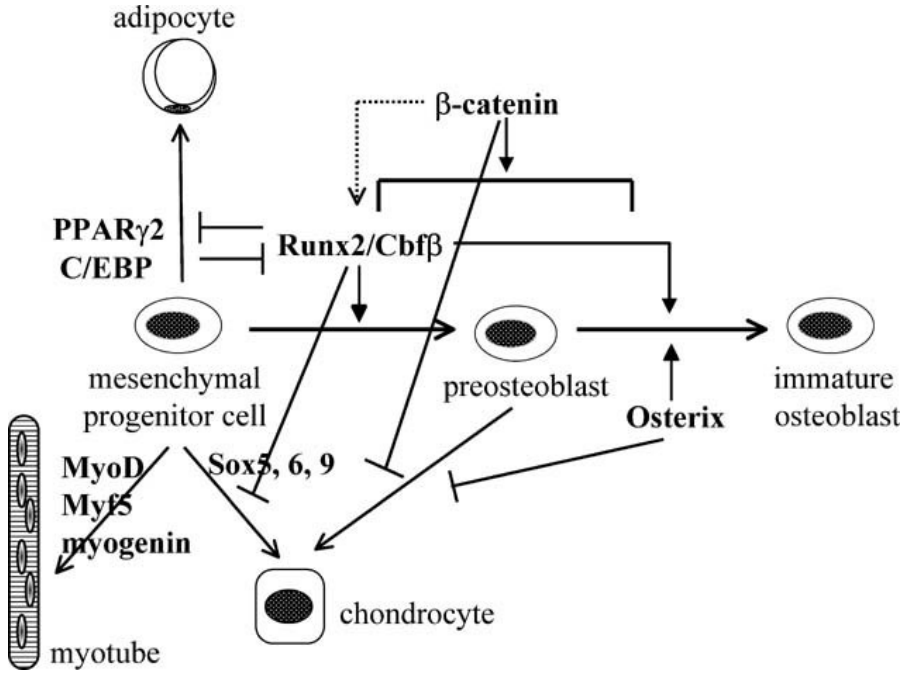


**Figure 6: Determination of osteoblastic lineage by transcription factors.** Adopted from (Komori, 2006)

As it was mentioned, cell differentiation is directed by various external processes and factors. Thus cell signalling including specific signalling molecules, growth factors, participates on it as well. Growth factors are substances (such as cytokines or hormons) with stimulating effects on cell growth, proliferation, differentiation or repair. Wide variety of their effects on cell behaviour and functions is known. The key growth factors are BMPs (bone morphogenetic proteins), FGFs (fibroblasts growth factors) and VEGF (vascular endothelial growth factos).

BMPs are group of multifunctional growth factors. Besides observed stimulation effects on cartilage, neural or heart development, these factors are key players in postnatal bone formation and homeostasis. Interestingly, they regulate activity of osteoblasts and osteoclasts by regulation of expression via important signalling pathways (e.g. ERK/MAPK) (Xiao et al., 2002). Key effects on bone homeostasis and formation are evident in some preclinical and clinical studies and results. For example, BMP-2 was applied and has been proven in various therapeutic procedures (bone defects, non-union fractures, spinal fusion, osteoporosis etc.) to support standard surgical interventions. Nowadays, there are also used recombinant variants of BMPs that show acceleration of bone regeneration (Cancedda et al., 2003; Carreira et al., 2014; Chen et al., 2004; Decambron et al., 2017; Kuboki et al., 1998; Laurencin et al., 2001; Sánchez-Duffhues et al., 2015). FGFs are crutial players in cell differentiation and proliferation; they participate in angiogenesis and reparation mechanisms. FGFs are called as promiscuous growth factors due to observed wide spectra of their actions (significant regulatory, morphological or

endocrine effects ) toward to various cell types (Green et al., 1996). VEGF directs organism to formation of new blood vessels to mediate oxygen supply to tissues via supporting of mitogenesis and migration (Palmer and Clegg, 2014). Next significant growth factors with impact on differentiation or regeneration are EGF (epidermal growth factor), NGF (nerve growth factor) or TGF (transforming growth factors, cytokines produced by white blood cells). Interestingly, it seems that none of growth factors has potential to direct cell differentiation exclusively to one cell type and thus the overall effect of the factors may be rather divided into groups with similar tendency of directed differentiation. For example, while BMP, FGF and EGF induced expression of ectodermal and mesodermal markers of cells, TGF induced expression of only mesodermal markers and NGF induced expression of ecto-, mezo- and endodermal markers (Schuldiner et al., 2000).

Despite the esentiality of growth factors in organism, the goal of tissue engineering is to induce cell differentiation without chemical suplements (Carreira et al., 2014; Dalby et al., 2007). It seems that differentiation without supplements can be sufficiently achieved by MSCs application. MSCs are widely used in tissue engineering due to their differentiation potential (in to osteoblasts, chondrocytes, myoblasts). MSCs produce various bioactive molecules including a variety of cytokines or growth factors with paracrine and autocrine activities in organism. These molecule display anti-apoptotic, immunomodulatory, angiogenic, anti-scarring, and chemoattractant properties. Thus, MSCs are effective and natural tool for induction of local regenerative environment *in vivo*. In summary, it was performed that these trophic effects are distinct from the direct differentiation of MSCs and that this is the next crutial MSC function which naturally participates in tissue repair. With regard to MSC application in tissue engineering and regenerative medicine, trophic function of MSC seems to be comparable or more important then their differentiation function (Camassola et al., 2012; Caplan and Dennis, 2006; da Silva Meirelles et al., 2009; Meirelles and Nardi, 2009).

In several independent studies it was shown that a topography pattern can crutially induce cell differentiation without chemical inducers of differentiation (Abagnale et al., 2015; Dalby et al., 2007, 2006; Deligianni et al., 2001; Karazisis et al., 2017; Streuli, 1999). Stem cells seem to be extremely sensitive to elasticity or stiffness of their surrounding. While soft material used to be neurogenic inducer, stiffer and rigid materials act as myogenic and osteogenic inducers. Interestingly, elasticity/stiffness can predominate in long-term effects of treatment over differentiation markers (Engler et al., 2006) or other environmental factors such as porosity or protein tehtering (Engler et al., 2006; Wen et al., 2014). Interestingly, porosity and pore-size seem to be rather complementary to differentiation due to not clear outcomes

about their ideal parameters (Kasten et al., 2008b; McCoy et al., 2012; van der Smissen et al., 2015). It seems that they rather depend on context of cell type, specifity of ECM and also on parameters such as mechanical stress or flow rate during cultivation (Altman et al., 2002; Jungreuthmayer et al., 2009; McCoy et al., 2012).

### 1.5.3 Cell Cultivation – Dynamics and Three-dimensional (3D) Conditions

With respect to the trend in tissue engineering to mimic organism and its natural conditions, also *in vitro* conditions (including the way of cells cultivation) need to mimic *in vivo* conditions. Because the native ECM provide 3D configuration, thus 3D way of cell cultivation (moving from cell monolayers to 3D cultures) has begun to replace traditional two-dimensional (2D) cultivation. It was soon confirmed that 3D culturing is clearly superior to 2D culturing and that combination of cells and 3D conditions (e.g. scaffolds or other carriers) provides more efficient cell culturing and has significantly higher potential for reparation of damaged tissue (Niemeyer et al., 2002; Sasaki et al., 2002).

Over time, the basic research turned out the impact of perfusion in (3D) cell cultivation that mimic dynamic conditions of organism. Interestingly, it was performed that perfused 3D culture supports the maintenance of cell in more natural state (Fernekorn et al., 2013). With respect to various results, it also seems that 3D cultivation together with dynamic culturing provides more physiological interactions of cells with ECM and with neighbouring cells. Both of them also support more efficient exchange of nutrients and induce many mechanical stimuli, which naturally occur in organism. In summary, they crutially affect cell adhesion, proliferation and differentiation and support self-renewal and differentiation potential of stem cells. In addition to better nutrient exchange, it was performed that dynamic cultivation elevates effectivity of 3D cultivation by easier delivery of oxygen in the volume of 3D environment. 3D culture *in vitro* is often associated with relevant oxygen gradients, which can cause inhomogeneous tissue quality, however, perfusion can help (at least partially) to eliminate these 3D culture–associated oxygen gradients and prevent cell death (Volkmer et al., 2008).

With the intension to ensure 3D and dynamic conditions under *in vitro* cultivation, a variety of bioreactors have been developed with the goal to provide controlled environment that mimic structural and dynamic conditions of organism and which can support more natural way of cell differentiation (Birgersdotter et al., 2005; Juhásová et al., 2011; Pampaloni et al., 2007; Tian et al., 2008; Ulloa-Montoya et al., 2005; Zhang et al., 2010). Positive impact of 3D and dynamic cultivation conditions including osteogenic differentiation was also performed in bone tissue engineering (Jungreuthmayer et al., 2009, 2008; McCoy et al., 2012; Stops et al., 2010;

Tian et al., 2008).

Results obtained from variable ways of cultivation do not only help to understand the basics about cell behaviour but also help to develop clinical (stem) cell applications and high-quality and perspective biomimetic cell carriers.

# 2 AIMS OF THE THESIS

This PhD thesis is composed of four parts (I-IV). The first three parts (I-III) are directly conected to various biomimetic materials – every part describes one material type and its impact on cells. The last part (IV) is focused on general description of cell adhesion process on standard cultivation surface i.e. it describes fundamental point of cell-surface interaction.

I To characterize cell response to **colloidal complexes of CTAB or Septonex with hyaluronic acid** - direct cell interactions with potential drug/nuclei acid/diagnostic dye delivery system or cosmetic agent with the respect to fetal bovine serum presence or absence during cultivation.

II To evaluate *in vitro* **collagen based scaffolds** and their suitability for stem cell therapy in bone surgery application by using mesenchymal stem cells derived from different organisms with respect to different cultivation conditions (static and dynamic).

III To evaluate *in vitro* **collagen/hydroxyapatite nano/micro structured resorbable layers with controlled elution of antibiotics** for pro-osteointegration support.

IV To describe an **early phase of cell adhesion of different cell types** in context of fetal bovine serum presence or absence under tissue culture conditions.

# 3 MATERIALS AND METHODS

Materials and methods are described in detail in publications A-G. The enclosed list contains methods that were performed by author of this thesis. Materials and methods of manuscript D, which is in preparation are described below in detail (see 3.1.), materials and methods of prepared manuscript F are identical to those of publication E.

**Tested Materials:**

- CTAB-HyA and Septonex-HyA complexes (in Publications A-B)
- Collagen based scaffolds consisted of: poly (DL-lactide) electrospun nano/sub-micronfibres (PDLLA), a natural collagen (type I) matrix supplemented with HyA and natural calcium phosphate nano-particles (bCaP) (in Publications C-D)
- Collagen/hydroxyapatite/vancomycin, collagen/hydroxyapatite/gentamicin and collagen/hydroxyapatite/vanco-gentamicin electrospun nanostructured layers (in Publications E-F)

**Culture of Cells:**

- Human osteoblast-like cell line (SAOS-2) (in Publications A-B,D, E-G)
- Spontaneously immortalised human keratinocyte cell line HaCaT (in Publication B)
- Human dermal fibroblasts (in Publications B, G)
- Human mesenchymal stem (stromal) cells (in Publication C, G)
- Porcine mesenchymal stem (stromal) cells (in Publication D)

**(Immuno)Fluorescence Staining of Cells, (stained Structures):**

- nuclei (in Publications B-G)
- actin stress fibers (in Publications C, E-G)
- CD44 (in Publication G)
- talin (in Publication G)
- vinculin (in Publication G)
- pERK1/2 (in Publication G)
- pFAK (in Publication G)

**Cell Imaging by Light Microscopy (in Publications A, B, G)**

**Cell Imaging by Fluorescence Wide-field Microscopy (in Publications B-C,E-F)**

**Cell Imaging by Fluorescence Confocal Microscopy (C-D)**

**Advanced Image Analyses:**

- Cell number determination (in Publications B)
- Cell area determination (in Publications G)
- Measurement of fluorescence intensity (in Publication G)
- 3D reconstruction of confocal microscope images (in Publications C-D)

(ImageJ (Rasband, W.S., ImageJ, U.S. National Institutes of Health, Bethesda, Maryland, USA, http://imagej.nih.gov/ij/, 1997-2016) and Cell Profiler (Broad Institute, USA) softwares were used)

- **Western blot analysis -** detection of pERK1/2 (in Publication G)
- **Enzyme-linked immunosorbent assay** (ELISA) - determination of the amount of pERK1/2 (in Publication G)

**Statistical Analyses:**

- Nonparametric Mann-Whitney U test (in Publication D, E, G)
- Nonparametric Kruskal-Wallis ANOVA with a subsequent post-hoc Multiple comparison test (in Publication B, C, D, E, F)
- Wilcoxon signed-rank test (in Publication A)

(STATISTICA Software (StatSoft, Czech Republic) was used)

## 3.1 Methods of Manuscript D

### 3.1.1 Cell Seeding onto Scaffolds and Cultivation

Cells were seeded onto scaffolds at a concentration of 200 000 cells for 2, 7 or 14 days of cultivation (controlled scaffolds were not colonized by cells). One-half of seeded scaffolds was exposed either to static (standard) cultivation conditions or to dynamic cultivation conditions (scaffolds were inserted to bioreactor cultivation chambers with arranged flow rate 30 μl/ min) for 6 hours. After this time period, all scaffolds were further cultivated under standard cultivation conditions for the rest of incubation time.

### 3.1.2 Fluorescence Staining of Cells

The cells on scaffolds were fixed in 4% paraformaldehyde in PBS at room temperature (RT) for 20 min after 2 days or 7 days of cell cultivation on the scaffolds. Cells were permeabilized by 0.1% Triton X-100 in PBS at RT for 20 min and their nucleai by DAPI at RT for 45 min (1:1000).

### 3.1.3 Imaging of Fluorescently Stained Cells

3D images of the cells on the scaffolds were acquired using a Leica SP8X microscope (Leica Microsystems, DE) equipped with a confocal scanning head, lens HC PL FL 10x/0.30 PH1 (W.D. 11.0mm) and excitation laser 405 (Leica Microsystems, DE). The emission was detected using a 470/40 nm band-pass filter. Images were rendered in a LasX software (Leica Microsystems, DE).

### 3.1.4 Determination of DNA Content

Cell seeded scaffolds were snap-frozen and stored at -20°C after 2 days or 7 days of cultivation. Scaffolds were then mechanically disrupted and then digested by proteinase K in TE buffer at 56°C for 16 hours. Digested scaffolds were centrifuged at 19 000 x g for 12 min, supernatants were transferred to new clean tube and centrifugation was repeated. Obtained supernatants were analyzed by Quant-iT™ PicoGreen® dsDNA Assay Kit according to the standard protocol based on 200 µl volume microplate reader analysis. Sample fluorescence was analysed by fluorescence microplate reader (excitation ~480 nm/ emission ~520 nm).

### 3.1.5 Gene Expression Analyses - qRT-PCR (Quantitative Polymerase Chain Reaction with Reverse Transcription)

Cell seeded scaffolds were snap-frozen and stored at -80°C after 2 days or 14 days of cultivation. Scaffolds were then homogenized using an iced manual homogenizer. Then samples were incubated with TRI Reagent® (Sigma, USA) solution for at least 30 min. at RT. After lysis the samples were centrifugated at 12 000 x g for 10 min at 4°C, supernatants were transferred to new clean tube and centrifugation was repeated. Next steps were performed according to manufacturer's protocol (RNA samples were precipitated in 75% EtOH over night at -20°C). Isolated RNA was analyzed on NanoDrop spectrophotometer ND-1000. If TRI Reagent® contamination occured, purification of RNA was additionaly performed according to protocol of Kerbs et al. (Krebs et al., 2009). Isolated RNA (20 - 50 ng) was used for reverse transcription by means of SuperScript III Reverse Transcriptase according to the

manufacturer´s protocol. Each qPCR reaction was performed in tetraplicates using a LightCycler 480 and using Universal Probe Library System Technology (Roche,Germany). The cDNA as a template was diluted prior to use in qPCR reaction. Controls with no template were used in each qPCR reaction. Forward (F) and reverse (R) primers sequences (*Sus scrofa*) were following: glyceraldehyde-3-phosphate dehydrogenase (GAPDH): F '5-gtcggttgtggatctgacct-3', R '5-gcctgcttcaccaccttct-3'; mitogen-activated protein kinase 3 (ERK1, MAPK3): F '5-agtcggaccccaaagctc-3'; R '5-tccgtttgttggggttaaag-3'; mitogen-activated protein kinase 14 (p38α, MAPK14): F '5-ttcacagggacctaaaacctagtaa-3', R '5-ccagtccgaaatccaaaatct-3'; runt-related transcription factor 2 (RUNX2): F '5-atggttaatctccgcaggtc-3', R '5-gcagccttaaatgcctctgt-3'; osterix (SP7): F '5-aaaaggttcacgcgttcg-3', R '5-tcttctcccgggtatgagtg-3'; collagen, type I, alpha 1 (COLI): F '5-ccaagaagaaggccaacaag-3', R '5-cacacgtctcggtcatggta-3'; peroxisome proliferator-activated receptor gamma (PPARG): F '5-tgaagctccaggactaccaaa-3', R '5-aataataaggcggggacaca-3'. qPCR data were analyzed by means of Double Delta Ct method (relative quantification). All qPCR data (Ct values – cycle threshold) were normalized to geometrical mean of GAPDH housekeeping gene.

### 3.1.6 Determination of Metalloproteinase Activity - Zymography

Supernatants (2-days-old conditioned media) of cell seeded scaffolds or control media were stored at -20°C. Then those were separated on one-dimensional SDS-PAGE (7.5% separating gel, 4% stacking gel) containing 0.05% gelatin. Gels were incubated. in gelatinase activation buffer (100 mM Tris-HCl, pH 7.4, 5 μM $CaCl_2$, 1 μM $ZnCl_2$) over night. Then gels were stained with Coomassie Brilliant Blue G-250. Matrix metalloproteinase (MMP)-2 and -9 activity was analysed by quantifying unstained bands by Gene Tools analysis software (Syngene, UK).

# 4 RESULTS

## 4.1 List of Original Publications Used for Phd Thesis

*PART I*

A. **Pavla Sauerová**, Martina Verdánová, Filip Mravec, Tereza Pilgrová, Tereza Venerová, Marie Hubálek Kalbáčová , Miloslav Pekař (2015): **Hyaluronic Acid as a Modulator of the Cytotoxic Effects of Cationic Surfactants.** Colloids and Surfaces A: Physicochem. Eng. Aspects 483, 155-161. IF = 2.752

B. **Pavla Sauerová,** Tereza Pilgrová, Miloslav Pekař and Marie Hubálek Kalbáčová (2017): **Hyaluronic Acid in Complexes with Surfactants: The Efficient Tool for Reduction of the Cytotoxic Effect of Surfactants on Human Cell Types.** Journal of Biological Macromolecules – accepted for publication. IF = 3.138

*PART II*

C. Tomáš Suchý, Monika Šupová, **Pavla Sauerová**, Martina Verdánová, Zbyněk Sucharda, Šárka Rýglová, Margit Žaloudková, Radek Sedláček and Marie Hubálek Kalbáčová (2015): **The Effects of Different Crosslinking Conditions on Collagen-Based Nanocomposite Scaffolds - An in Vitro Evaluation Using Mesenchymal Stem Cells.** Biomed Mater. 10, 065008. IF = 3.697

D. **Pavla Sauerová**, Tomáš Suchý, Monika Šupová, Zbyněk Sucharda, Šárka Rýglová, Margit Žaloudková, Tereza Kubíková, Zbyněk Tonar, Martin Bartoš, Jana Juhásová, Štefan Juhás, Jiří Klíma and Marie Hubálek Kalbáčová (2017): **Comparison of Seeding Efficiency on the Biodegradable Scaffolds of Different Composition and Cultivation Conditions.** Manuscript in preparation

*PART III*

E. Tomáš Suchý, Monika Šupová, Eva Klapková; Václava Adámková, Jan Závora,Margit Žaloudková, Šárka Rýglová, Rastislav Ballay, František Denk, Marek Pokorný, **Pavla Sauerová**, Marie Hubálek Kalbáčová, Lukáš Horný, Jan Veselý, Tereza Voňavková, Richard Průša (2017): **The Release Kinetics, Antimicrobial Activity and Cytocompatibility of Differently Prepared Collagen/Hydroxyapatite/Vancomycin Layers: Microstructure vs. Nanostructure.** European Journal of Pharmaceutical Sciences 100, 219-229. IF = 3.77

F. Tomáš Suchý, Monika Šupová; Eva Klapková; Václava Adámková; Jan Závora; Margit Žaloudková; Šárka Rýglová; Rastislav Ballay; František Denk; Marek Pokorný; **Pavla Sauerová**; Marie Hubálek Kalbáčová; Lukáš Horný; Jan Veselý; Tereza Voňavková; Richard Průša (2017): **Evaluation of Collagen/ Hydroxyapatite Layers Impregnated by Different Antibiotics – Novel Potential Local Drug Delivery for Bone Surgery**. Manuscript in preparation

*PART IV*

G. Martina Verdánová, **Pavla Sauerová**, Ute Hempel, Marie Hubálek Kalbáčová (2017): **Initial Cell Adhesion of Three Cell Types in the Presence and Absence of Serum Proteins.** Histochemistry and Cell biology 147 (5), published online. IF = 2.78

Mentioned accepted publications are included in full form in this thesis (see 10).

## 4.2 PART I: HyA- Surfactant Complexes (publications A - B)

Part I of this thesis is focused on characterization of cell behaviour affected by direct interactions of cells with **colloidal complexes of CTAB or Septonex with hyaluronic acid** for 24 h. The developed complexes have a primary potential as drug/nuclei acid/diagnostic dye delivery system, they have also potential as cosmetic agent. Therefore, the study of cell intreractions with complexes on survival and cytotoxicity level is fundamental step for sequential verification of their application potential. Moreover, this is the crucial phase of possible feedback modifications of complexes those enable an effective improvement of complex properties for next practical application. Because of more spheres of possible practical application, interactions of complexes were studied with more cell types. Moreover, selected experiments were performed under standard conditions (i.e. fetal bovine serum present for the whole time of cell cultivation with complexes (24h)) and under non-standard conditions (i.e. fetal bovine serum absent for the first four hours of whole time cell cultivation (24 h) with complexes).

Publication A describes interactions of complexes with only human osteoblasts (SAOS-2 cells; cell line derived from osteosarcoma) and under standard and non-standard conditions. Publication B (after feedback modification of complexes) describes complex interactions with not only osteoblastic cell line but also with human keratinocytes (HaCaT cells; spontaneously transformed aneuploid immortal keratinocyte cell line from adult human skin) and with primary human fibroblasts (primary dermal cells). Results of publication B provided more detailed characterisation of complexes under *in vitro* conditions in relation to cells. Only some analyses were performed under non-standard conditions due to confirmation of previsouly (publication A) observed trend.

This research is based on biological and chemical fields cooperation. Biological part was performed by the author of this thesis and it represents one of the thesis aims. Chemical research was performed by colleagues from Materials Research Centre of Faculty of Chemistry, Brno University of Technology.

### 4.2.1 Publication A: Hyaluronic Acid as a Modulator of the Cytotoxic Effects of Cationic Surfactants

**Pavla Sauerová**, Martina Verdánová, Filip Mravec, Tereza Pilgrová, Tereza Venerová, Marie Hubálek Kalbáčová , Miloslav Pekař (2015): Hyaluronic acid as a modulator of the cytotoxic effects of cationic surfactants. Colloids and Surfaces A: Physicochem. Eng. Aspects 483, 155-161. IF=2.76

CTAB-HyA and Septonex-HyA complexes were prepared as possible drug/ gene delivery system (Halasová et al., 2011). Function of developed complexes is based on possibility of cationic surfactants (CTAB and Septonex) to form micelles and to interact with negatively charged substances (some kinds of drugs, nucleic acids, cellular surface, etc.). Surfactant micelles can be ideal carriers of solubilized cargo and they can serve as an interesting tool in drug or gene cell delivery, for study of cell trafficking process or for other cell structures visualisation techniques. Additionally, thanks to antiseptic properties they can behave as antimicrobial agents for topical applications (cosmetic or pharamceutic industry) (Nakata et al., 2011). However, it is known that cationic surfactants (CTAB) exhibit the highest cytotoxicity in comparison to anionic (SDS) and non-ionic (Triton X-100) ones in general (Grant et al., 1992). Thus, hyaluronic acid seems to be as the ideal biocompatibile and naturally occurring tool for reduction of surfactant induced cytotoxicity (Halasová et al., 2013; Kalbáčová et al., 2014). HyA in complexes with surfactants should play more roles, not only it can protect cell but also it can help the complex to bind onto the cell surface (via its receptors) and subsequently to enter the cell. All of these properties seem to be ideal for drug delivery systems (Torchilin, 2001).

In this first paper, CTAB-HyA and Septonex-HyA complexes were tested for determination of the surfactants' cytotoxicity at various concentrations and for the ability of HyA bounded in complexes with these surfactants to reduce this cytotoxicity. Experiments were performed with human osteoblast cell line under standard cultivation conditions (and non-standard cultivation conditions for 24 h. After this incubation, all tested CTAB-HyA or Septonex-HyA complexes and controls (free HyA, free CTAB or Septonex and only medium for control untreated cells) were added to cells for additional 24 h. After this time, cell metabolic activity was measured by MTS assay. Solutions of complexes were prepared by our colleagues by mixing HyA and aqueous solutions of surfactant to obtain the desired final concentration. The surfactant solution was always added dropwise to the HyA solution. The concentrations of

CTAB in complex solutions were 40, 50, 80 and 100 μM. The concentrations of HyA (molecular weight of 1000 kDa) in CTAB complex solutions were : 5, 30 and 50 mg/l. The concentrations of Septonex in complex solutions were 30, 60 and 80 μM. Only one concentration of HyA (molecular weight of 936 kDa) in Septonex complex solutions was 1 g/l (see Table 1 of publication A). However, cells were treated by complexes diluted 1:9 in fresh cultivation medium, thus the final concentration of complexes was 10 times lower than concentration prepared by chemists.

Under standard conditions (Fig. 2 of publication A), metabolic activity of cells treated with all of used free CTAB concentrations were significantly decreased in comparison to control untreated cells. Cell metabolic activity after 4 μM or 5μM CTAB treatments reached 75% or 80%, resp. (cytotoxicity is often determined by drop of cell metabolic activity under 75 % (Flahaut et al., 2006)), after 8 μM or 10 μM CTAB treatment it reached 72% or 59%, respectively. The lowest HyA concentration (0.5 mg/l) was able to reduce negative effect of free CTAB at its lowest concentration used (4 μM). Higher HyA concentrations (3 mg/l and 5 mg/l) were able to significantly reduce negative effect of all higher CTAB concentrations (5 μM, 8 μM and 10 μM). The HyA regenerative ability increased proportionally with the increase of CTAB concentration. Under non-standard conditions (Fig. 3 in publication A), significant decrease of cell metabolic activity in most of free CTAB samples (but not at 4 μM CTAB concentration) compared to “only cells” control was observed. Contrary to standard conditions, even the lowest HyA concentration (0.5 mg/l) significantly reduced negative effects caused by 5 μM CTAB. Higher HyA concentrations (3 mg/l and 5 mg/l) in complexes with CTAB showed highly positive effect on cell metabolic activity - this effect rose proportionally with increasing of CTAB concentration again.

Cells under the standard conditions treated by Septonex (Fig. 4 in publication A) showed significant decrease of metabolic activity when treated with free Septonex and also with all of Septonex complexes with HyA in comparison to untretaed control. However, cytotoxicity was observed only at higher Septonex concentrations (6 μM and 8 μM). Statistically higher cell viability was observed in all Septonex complexes with HyA compared to free Septonex. HyA positive effect rose proportionally with increase of Septonex concentration, thus, HyA in complexes was also able to reduce Septonex induced cytotoxicity. Under non-standard conditions (Fig. 5 in publication A), the data showed significant drop of cell metabolic activity under the free Septonex treatment and also under the all of Septonex complexes treatment in comparison to untretaed control cells (the trend of metabolic activity in FBS absence and presence was similar but reduced in total). Cytotoxicity was observed when

6 μM Septonex and higher concentrations were used. This cytotoxicity was higher under non-standard conditions compared to standard conditions. For all that, significantly higher cell metabolic activity was detected when Septonex complexes were added to cells compared to free Septonex - higher Septonex concentrations (6 μM and 8 μM) were substantially reduced by HyA - this effect rose proportionally with increasing of Septonex concentration again.

In addition, changes in cell morphology of treated cells were observed by light microscopy (Fig. 1 of publication A). Results were in close agreement with all the metabolic activity results.

In this first publication A, we firstly tested created complexes of surfactants with HyA under *in vitro* conditions. We described the cytotoxic impact of created complexes on cell in comparison to free surfactants and free HyA. Besides HyA protectivity and FBS positivity in cell recovery under stress conditions, we demonstrated the potential of created complexes as possible future delivery system, in addition, usability of complexes under non-standard conditons was also performed.

### 4.2.2 Publication B: Hyaluronic Acid in Complexes with Surfactants: the Efficient Tool for Reduction of the Cytotoxic Effect of Surfactants on Human Cell Types

**Pavla Sauerová**, Tereza Pilgrová, Miloslav Pekař and Marie Hubálek Kalbáčová (2017): Hyaluronic acid in complexes with surfactants: the efficient tool for reduction of the cytotoxic effect of surfactants on human cell types. Journal of Biological Macromolecules. Accepted for publication. IF = 3.138

While the first observation (publication A) predicted HyA-srufactants complexes as the possible potential delivery system, we wanted to extend our results on various cell types – cell line of osteoblasts (SAOS-2), cell line of keratinocytes (HaCaT) and primary fibroblasts. Additionally, the concentrations of the surfactants and HyA in complexes were modified on the basis of a previous study (publication A, (Kalbáčová et al., 2014)) and aimed at exerting a reasonable effect on the cells. Further, the concentrations were selected bearing in mind the various colloidal aspects together to better comparison of both tested surfactants and their complexes with HyA.

Surfactant-HyA complex solutions were prepared by our colleagues by means of the gradual dropping of the surfactant stock solutions into the biopolymer stock solutions until the desired concentrations were obtained. The formation of induced micelles was confirmed by using pyrene as a fluorescence probe and by measurement of pyrene polarity index (Halasová et al., 2013). The concentrations of both surfactants in complex solutions were 3, 6 and 8 μM and concentration of HyA were 5 and 500 mg/l (molecular weight around 600 kDa).

Similarly to previous results, the degree of cell viability diminished with increasing concentrations of free surfactants. At the same time, the increase in viability in cases with the same amount of surfactant in CTAB-HyA and Septonex-HyA complexes was observed. In addition, reduction of cytotoxicity was dependent on surfactant and HyA concentrations (Fig. 1 and Fig. 2 of publication B). The treatment with surfactants or surfactant-HyA complexes exhibited a similar trend in all the three cell types tested. As figure 2 in publication B shows, concentration of 6 μM (and above) of both free surfactants led to cytotoxicity in all the cell types tested – cell viability was reduced below 75-80% of the control value (untreated cells). Similarly to results of publication A, the increase in viability and thus in the level of HyA protection was more apparent in cases of higher surfactant concentrations. However, unlike in previous experiments, the modification of complexes of different HyA concentration (5 or 500 mg/l) employed in this study allowed us to more accurately define the degree of HyA protection.

Protection was observed only in complexes with a lower HyA concentration (5 mg/l), whereas a higher HyA concentration (500 mg/l) caused either a markedly lower degree of protection or had no protective effect when compared to treatment with free surfactants. An analysis of metabolic activity changes at different cell type levels revealed that the fibroblasts (Fig.2A in publication B) and osteoblasts (Fig.2B of publication B) behaved in a more similar manner than did with the keratinocytes (Fig.2C of publication B) following general surfactant treatment. While the higher sensitivity to Septonex (than to CTAB) was evident in fibroblasts and osteoblasts, the extreme sensitivity to CTAB (not to Septonex) appeared in case of keratinocytes. As figure 2 in publication B shows, keratinocytes proved to be the most sensitive cell type of all the tested cell types to surfactant treatment. While the keratinocyte metabolism decreased rapidly below cytotoxic level (around 75%), as early as in the presence of the lowest (3 μM ) CTAB concentration, the metabolism of the fibroblasts and osteoblasts markedly decreased below this level only in the presence of higher CTAB concentrations (6 μM and more).

The analysis of the effect of surfactants and HyA-complexes thereof on cells was expanded to include the determination of nuclei number (cell number) beacuse of distinguishing between lethal cytotoxicity and sub-lethal cytotoxicity (Inácio et al., 2013). In general, cell number results (Fig.3 of publication B) corresponded with the trend of the MTS results thus indicating that MTS results reflect both cytotoxicity and cell number. However, despite the significant deviations in the cell number results, a certain percentage difference was noticeable between the nuclei number and metabolic activity results (Fig.2a in publication B). CTAB exerted a more marked influence in terms of reducing the number of cells than it did with concern to affecting metabolic activity, which did not decline with the same degree of intensity. However, a different situation from that of CTAB was observed with respect to Septonex treatment concerning which, in general, a higher level of similarity of cell number and metabolic activity was observed. It was indirectly shown that CTAB combines lethal toxicity with cell metabolism induction, while Septonex predominantly causes lethal toxicity concerning fibroblasts.

Due to the known instability of similar complexes over time (Li et al., 2012), the study included an investigation of possible changes affecting free surfactants and their complex analogues over time (testing of the same complex batches over time). The metabolic activity was determined of cells treated with freshly prepared, 4-week old and 10-week old solutions of free surfactants and their corresponding complex analogues. In order to ensure the highest degree of reproducibility of the obtained results, a well-defined immortalised osteoblast cell

line was used for this purpose. No significant changes in cell metabolic activity were identified following the treatment of the cells using the same, but varying in age, CTAB (Fig.4A in publication B) and Septonex (Fig.4 B in publication B) surfactants and their HyA-complexes.

Further, the well-defined osteoblast cell line was used for the verification of the effect of complexes on cells under standard (FBS present in the cultivation medium during whole of the incubation period) and non-standard conditions (FBS added only 4 h following cell seeding). Similarly to results of publication A, figure 5 in publication B demonstrates the positive role of FBS under stress conditions under which the cells were treated with the surfactant (CTAB). The trend of cell viability under non-standard conditions was similar to the one of standard conditions, although it was reduced in general. Despite a certain degree of viability reduction under non-standard conditions, the results confirmed the applicability of complexes under such conditions.

Finally, potential differences between complexes made up of HyA of differing molecular weights were determined because it was already demonstrated on similar system that the biological function of HyA depends on its molecular weight (Mizrahy et al., 2011a). Thus, complexes of CTAB with high molecular weight HyA (ca 900 kDa) and CTAB complex with lower molecular weight HyA (ca 600 kDa) were studied (Fig.6 in publication B) on osteoblasts under standard conditions. In addition, CTAB complexes composed of the highest surfactant concentration (8 μM) and a lower HyA concentration (5 mg/l) were tested since the protective role of HyA in this CTAB-HyA complex was found to be the most extensive and significant in comparison to free CTAB. Our results reveal no significant change in osteoblast metabolic activity following treatment with complexes of differing HyA molecular weight.

Also changes in cell morphology of treated cells were observed by light microscopy (Fig. 1 in publication B), results were in close agreement to all the metabolic activity results.

## 4.3 PART II: Collagen-Based Scaffolds as Cell Carriers (publications C-D)

The part II of thesis is focused on *in vitro* evaluation of **collagen based scaffolds** by means of different types of cells (MSCs of different origin and cell line of osteoblasts). Scaffold composition tries to mimics bone extracellular matrix, thus scaffolds have potential of structural substitution of bone and can serve for cell application. MSCs serve as a tool for study of cell-scaffold interactions and simultaneously they can verify scaffold suitability for mesenchymal stem cell therapy. While publication C is focused on cell interactions with one type of collagen-based scaffold treated by various crosslinking agents, manuscript in preparation D is focused on cell interactions with scaffold of different composition treated by same crosslinking agent. Moreover, scaffolds evaluated in manuscript D are colonized with cells by different processes - STATIC CULTIVATION (i.e. standardly used cultivation method when seeded cells are kept in stationary conditions for a whole time of cultivation with the scaffolds) and DYNAMIC CULTIVATION (i.e. cultivation method when medium flows through the scaffold with the aim to simulate natural conditions *in vivo*).

This research is based on biological and material fields' cooperation. Biological part was performed by author of this thesis and it represents one of the thesis aims. Material research was performed by colleagues from Department of Composites and Carbon Materials of Institute of Rock Structure and Mechanics, Academy of Sciences of the Czech Republic.

### 4.3.1 Publication C: The Effects of Different Crosslinking Conditions on Collagen-Based Nanocomposite Scaffolds - An *in Vitro* Evaluation Using Mesenchymal Stem Cells.

Tomáš Suchý, Monika Šupová, **Pavla Sauerová**, Martina Verdánová, Zbyněk Sucharda, Šárka Rýglová, Margit Žaloudková, Radek Sedláček and Marie Hubálek Kalbáčová (2015): The effects of different crosslinking conditions on collagen-based nanocomposite scaffolds - an in vitro evaluation using mesenchymal stem cells. Biomed Mater. 10, 065008. IF2014 = 3.697

The collagen-based scaffolds have potential to imitate an extracellular bone matrix and support hMSCs (human mesenchymal stem cell) adhesion, proliferation and osteogenic differentiation. However, the fast biodegradation rate and the low mechanical strength of the untreated collagen very often complicate *in vitro* and *in vivo* applications (Rault et al., 1996; Rýglová et al., 2017). The stability of collagen scaffolds can be enhanced by crosslinking. The purpose of publication C was to determine effective crosslinking conditions for scaffold based on a collagen matrix reinforced with poly(DL-lactide) sub-micron fibres and supplemented with bioapatite nano-particles and HyA. Thus, the impact of various crosslinking agents (genipin, EDC/NHS/EtOH or EDC/NHS/PBS (Chang et al., 2007; Chen et al., 2005; Ma et al., 2004b)) on scaffold (of one type) were tested *in vitro* in this study.

Based on evaluation of mechanical properties and structural stability of the tested scaffolds (provided by colleagues), the most effective crosslinking agents were found to be EDC/NHS/PBS and genipin. In addition, genipin scaffolds maintained constant mechanical properties without any change in contrast to the EDC/NHS/EtOH scaffolds which changed negatively following a longer incubation time. The EDC/NHS/EtOH scaffolds revealed the highest degradation rate together with a high swelling ratio after 1 to 8 days of incubation in the α-MEM medium. Moreover, a further advantage of the genipin crosslinked scaffold lies in pore size stability following crosslinking (pore size: approximately 300μm). Conversely, a reduction in pore size was observed with reference to the scaffolds crosslinked with other agents (pore size: 200 - 250μm).

Biological evaluation assessed scaffolds with respect to their suitability for cell application. With the respect to trend of cell therapy, hMSCs (isolated from a bone marrow) for all *in vitro* analyses were used.

Initially, hMSCs were cultivated in the infusions of the tested scaffolds (cross-linked with EDC/NHS/EtOH, genipin and EDC/NHS/PBS) in order to check the release of cytotoxic

agents from the individual scaffolds into the cultivation medium. Cell metabolic activity was determined following 2 and 7 days of infusion treatment. After 2 days of cultivation (Fig. 6A in publication C), the cell metabolic activity in all the infusions was found to be mutually comparable. After 7 days (Fig. 6B in publication C), the situation had changed markedly except for those cells in the genipin crosslinked scaffold infusion which maintained a similar level of metabolic activity as after 2 days of cultivation. The metabolic activity of the cells in the infusions from other scaffolds decreased but not under the cytotoxic leve. Thus, all the infusions were non-cytotoxic after short and long incubation.

In next step, cells were seeded directly on the infused scaffolds and cultivated for 2 and 7 days whereupon the number of adhered cells on the scaffolds was determined based on the measured cell metabolic activity. The amounts of cells adhered to the scaffolds were comparable for all three scaffolds at both time points (Fig. 7 in publication C). The cell amounts obtained reached approximately 50% of those of the control cells.

Finally, the cells which adhered to the scaffolds were visualised using wide-field microscopy (Fig. 8 of publication C) in order to determine cell morphology and their distribution on the samples. The ability of cells to adhere was observed with regard to all the tested samples. After 2 days a visible morphology difference was evident between the donor cells (not shown). However, the cells of all three donors used evinced the best appearance and symmetrical distribution on the genipin cross-linked scaffold. The cells on the EDC/NHS/EtOH and EDC/NHS/PBS cross-linked scaffolds were smaller and had a lower extend of spreading. Interestingly, after 7 days, the cells on all the scaffolds were similarly organised and displayed a comparable appearance – the differences in cell morphology and distribution were markedly less pronounced.

The cells adhered onto the scaffolds were also visualised in 3D using confocal microscopy (Fig. 9 of publication C). Despite „depth“ limits of scanning of this method, we determined cell ability to penetrate through the scaffold. The majority of adhered cells (cells of one donor were analysed) were observed on the surface of the scaffolds and up to a depth of 200 $\mu$m (i.e. 10–15% of scaffold depth).

In summary, the genipin cross-linked scaffold provided the best conditions for cultivation of hMSC for 2 and 7 days. In addition, it also maintained constant mechanical properties in contrast to the rest of cross-linked scaffolds. Thus, genipin crosslinked scaffolds were recommended for further advanced *in vitro* and subsequent *in vivo* analysis with emphasis to dynamic cultivation.

### 4.3.2 Manuscript in preparation D: Comparison of Seeding Efficiency on the Biodegradable Scaffolds of Different Composition and Cultivation Conditions

**Pavla Sauerová**, Tomáš Suchý, Monika Šupová, Zbyněk Sucharda, Šárka Rýglová, Margit Žaloudková, Tereza Kubíková, Zbyněk Tonar, Martin Bartoš, Jana Juhásová, Štefan Juhás, Jiří Klíma and Marie Hubálek Kalbáčová (2017). Manuscript in preparation.

Two types of collagen-based scaffolds differing in composition were developed for bone surgery application with the aim of bone ECM imitation and suitability for MSC therapy. Unlike previous scaffolds in publication B, these developed scaffolds were crosslinkend only by EDC/NHS in EtOH/$H_2O$ solution ($H_2O$ as a chemical reaction catalyst) which was selected as the most appropriate crosslinking agent with the respect to scaffold composition. The both scaffolds consisted of poly(DL-lactide) electrospun nano/sub-micronfibres (PDLLA), a natural collagen matrix supplemented with HyA and natural calcium phosphate nano-particles (bCaP). Both scaffolds (S4 and S6) differed in amounts of individual components (see Fig. D1).

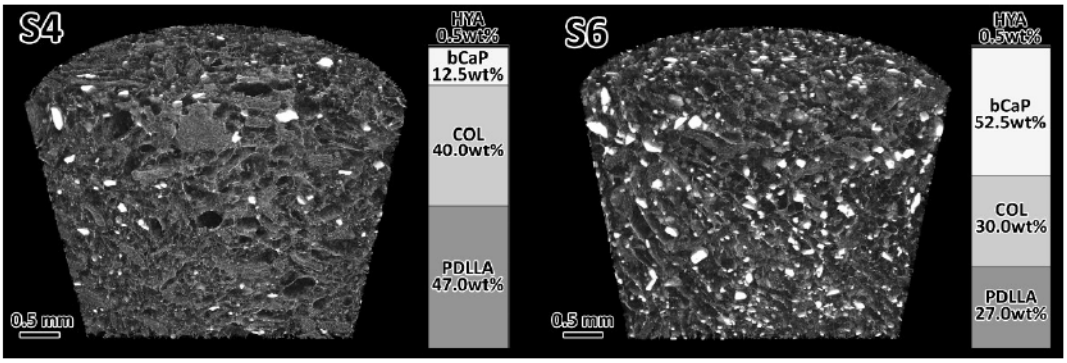


**Figure D1: MicroCT images and composition scaffolds S4 and S6.** Collagen matrix (COL),poly DL-lactide sub-micron fibres (PDLLA), bioapatite (bCaP) and sodium hyaluronate (HyA) powder. Picture provided by Tomáš Suchý and Martin Bartoš.

Based on mechanical evaluation including structural stability of the tested scaffolds, our colleagues determined both scaffolds as: low pore-size (< 200 μm) with high degree of open porosity (cca 85% of space inside the scaffold had connection with the scaffold surface). Unlike S4, swelling ratio of S6 remained almost unchanged over 1 day incubation in cultivation medium.

Biological evaluation assessed scaffolds with respect to their suitability for cell application in bone surgery and to subsequent *in vivo* analysis in porcine organism. Thus, the main focus of evalution was seeding efficiency of porcine MSCs (pMSCs) with respect to static

cultivation conditions (i.e. standardly used way of cultivation) and dynamic cultivation conditions (i.e. cultivation under constant flow of medium). The top of the scaffold (diameter of 5.5 mm and a thickness of 5 mm) was seeded by drop of pMSC suspension and then cultivated for the first 6 h under dynamic cultivation conditions in constant flow rate (30 ul/min) in multichamber bioreactor (see Fig.D2; perfusion platform developed for three-dimensional scaffolds which was adapted from a previous study (Piola et al., 2013)). After 6 hours, all of the scaffolds were cultivated under static cultivation conditions for the rest of incubation time (2 days, 7 days or 14 days).

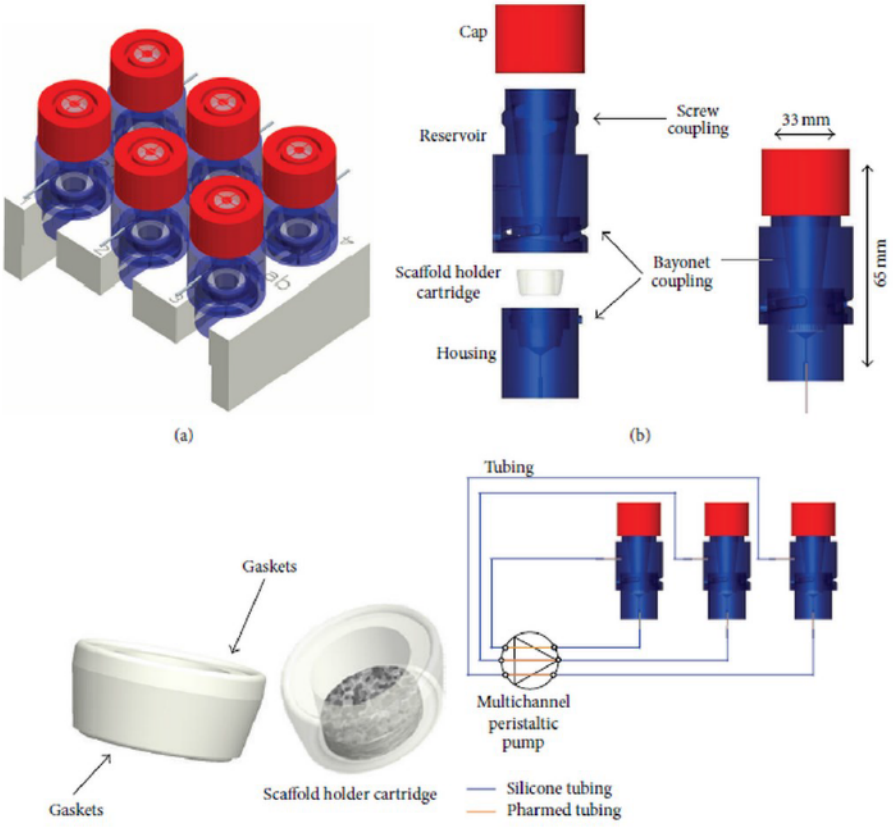


**Figure D2: Model of the six-chamber bioreactor** (a). Model of the single culture chamber: exploded and assembled view; the culture chamber is composed by a reservoir, a disposable screwcap, a housing, and a scaffold holder cartridge (b). Detail of a scaffold holder cartridge; the arrows indicate the upper and lower gaskets; the cartridge allows hosting matrices with different sizes and shapes (c). Sketch of the fluidic circuit with parallel culture chambers and perfusion circuits, actuated by a multichannel peristaltic pump (three out of six parallel circuits /chambers are shown) (d). Adopted from (Piola et al., 2013).

The cells adhered to the scaffolds were visualised 3D by confocal microscopy (Fig. D3). Despite „depth“ limits of scanning of this method, we determined cell ability to penetrate through the scaffold up to a maximall depth of 300 $\mu$m which was observed in samples after

dynamic cultivation either in S4 and S6 after 2 days or in S6 after 7 days. Our results showed differences between both scaffods and simultaneously between efficiency of both cultivation conditions as well. In contrast to S4 scaffold, we observed less cells on S6 surface but more cells in its volume after 2 days. After 7 days of cultivation, we determined general loss of cells in both scaffold in comparison to situation after 2 days. Comparison of both cutivation conditions determined either relatively narrow layer of cells on surface of scaffolds cultivated under static conditions or wider layer on surface of scaffolds cultivated under dynamic conditions. After 7 days, the level of penetration of cells had changed except for cells on S6 cultivated under dynamic conditions which preserved same level of penetration as after 2 days (300 μm). While penetration of the cells cultivated on S4 and S6 under static cultivation conditions was slightly elevated (growth to 150 →200 μm/S4 and 200 →250 μm/S6), penetration of cells on S4 under dynamic cultivation conditions was slightly reduced (to 300→250 μm). In general, penetration of cells under static cultivation didn´t overcome penetration reached under dynamic cultivation after both cultivation times.

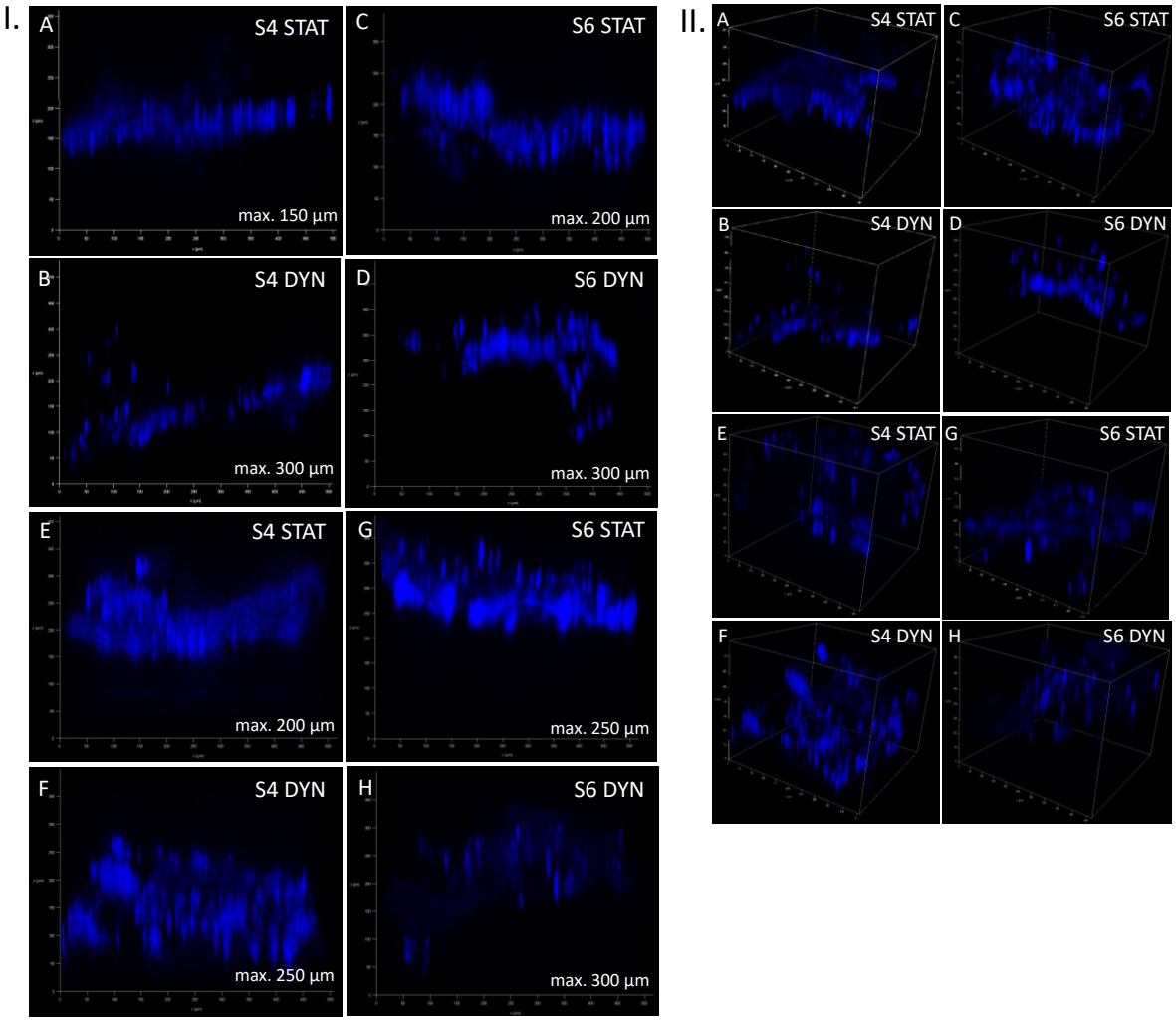


**Figure D3: 3D reconstruction of confocal microscope images of porcine MSC cultivated on scaffold S4 and S6 under static (STAT) or dynamic (DYN) cultivation conditions for 2 days (A-D) or 7days (E-F).** Fluorescence images in lateral (I.) projection (expression of cell penetration rate) and superior (II.) projection. The cell nuclei are stained in blue. Field size of scanning ~ 0,25 $mm^2$.

In the next step, we compared scaffods and both cultivation conditions at the level of cell amount determination using DNA content analysis. In general, insignificantly higher DNA content was detected on S4 scaffold in comparison to S6 (Fig. D4 A). After 2 days, S4 under static cultivation provided higher DNA content in comparison to its dynamic cultivation state. Opposite situation was observed in S6 scaffolds. After 7 days, we detected dramatic decreas of DNA content on both scaffolds (similarly to microscopy observation). Interestingly, more marked decrease was detected in both scaffolds cultivated under static cultivation conditions. Moreover, while S6 preserved the trend similar to that observed in 2 days cultivation (higher content of DNA was measured under dynamic cultivation in comparison to static cultivation), S4 performed opposite trend contrary to that of 2 days cultivation. Futhermore, we were

interested in seeding efficiency and scaffold colonization with respect to different cell types. Thus, we seeded osteoblasts (SAOS-2) on the tested scaffolds S4 and S6 (contrary to pMSC, osteoblasts' results reflected DNA content of seeded cells on scaffold without respect to cultivation conditions, time of cultivation was only 2-days (Fig. D4 B.)). Interestingly, results were in agreement with results obtained with pMSC, however the differences were significant. Significantly more cells were detected on S4 scaffold in comparison to S6. Surprisingly, 5 times higher quantity of DNA content was detected in scaffolds colonized by osteoblasts in comparison to scaffolds colonized by pMSC.

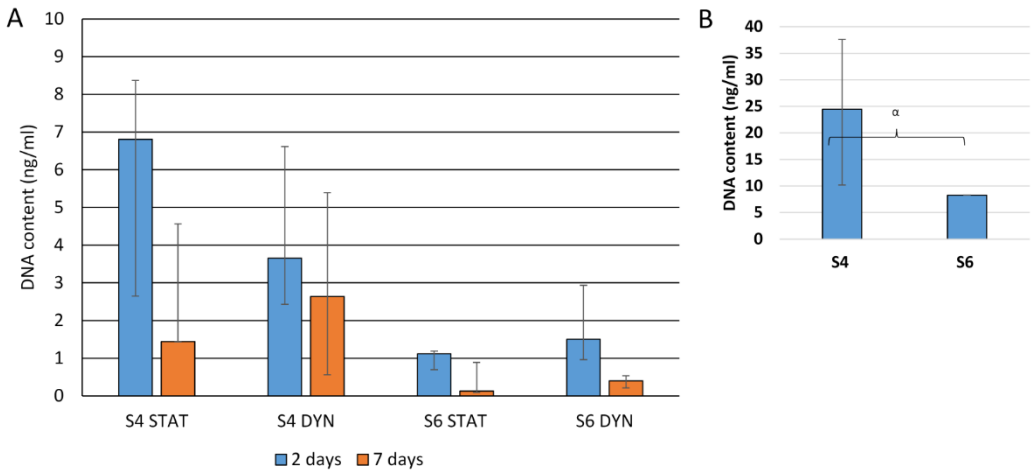


**Figure D4-A: DNA content after static (STAT) or dynamic (DYN) cultivation of porcine MSC on S4 and S6 scaffolds after 2 days and 7 days.** $ - significance at alpha level 0.05 compared to control (on polystyren seeded cells); * - significance at alpha level 0.05 same scaffolds under the different cultivation; # - significance at alpha level 0.05 between different scaffolds under the same cultivation; π - significance at alpha level 0.05 between different scaffolds under the different cultivation (based on non-parametric Kruskal-Wallis ANOVA with subsequent post-hoc Multiple comparison test). **B: DNA content after cultivation of osteoblasts on S4 and S6 scaffolds (**results reflects DNA content of seeded cells on scaffold without respect to cultivation conditions after 2 days). α - significance at alpha level 0.05 between different scaffolds (based on non-parametric Mann-Whithney U test).

With respect to intended application of scaffold in bone srugery, we interested in differences in expression of selected markers of differentiation after 2 days and 14 days of cultivation (Fig.D5). We selected genes related to signaling pathway (ERK1/2 and p38 kinases), the main gene related to adipo-diferentiation (Peroxisome proliferator-activated receptor gamma, PPARγ) and the genes related to osteodiferentiation (Collagen I, bone homeostasis regulators RUNX2 and Osterix (Sp7)) as markers of differentiation. The primary goal was the determination of any differentiation evidence with respect to scaffold composition, thus these results didn´t reflect different cultivation conditions. Two independent experiments were

performed in tetraplicates, expression level of tested differentiation markers were normalized to expression of GAPDH house-keeping gen. In general, no relevant expression profiles (up-regulation or down- regulation) of cells cultivated on scafolds were detected by qRT-PCR. After 2 days, cells on S4 were insignificantly up-regulated in expression of most of selected genes in comparison to S6. Interestingly, after 14 days, cells on S6 were insignificantly up-regulated in expression of most of selected genes in comparison to S4. With the respect to osteodifferentiation markers, S4 and S6 were comparable in cell expression after 14 days, however expression of genes of signaling patway predominated in S6.

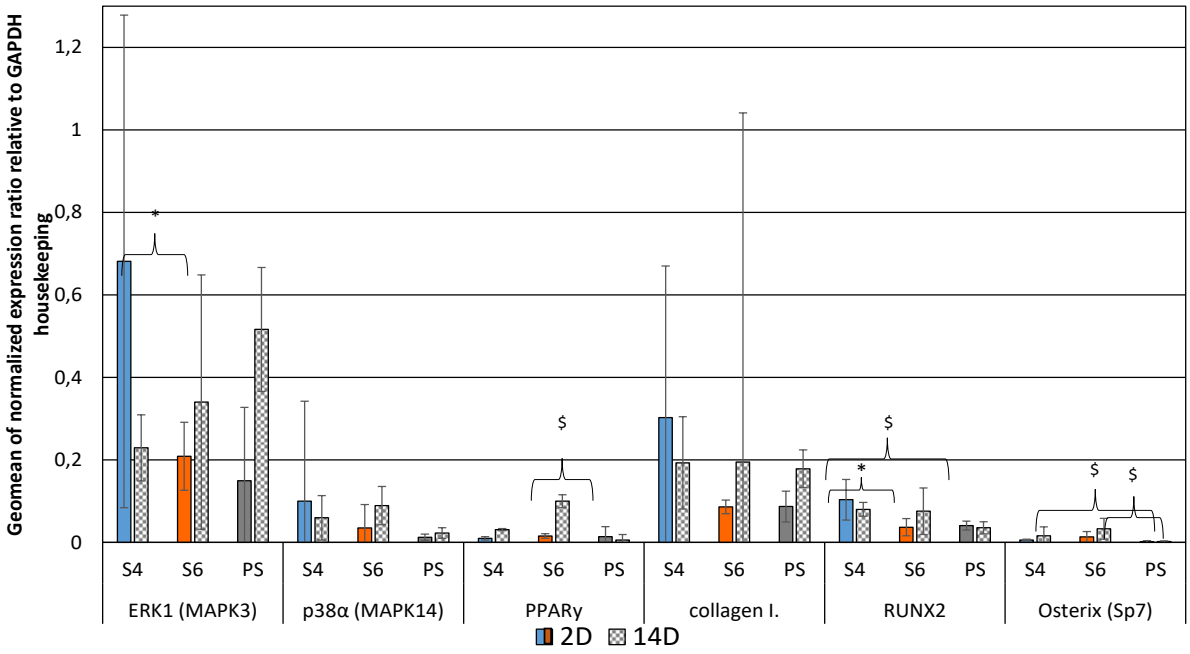


**Figure D5: Gene expression – change in time - relative to GAPDH housekeepig 2D or 14D after cultivation of porcine MSC on S4 and S6 scaffolds or on poylstyren surface (PS control).** $ - significance at alpha level 0.05 comparison to only cells (on polystyren seeded cells) under the same cultivation time; * - significance at alpha level 0.05 between different scaffolds under same cultivation time; # - significance at alpha level 0.05 between same scaffolds under different cultivation time (based on non-parametric Kruskal-Wallis ANOVA with subsequent post-hoc Multiple comparison test).

Finally, we were interested in scaffold matrix remodelation by seeded cells after 2 days of cultivation. Thus, we determined the activity of two matrix metalloproteinases (collagenases MMP2 and pro MMP9/MMP9) by zymography method (Fig. D6). In general, the higher activity of MMPs was observed in case of S4 in contrast to S6. In case of S4 only MMP2 activity was detected and it was higher under static cultivation conditions (in comparison to its dynamic cultivation conditions). In case of S6, only proMMP9/MMP9 activity under static cultivation conditions and activity of both MMPs under dynamic cultivated conditions was observed.

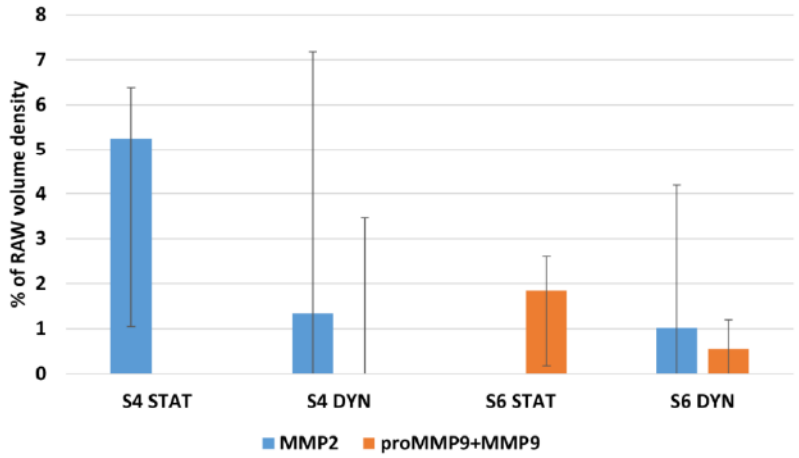


**Figure D6: Matrix proteinase activity expressed by zymography (in % of raw volume density related to controls scaffolds without cells) after static (STAT) or dynamic (DYN) cultivation of porcine MSC on S4 and S6 scaffolds after 2 days.** $ - significance at alpha level 0.05 compared to control (on polystyren seeded cells); * - significance at alpha level 0.05 same scaffolds under the different cultivation; # - significance at alpha level 0.05 between different scaffolds under the same cultivation; π - significance at alpha level 0.05 between different scaffolds under the different cultivation (based on non-parametric Kruskal-Wallis ANOVA with subsequent post-hoc Multiple comparison test).

With the respect to cell amount determination, our results indicated S4 scaffold as more suitable. However, with the respect to cell penetration, osteodifferentiation and observed adaptability within time, our results indicated S6 scaffold as more suitable for cell application in bone surgery, thus it seems to be also more perspective for its native colonization (invasion) by cells after implantation. In addtition, based on *in vitro* results, we confirmed the dynamic cultivation as more efficient for cell cultivation and penetration into scaffolds.

## 4.4 PART III: Collagen/Hydroxyapatite Nano/Micro-Structured Resorbable Layers Impregnated by Antibiotics (publications E-F)

The part III of this thesis is focused on *in vitro* evaluation of collagen/hydroxyapatite nano/micro structured resorbable layers impregnated by antibiotics. Composition and structure of layers were designed with respect to controlled elution of antibiotics and osteointegration enhancement. Thus, layers have potential for bone surgery application as a bone/implant bioactive interface to be used in the case of treatment of prosthetic joint infection or for infection prevention in joint replacement. Antibiotic susceptibility and antibiotic release from layers were determined before biological evalution (antibacterial activity with respect to four type of isolates: *Staphylococcus aureus* isolate, *Staphylococcus epidermidis* isolate (gentamicin-resistant), *Enterococcus faecalis* isolates and *Enterococcus faecalis* clinical isolates were determined).

The *in vitro* biological evaluation was conducted using osteoblasts (SAOS-2) in direct contact with the layers (for 2 or 8 days) or in their 1-day infusions. While publication E is focused on layers impregnated by vancomycin, publication F compares layers impregnated by vancomycin, gentamicin or their mixture. Except of antibiotic effect on human cells, both publications study changes in cell-layer interactions induced by different hydroxyapatite content in layers as well.

This research is based on biological and material fields' cooperation. Biological part was performed by the author of this thesis and it represents one of the thesis aims. Material research was performed by colleagues from Department of Composites and Carbon Materials of Institute of Rock Structure and Mechanics, Academy of Sciences of the Czech Republic.

### 4.4.1 Publication E: The Release Kinetics, Antimicrobial Activity and Cytocompatibility of Differently Prepared Collagen/Hydroxyapatite/Vancomycin Layers: Microstructure vs. Nanostructure.

Tomáš Suchý, Monika Šupová, Eva Klapková; Václava Adámková, Jan Závora, Margit Žaloudková, Šárka Rýglová, Rastislav Ballay, František Denk, Marek Pokorný, **Pavla Sauerová**, Marie Hubálek Kalbáčová, Lukáš Horný, Jan Veselý, Tereza Voňavková, Richard Průša (2017): The release kinetics, antimicrobial activity and cytocompatibility of differently prepared collagen/hydroxyapatite/vancomycin layers: microstructure vs. nanostructure. European Journal of Pharmaceutical Sciences 100, 219-229. IF = 3.77

Publication E is focused on *in vitro* evaluation of collagen/hydroxyapatite nano/micro structured resorbable layers impregnated by vancomycin (antibiotic). Layers have the potential for bone surgery application where antibiotics are key factors in the treatment of implant-associated bone infections and osteomyelitis. Just the local use of them is predicted to achieve high and long-term concentrations of the antimicrobial agents in the wound for eradication of the bacteria or at least for reduction of the bacterial load combined with low systemic concentration to eliminate systemic side effects. Additionally, in general, resorbable carrier systems lead to a material-tissue interaction with subsequent degradation of the material and without the need of subsequent removal by an additional surgical procedure (Alt et al., 2015). Besides profylaxis of osteomyelitis or its treatment, layers should also play a role as a bone/implant bioactive interface, thus composition and structure of layers should mimic bone matrix (collagen I and HA).

Layers were prepared as follows: collagen I was dispersed with three different HA concentrations (0%; 5% and 15% wt). Three different preparation methods were applied (Fig.E1). Collagen dispersion with HA and 10 %wt of vancomycin was i) lyophylized or ii) electrospun, respectively, and crosslinked. Finally, collagen dispersion with HA was electrospun and crosslinked and impregnated with 10 % wt of vancomycin (iii). Prepared layers were tested for structural and mechanical stability, for vancomycin release and its antimicrobial susceptibility. Three different preparation methods led to differences in inner structure of layers (micro vs. nano) and different binding of the antibiotic (mixing, electropinning and impregnation). Different preparation methods were compared based on the result of comprehensive evaluation and electrospun impregnated layers showed the best assumptions for future layer function. Colleagues determined the highest rates of antimicrobial activity (highest

concentrations of vancomycin active form) with the respect to the electrospun impregnated layers. Thus the potential of sufficient antibacterial activity (with respect to all tested *Staphylococci* isolates and gentamicin-resistant isolates) was confirmed (inhibition zones surrounding the samples were comparable to those of standardly used antibiotics). Taken together, based on antimicrobial activity, layers confirmed potential for clinical practise and thus, the next essentiality was *in vitro* evaluation of cytocompatibility of layers that is the fundamnetal step for next advanced *in vivo* testing and clinical application.

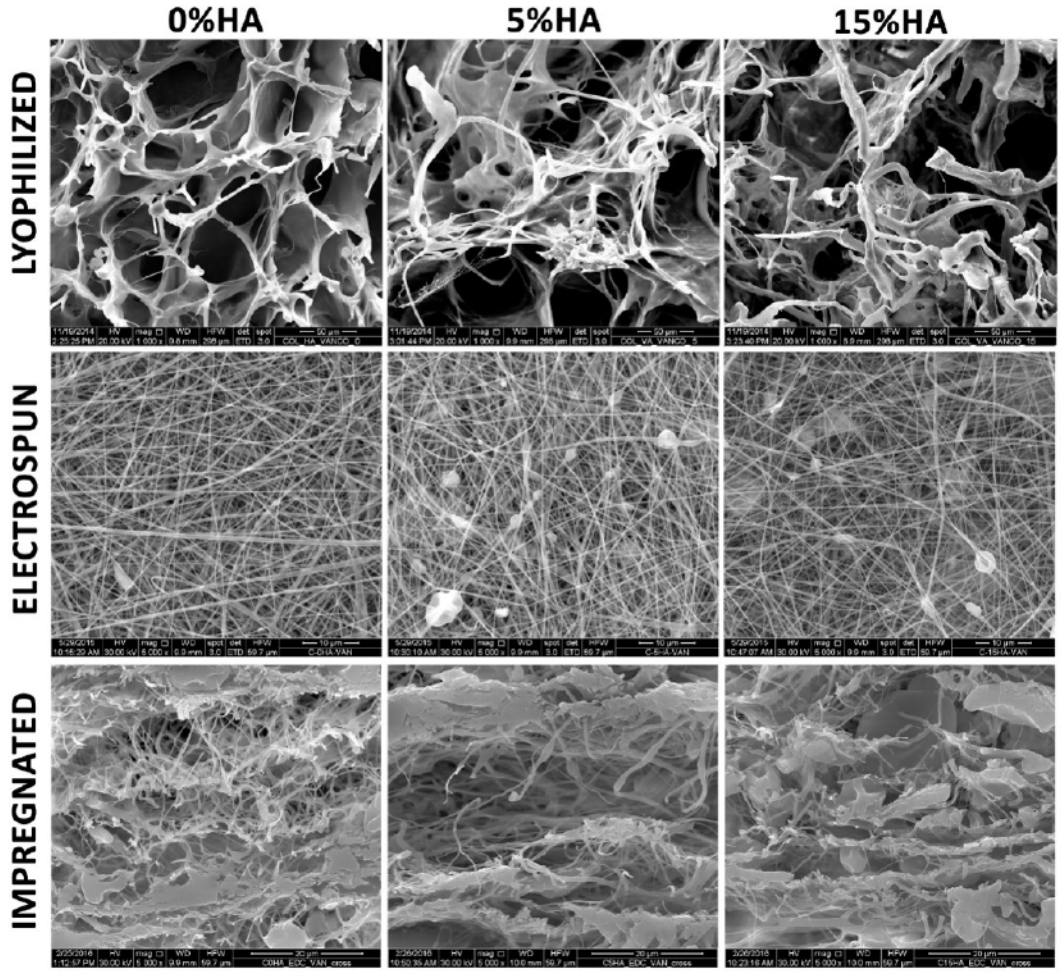


**Figure E1: Representative SEM images of lyophylized micro structured COL/HA/vancomycin layers (first row, mag.1000x), nano structured COL/HA/vancomycin electrospun layers (middle row, mag.5000x), and nano structured COL/HA/vancomycin electrospun impregnated layers (bottom, mag.5000x).** Picture provided by Tomáš Suchý.

Electrospun impregnated layers with 10% wt vancomycin (V) with three various HA contents (wt) - 0% (V0), 5 % (V5) and 15% (V15) (in publication E signed as EI0, EI5, EI15) were evaluated. Identical layers, however without vancomycin content were used as controls

(NK0, NK5 and NK15; in puclication E signed as N0 N5, N15). The aim of the *in vitro* tests was to verify whether eluted doses of vancomycin exert a negative effect on bone-like cell behaviour. In addition to the effect of vancomycin on bone cells, the influence of the composition of layers on cell behaviour was also investigated. This step was very important in the development process of layers and the results of the biological evaluation were the integral part of the the final design of implantable collagen/HA/vancomycin layers.

Initially, cytocompatibility was analysed at the level of layer infusions. All impregnated layers (V0, V5 and V15) and their appropriate controls without vancomycin (NK0, NK5 and NK15) were soaked in cultivation medium for 1 day. Obtained infusions were transferred on pre-seeded cells on polystyrene surface and then incubated together. After 1 day, cell metabolic activity was determined (Fig. 9A in publication E). As infusion results show, the metabolic activity of cells treated by the most of infusions was comparable to the polystyren control (PS). Only NK0, NK5 and V0 presented more significant decrease of metabolic activity, however values were above the limit of the cytotoxicity. Thus, with the respect to infusions, cytocompatibility of all layers tested was confirmed.

In next step, cells were seeded directly on the layers. After 2 days or 8 days of cultivation, cell growth (by metabolic activity analysis) and cell morphology (by fluorescent microscopy) were determined. After 2 days of incubation (Fig.9B in publication E), the metabolic activity of cells seeded on V0 and V5 layers was significantly inhibited in comparison to their controls (NK0 and NK5.) Suprisingly the metabolic activity of cells on the layer V15 with the highest content of HA (15 wt%) was the most elevated of all antibiotic impregnated layers. Moreover, it was comparable to its corresponding control NK15. Thus, the highest inihibiton of cells by vancomycin was found on the layer V0 without any HA. The trend of the inhibition was declining proportionaly to elevating of HA content. It demonstrated the positive effect of HA content on osteoblasts. After 8 days incubation (Fig.9C in publication E), the trend of vancomycin induced inhibition was similar to trend of 2 days cultivation; however, the inhibition was less significant in general. Surprisingly, previously observed positivity of V15 (EI15) on cell metabolism significantly excceded its corresponding control and all the tested layers. Thus, the inhibitory effect of vancomycin of this layer was markedly reduced in contrary to 2 days situation. Similarly to 2 days results, positive effect of increasing HA content on cell metabolic activity was confirmed as well.

To visualized cell morphology, staining of actin and nuclei and fluorescence microscopy was used for imaging of possible changes. As Fig.10 in publication E shows, after 2 days incubation, cells were predominantly of round shape with only poor distribution and in

reasonable amounts on the layers. Apparently lower cell amount in comparsion to corresponding controls (NK0, NK5 and NK15) was observed on all the tested layers (V0, V5 and V15). After 8 days of incubation, cell amount on all the tested layers including V0, V5 and V15 was markedly higher in comparison to 2 days situation. Cells were markedly spread and in higher amount and also distribution of cells was more homogenous. However, similarly to metabolic activity results, higher amounts of cells on NK0 and NK5 control layers were observed in contrast to corresponding vancomycin layers (V0 and V5). Thus, it confirmed its inhibitory effect on cells (performed by metabolic activity measurement). Similarly to metabolic activity results, the number of cells cultivated on V15 with the highest HA content was comparable with the cell amount observed on its corresponding control (NK15). Thus it confirmed metabolic activity results and also positive role of HA content on cells.

All results reflected that the behaviour of cells on layers is affected by two factors together – by vancomycin presence together with layer composition (HA content). We confirmed that bone-producing cells survive on these layers and that their metabolic activity increases side by sise with the degree of mineralisation. This suggests that COL/HA/vancomycin layers prepared by means of electrospinning with subsequent impregnation with vancomycin cannot be considered to be cytotoxic for newly-formed bone. It seems, the layers impregnated by vancomycin are suitable candidates for the preparation of bioactive and pro-osteo-integrating bone-implant interfaces. With respect to antimicrobial effects and vancomycin release, colleagues confirmed the potential of layers for local drug delivery.

### 4.4.2 Manuscript in preparation F: Evaluation of Collagen/Hydroxyapatite Layers Impregnated by Different Antibiotics – Novel Potential Local Drug Delivery for Bone Surgery

Tomáš Suchý, Monika Šupová; Eva Klapková; Václava Adámková; Jan Závora; Margit Žaloudková; Šárka Rýglová; Rastislav Ballay; František Denk; Marek Pokorný; **Pavla Sauerová**; Marie Hubálek Kalbáčová; Lukáš Horný; Jan Veselý; Tereza Voňavková; Richard Průša (2017). Manuscript in preparation.

Based on results presented in publication E, electrospun collagen/hydroxyapatite nano/micro structured resorbable layers impregnated by vancomycin (V) (used previously), gentamicin (G) and mixture of both antibiotics vancomycin and gentamicin (VG) were prepared.

Thus, *in vitro* evalution was performed by the same way as previously with the aim to extend the knowledge of the effect of gentamicin and vancomycin-gentamicin impregnated layers on cells (bacteria and human osteoblasts). Verified layers with the respect to sufficient antibiotic efficiency (determination of the highest released average concentration of specific antibiotic and analysis of antibacterial activity with respect to all the tested isolates - Staphylococci isolates and gentamicin-resistant isolates) were defined by *in vitro* evaluation. The cytocompatibility based on metabolic activity analysis including changes in cell morphology with the respect to layer composition was determined. Thus, we tested electrospun impregnated layers with three various contents of HA (0, 5 and 15% wt) with 1) 10% wt of vancomycin (V0, V5, V15); 2) 10% wt of gentamicin (G0, G5, G15); 3) 10% wt of vancomycin with gentamicin (1/1 w/w) (VG0, VG5, VG15); 4) antibiotic absence as corresponding controls (NK0, NK5, NK15).

Firstly, cytotoxicity was analysed by treatment of pre-seeded cells with 1-day infusions of all the tested layers. As figure F1 shows, the metabolic activity of cells incubated in all infusions was comparable to cells only cultivated on the polystyren control (PS). The metabolic activity of cells incubated in the most of infusions of antibiotic impregnated layers was also comparable to their appropriate controls without antibiotic impregnation (NK0, NK5 or NK15). Only G5 represented more significant decrease of metabolic activity, however this decrease didn´t reached the level of cytotoxicity. It means, the cytocompatibility of all the tested infusions was confirmed.

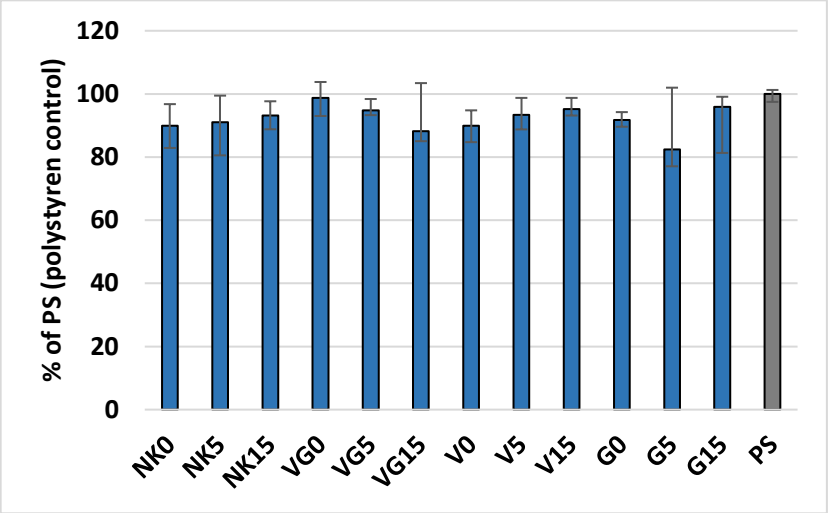


**Figure F1: Metabolic activity of osteoblasts (SAOS-2) incubated in 1-day infusions of different layers expressed as a percentage of metabolic activity of cells cultivated on polystyren surface without any infusions (PS).**

Amount of cells adhered on the layers were derived from the metabolic activity determination, thus the both the metabolic activity of cells (Fig.F2A) and the cell amount (Fig.F2B) provided comparable trend. The cell amount on layers after 2 days showed cca 1/3 or less of total amount of cell amount on PS. Simultaneously, values of metabolic activity of all the controls (NK0, NK5 and NK15) were the highest within every „group“ of layers with the same HA content (e.g. NK0 x VG0, V0 and G0, respectively). That means that the observed decrease of cell amount or metabolic activity resulted from the combination of cytotoxicity induced by antibiotics and by generally reduced adhesion of cells to the layers. Furthermore, increased HA content proportionaly elevated cell number in all the tested layers (with exception of V15 which was comparable its control layer NK15). After 8 days of cultivation, the trend similar to 2-days situation was detected; however, the values were generally elevated. Surprisingly, V15 significantly exceeded cell amount and metabolic activity of its corresponding control NK15. It also exceeded the rest of the tested layers in both parameters. In general, 8-days cultivation showed total increase in cell amount in all the tested layers. In addition, all layers impregnated with gentamicin induced the dramatic cytotoxicity to cells. The highest cell metabolic activity or cell number (with the respect to both cultivation times) were detected on VG5 and V15 layer. Furthermore, contrary to VG5, V15 provided more efficient cell recovery with respect to comparison results of both cultivation times.

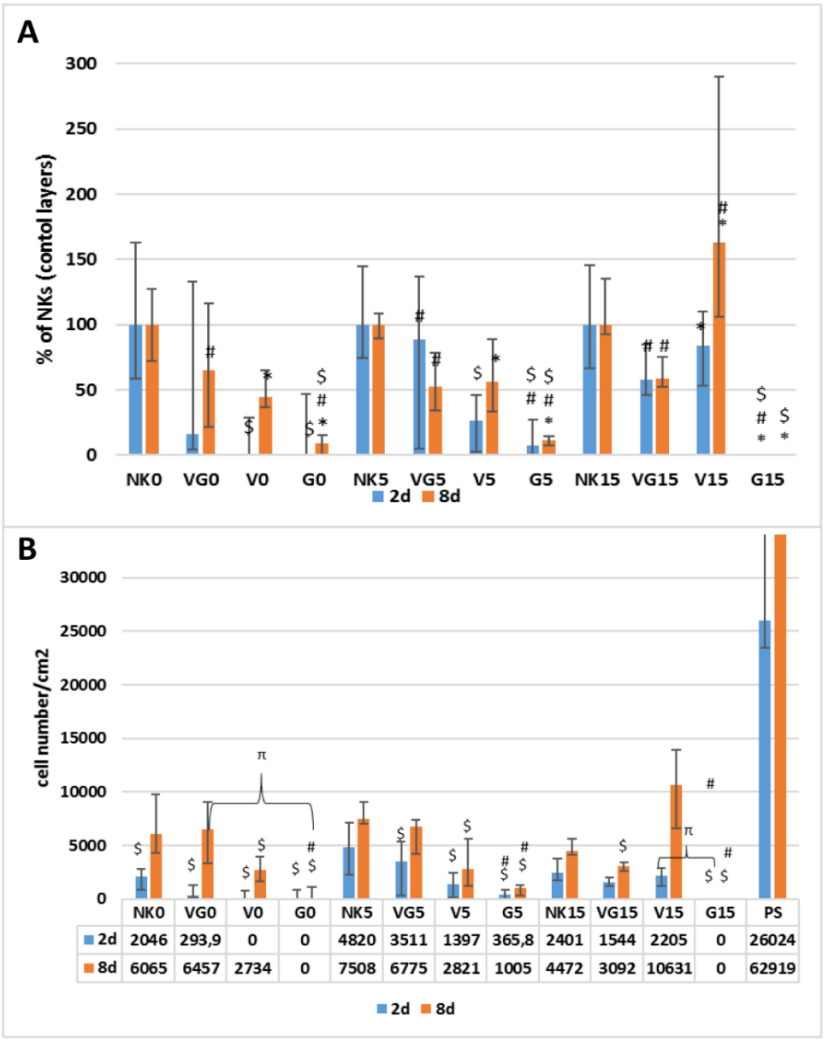


**Figure F2- A: Metabolic activity of osteoblasts cultivated on tested layers for 2 days and 8 days (B).** $ significance on the level of 0.05 to NK control and layers with the same content % HA; # significance on the level of 0.05 between layer with mixture of antibiotics (VG) and layer with one type of antibiotic (V or G); * significance on the level of 0.05 between layers with different antibiotics ( V x G)(Kruskal-Wallis with post-hoc multiple comparison test).
**B: Number of osteoblasts (per cm2) cultivated on tested layers for 2 days and 8 days (A).** $ significance on the level of 0.05 between PS control and any type of layer; # significance on the level of 0.05 between every type of NK (control layer) and its diffrerent antibiotic alternatives with same % of HA content (e.g. NK0 x VG0, V0 and G0); π significance on the level of 0.05 between diffrerent antibiotic alternatives with same % of HA content in every NK group (control layer) (e.g. NK0 x VG0, V0 and G0); * significance on the level of 0.05 between same antibiotics layers with only different % of HA content (Kruskal-Wallis with post-hoc multiple comparison test).

Similarly to 2-days results, the positive effect of HA content on cell survival was evident after 8 days. Interestingly, values measured after 2 days and 8 days showed limits of HA positive effect in relation to the antibiotic type. While layers with vancomycin seemed to be cytotoxic the least if it was combined with layers containing 15% of HA, gentamicin and vancomycin-gentamicin were cytotoxic the least in layers containing only 5% of HA.

Finally, staining of the actin cytoskeleton and nuclei was used to determine the cell morphology and quality of cells seeded on the layers. Fluorescence microscopy was performed to support the results of cell number and metabolic activity. As Fig.F3 shows, after 2-days incubation, cells were predominantly of round shape with only poor distribution and in reasonable amounts on the layers with exception of gentamicin impregnated layers that showed signicifant signs of cytotoxicity. Apparently, higher cell amount was observed on control layers in comparison to antibiotic-impregnated layers. After longer incubation (8 days), all observed changes in morphology and cell amount were more obvious. With exception of all gentamicin layers (G0, G5 and G15), higher cell amount and more cells with more spread morphology were observed on all the tested layers contrary to 2-days observation. Similarly to metabolic activity and cell amount determination, the highest cell amount with the best cell morphology was observed by microscopy on V15 and VG5 layers that were better or comparable to all control layers (NK0, NK5 and NK15). In agreement with metabolic activity and cell amount observations, the positive effect of HA content on cells was evident with mentioned limits (vancomicin was the least cytotoxic in layers with 15%wt of HA (V15), while layers with gentamicin and vancomycine-gentamicin were the least toxic in layers with 5% HA content (VG5 and G5)).

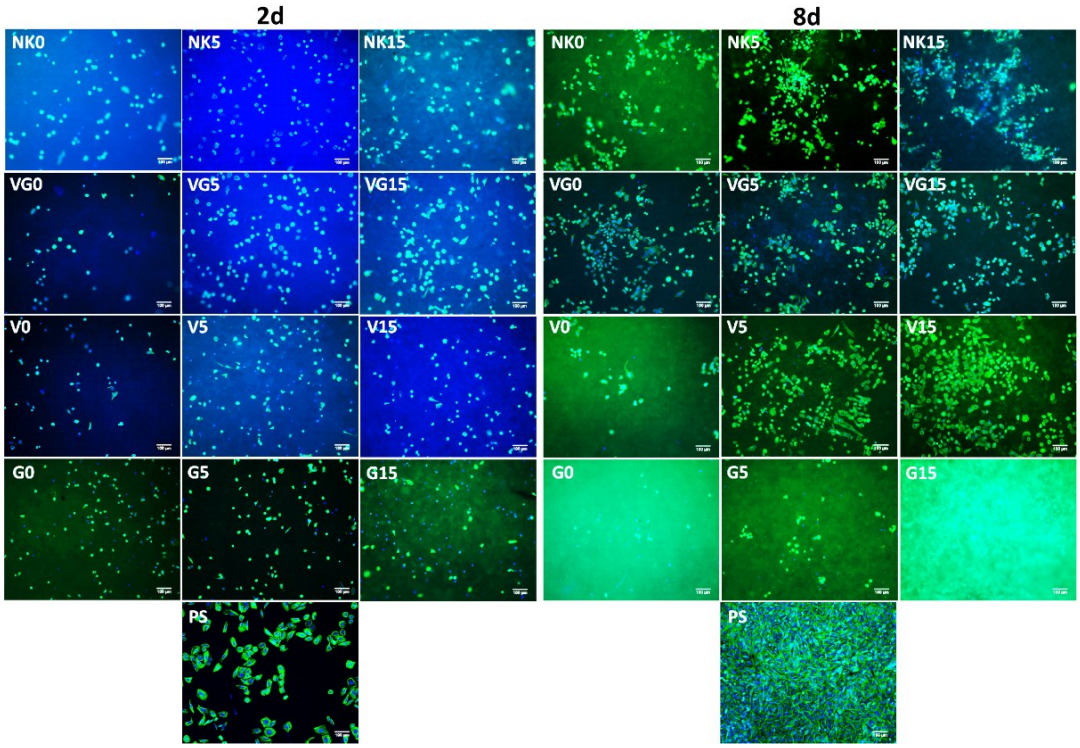


**Figure F3: Fluorescence images of osteoblasts cultivated for 2 and 8 days on tested layers.** Actin filaments representing cell morphology are stained in green, the cell nuclei in blue.

## 4.5 PART IV: Initial Cell Adhesion of Three Cell Types in the Presence and Absence of Serum Proteins (publication G)

Martina Verdánová, **Pavla Sauerová**, Ute Hempel, Marie Hubálek Kalbáčová (2017): Initial cell adhesion of three cell types in the presence and absence of serum proteins. Histochemistry and Cell biology 147 (5). Published online. IF = 2.780

Publication G is focused on early phase of adhesion of three selected cell types: osteoblastic cell line (SAOS-2), primary human fibroblasts and human mesenchymal stem cells (hMSCs). Publication compares differences in adhesion under standard cultivation conditions (FBS presence in medium) and non-standard cultivation conditions (FBS absence in medium). It was observed that these tested conditions induce significantly different reactions of cell to substrate. Changes were detected on the morphological level (cell shape and area), proliferation level (cell number) and on the level of expression and localization of various proteins participating either directly in cell adhesion (CD44, vinculin, talin, actin) or indirectly as messengers of signalisation of cell adhesion (pFAK, Rho-GTPases and pERK1/2). It was demonstrated that cells reacted differently to the presence and absence of FBS with respect to cell shape, area and number. However, the expression and localization of the various proteins involved in cell adhesion and signaling were, generally, similar in all the tested cell types but varied with respect to the presence or absence of FBS.

Cell morphology differed with respect to cultivation conditions (FBS presence or absence) (Fig.1 in publication G). Osteoblasts and hMSCs showed round shape in FBS presence and ragged shape in FBS absence. However, fibroblasts reacted inversely resulting in elongated and ragged shape in FBS presence. While cell area (Fig.2a in publication G) of osteoblasts was smaller in FBS presence contrary to FBS absence, fibroblasts reacted inversely and hMSCs show rather similar parameters under both conditions. Cell number (Fig.2b in publication G) of osteoblasts was lower in FBS presence contrary to FBS absence and fibroblasts and hMSCs reacted inversely again.

We were also interested in adhesion quality and mechanism under these two conditions. All of three cell types developed classical FAs (focal adehsions) with expression of vinculin, talin and activated pFAK in FBS presence (also participation of CD44 in classical focal adhesions was confirmed). In contrast, no classical focal adhesions were observed in FBS absence in all the tested cell types (Fig.3a-b in publication G). We also demonstrated different localisation of Rho and pERK1/2 proteins in fibroblasts in comparison to osteoblasts and hMCSs. Moreover, the observed localization was also affected by FBS presence or absence

(Fig.3c and Fig.4 in publication G). Significantly lower level of activated kinases pFAK and pERK1/2 in FBS absence indicated the development of some compensation signalling pathway in cell adhesion process. Taken together, it was confirmed that in contrast to cell number or shape, the process of FAs formation is not cell-type specific but it is mainly influenced by FBS presence/absence.

Based on our observation that classical focal adhesions are formed only in FBS presence (15% FBS content), we were interested in relation among various FBS contents with the respect to cell adhesion. However, no significant differences in cell adhesion were observed in the presence of 1%, 5% or 15% FBS in the cultivation medium (Fig.5 in publication G).

Finally, we were interested in the response of osteoblasts cultivated on the surface pre-treated with FN and VN in comparison to the surface pre-treated with FBS presence or the surface without any proteins after 2 h and 20 h of cultivation (Fig. 7 in publication G). After 2 h, osteoblasts cultivated on FN, VN and FBS proteins, showed comparable morphology, while morphology of osteoblasts adhered on naked surface (without proteins) was totally different. Similar situation was observed with FAs presence, those were well developed in FN, VN and FBS presence; however, they were very poor in the protein absence (Fig.7a-d in publication G). After 20 h, clear differences were observed in cell adhesion. Especially, FAs distribution differed according to type of the proteins on the surface (Fig.7e-h in publication G) – while cells cultivated on FN were large and separated with evenly distributed FAs, cells on VN were large with peripheral distribution of FAs and cells cultivated on FBS were smaller with FAs aggregates around cells. On naked surface, only few cells survived and those developed only few FAs in clusters in their filopodia. The cultivation after 20 h, clearly reflected the impact of tested proteins on cell shape and spreading (Fig.8 a-d in publication G): while FN induced large and well spread cells with elongated shape, VN induced similar effects but without elongation of cells. In contrast, FBS induced well spread morphology; however, with smaller and round shape cells. Cells cultivated without proteins were extremely elongated with poor adhesion. These results showed important participation of fibronectin and vitronectin in adhesion process (including FAs forming) and thus the impact of protein presence on the rate of cell survival.

# 5 DISCUSSION

This thesis is based on study of various biomimetic materials from the perspective of cell interactions. While first three parts are directly connected to specific biomimetic materials with different function in organism, the last part is focused on study of general cell adhesion, which is essential prediction for any stable interactions of cell with surface.

**The part I (publication A and B) of this thesis** is connected to biomimetic material with potential of systemic delivery system. Drug delivery systems are still developed with the goal to maximize the therapeutic effect with subsequent minimizing of negative-side effects of various agents such as drugs. The mechanisms of delivery systems often come from naturally occurring processes or compounds in organism (Torchilin, 2001). Various drug delivery systems developed in past reflected advantages and high potential of such entities as micelles, polymers, nanoparticles or nanotubes for delivery system (Cheung et al., 2012; Prestwich, 2011; Safari and Zarnegar, 2014). Just high surface-to-volume ratio and ability to form larger units can provide for delivery system the high cargo-loading capacity with subsequent releasing (He et al., 2007; Jie et al., 2005). Based on these facts, there were prepared CTAB-HyA and Septonex-HyA complexes (Halasová et al., 2011). Besides many positive effects on cells, it was predicted that HyA can also support binding and entrance of developed complex to cell via its CD44 celullar receptor (Aruffo et al., 1990; Ponta et al., 2003).

After chemical characterisation of created CTAB-HyA and Septonex-HyA complexes, *in vitro* biological evaluation was essential for characterisation of complex behaviour in context of cells and cultivation conditions. With the respect to future medical application and its limitation (high health risks connected with FBS, dysfunction of some materials or methods in FBS presence), some experiments were performed also under non-standard conditions (FBS absence for first 4h of cultivation) for determination of usability of complexes also in FBS absence (Lesniak et al., 2010; van der Valk et al., 2010). Therefore it was the first time when these complexes were tested in context of cells, all of experiments were focused on cytotoxicity, which is typical the first indicator of their biocompatibility and applicability.

Firstly we focused on cytotoxicity of complexes after 1-day cultivation time in context of osteoblast cell line which is well established in our laboratory. Under standard cultivation conditions, CTAB-HyA and Septonex-HyA complexes were found to reduce the cytotoxicity induced by free surfactants concerning all the tested concentrations (4, 5, 8 and 10 μM CTAB combined to 0.5, 3 or 5 mg/l HyA; 3, 6, 8 μM Septonex combined to 100 mg/l HyA). Reduction of cytotoxicity was dependent on surfactant and HyA concentrations. Cytotoxicity of tested

complexes of both surfactants wasn´t decreased under cytotoxicity limit, only complexes with highest concetrations of Septonex (6 and 8 μM) overcame limit of cytotoxicity. Thus, the key finding of this publication A was confirmation of predicted HyA protectivity when present in the form of a pre-prepared surfactant-HyA complex. This protectivity phenomenon is well supported by two different studies preformed in the past. The first study confirms our finding by demonstration of the HyA protectivity against surfactants, despite the experiments were performed by separated addition of HyA and surfactants to cells (Kalbáčová et al., 2014). The second study well supports our results from the perspective of HyA coating particles and it also confirms predicted potential of HyA in a complex enter the cell via affinity to CD44 (Mizrahy et al., 2014).

Next interesting finding of the publication A was that HyA protectivity is related to its concentration. We observed better protectivity of HyA of 5 mg/l concentration in comparison to 3 mg/l concentration. This observation is more discussed below (limits of HyA protectivity observed in publication B). Simultaneously, HyA protectivity was more efficient during the temporary absence of FBS. Thus, the combination of HyA and FBS can be very efficient form of cell protection.

Moreover, publication A demonstrates that FBS plays a positive role under the stress conditions induced by the presence of surfactant. Simultaneously metabolic activity reflected that FBS absence is generally stressful for cells. These results are in agreement with those from previous studies of our laboratory or other observations (Kalbáčová et al., 2014; Verdanova et al., 2012). Despite observed decrease of metabolic activity of cells treated by complexes under FBS absence, results confirmed complex functionality also under these non-standard conditions (no cytotoxicity observed). Only highest concetrations of free surfactants (8 and 10 μM CTAB and 6 and 8 μM Septonex) markedly reduced metabolic acitivity under the cytotoxic level (75% of metabolic activity (Flahaut et al., 2006)). Complexes composed of these highest concentrations were above or around limit of cytotoxicity. However, the comparison to FBS presence state showed that this cytotoxicity wasn´t caused primarily by FBS absence but it was induced rather by general cytotoxicity of surfactant in complexes.

With respect to future application, complexes were modified on the basis of a previous studies (publication A and (Kalbáčová et al., 2014)). Concentrations were dictated by the effort to avoid the precipitation of HyA-surfactant aggregates which occurs at elevated surfactant concentrations (not published results of our colleagues), modification also considered better comparison of both tested surfactants and their complexes with HyA. Publication A (CTAB experiments) determined that HyA concentration of 5 mg/l can induce the sufficient degree of

protectivity, thus it was used again. In experiments using Septonex (publication A), HyA concentration was even higher (100 mg/l) – this indicates that the HyA concentration in complexes could be significantly higher. Thus, complexes of CTAB and Septonex with the same surfactants´ concentrations (3, 6 and 8 μM) and with two types of HyA concentration (5 mg/l and 500 mg/l) were prepared and tested in the publication B.

Newly modified complexes verified our previous results (Kalbáčová et al., 2014) as well as results obtained by others (Inácio et al., 2011a;). Because osteoblasts treated by modified complexes showed similar or better results in comparison to our previous observation, we extended our experiments to other cell types (human fibroblasts and keratinocytes) and we were able to characterized the HyA-surfactant complexes more in detail. Metabolic activity analysis together with light microscopy confirmed a clear relationship between cytotoxicity and higher surfactant concentrations and positive effect of HyA presence in complex too (similar trend was observed in all three tested cell types).

The protective effect of HyA was more apparent in presence of higher surfactant concentrations. HyA protectivity was again observed and confirmed in all tested cell types. However, thanks to two different HyA concentration used in complexes, we demonstrated suprising limit of HyA protectivity. Protection was defined only with a lower HyA concentration (5 mg/l), whereas a higher HyA concentration (500 mg/l) caused either a markedly lower degree of protection or had no protective effect so far when compared to treatment with free surfactants. The existence of limit of HyA protective phenomenon is supported only by our first results, where 5 mg/l also shown the best protection. Interestingly, this result can explain firstly observed relatively low cell metabolic activities (on the level of 75% cytotoxicity limit) of osteoblasts in the presence of Septonex complexes with 100 mg/l HyA concetration. It indicates that not only 500 mg/l but also 100 mg/l HyA concentration can lack (at least in case of Septonex) protective effects. Our results suggest that excessive concentrations of HyA in the complex led to a loss of HyA protection ability. Moreover, our observation provides evidence that a reduction in HyA protection is directly connected to surfactant presence and its concentration, because the treatment of cells with both HyA concentrations (5 and 500 mg/l) in free form had comparable (neutral or positive) effect on cell viability. This finding is supported by Mizrahy, who demonstrated that the quality of HyA and its ability to interact with cells may be significantly altered if it is not free and interacts with other components (e.g. particles coated by HyA). Moreover, the degree of binding capacity of HyA molecule can be also altered by such molecular features as molecular weight. It seems that the presence of an attached hydrophobic tail or even micellar structures undoubtedly

cotribute to conformation changes (Mizrahy et al., 2011b). In addition, at higher concentrations, the polyelectrolyte binds more surfactant molecules than at lower concentrations (with the same surfactant concentration (Holmberg et al., 2002)). The resulting conformation of HyA in the complexes formed with higher concentrations thereof may hinder its cell protective effect.

Next important finding of our research demonstrated that cell reactions to free surfactants or complexes with HyA are also directed by a combination of cell origin and thus cell sensitivity to the structure of the surfactant and complexes. The dependence of toxicity only on the structure of the surfactant and its subsequent impact on different cell types has already been well described in the past by other authors (Inácio et al., 2011b) (Cornelis et al., 1992) (Lee et al., 2000) (Bigliardi et al., 1994). We observed higher sensitivity of keratinocytes to CTAB. However, osteoblasts and fibroblasts were more sensitive to Septonex. In addition, while keratinocyte metabolism decreased rapidly cytotoxic level as early as in the presence of the lowest (3 μM) CTAB concentration, the metabolism of the fibroblasts and osteoblasts markedly decreased to this level only in the presence of higher CTAB concentrations (6 μM and more). Similar differences between keratinocytes and osteoblasts were previously observed as well (Kalbáčová et al., 2014). Moreover, different cytotoxic effect of the surfactants on fibroblasts was described for the first time. It was indirectly shown that CTAB combines lethal toxicity with cell metabolism induction, while Septonex predominantly causes lethal toxicity concerning fibroblasts.

Due to the known instability of similar complexes over time (Li et al., 2012), we analysed complexes stored for various time in a fridge (0, 4 and 10 weeks). Surprisingly, no significant differences were observed. Indeed, this finding is supported by the good colloidal stability of the prepared complexes during storage. This stability confirmation also extended the potential of the prepared complexes.

Finally, we were interested in impact of molecular weight on HyA protectivity because this was already decribed by others in similar system (Mizrahy et al., 2011a). Moreover, it is known that high-molecular weight of HyA ($10^7$ Da) has immunosuppressive effects, in contrast, shorter or lower-molecular weight HA fragments are highly angiogenic, immunostimulatory, and inflammatory (Aya and Stern, 2014). We compared metabolic activity of osteoblasts treated with complexes of CTAB with high molecular weight HyA (ca 900 kDa) and complexes with lower molecular weight HyA (ca 600 kDa) under standard conditions. Results showed no significant changes in osteoblast metabolic activity in the presence of these two HyA of different molecular weights. This finding indicates that HyA protection is determined solely by its concentration and not by its molecular weight. This presumption is supported by Mizrahy et

al. (Mizrahy et al., 2011b), who demonstrated a linear relationship between the molecular weight of free HyA and its affinity to CD44 receptor (it means that molecular weight can trigger "HyA-cell" interactions and subsequent transport to the cell). Mizrahy also showed changes in HyA affinity to CD44 induced by HyA molecular weight when HyA is used for coating of nanoparticles (NPs). While the binding of free HyA of different molecular weights (132 kDa, 700 kDa and 1500 kDa) to CD44 was very similar, 132 kDa HyA-coated NPs bound less to cells than 700kDa or 1500kDa HyA-coated NPs. This can be caused by lower availability of CD44 binding sites which are already occupied by interactions with NPs. Thus with the respect to these conclusions, we can predict no significant difference in protectivity between 600 kDa and 900 kDa HyA, due to similarity of their molecular weight. Moreover, it means that molecular weight of 600 kDa is satisfactory for complex requirements (reduction of cytotoxicity and for potential cell interactions).

Taken togehter, besides confirmation of HyA protection ability and its limits with respect to CTAB and Septonex and different cell types, we confirmed the potential of developed complexes in serum-free systems and the long stability of complexes under *in vitro* conditions. All of our results strongly indicate that the system of cationic surfactant with HyA in the complex can be employed for "delivery system" purposes in various biomedical applications.

**The part II of this thesis** (publication C and results D) is focused on *in vitro* biological evaluation of collagen-based scaffolds with pottential of artificial bone structural substitution with suitability for cell application. The composition of these scaffolds was developed to mimic bone ECM using natural collagen, poly(DL-lactide) electrospun nanofibers, bCaP and HyA. The first section of results (included in publication C) was focused primary on testing of different crosslinking agents and their essentiality in a preparation of stable collagen-based materials. The second section (manuscript in preparation D) used the the same components as in publication C but modifies the ratios among them and uses only one type of crosslinking agent.

Collagen isolated for the preparation of studied scaffolds may be very unstable with regard to isolation procedure and post processing. Since the native structure of collagen in not preserved or is partialy destroyed without any subsequent treatment (e.g. proper crosslinking), such material can be prone to the fast biodegradation rate and insufficient mechanical properties that very often complicates *in vitro* and *in vivo* application. Stability of collagen scaffolds can be enhanced by crosslinking (Rault et al., 1996; Rýglová et al., 2017). In practise, there are used various crosslinking agents (Chang et al., 2007; Chen et al., 2005; Ma et al., 2004b), however,

our developed scaffold was treated by genipin, EDC/NHS/EtOH or EDC/NHS/PBS) (publication C). In our study, hMSC were used as a tool for biological evaluation of differently crosslinked scaffolds with the respect to the potential of scaffold application in cell therapy.

Firstly, prepared scaffolds were soaked in cultivation medium for 24 h and obtained infusions were used for cell treatment. All the infusions were considered as non-cytotoxic after 2 and 7 days, thus these results indicate cytocompatibility of scaffolds. Only the metabolic activity of the cells cultivated in the EDC/NHS/PBS crosslinked scaffold infusion decreased significantly to 83%, however the cytotoxicity is often determined by a decrease in cell metabolic activity under 75% (Flahaut et al., 2006). Moreover, the observed decrease of metabolic activity of cells in infusion of EDC/NHS/PBS crosslinked scaffold also reflects that crosslinking agents can influence cell viability and scaffold behaviour (via any cytotoxic agent or any degradation product released from scaffold after longer incubation time). Thus, these findings also confirm the necessity of the *in vitro* biological evaluation of the prepared biomaterials.

Secondly, cells were seeded on prepared scaffolds. The amounts of adhered cells were comparable for all the three scaffolds used at both time points. However, the cell amounts obtained from scaffolds reached approximately 50% of those of the control cells. The control polystyrene (PS) surface is non-porous, solid and flat unlike the tested scaffolds which were porous, pliable and uneven. Thus, the observed substantial reduction in cell adhesion and different cell morphology on the scaffolds in comparison to the control cells on PS could be reasonably predicted. This is in correlation with a previously published report which revealed that substrate stiffness can have a marked effect on cell morphology (Walters and Gentleman, 2015). Also the scaffold porosity and heterogeneity of the pores undoubtedly can play a key role in terms of cell adhesion (O'Brien et al., 2005). Moreover, there is known MSC sensitivity to porosity, pore-size and other mechanical properties (Evans and Gentleman, 2014; Kasten et al., 2008b). Also accessibility of specific adhesion motifs of collagen can be affected by crosslinking (Xu et al., 2012) or specific nano-spacing of scaffold could have affected hMSC adhesion (Wang et al., 2013).

Despite the similarity of metabolic activity among tested scaffolds, visualisation of adhered cells demonstrated significant differences. After 2 days, best appearance and symmetrical distribution of cells was obtained on the genipin crosslinked scaffold. The cells on the EDC/NHS/EtOH and EDC/NHS/PBS cross-linked scaffolds were smaller and spread to lower extent. However, after 7 days, cell morphology and organisation were comparable on all the scaffolds used. The cause of the observed difference after 2 days was most likely due to

higher swelling ratio of scaffolds crosslinked with EDC/NHS/EtOH and EDC/NHS/PBS in comparison to genipin crosslinked scaffold. The stiffness of collagen scaffolds is affected by swelling. And as it was shown, rate of crosslinking, stiffness and other mechanical properties can fundamentally direct cell attachment, proliferation and migration. Our observation is supported by previous finding that the higher scaffold stiffness is proportional to the higher cell number and more homogenous cellular distribution (Haugh et al., 2011). In addition, as it was demonstrated in past (Engler et al., 2006), material rigidity determines stem cell fate and its differentiation. The stiffer materials can act as osteogenic inducers. Thus, our results of low swelling and thus higher mechanical stability of genipin crosslinked scaffold predict this scaffold as the most perspective for MSC differentiation into bone. Moreover, genipin crosslinked scaffold provided pore size approximately of 300µm, however, the pore size of EDC/NHS/EtOH and EDC/NHS/PBS cross-linked scaffolds was only around 200 - 250µm. Despite of no clear definition about ideal pore-size of biomimetic materials (there are various studies with pore-size in wide range 0.5 – 600 µm) or their ideal porosity (in average 25-75%) (Akin et al., 2001; Grier et al., 2017; Kasten et al., 2008a; Murphy et al., 2010; Mygind et al., 2007; Zhang et al., 2015), we could conclude that hMSC used in our study prefered larger pore size (300µm) for their "early" adhesion, which moderates their homogenous distribution on the sruface (up to 2 days). Murphy et al. shows similar surface preference of cells on collagen–glycosaminoglycan scaffolds colonised by osteoblasts, where the specific surface area of the scaffolds was important in terms of initial adhesion (2 days). Also increased cell migration and reduction of cell aggregates formation were observed on scaffold with pore size greater that 300µm. (Murphy et al., 2010).

The last finding of publication C was disability of the cells to freely penetrate into the scaffold (the majority of adhered cells were observed on the surface of the scaffolds and up to a depth of 200µm (i.e. 10 – 20% of scaffold depth)). Low ability of cells to penetrate through the scaffold can be due to the inner structure of the scaffold – the unevenness of the crosslinking and the above mentioned pore size variability (O'Brien et al., 2005), specific collagen sequence/motif accessibility (Xu et al., 2012) and nano-spacing of cell-attractive motifs (Wang et al., 2013). Also seeding method and low availability of nutrients and gases in depth of the scaffold in comparison to scaffold surface can cause poor penetration of cells to the scaffold volume. To improve cell colonization by cells, dynamic cell cultivation was recommended, which can be reached with ideal flow of culturing media through the scaffolds during cultivation (McCoy et al., 2012).

With regard to the structural and mechanical stability of the tested scaffolds, the most effective crosslinking agents were found to be genipin and EDC/NHS/PBS. The genipin cross-linked scaffold provided the best conditions for human mesenchymal stem cells cultivation bacause it maintained constant mechanical properties in contrast to the rest of cross-linked scaffolds. Genipin was selected as the best crosslinking agent for developed type of scaffold and thus was recommended for further advanced *in vitro* (dynamic cultivation) and subsequent *in vivo* studies.

In response to results of publication C, our colleagues developed two new types of collagen-based scaffolds (S4 and S6) differing in their composition (origins and ratios of components). In contrast to publication C which used fish collagen I, new scaffolds were prepared form bovine collagen I. Thus, as we demonstrated in publication C, selection of suitable crosslinikg agent needs to respect specifity of developed collagen-based scaffold, the newly developed scaffolds were treated by optimized combination of EDC/NHS in EtOH/$H_2O$solution selected as the most appropriate crosslinking agent for this purpose. While the collagen and PDLLA content of both scaffold varied by only 10 % and 20 % respectively, the bCaP content in both scaffolds differed significantly (S4 provided only 12.5%, while S6 provided 52.5 %). Biological evaluation was primary focused on cell seeding, scaffold colonization and their efficiency with respect to standardly used static cultivation and dynamic cultivation. As the trend of development of bioartificial bone substitutes shows, static cultivation of 3D tissue-like grafts is unsuitable due to limitations in cell density and nutrition and oxygen support. In contrast, dynamic cultivation in a bioreactor system can significantly reduce these insufficiences and additionally it can allow the environment control (such factors as pH, oxygen content, and temperature). Additionally, these appropriate 3D/dynamic conditions can support bone lineage specific growth (Diederichs et al., 2009).

The cells adhered to the scaffolds were at first 3D visualised by confocal microscopy because of facilitated the visualisation of cell penetration through the scaffolds. Due to the scanning limits of the confocal method, observed penetration level expressed only the majority trend of cell penetration but not maximal penetration in scaffold volume. Maximal penetration can be reliably confirmed by histological analysis of real scaffold sections (these results are not still provided by the colleagues). We observed the majority of adhered cells on the surface of both scaffolds cultivated under both conditions up to a depth of 300µm (i.e. 6 % of scaffold depth). These results reflect relatively low ability of cells to penetrate into scaffold. If we take into account observed reduction of cell amount on both scaffold (provided by DNA content analysis) in time, poor penetration will be probably connected to poor nutrition availability to

cells in scaffold volume. Just the oxygen content is often critical point in efficiency of scaffold colonization. Inhomogenity of scaffold is often the cause of hypoxia, which leads to cell death in scaffold volume (Volkmer et al., 2008). Thus, it seems that the observed lower level of cell penetration and also DNA content were caused by relevant oxygen gradient induced by inhomogenity of scaffold. In addition, the idea of low oxygen nutrition in scaffolds is also supported by observed higher efficiency of dynamic cultivation on cell penetration and DNA content level.

In general, observed higher effectivity of dynamic cultivation contrary to standard static cultivation is confirmed by lots of previous studies aimed to development of the most efficient colonization of 3D strucutres (Diederichs et al., 2009; Gerecht-Nir et al., 2004; Schumacher et al., 2010). Furthermore, as mentioned, DNA content analysis also confirmed higher effectivity of dynamic cultivation. Observed positive effect of dynamic cultivation on cell amount is in agreement with Schumacher, who detected cell number decreased in case of static conditions, while dynamic cultivation allowed homogeneous cell growth in scaffold (Schumacher et al., 2010). Simultaneously, regardless of the way of cultivation, our results of penetration and DNA content also showed impact of scaffold content on efficiency of scaffold colonization by cells. While higher amounts of cells were observed on S4, more efficient penetration and thus higher amounts of cells in scaffold volume were observed on S6 after both incubation times. It reflects that S6 compostion supports better cell migration and better nutrient supplement to deeper structures. Better cell migration and nutrient supplement is probably affected just by high bCaP (HA) contents in S6 (Deligianni et al., 2001). Furthermore, higher suitability of S6 for cell migration and nutrition is also closely connected to minimal swelling in time in comparison to S4 (unpublished data of colleagues). Lower swelling is probably caused by lower protein content in S6, wich subsequently means lower binding of water molecules (Dutta et al., 1997). The high HA content in S6 can also contributes to S6 suitability for cells by reduction of collagen swelling via high bCaP (HA)-collagen interactions that lead to higher collagen compactness and stability (Huang et al., 2012).

However, general loss of cell amount in both scaffold after 7 days of cultivation in comparison to 2-days situation was determined. It is probable that a reduced cell amount was associated with a too short time for adapting of cells to a new matrix. And it can be assumed that after a longer time and thus longer time for adaptation, the cell amount can be elevated (Schumacher et al., 2010). Theory of delayed adaptation of pMSC to scaffold matrix is also supported by our observation of better colonization of scaffolds by osteoblasts contrary to pMSC after 2 days. Contrary to pMSC, osteoblasts prefer matrices imitating their native

environment, thus their proliferation can be enhanced on more rigid scaffolds . Thus, our results also show the preference of various cells to various substrate given by their tissue origin. Additionaly, lower amount of pMSC can be due to longer pMSC doubling time (around 50 hours, unpublished data) in comparison to osteobalsts' doubling time (around 44 hours). Thus it confirms that pMSC can need longer time for their adaptation than cell line of osteoblasts. However, thanks to osteoblasts´ analysis, we also confirmed the potential of scaffold to be naturally colonized by bone cells after implantation.

Next factor playing rol in cell number reduction can be insufficient level of flow rate as parameter of dynamic cultivation which is closely related to mentioned oxygen suppply and which can direct the level of colonization of sccaffold volume and subsequent cell survival(Volkmer et al., 2008). Insufficient flow rate can also means the poor mechanical stimulation of cells, which naturally occures in native tissues. As it was demonstrated on various developed bone graft substitutes, if ideal flow rate is achieved in developed bioreactor, native conditions are imitated and subsequent proliferation or differentiation of cells are significantly elevated. In general, the ideal flow rate needs to be enough strong to induce sufficient mechanical stimuli (and thus cell stimulation) and simultaenously it needs to be sufficiently regardful to minimize cell detachment from the scaffold (McCoy et al., 2012). Thus, with respect to our conditions (30 µl/min flow rate and 6h dynamic cultivation), we can confirm the time of dynamic cultivation together with total time of cell cultivation on scaffolds as key factors for resulting colonization of scaffold by cells (in addition, both parametres were demonstrated as enhancers of osteo-differentiation). It is well suported by results of Schumacher et al., who expossed cells seeded on scaffolds to static or dynamic culture conditions for whole incubation time which was markedly longer (17 days). Thus, it means that in case of future modification of our experimental parametres, these two key factors should be taken into acount - elevation of flow rate together with extension of period of dynamic cultivation (Schumacher et al., 2010).

With respect to expression of selected markers of differentiation (after 2 days and 14 days), we detected no relevant expression changes. Despite any observed up-regulation of tested markers, we detected interesting trends in expression overall. In general, cells seeded on S4 were insignificantly up-regulated in expression after short incubation time, S6 were insignificantly up-regulated in expression after longer incubation time. Thus, comparison of 2- and 14-days expression trends indicates that S6 support the total (insignificant) up-regulation of expression of all tested markers within time contrary to S4. Despite that the expression of osteodifferentiation markers was comparable between cells on S4 and S6 after 14 days, next

long-term increase of expression of cells on S6 and next decrease of the expression of cells on S4 can be predicted. With respect to it, S6 can be estimated as more suitable scaffold for bone surgery. In general, this S6 suitability is also probably supported by S6 high bCaP (HA) content, which is known for its osteoinductive effects (Deligianni et al., 2001; Novotna et al., 2014; Prosecká et al., 2015). Also the expression at the level of signaling molecules (ERK1/2 and p38) predicts S6 for long-term suitability. In comparsion to S4, S6-induced expression is elevated within time in ERK1/2 and also in p38. Interestingly, elevated activity of ERK1/2 signalling was closely connected to elevated concentration of growth factors (Chen et al., 1992). It can reflect that cells are less deprivated on S6 with increasing time in comparsion to S4. Thus we can speculate that observed elevated expression of ERK1/2 and p38 in S6 in time reflects less cell deprivation on S6 due to gradual adaptation to novel environment (and gradual reduction of stressful contitions). The less deprivation of cells can be accompanied by production of various trophic factors to surrounding that are key participants in natural regenerative processes in organism (Caplan and Dennis, 2006). Estimation of gradual reduction of stressful contitions on S6 in time is supported by results presented in publication G. There, activity of ERK1/2 kinase correlated with development of classical focal adhesion that were developed only under standard (non-stressed) conditios. Thus it seems that triggering of standard signaling patway via elevation of ERK1/2 or p38 expression in time can realy mean less-stressed pMSCs with enhanced adaptability on S6 (contrary to S4).

Interestingly, ERK1/2 can be connected to osteodifferentiation as well. As it was shown, ERK1/2 kinases is closely connected to FAK activity (Chaturvedi et al., 2007). FAK signaling plays an important role in regulation of ECM-induced osteogenic differentiation of hMSC (Salasznyk et al., 2007) via activation of osterix transcriptional activity (interestingly, during exprerimental FAK inhibition, lowered expression of osteogenic genes was detected). Thus, additionaly, this can be the next support for S6 suitability at the level of osteodifferentiation.

Finally, we interested in cell adaptability using analysis of remodelation activity of cells seeded on scaffolds. Activity of MMP2 and proMMP9/MMP9 collagenases was analysed in supernatants from cells seeded on scaffolds for 2 days. In general, S4 provided the higher MMP activity in comparsion to S6. Nevertheless, S4 shows activity of only MMP2 collagenase – its activity was elevated only under static cultivation. In contrast, in supernatants from cells incubated on S6 activity of both collagenases (MMP2 and proMMP9/MMP9) under dynamic cultivated conditions were determined as well as activity of only proMMP9/MMP9 collagenase under static cultivation. Interestingly, similarity between MMP activity and DNA content trend shows that activities are correlate with cell amounts. Generally, elevated activity of MMPs in

supernatants from S4 can reflect impaired penetration of cell to S4 contrary to S6 and simultaneously it can reflect worse cell penetration to S4 under static conditions contrary to dynamic conditions. This observation is in agreement with typical phenomenon observed in cancer cells that degrade the ECM by MMPs with the aim to prepare the path for tumor cells to migrate, invade and spread to distant secondary areas (Bourboulia and Stetler-Stevenson, 2010).

In summary, with the respect to cell amount determination, our results indicated S4 scaffold as more suitable for its application in regenerative medicine. However, with the respect to cell penetration, osteodifferentiation and adaptability, our results indicated S6 scaffold as the more suitable for cell application in bone surgery. In addtition, based on *in vitro* results, we confirmed the dynamic cultivation as more efficient for cell cultivation and their penetration into the scaffold.

**The part III of this thesis** (publication E and results F) is focused on evaluation of material with application for local drug delivery. The aim of this research was to develop an osteo-inductive biodegradable composite layer allowing the controlled elution of antibiotics to be used as a bone/implant bioactive interface especially in the case of prosthetic joint infections, or as a preventative procedure with respect to primary joint replacement at a potentially infected site. The bioactive interface was represented by layer composition, which mimics bone ECM. Namely, there were used collagen I and HA (pure, commercial HA) at three different concentrations (0%; 5% and 15% wt of HA). They are not only the main compounds of native bone ECM, but also they are key factors of biomineralisation and collagen self-assembly essential for bone tissue structure and function. As Huant et al. demonstated under *in vitro* conditions, coordinate bonds generated between collagen I and calcium of HA are just key points those direct collagen I self-assembly and are the cause of better and more compact appearance of collagen I in HA presence (Huang et al., 2012). Moreover, collagen I and HA were observed as regulators of cell behaviour - adhesion, migration or differentiation (Deligianni et al., 2001; Mygind et al., 2007; Taubenberger et al., 2010; Wolf et al., 2009; Q. Zhang et al., 2014). Just all of these „cellular“ positive effects were predicted to support better intergation of layers to bone and to potentiate osteo-inductivity. Finally, the possibility to process the collagen I by electrospinning method extended the potential of the layers in drug delivery. Electrospinning is thought to be perspective for drug delivery, because of production of nano- or microfibers that are in general efficient drug delivery agent due to high surface-area-to-volume ratio, high porosity and 3D open porous structures (Rogina, 2014). Moreover,

as results of publication E showed, the electrospinning was really the most efficient method with the respect to desired layer properties and elevation of perspectivity of layers in drug delivery. Taken togehter, all of four mentioned points were clear arguments for development of collagen-based layers enriched by HA. In addition, it was also supported by current trend that considers collagen-based, calcium phosphate–based or calcium sulfate–based materials as typical biodegradable carriers with perspectivity for the local delivery of antibiotics in bone surgery (Alt et al., 2015).

With the respect to layer characterisation provided by our colleagues (such as analyses of structural and mechanical stability and determination of antibiotic release) including the confirmation of sufficient antimicrobial effect of the layers, the next essential step was to perform the *in vitro* evaluation with the focus on cytoxicity and cytocompatibility of these layers. The aim of the biological tests was to verify whether eluted doses of antibiotics have a negative effect on bone-like cell behaviour. Not only effects of antibiotics on bone cells were investigated but also the influence of the layer composition (HA content).

Publication E focused on layers impregnated only by vancomycin. The results presented in publication F confirmed previously observed results obtained from vankomycin modified layers (V) (publication E) and also extended results by evaluation of gentamicin (G) and mixture of vamcomycin and gentamicin (VG) impregnated layers. Vancomycin and gentamicin are the most frequently used antibiotics in bone surgery, especially in septic surgery (Alt et al., 2015; Bertazzoni Minelli et al., 2004; Sugo et al., 2016). A system of mammalian cells was used for biological evaluation due to desired clinical application. First, the level of cytotoxicity was determined treating the pre-seeded cells with infusions obtained from layers soaked for 1 day in cultivation medium. Just infusions are the fine tool for the basic cytotoxicity determination because pre-seeded cells are treated and these are more stable and thus more resistant to various agents in comparison to freshly seeded cells on the layers or scaffolds. Infusion results showed that all of tested layers are not cytotoxic, metabolic activities of all the infusions tested were either comparable to the control sample or only slighly reduced (approximatelly a 10% decrease). Only G5 (gentamicin impregnated layer with 5% HA content) showed more marked decerase of metabolic activity, but it didn´t reach the level of cytotoxicity (cca 75 % of metabolisc activity; (Flahaut et al., 2006)). However, higher cytotoxicity of gentamicin impregnated layers in comparison to vancomycin impregnated layers was predicted due to known cytotoxic effects of gentamicin on cells or tissues of organism (Elyasi et al., 2012; Rathbone et al., 2011; Sahu et al., 2014). Neverthelss, the cytocompatibility of infusions of all the layers was confirmed and it was concluded that the compounds released from the layers

(such as active and degradated forms of antibiotics together with other substances released from layers) did not have a cytotoxic effect on the human osteoblastic cell line. This was extended by next results in publication E where our colleagues found out that ca 800 mg/l of vancomycin is released from the layer after 1 day (gentamicin and vancomycin-gentamicin results are not still provided by the colleagues). While we didn´t detected any cytotoxic effect of vancomycin infusions, we can predict that such concentration is not cytotoxic for human osteoblastic cells. This is in agreement with data describing the local administration of vancomycin to osteoblastic cells (MG-63) , when concentrations of 1 g/l and less had no negative effect on these cells (Edin et al., 1996). In addition, relative safety of vancomycin and its potential for local administration was also confirmed by testing of the wide range of doses (0-5000 mg/l) in the presence of pre-seeded osteoblasts by Rathbone et al. Vancomycin was confirmed as the one of the least cytotoxic antibiotics and only the high concentration (5000 mg/l) induced the first signs of cytotoxicity. Its doses between 500 – 1000 mg/l reduced cell number but not to cytotoxic level of 25% of control cells, thus it was also not cytotoxic (Rathbone et al., 2011). Thus both of mentioned studies support our conclusion that 800 mg/l of vancomycin active form released from the prepared layer is not cytotoxic and thus it explains also observed cytocompatibility of infusion.

Next, cells were seeded directly on layers´ surfaces and metabolic activity and cell number were determined after 2 days and 8 days. Results demonstrated reduced ability of cells to adhere onto the surface of all the layers in contrast to the ideal adhesive surface such as PS. Nevertheless, dramatic difference between PS and the layers was expected, because used PS is specifically treated surface for cell adhesion. Without regard to HA content, results also showed the clear difference between cytotoxicity of both tested antibiotics. While G layers dramatically reduced cell metabolic activity and cell amounts at both incubation times, V layers seemed to be markedly less cytotoxic. VG layers showed the best results of all the tested layers. Vancomycin-gentamicin positivity can be explained by half amount of both antibiotics in VG layers in comparison to layers impregnated only in single antibiotic. Dramatic cytotoxicity of G layers can be caused by higher amount of released gentamicin from the layer in comaparison to vancomycin (results of colleagues are still in process). Observed results of cytotoxicity are in agreement with various studies (Edin et al., 1996; Isefuku et al., 2003; Negrette-Guzmán et al., 2015; Rathbone et al., 2011). The exact mechanism of gentamicin toxicity is not still clear and thus there are studies with oposite effects of gentamicin on human cells. For example, while Isefuku et al. observed higher concentrations of gentamicin (≥700 mg/l) as inhibitory for cells (Isefuku et al., 2003), other studies demonstrated close relation between gentamicin and

mitochondrial dysfunction and apoptosis which is the indicator of lethality (Negrette-Guzmán et al., 2015; Sahu et al., 2014).

The next important finding was the confirmation of positive effect of HA content on cells and thus HA-induced reduction of cytotoxicity. Positivity of HA was predicted based on various observations that demonstrated HA regulation of such processes as cell adhesion, cell spreading morphology and migration (Deligianni et al., 2001; Novotna et al., 2014). However, the real surprising were limits of HA positive effect (content which was able to reduce of the cytotoxicity) in relation to the antibiotic type. Whereas, G and VG layers provided the best conditions for cells in 5% HA presence (thus G5 and VG5 were the best), V layers provided the best conditions in the presence of 15% HA (thus V15 was the best). Furthermore, we also detected the cell number increase as general adaptability on stressful conditions induced by antibiotic within time. Besides the positivity of HA content in sence of cell adhesion support, the key factor of adaptability was probably gradual decrease of antibiotic release from layers. This can be well supported by vancomycin results provided by the colleagues in publication E (gentamicin and vancomycin-gentamicin results are still in process), where they showed changes in release of vancomycin amount in time (the gradual decrease 2-8 day). While gradual release (steady decrease in the release) was exhibited by V0 layer, more precipitous (uneven) release was exhibited in V5 and V15 (the extreme decrease of release was measured during the first 100 hours). Firstly, this result can explain our observation that cytotoxicity of antibiotics is affected by HA content. Secondly, V15 results also showed that not only HA content influences the cytotoxicity but also another factor. If cytotoxicity is affected only by HA content, V15 should be more toxic than V0 and V5 layers. We can´t also exlude the possibility of cell adaptation to high released vancomycin concetrations measured during the experiment. The next explanation of the best features of V15, despite high amounts of released vancomycin, can be the BSA presence in cultivation medium. Two facts support it; BSA is the adhesion-inhibiting protein (Carré and Lacarrière, 2010; Wei et al., 2009) and vancomycin can interact with BSA and alter its conformation (Wu et al., 2013). Thus, despite the high vancomycin concetration in V15, the cell viability can be increased due to inteaction of vancomycin with BSA which can reduce cytotoxic effect of vancomycin and simultaneously alteration of BSA can provid better adhesion conditions (adhesion-promoting proteins from FBS). Our results also show the cell recovery on layers after 8 days (with exception to G0 and G15 where cytotoxicity was still dramatic). It is the next important indicator of cytocompatibility and it can predict the osteo-inductive potential of layers. With the respect to it, layers possibly used for next testing are V15> VG5> G5.

Obtained results from biochemical analyses were confirmed by the microscopic determination of cell morphology and quality of cells seeded on the layers. After 2 days, cells were predominantly of round shape with only poor distribution and in small amounts on the layers; it reflected reduced adhesion to the layers and also the cytotoxic effect of antibiotics. Dramatic cytotoxicity of gentamicin was also evident. After 8 days, higher amounts of cells with more spread morphology confirmed the trend of cell recovery (with exception of all gentamicin layers (G0 and G15)). From these results, the best conditions were provided by V15> VG5> G5.

Taken together, *in vitro* evalution determined V15, VG5 and G5 layers as the best representatives of each type of antibiotic impregnated layer. We demonstrated that bone-producing cells can survive on these layers (with exception to G0 and G15) and that their metabolic activity depends on the type of antibiotic used together with degree of layer mineralisation. With respect to changes in time, sufficient antimicrobial activity, cytocompatibility, the lowest negative effects on bone-like cells and the highest potential of cell recovery, the layer with the highest perspectivity for bone surgery application was V15. V15 was also recommended as the best candidate for subsequent *in vivo* evaluation.

**Part IV of this thesis** is covered by publication G. While previous sections are focused on the study of cells in the context of various arfiticial environments where the results are in principle rather more general and cells are primarily the tool for biomaterial exploration, in this last part, cells are primary the objects of the exploration. The cell is a perfect microsystem and achieved knowledge is the essential assumption for regenerative medicine and effective tissue engineering and cell therapy.

Results of publication G are focused on initial phase of cell adhesion, which is the primary and key point of cell survival and the first determinant of cell fate. The early phase of adhesion was studied with three selected human cell types - osteoblastic cell line (SAOS-2), primary human fibroblasts and human mesenchymal stem cells (hMSC). Experiments were performed under standard (FBS presence) and non-standard cultivation conditions (FBS absence). The reason of these two experimental conditions are similar to the first part of this thesis: 1) standardly used FBS or other external proteins (as supplements of culturing medium in *in vitro* research) can highly impact various cell interactions with environment and it may also distort real behaviour of cells *in vitro*, 2) there are lots of methods or materials in research practise that can´t be used in the presence of FBS or any other proteins, 3) medical application tries to reduce or exclude the use of FBS due to high health risks.

It was shown that the various cells reacted differently to the presence or absence of FBS with respect to cell shape, area and number; it was concluded that the differing cell reactions were probably connected to the origin of the cells. SAOS-2 cells are osteosarcoma cell line that is generally used in the form of a permanent line of human osteoblast-like cells (Rodan et al., 1987). The osteoblast cancer cell line possesses certain characteristic features (PAUTKE et al., 2004) that may differ from those of primary and healthy cells such as primary human dermal fibroblasts and hMSCs. Literature has described different adhesion of fibroblastic and melanoma cells to fibronectin (Humphries et al., 1986). Due to the high functional variability among tested cell types, observed differences originate in basic features of cells under their native conditions (Meirelles et al., 2006). Results reflect general difference between pluripotent MSCs and differentiated cells. Simultaneously there are also evident differences between two types of differentiated cells. Thus it seems that hMSCs results stay somewhere between results obtained from osteoblasts and fibroblasts. While hMSCs correspond to osteoblasts in the cell shape, they differ in cell amount on the polystyrene surface. Higher tendency of hMSCs to proliferate could be affected by high sensitivity of hMSCs to growth factors or non-stressed conditions provided by FBS presence (in contrast to differentiated cells). On the other hand, the increase in cell number of hMSC could be induced by higher sensitivity of hMSC to stiffness or flatness of cultivation surface that can stimulate their proliferation (Engler et al., 2006; Schuldiner et al., 2000; Uccelli et al., 2008; Wen et al., 2014). The decrease of osteoblasts amount in FBS presence can be affected also by their cancer character, because it was showed that under natural conditions cancer cells perform lower adhesion (natural conditions are provided just by FBS for *in vitro* experiments) (Khalili and Ahmad, 2015). We can´t also exclude the impact of stiff and flat surface (provided by polystyrene surface) on resulting cell morphology due to different tendency of cells to remodelate underlying surface for better adhesion (Engler et al., 2006; Wen et al., 2014). In the past, it was observed that just surface parametres can affect proliferation and shape changes of fibroblasts (Dalby et al., 2003). Interestingly, it was also shown that the cell shape can direct cell behaviour and cell fate (McBeath et al., 2004), thus observed shape differences induced by FBS presence or absence can affect resulting proliferation of cells. Nevertheless, all results describe only short-term cultivation and this must be taken into account. This trend is also suported by our results obtained at 2 h and 20 h as well, that refleted more significant differences in adhesion after a longer time. As it was previously shown, just long-term cultivation (days or weeks) can affect some of parameters of cell behaviour due to cell adaptation to environment (Dalby et al., 2003; Deligianni et al., 2001; Engler et al., 2006).

While change in morphology and cell amount were dependent on cell type and FBS presence or absence, the expression and localization of proteins of FA didn´t show significant differences at the level of cell types. Both parameters reveal significant changes only under various conditions. With the respect to cell adhesion, we were also interested in the quality and mechanism of adhesion process. We observed that all the three cell types used developed classical FAs with expression of vinculin, talin and activated pFAk in FBS presence. Additionally, we also demonstrated the participation of CD44 in classical FAs, which is in agreement with study showing HyA as a participant of very early phase of cell-matrix interactions in some cell types (Zimmerman et al., 2002). Moreover, CD44 participation in cell adhesion is also supported by study that showed the formation of growth-promoting complex containing CD44 molecules in the presence of growth factors (can be provided by FBS) (Ponta et al., 2003).

In comparison to situation in FBS presence, no classical focal adhesions were observed under non-standard conditions. Moreover, lower levels of activated kinases pFAK and pERK1/2 were observed. With respect to decrease in expression and localization of both kinases (Saoncella et al., 1999), we suggest that cells use alternative signalling pathway for adhesion process under stress conditions (such as FBS absence). Thus in agreement with research of others, we showed the key signaling role of ERK1/2 and FAK kinases in standard cell adhesion process which are in functional interconnection(Salasznyk et al., 2007, 2004a). Observed low amounts of activated (phophorylated) kinases in FBS absence (lack of growth factors) was also confirmed by Chen et al., who demonstrated increased phophorylated form of ERK 1/2 kinase when serum-deprived cell were treated by growth factors (Chen et al., 1992).

As it was mentioned, classical focal adhesions were formed only in FBS presence (15% FBS). However, we tested other concetrations of FBS in the medium and no significant differences between 1%, 5% or 15% FBS contents were found. It means that the lowest FBS content was sufficient for formation of standard adhesion structures (probably via FN and VN) (Krebs, 1950). It was confirmed by our results derived from cultivation of cells on surfaces pre-treated only with FN or VN where clasical FAs formation was evident as well. While effects of both proteins were comparable in FBS presence after 2h (Lenselink, 2015; Pankov and Yamada, 2002; Preissner, 1991; Ruoslahti, 1996; Williams et al., 2008), longer incubation (20h) indicated various level of cell adaptability under various conditions, which probably refleted various tendency of cells to remodelate their ECM (Bonnans et al., 2014; Carré and Lacarrière, 2010; Dalby et al., 2006, 2003). Comparison of standardly used FBS with preadsorbed FN and VN also pointed out their various impact on resulting cell adhesion and

morphology, thus it also reflects disadvantages of using of undefined and heterogenous FBS for *in vitro* analyses (van der Valk et al., 2010). In summary, these results demonstrated the importance of initial protein layer in cell adhesion process (Anselme et al., 2012) and also crutial role of matrix composition and its dominant impact on cell morphology (Kim et al., 1992; Salasznyk et al., 2004b; Walters and Gentleman, 2015). Furthermore, similarly to previous study (McBeath et al., 2004), we can predict the impact of cell morphology on cell behaviour such as cell survival, changes in signalisation, or cytoskeletal rearrangement that can finally affect cell fate (such as proliferation, migration and probably differentiation).

Generally, we demonstrated that cell adhesion mediated by FBS proteins differs greatly from "direct" cell adhesion to surface without FBS protein contribution. The diverse intensity and localization of membrane, signalling and structural proteins involved in cell adhesion were observed. Moreover, cell area and shape were also strongly affected by cell type. For the first time, the cell-substrate contact in the absence of serum proteins for anchorage-dependent cells was described in detail. All of these results showed the importance of initial cell adhesion for cell fate including the key role of ECM composition, its organization, role of protein layer in initial cell adhesion and its high impact on bidirectional communication between cell and matrix (Pelham and Wang, 1997; Walters and Gentleman, 2015).

Results of every part of this thesis helped to evaluate, characterize or modify the developed material under *in vitro* conditions. Moreover, these results subsequently contributed to prediction of the potential of the material for subsequent *in vivo* analysis and its future clinical application. It was shown that every tested biomaterial in this thesis has potential to support established medical procedures or to become the new alternative of treatment in the regenerative medicine. Our results also demonstrated the importance of *in vitro* biological evaluantion of developed modificated materials. In more general perspective, the possibility to study three different biomimetic materials based on various principles or functions in organism, helped to verify in practise: the enormous impact of surrounding environment on cell behaviour and cell interactions including the key role of ECM in various cellular processes. It also reflected the different adaptability of different types of cells under various conditions and the complexity and reciprocity (bidirectionality) of cellular processes.

# 6 CONCLUSIONS

I We characterized the response of cells to **colloidal complexes of CTAB or Septonex with hyaluronic acid** (HyA) (potential drug/nuclei acid/diagnostic dye delivery system or cosmetic agent) with the respect to fetal bovine serum presence or absence during cultivation. Generally, HyA protection ability with respect to cationic surfactant (CTAB and Septonex)-induced cytotoxicity was confirmed. Also detailed definition of the limits of HyA protection was provided. In addition, HyA protection ability and the limits in respect to different cell types were demonstrated. Moreover, the study of various cell types and differently modified complexes enhanced knowledge about surfactant-induced cytotoxicity and its reduction by prepared complexes with HyA. We revealed the positive effect of FBS on cells under stress conditions (surfactant presence). We also confirmed the cell protective function of HyA in complexes containing surfactants under non-standard conditions, thus we verified the potential of the use of the complexes in serum-free systems. Our results strongly indicated the potential of cationic surfactant-HyA complex systems as "delivery system" in various biomedical applications.

II We evaluated **collagen based scaffolds** with suitability for stem cell therapy in bone surgery application *in vitro* by using MSCs derived from different organisms. Firstly, we evaluated developed scaffolds with the respect to various crosslinking agents and with the focus on cytotoxicity determination and adhesion, proliferation and penetration of cells into scaffolds. The most effective crosslinking agents to improve medicinal properties of the scaffold were found to be genipin and EDC/NHS/PBS. Genipin cross-linked scaffolds provided the best conditions for MSCs presented by proper cell morphology and their homogenous distribution on scaffold surface 2 days and 7 days of cultivation. In comparison, the cells on EDC/NHS/EtOH and EDC/NHS/PBS cross-linked scaffolds were found to be less spread after 2 days. Based on *in vitro* testing, the genipin cross-linked scaffold was recommended for further *in vitro* and *in vivo* testing with emphasis for dynamic cultivation. Secondly, two types of developed collagen-based scaffolds (with lower and higher CaP content) were evaluated by advanced methods with the focus on static and dynamic cultivation of cells. Effectivity of both cultivation conditions was determined with the respect to cell

colonization and penetration into the scaffold depth, and also with respect to potential application of scaffolds for cell therapy. Results confirmed the higher effectivity of dynamic cultivation in comparison to static cultivation. Moreover, the scaffold with the higher content of CaP was selected as better one for cell colonization and penetration into scaffold depth. Based on our results, the recommended type of scaffold was used for *in vivo* tests.

III We evaluated *in vitro* **collagen/hydroxyapatite nano/micro structured resorbable layers with controlled elution of antibiotics** (vancomycin, gentamicin and mixture of both) for osteointegration support. Based on cytotoxicity, metabolic activity and cell morphological analaysis, we confirmed V15 (vancomycin impregnated layer with 15% content of HA), VG5 (vancomycin/gentamicin impregnated layer with 5% content of HA) and G5 (gentamicin impregnated layer with 5% content of HA) layers as the best representatives of each used type of antibiotic. It was demonstrated that bone-producing cells can survive on all the layers used with exception of G0 (gentamicin impregnated layer with 0% content of HA) and G15 (gentamicin impregnated layer with 15% content of HA) layers. Interestingly, it was found out that antibiotic impregnation together with the degree of HA mineralisation of layer participate in resulting cell number and affect cell metabolic activity. With respect to cytocompatibility, the highest potential of cell recovery had cells on V15 layer. It provided such doses of vancomycin that exerted the lowest negative effect on bone-like cell behaviour and on the other hand ensured sufficient antibacterial activity. Thus, V15 was recommended as the best candidate for subsequent *in vivo* evaluation. In general, developed nanostructured layers (prepared by means of electrospinning from collagen/HA dispersion, subsequently cross-linked with EDC/NHS and finally impregnated with vancomycin) were confirmed as suitable candidates for the preparation of bioactive and pro-osteo-integrating bone-implant interfaces and for local drug delivery.

IV We described an **early phase of cell adhesion of** osteosarcoma cell line SAOS-2, primary human fibroblasts and hMSCs in the context of FBS presence or absence in the cultivation medium. Generally, it was demonstrated that cell adhesion mediated by FBS proteins differs greatly from "direct" cell adhesion on protein-free surface. The diverse intensity and localization of membrane, signalling and FAs structural proteins involved in cell adhesion were observed. With the respect to all three tested cell types,

it was found out that no classic focal adhesions were formed during cell adhesion in the absence of FBS proteins. The alternative signalisation of cells under stress conditions such as FBS absence was also outlined. Finally, it was confirmed that parameters such as cell area and shape are determined also by cell type. For the first time, the cell-substrate contact in the absence of serum proteins for anchorage-dependent cells was described in detail.

# 7 COMPLETE LISTS OF AUTHOR'S PUBLICATIONS

**Pavla Sauerová**, Martina Verdánová, Filip Mravec, Tereza Pilgrová, Tereza Venerová, Marie Hubálek Kalbáčová , Miloslav Pekař (2015): **Hyaluronic Acid as a Modulator of the Cytotoxic Effects of Cationic Surfactants.** Colloids and Surfaces A: Physicochem. Eng. Aspects 483, 155-161. IF = 2.752

**Pavla Sauerová,** Tereza Pilgrová, Miloslav Pekař and Marie Hubálek Kalbáčová (2017): **Hyaluronic Acid in Complexes with Surfactants: The Efficient Tool for Reduction of the Cytotoxic Effect of Surfactants on Human Cell Types.** Journal of Biological Macromolecules – accepted for publication. IF = 3.138

Tomáš Suchý, Monika Šupová, **Pavla Sauerová**, Martina Verdánová, Zbyněk Sucharda, Šárka Rýglová, Margit Žaloudková, Radek Sedláček and Marie Hubálek Kalbáčová (2015): **The Effects of Different Crosslinking Conditions on Collagen-Based Nanocomposite Scaffolds - An in Vitro Evaluation Using Mesenchymal Stem Cells.** Biomed Mater. 10, 065008. IF = 3.697

Tomáš Suchý, Monika Šupová, Eva Klapková; Václava Adámková, Jan Závora,Margit Žaloudková, Šárka Rýglová, Rastislav Ballay, František Denk, Marek Pokorný, **Pavla Sauerová**, Marie Hubálek Kalbáčová, Lukáš Horný, Jan Veselý, Tereza Voňavková, Richard Průša (2017): **The Release Kinetics, Antimicrobial Activity and Cytocompatibility of Differently Prepared Collagen/Hydroxyapatite/Vancomycin Layers: Microstructure vs. Nanostructure.** European Journal of Pharmaceutical Sciences 100, 219-229. IF = 3.77

Martina Verdánová, **Pavla Sauerová**, Ute Hempel, Marie Hubálek Kalbáčová (2017): **Initial Cell Adhesion of Three Cell Types in the Presence and Absence of Serum Proteins.** Histochemistry and Cell biology 147 (5), published online. IF = 2.78

Tomáš Suchý, Monika Šupová, Martin Bartoš, Radek Sedláček, Marco Piola, Monica Soncini, Gianfranco Beniamino Fiore, **Pavla Sauerová**, Marie Hubálek Kalbáčová (2017): **Dry versus hydrated collagen scaffolds: are dry states representative of hydrated states. Biomedical Materials** – submitted.

# 8 LIST OF ABBREVIATIONS

| | |
|---|---|
| 2D | two-dimensional |
| 3D | three-dimensional |
| ANOVA | analysis of variance |
| bCaP | bioapatite (bio calcium phosphate) |
| BMP | bone morphogenetic proteins |
| BSA | bovine serum albumin |
| C/EBP | CCAAT-enhancer-binding protein |
| CAMs | cell adhesion molecules |
| CaP | calcium phosphate |
| CD44 | cluster of differentiation 44 |
| cDNA | complementary deoxyribonucleic acid |
| COL I | collagen I |
| CTAB | cetrimonium bromide; cetyltrimethylammonium bromide |
| DAPI | 4',6-diamidino-2-phenylindole |
| DNA | deoxyribonucleic acid |
| ECM | extracelular matrix |
| EDC/NHS/EtOH | N-(3 dimethylaminopropyl)-N-ethylcarbodiimide hydrochloride (EDC)/N-hydroxysuccinimide (NHS) in ethanol |
| EDC/NHS/PBS | N-(3 dimethylaminopropyl)-N-ethylcarbodiimide hydrochloride (EDC)/N-hydroxysuccinimide (NHS) in phospate buffer |
| EGF | epidermal growth factor |
| EI0, EI5 and E15 | vancomycin (10 % wt) impregnated electrospun layers with 0, 5 and 15% wt of HA content |
| ERK1/2 | extracellular signal-regulated kinases 1 and 2 |
| FA(s) | focal adhesion(s) |
| FAK | focal adhesion kinase |
| FGF | fibroblasts growth factors |
| FN | fibronectin |
| G | gentamicin impregnated layer |
| G0, G5 and G15 | gentamicin (10 % wt) impregnated electrospun layers with 0, 5 and 15% wt of HA content |
| GAGs | glykosaminoglycans |
| GAPDH | glyceraldehyde-3-phosphate dehydrogenase |
| HA | hydroxylapatite |
| HaCaT | spontaneously transformed aneuploid immortal keratinocyte cell line from adult human skin |
| hMSC | human mesenchymal stem cell |
| HyA | hyaluronic Acid |
| kDa | kilodalton |
| MAPK | mitogen-activated protein kinase |
| MEK 1/2 | mitogen-activated protein kinase (MAP)/ERK kinase |
| MMP2 | matrix metalloproteinase 2 |
| MMP9 | matrix metalloproteinase 9 |
| MMPs | matrix metalloproteinases |
| MSC | mesenchymal stem cell |
| Nanog | NK-2 type homeodomain trancription factor |

| | |
|---|---|
| NGF | nerve growth factor |
| NK0, NK5 and NK15 | non-impregnated electrospun layers with 0, 5 and 15% wt of HA content |
| Oct4 | octamer-binding transcription factor 4 |
| p38 | p 38 kinase |
| PBS | phosphate Buffered Saline |
| PCL | poly(ε-caprolactone) |
| PDLLA | poly(DL-lactide) |
| pERK1/2 | phosphorylated extracellular signal-regulated kinases 1 and 2 |
| pFAK | phosphorylated focal adhesion kinase |
| PGA | polyglycolide |
| PGs | proteoglycans |
| PLA | polylactide |
| PLGA | poly(lactide-*co*-glycolide) |
| pMSC | porcine mesenchymal stem cell |
| PPARγ | Peroxisome proliferator-activated receptor gamma |
| ppm | parts per million |
| proMMP9 | matrix prometalloproteinase 9 |
| PS | polystyren surface control |
| qPCR | quantitative polymerase chain reaction |
| RGD peptide | arginine-glycine-aspartic acid peptide |
| Rho-GTPase | Rho-GTP(Guanosintrifosfát)-binding protein |
| RNA | ribonucleic acid |
| RT | room temperature |
| RTqPCR | quantitative Polymerase Chain Reaction with Reverse Transcription |
| RUN X | Runt-related transcription factor |
| S4 | scaffold composed of poly(DL-lactide) (47 wt %), collagen I (40 wt %), natural calcium phosphate (12,5 wt %), hyaluronan (0,5 wt%) |
| S6 | scaffold composed of poly(DL-lactide) (27 wt %), collagen I(30 wt %), natural calcium phosphate (42,5 wt %), hyaluronan (0,5 wt%) |
| SAOS-2 | sarcoma osteogenic cell line |
| SDS | sodium dodecyl sulfate |
| SDS-PAGE | sodium dodecyl sulfate - polyacrylamide gel electrophoresis |
| Sox2 | SRY (sex determining region Y)-box 2 trancription factor |
| SP7 | osterix ,transcription factor |
| TE buffer | Tris-EDTA |
| TGF | transforming growth factor |
| TIMs | tissue inhibitors of MMPs |
| V | vancomycin impregnated layer |
| V0, V5 and V15 | vancomycin (10 % wt) impregnated electrospun layers with 0, 5 and 15% wt of HA content |
| VASP | vasodilator-stimulated phosphoprotein |
| VEGF | vascular endothelial growth factos |
| VG | vancomycin-gentamicin (mixture) impregnated layer |
| VG0, VG5 and VG15 | vancomycin-gentamicin (10 % wt) impregnated electrospun layers with 0, 5 and 15% wt of HA content |
| VN | vitronectin |

# 9 REFERENCES


Abagnale, G., Steger, M., Nguyen, V.H., Hersch, N., Sechi, A., Joussen, S., Denecke, B., Merkel, R., Hoffmann, B., Dreser, A., Schnakenberg, U., Gillner, A., Wagner, W., 2015. Surface topography enhances differentiation of mesenchymal stem cells towards osteogenic and adipogenic lineages. Biomaterials 61, 316–326. doi:10.1016/j.biomaterials.2015.05.030

Akin, F.A., Zreiqat, H., Jordan, S., Wijesundara, M.B.J., Hanley, L., 2001. Preparation and analysis of macroporous TiO2 films on Ti surfaces for bone–tissue implants. J. Biomed. Mater. Res. 57, 588–596. doi:10.1002/1097-4636(20011215)57:4<588::AID-JBM1206>3.0.CO;2-Y

Alford, A.I., Kozloff, K.M., Hankenson, K.D., 2015. Extracellular matrix networks in bone remodeling. Int. J. Biochem. Cell Biol. 65, 20–31. doi:10.1016/j.biocel.2015.05.008

Allain, F., Vanpouille, C., Carpentier, M., Slomianny, M.-C., Durieux, S., Spik, G., 2002. Interaction with glycosaminoglycans is required for cyclophilin B to trigger integrin-mediated adhesion of peripheral blood T lymphocytes to extracellular matrix. Proc. Natl. Acad. Sci. 99, 2714–2719. doi:10.1073/pnas.052284899

Almalik, A., Donno, R., Cadman, C.J., Cellesi, F., Day, P.J., Tirelli, N., 2013. Hyaluronic acid-coated chitosan nanoparticles: Molecular weight-dependent effects on morphology and hyaluronic acid presentation. J. Controlled Release 172, 1142–1150. doi:10.1016/j.jconrel.2013.09.032

Alt, V., Franke, J., Schnettler, R., 2015. Local delivery of antibiotics in the surgical treatment of bone infections. Tech. Orthop. 30, 230–235.

Altman, G.H., Horan, R.L., Martin, I., Farhadi, J., Stark, P.R.H., Volloch, V., Richmond, J.C., Vunjak-Novakovic, G., Kaplan, D.L., 2002. Cell differentiation by mechanical stress. FASEB J. Off. Publ. Fed. Am. Soc. Exp. Biol. 16, 270–272. doi:10.1096/fj.01-0656fje

Anselme, K., Ploux, L., Ponche, A., 2012. Cell/Material Interfaces: Influence of Surface Chemistry and Surface Topography on Cell Adhesion. J. Adhes. Sci. Technol. doi:10.1163/016942409X12598231568186

Arnold, M., Cavalcanti-Adam, E.A., Glass, R., Blümmel, J., Eck, W., Kantlehner, M., Kessler, H., Spatz, J.P., 2004. Activation of Integrin Function by Nanopatterned Adhesive Interfaces. ChemPhysChem 5, 383–388. doi:10.1002/cphc.200301014

Aruffo, A., Stamenkovic, I., Melnick, M., Underhill, C.B., Seed, B., 1990. CD44 is the principal cell surface receptor for hyaluronate. Cell 61, 1303–1313. doi:10.1016/0092-8674(90)90694-A

Aya, K.L., Stern, R., 2014. Hyaluronan in wound healing: rediscovering a major player. Wound Repair Regen. 22, 579–593.

BaoLin, G., MA, P.X., 2014. Synthetic biodegradable functional polymers for tissue engineering: a brief review. Sci. China Chem. 57, 490–500.

Barrilleaux, B., Phinney, D.G., Prockop, D.J., O'Connor, K.C., 2006. Review: ex vivo engineering of living tissues with adult stem cells. Tissue Eng. 12, 3007–3019. doi:10.1089/ten.2006.12.3007

Bertazzoni Minelli, E., Benini, A., Magnan, B., Bartolozzi, P., 2004. Release of gentamicin and vancomycin from temporary human hip spacers in two-stage revision of infected arthroplasty. J. Antimicrob. Chemother. 53, 329–334. doi:10.1093/jac/dkh032

Bigliardi, P.L., Herron, M.J., Nelson, R.D., Dahl, M.V., 1994. Effects of detergents on proliferation and metabolism of human keratinocytes. Exp. Dermatol. 3, 89–94. doi:10.1111/j.1600-0625.1994.tb00053.x

Birgersdotter, A., Sandberg, R., Ernberg, I., 2005. Gene expression perturbation in vitro—A growing case for three-dimensional (3D) culture systems. Semin. Cancer Biol. 15, 405–412. doi:10.1016/j.semcancer.2005.06.009

Bissell, M.J., Aggeler, J., 1987. Dynamic reciprocity: how do extracellular matrix and hormones direct gene expression? Prog. Clin. Biol. Res. 249, 251–262.

Black, C.R.M., Goriainov, V., Gibbs, D., Kanczler, J., Tare, R.S., Oreffo, R.O.C., 2015. Bone Tissue Engineering. Curr. Mol. Biol. Rep. 1, 132–140. doi:10.1007/s40610-015-0022-2

Bonnans, C., Chou, J., Werb, Z., 2014. Remodelling the extracellular matrix in development and disease. Nat. Rev. Mol. Cell Biol. 15, 786–801. doi:10.1038/nrm3904

Bourboulia, D., Stetler-Stevenson, W.G., 2010. Matrix metalloproteinases (MMPs) and tissue inhibitors of metalloproteinases (TIMPs): Positive and negative regulators in tumor cell adhesion. Semin. Cancer Biol., Adhesive interactions: The multi-task biochemical toolbox of cancer cells 20, 161–168. doi:10.1016/j.semcancer.2010.05.002

Busscher, H.J., Mei, H.C. van der, Subbiahdoss, G., Jutte, P.C., Dungen, J.J.A.M. van den, Zaat, S.A.J., Schultz, M.J., Grainger, D.W., 2012. Biomaterial-Associated Infection: Locating the Finish Line in the Race for the Surface. Sci. Transl. Med. 4, 153rv10-153rv10. doi:10.1126/scitranslmed.3004528

Camassola, M., de Macedo Braga, L.M.G., Chagastelles, P.C., Nardi, N.B., 2012. Methodology, biology and clinical applications of human mesenchymal stem cells. Methods Mol. Biol. Clifton NJ 879, 491–504. doi:10.1007/978-1-61779-815-3_30

Cancedda, R., Dozin, B., Giannoni, P., Quarto, R., 2003. Tissue engineering and cell therapy of cartilage and bone. Matrix Biol. 22, 81–91. doi:10.1016/S0945-053X(03)00012-X

Cancedda, R., Giannoni, P., Mastrogiacomo, M., 2007. A tissue engineering approach to bone repair in large animal models and in clinical practice. Biomaterials 28, 4240–4250. doi:10.1016/j.biomaterials.2007.06.023

Caplan, A.I., 1991. Mesenchymal stem cells. J. Orthop. Res. 9, 641–650. doi:10.1002/jor.1100090504

Caplan, A.I., Dennis, J.E., 2006. Mesenchymal stem cells as trophic mediators. J. Cell. Biochem. 98, 1076–1084. doi:10.1002/jcb.20886

Carré, A., Lacarrière, V., 2010. How Substrate Properties Control Cell Adhesion. A Physical–Chemical Approach. J. Adhes. Sci. Technol. 24, 815–830. doi:10.1163/016942409X12598231567862

Carreira, A.C., Alves, G.G., Zambuzzi, W.F., Sogayar, M.C., Granjeiro, J.M., 2014. Bone Morphogenetic Proteins: Structure, biological function and therapeutic applications. Arch. Biochem. Biophys., Bone: A dynamic and integrating tissue 561, 64–73. doi:10.1016/j.abb.2014.07.011

Chang, J.-Y., Lin, J.-H., Yao, C.-H., Chen, J.-H., Lai, T.-Y., Chen, Y.-S., 2007. In Vivo Evaluation of a Biodegradable EDC/NHS-Cross-Linked Gelatin Peripheral Nerve Guide Conduit Material. Macromol. Biosci. 7, 500–507. doi:10.1002/mabi.200600257

Chang, S.-J., Chen, Y.-C., Yang, C.-H., Huang, S.-C., Huang, H.-K., Li, C.-C., Harn, H.I.-C., Chiu, W.-T., 2017. Revealing the three dimensional architecture of focal adhesion components to explain Ca2 +-mediated turnover of focal adhesions. Biochim. Biophys. Acta BBA - Gen. Subj. 1861, 624–635. doi:10.1016/j.bbagen.2017.01.002

Chaturvedi, L.S., Marsh, H.M., Basson, M.D., 2007. Src and focal adhesion kinase mediate mechanical strain-induced proliferation and ERK1/2 phosphorylation in human H441 pulmonary epithelial cells. Am. J. Physiol. - Cell Physiol. 292, C1701–C1713. doi:10.1152/ajpcell.00529.2006

Chen, D., Zhao, M., Mundy, G.R., 2004. Bone Morphogenetic Proteins. Growth Factors 22, 233–241. doi:10.1080/08977190412331279890

Chen, D.W., Hsu, Y.-H., Liao, J.-Y., Liu, S.-J., Chen, J.-K., Ueng, S.W.-N., 2012. Sustainable release of vancomycin, gentamicin and lidocaine from novel electrospun sandwich-structured PLGA/collagen nanofibrous membranes. Int. J. Pharm. 430, 335–341. doi:10.1016/j.ijpharm.2012.04.010

Chen, G., Ushida, T., Tateishi, T., 2002. Scaffold design for tissue engineering. Macromol. Biosci. 2, 67–77.

Chen, J., Chu, B., Hsiao, B.S., 2006. Mineralization of hydroxyapatite in electrospun nanofibrous poly (L-lactic acid) scaffolds. J. Biomed. Mater. Res. A 79, 307–317.

Chen, R.H., Sarnecki, C., Blenis, J., 1992. Nuclear localization and regulation of erk- and rsk-encoded protein kinases. Mol. Cell. Biol. 12, 915–927. doi:10.1128/MCB.12.3.915

Chen, Y.-S., Chang, J.-Y., Cheng, C.-Y., Tsai, F.-J., Yao, C.-H., Liu, B.-S., 2005. An in vivo evaluation of a biodegradable genipin-cross-linked gelatin peripheral nerve guide conduit material. Biomaterials 26, 3911–3918. doi:10.1016/j.biomaterials.2004.09.060

Cheng, Y., Ramos, D., Lee, P., Liang, D., Yu, X., Kumbar, S.G., 2014. Collagen Functionalized Bioactive Nanofiber Matrices for Osteogenic Differentiation of Mesenchymal Stem Cells: Bone Tissue Engineering. J. Biomed. Nanotechnol. 10, 287–298. doi:10.1166/jbn.2014.1753

Cheung, K.L., Chen, H., Chen, Q., Wang, J., Ho, H.P., Wong, C.K., Kong, S.K., 2012. CTAB-coated gold nanorods elicit allergic response through degranulation and cell death in human basophils. Nanoscale 4, 4447–4449. doi:10.1039/C2NR30435J

Cheung, W.-F., Cruz, T.F., Turley, E.A., 1999. RECEPTOR FOR HYALURONAN-MEDIATED MOTILITY (RHAMM), A HYALADHERIN THAT REGULATES CELL RESPONSES TO GROWTH FACTORS. Biochem. Soc. Trans. 27, 135–142.

Chiarugi, P., Giannoni, E., 2008. Anoikis: a necessary death program for anchorage-dependent cells. Biochem. Pharmacol. 76, 1352–1364.

Chou, Y.-C., Cheng, Y.-S., Hsu, Y.-H., Yu, Y.-H., Liu, S.-J., 2016. A bio-artificial poly([d,l]-lactide-co-glycolide) drug-eluting nanofibrous periosteum for segmental long bone open fractures with significant periosteal stripping injuries. Int. J. Nanomedicine 11, 941–953. doi:10.2147/IJN.S99791

Chou, Y.-F., Dunn, J.C., Wu, B.M., 2005. In vitro response of MC3T3-E1 preosteoblasts within three-dimensional apatite-coated PLGA scaffolds. J. Biomed. Mater. Res. B Appl. Biomater. 75, 81–90.

Christophersen, N.S., Helin, K., 2010. Epigenetic control of embryonic stem cell fate. J. Exp. Med. 207, 2287–2295. doi:10.1084/jem.20101438

Collins, M.N., Birkinshaw, C., 2013. Hyaluronic acid based scaffolds for tissue engineering—A review. Carbohydr. Polym. 92, 1262–1279. doi:10.1016/j.carbpol.2012.10.028

Cooper, D.M.L., Matyas, J.R., Katzenberg, M.A., Hallgrimsson, B., 2004. Comparison of Microcomputed Tomographic and Microradiographic Measurements of Cortical Bone Porosity. Calcif. Tissue Int. 74, 437–447. doi:10.1007/s00223-003-0071-z

Cornelis, M., Dupont, C., Wepierre, J., 1992. Prediction of eye irritancy potential of surfactants by cytotoxicity tests in vitro on cultures of human skin fibroblasts and keratinocytes. Toxicol. In Vitro 6, 119–128. doi:10.1016/0887-2333(92)90004-B

da Silva Meirelles, L., Fontes, A.M., Covas, D.T., Caplan, A.I., 2009. Mechanisms involved in the therapeutic properties of mesenchymal stem cells. Cytokine Growth Factor Rev., Bone Morphogenetic Proteins, Stem Cells and Regenerative Medicine 20, 419–427. doi:10.1016/j.cytogfr.2009.10.002

Dalby, M.J., Childs, S., Riehle, M.O., Johnstone, H.J.H., Affrossman, S., Curtis, A.S.G., 2003. Fibroblast reaction to island topography: changes in cytoskeleton and morphology with time. Biomaterials 24, 927–935. doi:10.1016/S0142-9612(02)00427-1

Dalby, M.J., Gadegaard, N., Oreffo, R.O.C., 2014. Harnessing nanotopography and integrin-matrix interactions to influence stem cell fate. Nat. Mater. 13, 558–569. doi:10.1038/nmat3980

Dalby, M.J., Gadegaard, N., Tare, R., Andar, A., Riehle, M.O., Herzyk, P., Wilkinson, C.D.W., Oreffo, R.O.C., 2007. The control of human mesenchymal cell differentiation using nanoscale symmetry and disorder. Nat. Mater. 6, 997–1003. doi:10.1038/nmat2013

Dalby, M.J., McCloy, D., Robertson, M., Agheli, H., Sutherland, D., Affrossman, S., Oreffo, R.O.C., 2006. Osteoprogenitor response to semi-ordered and random nanotopographies. Biomaterials 27, 2980–2987. doi:10.1016/j.biomaterials.2006.01.010

Decambron, A., Fournet, A., Bensidhoum, M., Manassero, M., Sailhan, F., Petite, H., Logeart-Avramoglou, D., Viateau, V., 2017. Low-dose BMP-2 and MSC dual delivery onto coral scaffold for critical-size bone defect regeneration in sheep. J. Orthop. Res. n/a-n/a. doi:10.1002/jor.23577

Delabarde, C., Plummer, C.J., Bourban, P.-E., M\a anson, J.-A.E., 2012. Biodegradable polylactide/hydroxyapatite nanocomposite foam scaffolds for bone tissue engineering applications. J. Mater. Sci. Mater. Med. 23, 1371–1385.

Deligianni, D.D., Katsala, N.D., Koutsoukos, P.G., Missirlis, Y.F., 2001. Effect of surface roughness of hydroxyapatite on human bone marrow cell adhesion, proliferation, differentiation and detachment strength. Biomaterials 22, 87–96.

Dicker, K.T., Gurski, L.A., Pradhan-Bhatt, S., Witt, R.L., Farach-Carson, M.C., Jia, X., 2014. Hyaluronan: A simple polysaccharide with diverse biological functions. Acta Biomater. 10, 1558–1570. doi:10.1016/j.actbio.2013.12.019

Diederichs, S., Röker, S., Marten, D., Peterbauer, A., Scheper, T., van Griensven, M., Kasper, C., 2009. Dynamic cultivation of human mesenchymal stem cells in a rotating bed bioreactor system based on the Z® RP Platform. Biotechnol. Prog. 25, 1762–1771.

Dingli, D., Traulsen, A., Michor, F., 2007. (A)Symmetric Stem Cell Replication and Cancer. PLOS Comput. Biol. 3, e53. doi:10.1371/journal.pcbi.0030053

Dohan Ehrenfest, D.M., Coelho, P.G., Kang, B.-S., Sul, Y.-T., Albrektsson, T., 2010. Classification of osseointegrated implant surfaces: materials, chemistry and topography. Trends Biotechnol. 28, 198–206. doi:10.1016/j.tibtech.2009.12.003

Dong, C., Lv, Y., 2016. Application of Collagen Scaffold in Tissue Engineering: Recent Advances and New Perspectives. Polymers 8, 42. doi:10.3390/polym8020042

Dutta, P., Hajra, S., Chattoraj, D.K., 1997. Binding of water and solute to protein-mixture and protein-coated alumina. Indian J. Biochem. Biophys. 34, 449–460.

Edin, M.L., Miclau, T., Lester, G.E., Lindsey, R.W., Dahners, L.E., 1996. Effect of cefazolin and vancomycin on osteoblasts in vitro. Clin. Orthop. 333, 245–251.

Elyasi, S., Khalili, H., Dashti-Khavidaki, S., Mohammadpour, A., 2012. Vancomycin-induced nephrotoxicity: mechanism, incidence, risk factors and special populations. A literature review. Eur. J. Clin. Pharmacol. 68, 1243–1255. doi:10.1007/s00228-012-1259-9

Engler, A.J., Sen, S., Sweeney, H.L., Discher, D.E., 2006. Matrix Elasticity Directs Stem Cell Lineage Specification. Cell 126, 677–689. doi:10.1016/j.cell.2006.06.044

Evans, N.D., Gentleman, E., 2014. The role of material structure and mechanical properties in cell–matrix interactions. J. Mater. Chem. B 2, 2345–2356. doi:10.1039/C3TB21604G

Fang, T., Wen, J., Zhou, J., Shao, Z., Dong, J., 2012. Poly (ε-caprolactone) coating delays vancomycin delivery from porous chitosan/β-tricalcium phosphate composites. J. Biomed. Mater. Res. B Appl. Biomater. 100B, 1803–1811. doi:10.1002/jbm.b.32747

Fasano, M., Curry, S., Terreno, E., Galliano, M., Fanali, G., Narciso, P., Notari, S., Ascenzi, P., 2005. The extraordinary ligand binding properties of human serum albumin. IUBMB Life 57, 787–796. doi:10.1080/15216540500404093

Feng, B., Chen, J., Zhang, X., 2002. Interaction of calcium and phosphate in apatite coating on titanium with serum albumin. Biomaterials 23, 2499–2507.

Fernekorn, U., Hampl, J., Augspurger, C., Hildmann, C., Weise, F., Klett, M., Läffert, A., Gebinoga, M., Williamson, A., Schober, A., 2013. In vitro cultivation of biopsy derived primary hepatocytes leads to a more metabolic genotype in perfused 3D scaffolds than static 3D cell culture. RSC Adv. 3, 16558–16568. doi:10.1039/C3RA42358A

Flahaut, E., Durrieu, M.C., Remy-Zolghadri, M., Bareille, R., Baquey, C., 2006. Investigation of the cytotoxicity of CCVD carbon nanotubes towards human umbilical vein endothelial cells. Carbon 44, 1093–1099. doi:10.1016/j.carbon.2005.11.007

Frisch, S.M., Francis, H., 1994. Disruption of epithelial cell-matrix interactions induces apoptosis. J. Cell Biol. 124, 619–626.

Ga, E., Sr, B., Jg, L., 1991. Viral contamination of fetal bovine serum used for tissue culture: risks and concerns. Dev. Biol. Stand. 75, 173–175.

Gattazzo, F., Urciuolo, A., Bonaldo, P., 2014. Extracellular matrix: A dynamic microenvironment for stem cell niche. Biochim. Biophys. Acta BBA - Gen. Subj., Matrix-mediated cell behaviour and properties 1840, 2506–2519. doi:10.1016/j.bbagen.2014.01.010

Gay, D., 2014. Composite Materials: Design and Applications, Third Edition. CRC Press.

Geiger, B., Yamada, K.M., 2011. Molecular Architecture and Function of Matrix Adhesions. Cold Spring Harb. Perspect. Biol. 3, a005033. doi:10.1101/cshperspect.a005033

Gelse, K., Pöschl, E., Aigner, T., 2003. Collagens—structure, function, and biosynthesis. Adv. Drug Deliv. Rev., Collagen in drug delivery and tissue engineering 55, 1531–1546. doi:10.1016/j.addr.2003.08.002

Gerecht-Nir, S., Cohen, S., Itskovitz-Eldor, J., 2004. Bioreactor cultivation enhances the efficiency of human embryoid body (hEB) formation and differentiation. Biotechnol. Bioeng. 86, 493–502.

Giancotti, F.G., 2000. Complexity and specificity of integrin signalling. Nat. Cell Biol. 2, E13–E13.

Gordon, M.K., Hahn, R.A., 2010. Collagens. Cell Tissue Res. 339, 247. doi:10.1007/s00441-009-0844-4

Grant, R.L., Yao, C., Gabaldon, D., Acosta, D., 1992. Evaluation of surfactant cytotoxicity potential by primary cultures of ocular tissues: I. Characterization of rabbit corneal epithelial cells and initial injury and delayed toxicity studies. Toxicology 76, 153–176. doi:10.1016/0300-483X(92)90162-8

Green, P.J., Walsh, F.S., Doherty, P., 1996. Promiscuity of fibroblast growth factor receptors. BioEssays News Rev. Mol. Cell. Dev. Biol. 18, 639–646. doi:10.1002/bies.950180807

Grier, W.K., Iyoha, E.M., Harley, B.A.C., 2017. The influence of pore size and stiffness on tenocyte bioactivity and transcriptomic stability in collagen-GAG scaffolds. J. Mech. Behav. Biomed. Mater. 65, 295–305. doi:10.1016/j.jmbbm.2016.08.034

Grishko, V., Xu, M., Ho, R., Mates, A., Watson, S., Kim, J.T., Wilson, G.L., Pearsall, A.W., 2009. Effects of Hyaluronic Acid on Mitochondrial Function and Mitochondria-driven Apoptosis following Oxidative Stress in Human Chondrocytes. J. Biol. Chem. 284, 9132–9139. doi:10.1074/jbc.M804178200

Gstraunthaler Gerhard, 2003. Alternatives to the Use of Fetal Bovine Serum: Serum-free Cell Culture - Google Scholar [WWW Document]. URL https://scholar.google.cz/scholar?q=Alternatives+to+the+Use+of+Fetal+Bovine+Serum%3A+Serum-free+Cell+Culture&btnG=&hl=cs&as_sdt=0%2C5 (accessed 2.8.17).

Gupta, B., Revagade, N., Hilborn, J., 2007. Poly (lactic acid) fiber: an overview. Prog. Polym. Sci. 32, 455–482.

Halasová, T., Krouská, J., Mravec, F., Pekař, M., 2011. Hyaluronan-surfactant interactions in physiological solution studied by tensiometry and fluorescence probe techniques. Colloids Surf. Physicochem. Eng. Asp. 391, 25–31. doi:10.1016/j.colsurfa.2011.05.035

Halasová, T., Mravec, F., Pekař, M., 2013. The effect of hyaluronan on the aggregation of hydrophobized amino acids—A fluorescence study. Carbohydr. Polym. 97, 34–37. doi:10.1016/j.carbpol.2013.04.051

Harada, H., Takahashi, M., 2007. CD44-dependent Intracellular and Extracellular Catabolism of Hyaluronic Acid by Hyaluronidase-1 and -2. J. Biol. Chem. 282, 5597–5607. doi:10.1074/jbc.M608358200

Haugh, M.G., Murphy, C.M., McKiernan, R.C., Altenbuchner, C., O'Brien, F.J., 2011. Crosslinking and mechanical properties significantly influence cell attachment, proliferation, and migration within collagen glycosaminoglycan scaffolds. Tissue Eng. Part A 17, 1201–1208.

He, G., Ma, L.L., Pan, J., Venkatraman, S., 2007. ABA and BAB type triblock copolymers of PEG and PLA: A comparative study of drug release properties and "stealth" particle characteristics. Int. J. Pharm. 334, 48–55. doi:10.1016/j.ijpharm.2006.10.020

He, Q., Shi, J., Chen, F., Zhu, M., Zhang, L., 2010. An anticancer drug delivery system based on surfactant-templated mesoporous silica nanoparticles. Biomaterials 31, 3335–3346. doi:10.1016/j.biomaterials.2010.01.015

Hemeda, H., Giebel, B., Wagner, W., 2014. Evaluation of human platelet lysate versus fetal bovine serum for culture of mesenchymal stromal cells. Cytotherapy 16, 170–180. doi:10.1016/j.jcyt.2013.11.004

Hempel, U., Preissler, C., Vogel, S., M&#xf6, Ller, S., Hintze, V., Becher, J., Schnabelrauch, M., Rauner, M., Hofbauer, L.C., Dieter, P., 2014. Artificial Extracellular Matrices with Oversulfated Glycosaminoglycan Derivatives Promote the Differentiation of Osteoblast-Precursor Cells and Premature Osteoblasts. BioMed Res. Int. 2014, e938368. doi:10.1155/2014/938368

Hofinger, E.S.A., Hoechstetter, J., Oettl, M., Bernhardt, G., Buschauer, A., 2008. Isoenzyme-specific differences in the degradation of hyaluronic acid by mammalian-type hyaluronidases. Glycoconj. J. 25, 101–109. doi:10.1007/s10719-007-9058-8

Holmberg, K., Jönsson, B., Kronberg, B., Lindman, B., 2002. Surfactant Micellization, in: Surfactants and Polymers in Aqueous Solution. John Wiley & Sons, Ltd, pp. 39–66. doi:10.1002/0470856424.ch2

Holzwarth, J.M., Ma, P.X., 2011. 3D nanofibrous scaffolds for tissue engineering. J. Mater. Chem. 21, 10243–10251.

Hong, D.-W., Lai, P.-L., Ku, K.-L., Lai, Z.-T., Chu, I.-M., 2013. Biodegradable in situ gel-forming controlled vancomycin delivery system based on a thermosensitive mPEG-PLCPPA hydrogel. Polym. Degrad. Stab. 98, 1578–1585. doi:10.1016/j.polymdegradstab.2013.06.027

Hu, E., Tontonoz, P., Spiegelman, B.M., 1995. Transdifferentiation of myoblasts by the adipogenic transcription factors PPAR gamma and C/EBP alpha. Proc. Natl. Acad. Sci. 92, 9856–9860.

Huang, Z.L., Liu, G.Y., He, Y., Yi, Z.Z., Guo, J.M., 2012. Interaction between Hydroxyapatite and Collagen. Adv. Mater. Res. 412, 384–387. doi:10.4028/www.scientific.net/AMR.412.384

Humphrey, J.D., Dufresne, E.R., Schwartz, M.A., 2014. Mechanotransduction and extracellular matrix homeostasis. Nat. Rev. Mol. Cell Biol. 15, 802–812. doi:10.1038/nrm3896

Humphries, J.D., Wang, P., Streuli, C., Geiger, B., Humphries, M.J., Ballestrem, C., 2007. Vinculin controls focal adhesion formation by direct interactions with talin and actin. J. Cell Biol. 179, 1043–1057. doi:10.1083/jcb.200703036

Humphries, M.J., Olden, K., Yamada, K.M., 1986. A synthetic peptide from fibronectin inhibits experimental metastasis of murine melanoma cells. Science 233, 467–470.

Hynes, R.O., Naba, A., 2012. Overview of the Matrisome—An Inventory of Extracellular Matrix Constituents and Functions. Cold Spring Harb. Perspect. Biol. 4. doi:10.1101/cshperspect.a004903

Ikeda, T., Kawaguchi, H., Kamekura, S., Ogata, N., Mori, Y., Nakamura, K., Ikegawa, S., Chung, U., 2005. Distinct roles of Sox5, Sox6, and Sox9 in different stages of chondrogenic differentiation. J. Bone Miner. Metab. 23, 337–340. doi:10.1007/s00774-005-0610-y

Inácio, Â.S., Costa, G.N., Domingues, N.S., Santos, M.S., Moreno, A.J.M., Vaz, W.L.C., Vieira, O.V., 2013. Mitochondrial Dysfunction Is the Focus of Quaternary Ammonium Surfactant Toxicity to Mammalian Epithelial Cells. Antimicrob. Agents Chemother. 57, 2631–2639. doi:10.1128/AAC.02437-12

Inácio, Â.S., Mesquita, K.A., Baptista, M., Ramalho-Santos, J., Vaz, W.L.C., Vieira, O.V., 2011a. In Vitro Surfactant Structure-Toxicity Relationships: Implications for Surfactant Use in Sexually Transmitted Infection Prophylaxis and Contraception. PLoS ONE 6, e19850. doi:10.1371/journal.pone.0019850

Inácio, Â.S., Mesquita, K.A., Baptista, M., Ramalho-Santos, J., Vaz, W.L.C., Vieira, O.V., 2011b. In vitro surfactant structure-toxicity relationships: implications for surfactant use in sexually transmitted infection prophylaxis and contraception. PloS One 6, e19850. doi:10.1371/journal.pone.0019850

Isefuku, S., Joyner, C.J., Simpson, A.H.R., 2003. Gentamicin may have an adverse effect on osteogenesis. J. Orthop. Trauma 17, 212–216.

Jang, C.H., Cho, Y.B., Jang, Y.S., Kim, M.S., Kim, G.H., 2015. Antibacterial effect of electrospun polycaprolactone/polyethylene oxide/vancomycin nanofiber mat for prevention of periprosthetic infection and biofilm formation. Int. J. Pediatr. Otorhinolaryngol. 79, 1299–1305. doi:10.1016/j.ijporl.2015.05.037

Jhala, D., Vasita, R., 2015. A Review on Extracellular Matrix Mimicking Strategies for an Artificial Stem Cell Niche. Polym. Rev. 55, 561–595. doi:10.1080/15583724.2015.1040552

Jie, P., Venkatraman, S.S., Min, F., Freddy, B.Y.C., Huat, G.L., 2005. Micelle-like nanoparticles of star-branched PEO–PLA copolymers as chemotherapeutic carrier. J. Controlled Release 110, 20–33. doi:10.1016/j.jconrel.2005.09.011

Juhásová, J., Juhás, S., Klíma, J., Strnádel, J., Holubová, M., Motlík, J., 2011. Osteogenic differentiation of miniature pig mesenchymal stem cells in 2D and 3D environment. Physiol. Res. 60, 559–571.

Jungreuthmayer, C., Donahue, S.W., Jaasma, M.J., Al-Munajjed, A.A., Zanghellini, J., Kelly, D.J., O'Brien, F.J., 2008. A Comparative Study of Shear Stresses in Collagen-Glycosaminoglycan and Calcium Phosphate Scaffolds in Bone Tissue-Engineering Bioreactors. Tissue Eng. Part A 15, 1141–1149. doi:10.1089/ten.tea.2008.0204

Jungreuthmayer, C., Jaasma, M.J., Al-Munajjed, A.A., Zanghellini, J., Kelly, D.J., O'Brien, F.J., 2009. Deformation simulation of cells seeded on a collagen-GAG scaffold in a flow perfusion bioreactor using a sequential 3D CFD-elastostatics model. Med. Eng. Phys., Finite Element Modelling of Medical Devices 31, 420–427. doi:10.1016/j.medengphy.2008.11.003

Kalbáčová, M., Verdánová, M., Mravec, F., Halasová, T., Pekař, M., 2014. Effect of CTAB and CTAB in the presence of hyaluronan on selected human cell types. Colloids Surf. Physicochem. Eng. Asp. 460, 204–208. doi:10.1016/j.colsurfa.2013.12.048

Kanchanawong, P., Shtengel, G., Pasapera, A.M., Ramko, E.B., Davidson, M.W., Hess, H.F., Waterman, C.M., 2010. Nanoscale architecture of integrin-based cell adhesions. Nature 468, 580–584. doi:10.1038/nature09621

Karazisis, D., Petronis, S., Agheli, H., Emanuelsson, L., Norlindh, B., Johansson, A., Rasmusson, L., Thomsen, P., Omar, O., 2017. The influence of controlled surface nanotopography on the early biological events of osseointegration. Acta Biomater. 53, 559–571. doi:10.1016/j.actbio.2017.02.026

Karp, J.M., Dalton, P.D., Shoichet, M.S., 2003. Scaffolds for Tissue Engineering. MRS Bull. 28, 301–306. doi:10.1557/mrs2003.85

Kasten, P., Beyen, I., Niemeyer, P., Luginbühl, R., Bohner, M., Richter, W., 2008a. Porosity and pore size of β-tricalcium phosphate scaffold can influence protein production and osteogenic differentiation of human mesenchymal stem cells: An in vitro and in vivo study. Acta Biomater. 4, 1904–1915. doi:10.1016/j.actbio.2008.05.017

Kasten, P., Vogel, J., Luginbühl, R., Niemeyer, P., Tonak, M., Lorenz, H., Helbig, L., Weiss, S., Fellenberg, J., Leo, A., Simank, H.-G., Richter, W., 2005. Ectopic bone formation associated with mesenchymal stem cells in a resorbable calcium deficient hydroxyapatite carrier. Biomaterials 26, 5879–5889. doi:10.1016/j.biomaterials.2005.03.001

Keaveny, T.M., Morgan, E.F., Niebur, G.L., Yeh, O.C., 2001. Biomechanics of Trabecular Bone. Annu. Rev. Biomed. Eng. 3, 307–333. doi:10.1146/annurev.bioeng.3.1.307

Kemppainen, J.M., Hollister, S.J., 2010. Differential effects of designed scaffold permeability on chondrogenesis by chondrocytes and bone marrow stromal cells. Biomaterials 31, 279–287. doi:10.1016/j.biomaterials.2009.09.041

Khalili, A.A., Ahmad, M.R., 2015. A Review of Cell Adhesion Studies for Biomedical and Biological Applications. Int. J. Mol. Sci. 16, 18149–18184. doi:10.3390/ijms160818149

Kim, J.P., Zhang, K., Chen, J.D., Wynn, K.C., Kramer, R.H., Woodley, D.T., 1992. Mechanism of human keratinocyte migration on fibronectin: Unique roles of RGD site and integrins. J. Cell. Physiol. 151, 443–450. doi:10.1002/jcp.1041510303

Klim, J.R., Li, L., Wrighton, P.J., Piekarczyk, M.S., Kiessling, L.L., 2010. A defined glycosaminoglycan-binding substratum for human pluripotent stem cells. Nat. Methods 7, 989–994. doi:10.1038/nmeth.1532

Knudson, C.B., 2003. Hyaluronan and CD44: Strategic players for cell–matrix interactions during chondrogenesis and matrix assembly. Birth Defects Res. Part C Embryo Today Rev. 69, 174–196. doi:10.1002/bdrc.10013

Komori, T., 2006. Regulation of osteoblast differentiation by transcription factors. J. Cell. Biochem. 99, 1233–1239. doi:10.1002/jcb.20958

Koshikawa, N., Giannelli, G., Cirulli, V., Miyazaki, K., Quaranta, V., 2000. Role of Cell Surface Metalloprotease Mt1-Mmp in Epithelial Cell Migration over Laminin-5. J. Cell Biol. 148, 615–624. doi:10.1083/jcb.148.3.615

Krebs, H.A., 1950. Chemical Composition of Blood Plasma and Serum. Annu. Rev. Biochem. 19, 409–430. doi:10.1146/annurev.bi.19.070150.002205

Krebs, S., Fischaleck, M., Blum, H., 2009. A simple and loss-free method to remove TRIzol contaminations from minute RNA samples. Anal. Biochem. 387, 136–138. doi:10.1016/j.ab.2008.12.020

Kuboki, Y., Takita, H., Kobayashi, D., Tsuruga, E., Inoue, M., Murata, M., Nagai, N., Dohi, Y., Ohgushi, H., 1998. BMP-induced osteogenesis on the surface of hydroxyapatite with geometrically feasible and nonfeasible structures: topology of osteogenesis. J. Biomed. Mater. Res. 39, 190–199.

Kubow, K.E., Vukmirovic, R., Zhe, L., Klotzsch, E., Smith, M.L., Gourdon, D., Luna, S., Vogel, V., 2015. Mechanical forces regulate the interactions of fibronectin and collagen I in extracellular matrix. Nat. Commun. 6. doi:10.1038/ncomms9026

Kuo, Y.-C., Yeh, C.-F., 2011. Effect of surface-modified collagen on the adhesion, biocompatibility and differentiation of bone marrow stromal cells in poly(lactide-co-glycolide)/chitosan scaffolds. Colloids Surf. B Biointerfaces 82, 624–631. doi:10.1016/j.colsurfb.2010.10.032

Laurencin, C.T., Attawia, M.A., Lu, L.Q., Borden, M.D., Lu, H.H., Gorum, W.J., Lieberman, J.R., 2001. Poly(lactide-co-glycolide)/hydroxyapatite delivery of BMP-2-producing cells: a regional gene therapy approach to bone regeneration. Biomaterials 22, 1271–1277. doi:10.1016/S0142-9612(00)00279-9

Lee, J.K., Kim, D.B., Kim, J.I., Kim, P.Y., 2000. In vitro cytotoxicity tests on cultured human skin fibroblasts to predict skin irritation potential of surfactants. Toxicol. In Vitro 14, 345–349. doi:10.1016/S0887-2333(00)00028-X

Lenselink, E.A., 2015. Role of fibronectin in normal wound healing. Int. Wound J. 12, 313–316. doi:10.1111/iwj.12109

Lesniak, A., Campbell, A., Monopoli, M.P., Lynch, I., Salvati, A., Dawson, K.A., 2010. Serum heat inactivation affects protein corona composition and nanoparticle uptake. Biomaterials 31, 9511–9518. doi:10.1016/j.biomaterials.2010.09.049

Lewis, P.N., Pinali, C., Young, R.D., Meek, K.M., Quantock, A.J., Knupp, C., 2010. Structural Interactions between Collagen and Proteoglycans Are Elucidated by Three-Dimensional Electron Tomography of Bovine Cornea. Structure 18, 239–245. doi:10.1016/j.str.2009.11.013

Li, D., Kelkar, M.S., Wagner, N.J., 2012. Phase Behavior and Molecular Thermodynamics of Coacervation in Oppositely Charged Polyelectrolyte/Surfactant Systems: A Cationic Polymer JR 400 and Anionic Surfactant SDS Mixture. Langmuir 28, 10348–10362. doi:10.1021/la301475s

Li, W.-J., Laurencin, C.T., Caterson, E.J., Tuan, R.S., Ko, F.K., 2002. Electrospun nanofibrous structure: A novel scaffold for tissue engineering. J. Biomed. Mater. Res. 60, 613–621. doi:10.1002/jbm.10167

Little, W.C., Schwartlander, R., Smith, M.L., Gourdon, D., Vogel, V., 2009. Stretched Extracellular Matrix Proteins Turn Fouling and Are Functionally Rescued by the Chaperones Albumin and Casein. Nano Lett. 9, 4158–4167. doi:10.1021/nl902365z

Liu, S., Thomas, S.M., Woodside, D.G., Rose, D.M., Kiosses, W.B., Pfaff, M., Ginsberg, M.H., 1999. Binding of paxillin to α4 integrins modifies integrin-dependent biological responses. Nature 402, 676–681. doi:10.1038/45264

Ma, L., Gao, C., Mao, Z., Zhou, J., Shen, J., 2004a. Enhanced biological stability of collagen porous scaffolds by using amino acids as novel cross-linking bridges. Biomaterials 25, 2997–3004. doi:10.1016/j.biomaterials.2003.09.092

Magnusson, J.P., Saeed, A.O., Fernández-Trillo, F., Alexander, C., 2011. Synthetic polymers for biopharmaceutical delivery. Polym. Chem. 2, 48–59.

Makhlouf, A.S.H., Scharnweber, D., 2015. Handbook of Nanoceramic and Nanocomposite Coatings and Materials. Butterworth-Heinemann.

Matthews, J.A., Wnek, G.E., Simpson, D.G., Bowlin, G.L., 2002. Electrospinning of collagen nanofibers. Biomacromolecules 3, 232–238.

McBeath, R., Pirone, D.M., Nelson, C.M., Bhadriraju, K., Chen, C.S., 2004. Cell Shape, Cytoskeletal Tension, and RhoA Regulate Stem Cell Lineage Commitment. Dev. Cell 6, 483–495. doi:10.1016/S1534-5807(04)00075-9

McCoy, R. j., Jungreuthmayer, C., O'Brien, F. j., 2012. Influence of flow rate and scaffold pore size on cell behavior during mechanical stimulation in a flow perfusion bioreactor. Biotechnol. Bioeng. 109, 1583–1594. doi:10.1002/bit.24424

McCulloch, E.A., Till, J.E., 2005. Perspectives on the properties of stem cells. Nat. Med. 11, 1026–1028. doi:10.1038/nm1005-1026

McDade, J.K., Brennan-Pierce, E.P., Ariganello, M.B., Labow, R.S., Lee, J.M., 2013. Interactions of U937 macrophage-like cells with decellularized pericardial matrix materials: Influence of crosslinking treatment. Acta Biomater. 9, 7191–7199.

Meirelles, L. da S., Chagastelles, P.C., Nardi, N.B., 2006. Mesenchymal stem cells reside in virtually all post-natal organs and tissues. J. Cell Sci. 119, 2204–2213. doi:10.1242/jcs.02932

Meirelles, L. da S., Nardi, N.B., 2009. Methodology, biology and clinical applications of mesenchymal stem cells. Front. Biosci. Landmark Ed. 14, 4281–4298.

Mitalipov, S., Wolf, D., 2009. Totipotency, Pluripotency and Nuclear Reprogramming. Adv. Biochem. Eng. Biotechnol. 114, 185–199. doi:10.1007/10_2008_45

Mitra, S.K., Hanson, D.A., Schlaepfer, D.D., 2005. Focal adhesion kinase: in command and control of cell motility. Nat. Rev. Mol. Cell Biol. 6, 56–68. doi:10.1038/nrm1549

Mizrahy, S., Goldsmith, M., Leviatan-Ben-Arye, S., Kisin-Finfer, E., Redy, O., Srinivasan, S., Shabat, D., Godin, B., Peer, D., 2014. Tumor targeting profiling of hyaluronan-coated lipid based-nanoparticles. Nanoscale 6, 3742–3752. doi:10.1039/C3NR06102G

Mizrahy, S., Raz, S.R., Hasgaard, M., Liu, H., Soffer-Tsur, N., Cohen, K., Dvash, R., Landsman-Milo, D., Bremer, M.G.E.G., Moghimi, S.M., Peer, D., 2011b. Hyaluronan-coated nanoparticles: The influence of the molecular weight on CD44-hyaluronan interactions and on the immune response. J. Controlled Release 156, 231–238. doi:10.1016/j.jconrel.2011.06.031

Morrison, S.J., Kimble, J., 2006. Asymmetric and symmetric stem-cell divisions in development and cancer. Nature 441, 1068–1074. doi:10.1038/nature04956

Murphy, C.M., Haugh, M.G., O'Brien, F.J., 2010. The effect of mean pore size on cell attachment, proliferation and migration in collagen–glycosaminoglycan scaffolds for bone tissue engineering. Biomaterials 31, 461–466. doi:10.1016/j.biomaterials.2009.09.063

Murphy, L.O., Smith, S., Chen, R.-H., Fingar, D.C., Blenis, J., 2002. Molecular interpretation of ERK signal duration by immediate early gene products. Nat. Cell Biol. 4, 556–564. doi:10.1038/ncb822

Murphy, W.L., McDevitt, T.C., Engler, A.J., 2014. Materials as stem cell regulators. Nat. Mater. 13, 547–557. doi:10.1038/nmat3937

Mygind, T., Stiehler, M., Baatrup, A., Li, H., Zou, X., Flyvbjerg, A., Kassem, M., Bünger, C., 2007. Mesenchymal stem cell ingrowth and differentiation on coralline hydroxyapatite scaffolds. Biomaterials 28, 1036–1047. doi:10.1016/j.biomaterials.2006.10.003

Nagase, H., Visse, R., Murphy, G., 2006. Structure and function of matrix metalloproteinases and TIMPs. Cardiovasc. Res. 69, 562–573. doi:10.1016/j.cardiores.2005.12.002

Nagase, H., Woessner, J.F., 1999. Matrix Metalloproteinases. J. Biol. Chem. 274, 21491–21494. doi:10.1074/jbc.274.31.21491

Nair, L.S., Laurencin, C.T., 2007. Biodegradable polymers as biomaterials. Prog. Polym. Sci. 32, 762–798.

Nair, M.B., Kretlow, J.D., Mikos, A.G., Kasper, F.K., 2011. Infection and tissue engineering in segmental bone defects — a mini review. Curr. Opin. Biotechnol., Tissue, cell and pathway engineering 22, 721–725. doi:10.1016/j.copbio.2011.02.005

Naka, M.H., Morita, Y., Ikeuchi, K., 2005. Influence of proteoglycan contents and of tissue hydration on the frictional characteristics of articular cartilage. Proc. Inst. Mech. Eng. [H] 219, 175–182. doi:10.1243/095441105X34220

Nakata, K., Tsuchido, T., Matsumura, Y., 2011. Antimicrobial cationic surfactant, cetyltrimethylammonium bromide, induces superoxide stress in Escherichia coli cells. J. Appl. Microbiol. 110, 568–579. doi:10.1111/j.1365-2672.2010.04912.x

Negrette-Guzmán, M., García-Niño, W.R., Tapia, E., Zazueta, C., Huerta-Yepez, S., León-Contreras, J.C., Hernández-Pando, R., Aparicio-Trejo, O.E., Madero, M., Pedraza-Chaverri, J., 2015. Curcumin attenuates gentamicin-induced kidney mitochondrial alterations: possible role of a mitochondrial biogenesis mechanism. Evid. Based Complement. Alternat. Med. 2015.

Ngiam, M., Liao, S., Patil, A.J., Cheng, Z., Chan, C.K., Ramakrishna, S., 2009. The fabrication of nano-hydroxyapatite on PLGA and PLGA/collagen nanofibrous composite scaffolds and their effects in osteoblastic behavior for bone tissue engineering. Bone 45, 4–16.

Niemeyer, P., Krause, U., Punzel, M., Fellenberg, J., Simank, H.G., 2002. Mesenchymal stem cells for tissue engineering of bone: 3D-cultivation and osteogenic differentiation on mineralized collagen. Z. Orthop. Ihre Grenzgeb. 141, 712–717.

Nishio, Y., Dong, Y., Paris, M., O'Keefe, R.J., Schwarz, E.M., Drissi, H., 2006. Runx2-mediated regulation of the zinc finger Osterix/Sp7 gene. Gene 372, 62–70. doi:10.1016/j.gene.2005.12.022

Noel, S.P., Courtney, H.S., Bumgardner, J.D., Haggard, W.O., 2010. Chitosan Sponges to Locally Deliver Amikacin and Vancomycin: A Pilot In Vitro Evaluation. Clin. Orthop. Relat. Res. 468, 2074–2080. doi:10.1007/s11999-010-1324-6

Novotna, K., Zajdlova, M., Suchy, T., Hadraba, D., Lopot, F., Zaloudkova, M., Douglas, T.E.L., Munzarova, M., Juklickova, M., Stranska, D., Kubies, D., Schaubroeck, D., Wille, S., Balcaen, L., Jarosova, M., Kozak, H., Kromka, A., Svindrych, Z., Lisa, V., Balik, K., Bacakova, L., 2014. Polylactide nanofibers with hydroxyapatite as growth substrates for osteoblast-like cells. J. Biomed. Mater. Res. A 102, 3918–3930. doi:10.1002/jbm.a.35061

Oakes, P.W., Gardel, M.L., 2014. Stressing the limits of focal adhesion mechanosensitivity. Curr. Opin. Cell Biol., Cell adhesion and migration 30, 68–73. doi:10.1016/j.ceb.2014.06.003

O'Brien, F.J., Harley, B.A., Yannas, I.V., Gibson, L.J., 2005. The effect of pore size on cell adhesion in collagen-GAG scaffolds. Biomaterials 26, 433–441. doi:10.1016/j.biomaterials.2004.02.052

Özbek, S., Balasubramanian, P.G., Chiquet-Ehrismann, R., Tucker, R.P., Adams, J.C., 2010. The Evolution of Extracellular Matrix. Mol. Biol. Cell 21, 4300–4305. doi:10.1091/mbc.E10-03-0251

Palmer, B.F., Clegg, D.J., 2014. Oxygen sensing and metabolic homeostasis. Mol. Cell. Endocrinol., Cellular energy sensors and endocrine function 397, 51–58. doi:10.1016/j.mce.2014.08.001

Pampaloni, F., Reynaud, E.G., Stelzer, E.H.K., 2007. The third dimension bridges the gap between cell culture and live tissue. Nat. Rev. Mol. Cell Biol. 8, 839–845. doi:10.1038/nrm2236

Pankov, R., Yamada, K.M., 2002. Fibronectin at a glance. J. Cell Sci. 115, 3861–3863. doi:10.1242/jcs.00059

Park, S.-N., Park, J.-C., Kim, H.O., Song, M.J., Suh, H., 2002. Characterization of porous collagen/hyaluronic acid scaffold modified by 1-ethyl-3-(3-dimethylaminopropyl) carbodiimide cross-linking. Biomaterials 23, 1205–1212.

Parsons, J.T., 2003. Focal adhesion kinase: the first ten years. J. Cell Sci. 116, 1409–1416.

PAUTKE, C., SCHIEKER, M., TISCHER, T., KOLK, A., NETH, P., MUTSCHLER, W., MILZ, S., 2004. Characterization of osteosarcoma cell lines MG-63, Saos-2 and U-2 OS in comparison to human osteoblasts. Anticancer Res. 24, 3743–3748.

Pelham, R.J., Wang, Y. l, 1997. Cell locomotion and focal adhesions are regulated by substrate flexibility. Proc. Natl. Acad. Sci. U. S. A. 94, 13661–13665.

Piola, M., Soncini, M., Cantini, M., Sadr, N., Ferrario, G., Fiore, G.B., 2013. Design and functional testing of a multichamber perfusion platform for three-dimensional scaffolds. Sci. World J. 2013.

Polo, J.M., Liu, S., Figueroa, M.E., Kulalert, W., Eminli, S., Tan, K.Y., Apostolou, E., Stadtfeld, M., Li, Y., Shioda, T., Natesan, S., Wagers, A.J., Melnick, A., Evans, T., Hochedlinger, K., 2010. Cell type of origin influences the molecular and functional properties of mouse induced pluripotent stem cells. Nat. Biotechnol. 28, 848–855. doi:10.1038/nbt.1667

Ponta, H., Sherman, L., Herrlich, P.A., 2003. CD44: From adhesion molecules to signalling regulators. Nat. Rev. Mol. Cell Biol. 4, 33–45. doi:10.1038/nrm1004

Preissner, K.T., 1991. Structure and Biological Role of Vitronectin. Annu. Rev. Cell Biol. 7, 275–310. doi:10.1146/annurev.cb.07.110191.001423

Prestwich, G.D., 2011. Hyaluronic acid-based clinical biomaterials derived for cell and molecule delivery in regenerative medicine. J. Controlled Release 155, 193–199. doi:10.1016/j.jconrel.2011.04.007

Prosecká, E., Rampichová, M., Litvinec, A., Tonar, Z., Králíčková, M., Vojtova, L., Kochova, P., Plencner, M., Buzgo, M., Míčková, A., others, 2015. Collagen/hydroxyapatite scaffold enriched with polycaprolactone nanofibers, thrombocyte-rich solution and mesenchymal stem cells promotes regeneration in large bone defect in vivo. J. Biomed. Mater. Res. A 103, 671–682.

Qiu, L., Li, Z., Qiao, M., Long, M., Wang, M., Zhang, X., Tian, C., Chen, D., 2014. Self-assembled pH-responsive hyaluronic acid–g-poly(l-histidine) copolymer micelles for targeted intracellular delivery of doxorubicin. Acta Biomater. 10, 2024–2035. doi:10.1016/j.actbio.2013.12.025

Raiskup, F., Spoerl, E., 2013. Corneal Crosslinking with Riboflavin and Ultraviolet A. I. Principles. Ocul. Surf. 11, 65–74. doi:10.1016/j.jtos.2013.01.002

Rampichová, M., Chvojka, J., Buzgo, M., Prosecká, E., Mikeš, P., Vysloužilová, L., Tvrdík, D., Kochová, P., Gregor, T., Lukáš, D., Amler, E., 2013. Elastic three-dimensional poly (ε-caprolactone) nanofibre scaffold enhances migration, proliferation and osteogenic differentiation of mesenchymal stem cells. Cell Prolif. 46, 23–37. doi:10.1111/cpr.12001

Rasmussen, J.W., Martinez, E., Louka, P., Wingett, D.G., 2010. Zinc oxide nanoparticles for selective destruction of tumor cells and potential for drug delivery applications. Expert Opin. Drug Deliv. 7, 1063–1077. doi:10.1517/17425247.2010.502560

Rathbone, C.R., Cross, J.D., Brown, K.V., Murray, C.K., Wenke, J.C., 2011. Effect of various concentrations of antibiotics on osteogenic cell viability and activity. J. Orthop. Res. 29, 1070–1074.

Rault, I., Frei, V., Herbage, D., Abdul-Malak, N., Huc, A., 1996. Evaluation of different chemical methods for cros-linking collagen gel, films and sponges. J. Mater. Sci. Mater. Med. 7, 215–221. doi:10.1007/BF00119733

Reinhard, M., Jouvenal, K., Tripier, D., Walter, U., 1995. Identification, purification, and characterization of a zyxin-related protein that binds the focal adhesion and microfilament protein VASP (vasodilator-stimulated phosphoprotein). Proc. Natl. Acad. Sci. U. S. A. 92, 7956–7960.

Reneker, D.H., Yarin, A.L., Zussman, E., Xu, H., 2007. Electrospinning of nanofibers from polymer solutions and melts. Adv. Appl. Mech. 41, 43–346.

Reznikov, N., Shahar, R., Weiner, S., 2014. Bone hierarchical structure in three dimensions. Acta Biomater., Biomineralization 10, 3815–3826. doi:10.1016/j.actbio.2014.05.024

Rodan, S.B., Imai, Y., Thiede, M.A., Wesolowski, G., Thompson, D., Bar-Shavit, Z., Shull, S., Mann, K., Rodan, G.A., 1987. Characterization of a human osteosarcoma cell line (Saos-2) with osteoblastic properties. Cancer Res. 47, 4961–4966.

Rogina, A., 2014. Electrospinning process: Versatile preparation method for biodegradable and natural polymers and biocomposite systems applied in tissue engineering and drug delivery. Appl. Surf. Sci. 296, 221–230. doi:10.1016/j.apsusc.2014.01.098

Roskoski Jr., R., 2012. ERK1/2 MAP kinases: Structure, function, and regulation. Pharmacol. Res. 66, 105–143. doi:10.1016/j.phrs.2012.04.005

Ruoslahti, E., 1996. Rgd and Other Recognition Sequences for Integrins. Annu. Rev. Cell Dev. Biol. 12, 697–715. doi:10.1146/annurev.cellbio.12.1.697

Ruoslahti, E., Yamaguchi, Y., 1991. Proteoglycans as modulators of growth factor activities. Cell 64, 867–869. doi:10.1016/0092-8674(91)90308-L

Rýglová, Š., Braun, M., Suchý, T., 2017. Collagen and Its Modifications—Crucial Aspects with Concern to Its Processing and Analysis. Macromol. Mater. Eng. n/a-n/a. doi:10.1002/mame.201600460

Saadat, E., Amini, M., Dinarvand, R., Dorkoosh, F.A., 2014. Polymeric micelles based on hyaluronic acid and phospholipids: Design, characterization, and cytotoxicity. J. Appl. Polym. Sci. 131, n/a-n/a. doi:10.1002/app.40944

Safari, J., Zarnegar, Z., 2014. Advanced drug delivery systems: Nanotechnology of health design A review. J. Saudi Chem. Soc. 18, 85–99. doi:10.1016/j.jscs.2012.12.009

Sahu, B.D., Tatireddy, S., Koneru, M., Borkar, R.M., Kumar, J.M., Kuncha, M., Srinivas, R., Sistla, R., others, 2014. Naringin ameliorates gentamicin-induced nephrotoxicity and associated mitochondrial dysfunction, apoptosis and inflammation in rats: possible mechanism of nephroprotection. Toxicol. Appl. Pharmacol. 277, 8–20.

Salasznyk, R.M., Klees, R.F., Hughlock, M.K., Plopper, G.E., 2004a. ERK Signaling Pathways Regulate the Osteogenic Differentiation of Human Mesenchymal Stem Cells on Collagen I and Vitronectin. Cell Commun. Adhes. 11, 137–153. doi:10.1080/15419060500242836

Salasznyk, R.M., Klees, R.F., Williams, W.A., Boskey, A., Plopper, G.E., 2007. Focal adhesion kinase signaling pathways regulate the osteogenic differentiation of human mesenchymal stem cells. Exp. Cell Res. 313, 22–37. doi:10.1016/j.yexcr.2006.09.013

Salasznyk, R.M., Williams, W.A., Boskey, A., Batorsky, A., Plopper, G.E., 2004b. Adhesion to Vitronectin and Collagen I Promotes Osteogenic Differentiation of Human Mesenchymal Stem Cells. BioMed Res. Int. 2004, 24–34. doi:10.1155/S1110724304306017

Sánchez-Duffhues, G., Hiepen, C., Knaus, P., ten Dijke, P., 2015. Bone morphogenetic protein signaling in bone homeostasis. Bone, Muscle Bone Interactions 80, 43–59. doi:10.1016/j.bone.2015.05.025

Saoncella, S., Echtermeyer, F., Denhez, F., Nowlen, J.K., Mosher, D.F., Robinson, S.D., Hynes, R.O., Goetinck, P.F., 1999. Syndecan-4 signals cooperatively with integrins in a Rhodependent manner in the assembly of focal adhesions and actin stress fibers. Proc. Natl. Acad. Sci. 96, 2805–2810. doi:10.1073/pnas.96.6.2805

Sasaki, T., Takagi, M., Soma, T., Yoshida, T., 2002. 3D culture of murine hematopoietic cells with spatial development of stromal cells in nonwoven fabrics. Cytotherapy 4, 285–291.

Schlapp, M., Friess, W., 2003. Collagen/PLGA microparticle composites for local controlled delivery of gentamicin. J. Pharm. Sci. 92, 2145–2151. doi:10.1002/jps.10460

Schuldiner, M., Yanuka, O., Itskovitz-Eldor, J., Melton, D.A., Benvenisty, N., 2000. Effects of eight growth factors on the differentiation of cells derived from human embryonic stem cells. Proc. Natl. Acad. Sci. 97, 11307–11312. doi:10.1073/pnas.97.21.11307

Schumacher, M., Uhl, F., Detsch, R., Deisinger, U., Ziegler, G., 2010. Static and dynamic cultivation of bone marrow stromal cells on biphasic calcium phosphate scaffolds derived from an indirect rapid prototyping technique. J. Mater. Sci. Mater. Med. 21, 3039–3048.

Segalés, J., Perdiguero, E., Muñoz-Cánoves, P., 2016. Regulation of Muscle Stem Cell Functions: A Focus on the p38 MAPK Signaling Pathway. Front. Cell Dev. Biol. 4, 91. doi:10.3389/fcell.2016.00091

Sell, S.A., Francis, M.P., Garg, K., McClure, M.J., Simpson, D.G., Bowlin, G.L., 2008. Cross-linking methods of electrospun fibrinogen scaffolds for tissue engineering applications. Biomed. Mater. 3, 045001.

Sergé, A., 2016. The Molecular Architecture of Cell Adhesion: Dynamic Remodeling Revealed by Videonanoscopy. Front. Cell Dev. Biol. 4. doi:10.3389/fcell.2016.00036

Shin, H., Jo, S., Mikos, A.G., 2003. Biomimetic materials for tissue engineering. Biomaterials, Synthesis of Biomimetic Polymers 24, 4353–4364. doi:10.1016/S0142-9612(03)00339-9

Sieg, D.J., Hauck, C.R., Ilic, D., Klingbeil, C.K., Schaefer, E., Damsky, C.H., Schlaepfer, D.D., 2000. FAK integrates growth-factor and integrin signals to promote cell migration. Nat. Cell Biol. 2, 249–256. doi:10.1038/35010517

Simchi, A., Tamjid, E., Pishbin, F., Boccaccini, A.R., 2011. Recent progress in inorganic and composite coatings with bactericidal capability for orthopaedic applications. Nanomedicine Nanotechnol. Biol. Med. 7, 22–39. doi:10.1016/j.nano.2010.10.005

Song, X., Ling, F., Ma, L., Yang, C., Chen, X., 2013. Electrospun hydroxyapatite grafted poly(l-lactide)/poly(lactic-co-glycolic acid) nanofibers for guided bone regeneration membrane. Compos. Sci. Technol. 79, 8–14. doi:10.1016/j.compscitech.2013.02.014

Sonseca, A., Peponi, L., Sahuquillo, O., Kenny, J.M., Giménez, E., 2012. Electrospinning of biodegradable polylactide/hydroxyapatite nanofibers: study on the morphology, crystallinity structure and thermal stability. Polym. Degrad. Stab. 97, 2052–2059.

Stops, A.J.F., Heraty, K.B., Browne, M., O'Brien, F.J., McHugh, P.E., 2010. A prediction of cell differentiation and proliferation within a collagen–glycosaminoglycan scaffold subjected to mechanical strain and perfusive fluid flow. J. Biomech. 43, 618–626. doi:10.1016/j.jbiomech.2009.10.037

Streuli, C., 1999. Extracellular matrix remodelling and cellular differentiation. Curr. Opin. Cell Biol. 11, 634–640. doi:10.1016/S0955-0674(99)00026-5

Subbiahdoss, G., Kuijer, R., Grijpma, D.W., van der Mei, H.C., Busscher, H.J., 2009. Microbial biofilm growth vs. tissue integration: "The race for the surface" experimentally studied. Acta Biomater. 5, 1399–1404. doi:10.1016/j.actbio.2008.12.011

Suchý, T., Šupová, M., Klapková, E., Adamková, V., Závora, J., Žaloudková, M., Rýglová, Š., Ballay, R., Denk, F., Pokorný, M., Sauerová, P., Hubálek Kalbáčová, M., Horný, L., Veselý, J., Voňavková, T., Průša, R., 2017. The release kinetics, antimicrobial activity and cytocompatibility of differently prepared

collagen/hydroxyapatite/vancomycin layers: Microstructure vs. nanostructure. Eur. J. Pharm. Sci. 100, 219–229. doi:10.1016/j.ejps.2017.01.032

Sugo, K., Uchida, K., Naruse, K., Uchino, M., Hirakawa, N., Toyama, M., Miyajima, G., Ikeda, S., Urabe, K., 2016. ELUTION MECHANISM OF VANCOMYCIN AND GENTAMICIN FROM CALCIUM PHOSPHATE CEMENT. Phosphorus Res. Bull. 32, 1–4.

Sundin, M., Ringdén, O., Sundberg, B., Nava, S., Götherström, C., Blanc, K.L., 2007. No alloantibodies against mesenchymal stromal cells, but presence of anti-fetal calf serum antibodies, after transplantation in allogeneic hematopoietic stem cell recipients. Haematologica 92, 1208–1215. doi:10.3324/haematol.11446

Šupová, M., Suchý, T., 2015. Chapter 2 - Bio-nanoceramics and Bio-nanocomposites, in: Handbook of Nanoceramic and Nanocomposite Coatings and Materials. Butterworth-Heinemann, pp. 29–58. doi:10.1016/B978-0-12-799947-0.00002-X

Swinehart, I.T., Badylak, S.F., 2016. Extracellular matrix bioscaffolds in tissue remodeling and morphogenesis. Dev. Dyn. 245, 351–360. doi:10.1002/dvdy.24379

Tabar, V., Studer, L., 2014. Pluripotent stem cells in regenerative medicine: challenges and recent progress. Nat. Rev. Genet. 15, 82–92. doi:10.1038/nrg3563

Takahashi, K., Yamanaka, S., 2006. Induction of Pluripotent Stem Cells from Mouse Embryonic and Adult Fibroblast Cultures by Defined Factors. Cell 126, 663–676. doi:10.1016/j.cell.2006.07.024

Taubenberger, A.V., Woodruff, M.A., Bai, H., Muller, D.J., Hutmacher, D.W., 2010. The effect of unlocking RGD-motifs in collagen I on pre-osteoblast adhesion and differentiation. Biomaterials 31, 2827–2835. doi:10.1016/j.biomaterials.2009.12.051

Tian, X.-F., Heng, B.-C., Ge, Z., Lu, K., Rufaihah, A.J., Fan, V.T.-W., Yeo, J.-F., Cao, T., 2008. Comparison of osteogenesis of human embryonic stem cells within 2D and 3D culture systems. Scand. J. Clin. Lab. Invest. 68, 58–67. doi:10.1080/00365510701466416

Torchilin, V.P., 2001. Structure and design of polymeric surfactant-based drug delivery systems. J. Controlled Release 73, 137–172. doi:10.1016/S0168-3659(01)00299-1

Uccelli, A., Moretta, L., Pistoia, V., 2008. Mesenchymal stem cells in health and disease. Nat. Rev. Immunol. 8, 726–736. doi:10.1038/nri2395

Ulloa-Montoya, F., Verfaillie, C.M., Hu, W.-S., 2005. Culture systems for pluripotent stem cells. J. Biosci. Bioeng. 100, 12–27. doi:10.1263/jbb.100.12

Vago, R., Plotquin, D., Bunin, A., Sinelnikov, I., Atar, D., Itzhak, D., 2002. Hard tissue remodeling using biofabricated coralline biomaterials. J. Biochem. Biophys. Methods 50, 253–259. doi:10.1016/S0165-022X(01)00235-4

van der Smissen, A., Hoffmeister, P.-G., Friedrich, N., Watarai, A., Hacker, M.C., Schulz-Siegmund, M., Anderegg, U., 2015. Artificial extracellular matrices support cell growth and matrix synthesis of human dermal fibroblasts in macroporous 3D scaffolds. J. Tissue Eng. Regen. Med. n/a-n/a. doi:10.1002/term.2037

van der Valk, J., Brunner, D., De Smet, K., Fex Svenningsen, Å., Honegger, P., Knudsen, L.E., Lindl, T., Noraberg, J., Price, A., Scarino, M.L., Gstraunthaler, G., 2010. Optimization of chemically defined cell culture media – Replacing fetal bovine serum in mammalian in vitro methods. Toxicol. In Vitro 24, 1053–1063. doi:10.1016/j.tiv.2010.03.016

van der Valk, J., Mellor, D., Brands, R., Fischer, R., Gruber, F., Gstraunthaler, G., Hellebrekers, L., Hyllner, J., Jonker, F.H., Prieto, P., Thalen, M., Baumans, V., 2004. The humane collection of fetal bovine serum and possibilities for serum-free cell and tissue culture. Toxicol. In Vitro 18, 1–12. doi:10.1016/j.tiv.2003.08.009

Van Vlierberghe, S., Dubruel, P., Schacht, E., 2011. Biopolymer-based hydrogels as scaffolds for tissue engineering applications: a review. Biomacromolecules 12, 1387–1408.

Vandenbroucke, R.E., Libert, C., 2014. Is there new hope for therapeutic matrix metalloproteinase inhibition? Nat. Rev. Drug Discov. 13, 904–927. doi:10.1038/nrd4390

Ventre, M., Natale, C.F., Rianna, C., Netti, P.A., 2014. Topographic cell instructive patterns to control cell adhesion, polarization and migration. J. R. Soc. Interface 11, 20140687. doi:10.1098/rsif.2014.0687

Venugopal, J., Ramakrishna, S., 2005. Applications of Polymer Nanofibers in Biomedicine and Biotechnology. Appl. Biochem. Biotechnol. 125, 147–158. doi:10.1385/ABAB:125:3:147

Verdanova, M., Broz, A., Kalbac, M., Kalbacova, M., 2012. Influence of oxygen and hydrogen treated graphene on cell adhesion in the presence or absence of fetal bovine serum. Phys. Status Solidi B 249, 2503–2506. doi:10.1002/pssb.201200099

Vodička, P., Smetana, K., Dvořánková, B., Emerick, T., Xu, Y.Z., Ourednik, J., Ourednik, V., Motlík, J., 2005. The Miniature Pig as an Animal Model in Biomedical Research. Ann. N. Y. Acad. Sci. 1049, 161–171. doi:10.1196/annals.1334.015

Volkmer, E., Drosse, I., Otto, S., Stangelmayer, A., Stengele, M., Kallukalam, B.C., Mutschler, W., Schieker, M., 2008. Hypoxia in Static and Dynamic 3D Culture Systems for Tissue Engineering of Bone. Tissue Eng. Part A 14, 1331–1340. doi:10.1089/ten.tea.2007.0231

Waeiss, R.A., Negrini, T.C., Arthur, R.A., Bottino, M.C., 2014. Antimicrobial Effects of Drug-Containing Electrospun Matrices on Osteomyelitis-Associated Pathogens. J. Oral Maxillofac. Surg. 72, 1310–1319. doi:10.1016/j.joms.2014.01.007

Walters, B.D., Stegemann, J.P., 2014. Strategies for directing the structure and function of three-dimensional collagen biomaterials across length scales. Acta Biomater., Biological Materials 10, 1488–1501. doi:10.1016/j.actbio.2013.08.038

Walters, N.J., Gentleman, E., 2015. Evolving insights in cell–matrix interactions: Elucidating how non-soluble properties of the extracellular niche direct stem cell fate. Acta Biomater. 11, 3–16. doi:10.1016/j.actbio.2014.09.038

Wang, H., Lee, J.-K., Moursi, A., Lannutti, J.J., 2003. Ca/P ratio effects on the degradation of hydroxyapatite in vitro. J. Biomed. Mater. Res. A 67A, 599–608. doi:10.1002/jbm.a.10538

Wang, M., 2003. Developing bioactive composite materials for tissue replacement. Biomaterials, Focus on Biomaterials Science in Asia 24, 2133–2151. doi:10.1016/S0142-9612(03)00037-1

Wang, N., Butler, J.P., Ingber, D.E., 1993. Mechanotransduction across the cell surface and through the cytoskeleton. Science 260, 1124–1127.

Wang, S., Liu, Y., Fang, D., Shi, S., 2007. The miniature pig: a useful large animal model for dental and orofacial research. Oral Dis. 13, 530–537. doi:10.1111/j.1601-0825.2006.01337.x

Wang, X., Yan, C., Ye, K., He, Y., Li, Z., Ding, J., 2013. Effect of RGD nanospacing on differentiation of stem cells. Biomaterials 34, 2865–2874. doi:10.1016/j.biomaterials.2013.01.021

Wei, G., Ma, P.X., 2009. Partially nanofibrous architecture of 3D tissue engineering scaffolds. Biomaterials 30, 6426–6434.

Wei, J., Igarashi, Toshio, Okumori, N., Igarashi, Takayasu, Maetani, T., Liu, B., Masao Yoshinari, 2009. Influence of surface wettability on competitive protein adsorption and initial attachment of osteoblasts. Biomed. Mater. 4, 045002. doi:10.1088/1748-6041/4/4/045002

Weiner, S., Wagner, and H.D., 1998. THE MATERIAL BONE: Structure-Mechanical Function Relations. Annu. Rev. Mater. Sci. 28, 271–298. doi:10.1146/annurev.matsci.28.1.271

Wen, J.H., Vincent, L.G., Fuhrmann, A., Choi, Y.S., Hribar, K.C., Taylor-Weiner, H., Chen, S., Engler, A.J., 2014. Interplay of matrix stiffness and protein tethering in stem cell differentiation. Nat. Mater. 13, 979–987. doi:10.1038/nmat4051

Williams, C.M., Engler, A.J., Slone, R.D., Galante, L.L., Schwarzbauer, J.E., 2008. Fibronectin Expression Modulates Mammary Epithelial Cell Proliferation during Acinar Differentiation. Cancer Res. 68, 3185–3192. doi:10.1158/0008-5472.CAN-07-2673

Williams, D., 2003. Revisiting the definition of biocompatibility. Med. Device Technol. 14, 10–13.

Wilson, C.J., Clegg, R.E., Leavesley, D.I., Pearcy, M.J., 2005. Mediation of Biomaterial–Cell Interactions by Adsorbed Proteins: A Review. Tissue Eng. 11, 1–18. doi:10.1089/ten.2005.11.1

Wolf, K., Alexander, S., Schacht, V., Coussens, L.M., von Andrian, U., van Rheenen, J., Deryugina, E., Friedl, P., 2009. Collagen-based cell migration models in vitro and in vivo. Semin. Cell Dev. Biol. 20, 931–941. doi:10.1016/j.semcdb.2009.08.005

Wollensak, G., Spoerl, E., 2004. Collagen crosslinking of human and porcine sclera. J. Cataract Refract. Surg. 30, 689–695. doi:10.1016/j.jcrs.2003.11.032

Wu, J., Wei, R., Wang, H., Li, T., Ren, W., 2013. Underlying the mechanism of vancomycin and human serum albumin interaction: a biophysical study. J. Biochem. Mol. Toxicol. 27, 463–470. doi:10.1002/jbt.21511

Wu, Y., Yang, Z., Law, J.B.K., He, A.Y., Abbas, A.A., Denslin, V., Kamarul, T., Hui, J.H.., Lee, E.H., 2016. The Combined Effect of Substrate Stiffness and Surface Topography on Chondrogenic Differentiation of Mesenchymal Stem Cells. Tissue Eng. Part A 23, 43–54. doi:10.1089/ten.tea.2016.0123

Xiao, G., Gopalakrishnan, R., Jiang, D., Reith, E., Benson, M.D., Franceschi, R.T., 2002. Bone Morphogenetic Proteins, Extracellular Matrix, and Mitogen-Activated Protein Kinase Signaling Pathways Are Required for Osteoblast-Specific Gene Expression and Differentiation in MC3T3-E1 Cells. J. Bone Miner. Res. 17, 101–110. doi:10.1359/jbmr.2002.17.1.101

Xu, B., Ju, Y., Song, G., 2014. Role of p38, ERK1/2, focal adhesion kinase, RhoA/ROCK and cytoskeleton in the adipogenesis of human mesenchymal stem cells. J. Biosci. Bioeng. 117, 624–631. doi:10.1016/j.jbiosc.2013.10.018

Xu, H., Bihan, D., Chang, F., Huang, P.H., Farndale, R.W., Leitinger, B., 2012. Discoidin Domain Receptors Promote α1β1- and α2β1-Integrin Mediated Cell Adhesion to Collagen by Enhancing Integrin Activation. PLoS ONE 7, e52209. doi:10.1371/journal.pone.0052209

Yao, C.-H., Liu, B.-S., Hsu, S.-H., Chen, Y.-S., Tsai, C.-C., 2004. Biocompatibility and biodegradation of a bone composite containing tricalcium phosphate and genipin crosslinked gelatin. J. Biomed. Mater. Res. A 69A, 709–717. doi:10.1002/jbm.a.30045

Yu, J., Vodyanik, M.A., Smuga-Otto, K., Antosiewicz-Bourget, J., Frane, J.L., Tian, S., Nie, J., Jonsdottir, G.A., Ruotti, V., Stewart, R., Slukvin, I.I., Thomson, J.A., 2007. Induced Pluripotent Stem Cell Lines Derived from Human Somatic Cells. Science 318, 1917–1920. doi:10.1126/science.1151526

Zaidel-Bar, R., Ballestrem, C., Kam, Z., Geiger, B., 2003. Early molecular events in the assembly of matrix adhesions at the leading edge of migrating cells. J. Cell Sci. 116, 4605–4613. doi:10.1242/jcs.00792

Zaidel-Bar, R., Cohen, M., Addadi, L., Geiger, B., 2004. Hierarchical assembly of cell–matrix adhesion complexes. Biochem. Soc. Trans. 32, 416–420. doi:10.1042/bst0320416

Zhang, Q., Lu, H., Kawazoe, N., Chen, G., 2014. Pore size effect of collagen scaffolds on cartilage regeneration. Acta Biomater. 10, 2005–2013. doi:10.1016/j.actbio.2013.12.042

Zhang, R., Ma, P.X., 1999. Poly (α-hydroxyl acids)/hydroxyapatite porous composites for bone-tissue engineering. I. Preparation and morphology.

Zhang, S., Ermann, J., Succi, M.D., Zhou, A., Hamilton, M.J., Cao, B., Korzenik, J.R., Glickman, J.N., Vemula, P.K., Glimcher, L.H., Traverso, G., Langer, R., Karp, J.M., 2015. An inflammation-targeting hydrogel for local drug delivery in inflammatory bowel disease. Sci. Transl. Med. 7, 300ra128-300ra128. doi:10.1126/scitranslmed.aaa5657

Zhang, X., Chen, X., Yang, T., Zhang, N., Dong, L., Ma, S., Liu, X., Zhou, M., Li, B., 2014. The effects of different crossing-linking conditions of genipin on type I collagen scaffolds: an in vitro evaluation. Cell Tissue Bank. 15, 531–541.

Zhang, Z.-Y., Teoh, S.H., Teo, E.Y., Khoon Chong, M.S., Shin, C.W., Tien, F.T., Choolani, M.A., Chan, J.K.Y., 2010. A comparison of bioreactors for culture of fetal mesenchymal stem cells for bone tissue engineering. Biomaterials 31, 8684–8695. doi:10.1016/j.biomaterials.2010.07.097

Zimmerman, E., Geiger, B., Addadi, L., 2002. Initial stages of cell-matrix adhesion can be mediated and modulated by cell-surface hyaluronan. Biophys. J. 82, 1848–1857. doi:10.1016/S0006-3495(02)75535-5

Zollinger, A.J., Smith, M.L., 2016. Fibronectin, the extracellular glue. Matrix Biol. J. Int. Soc. Matrix Biol. doi:10.1016/j.matbio.2016.07.011

# 10 ORIGINAL PUBLICATIONS USED FOR PH.D. THESIS IN FULL

**A. Pavla Sauerová**, Martina Verdánová, Filip Mravec, Tereza Pilgrová, Tereza Venerová, Marie Hubálek Kalbáčová , Miloslav Pekař (2015): **Hyaluronic Acid as a Modulator of the Cytotoxic Effects of Cationic Surfactants.** Colloids and Surfaces A: Physicochem. Eng. Aspects 483, 155-161. IF = 2.752

Colloids and Surfaces A: Physicochem. Eng. Aspects 483 (2015) 155–161

Contents lists available at ScienceDirect

Colloids and Surfaces A: Physicochemical and Engineering Aspects

journal homepage: www.elsevier.com/locate/colsurfa

# Hyaluronic acid as a modulator of the cytotoxic effects of cationic surfactants

Pavla Sauerová[a], Martina Verdánová[b,c], Filip Mravec[d], Tereza Pilgrová[d], Tereza Venerová[d], Marie Hubálek Kalbáčová[a,c,e], Miloslav Pekař[d,*]

[a] Biomedical Centre, Faculty of Medicine in Pilsen, Charles University in Prague, alej Svobody 1655/76, Pilsen 323 00, Czech Republic
[b] Department of Genetics and Microbiology, Faculty of Science, Charles University in Prague, Albertov 6, Prague 2 128 43, Czech Republic
[c] Institute of Inherited Metabolic Disorders, 1st Faculty of Medicine, Charles University in Prague, Ke Karlovu 2, Prague 2 128 08, Czech Republic
[d] Materials Research Centre, Faculty of Chemistry, Brno University of Technology, Purkyňova 464/118, Brno 612 00, Czech Republic
[e] Department of Histology and Embryology, Faculty of Medicine in Pilsen, Charles University in Prague, Karlovarská 48, Pilsen 301 66, Czech Republic

## HIGHLIGHTS

- Surfactants (CTAB and Septonex) are toxic for osteoblasts.
- When complexed with hyaluronan their cytotoxicity is suppressed.
- Fetal bovine serum plays a positive role in the cytotoxicity suppression.

## GRAPHICAL ABSTRACT

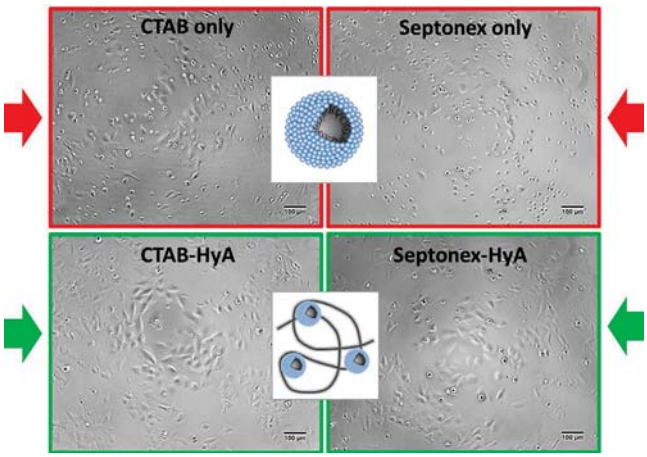


## ARTICLE INFO

*Article history:*
Received 18 May 2015
Accepted 29 June 2015
Available online 17 July 2015

*Keywords:*
Cytotoxicity
Cell metabolic activity
Human osteoblasts
Hyaluronan
Surfactant
CTAB
Septonex

## ABSTRACT

CTAB (cetyltrimethylammonium bromide) and Septonex (carbethoxypendecinium bromide) are cationic surfactants known for harmful effects on different cell types (bacteria, fungi, mammal cells, etc.). Colloidal complexes of CTAB or Septonex with oppositely charged hyaluronic acid (HyA), based primarily on electrostatic interactions, were prepared with the aim to test potential modulation of surfactants cytotoxic effects. Complexes were tested for their cytotoxicity on human osteoblasts—the cell metabolic activity was determined after 24 h of treatment. Our data show that CTAB–HyA or Septonex–HyA complexes reduce (in different rate according to the used surfactant and HyA concentrations) cytotoxicity of both surfactants in all tested concentrations. In addition, a significant role of fetal bovine serum (important supplement of cell culture medium) in cell recovery under the stress conditions like CTAB or Septonex presence was observed. Taken together, HyA could be a useful modulator of CTAB or Septonex effects on cells at diverse levels. Drug or nucleic acid delivery system, diagnostic dye carriers or cosmetic industry are the possible applications of prepared complexes.



* Corresponding author.
*E-mail address:* pekar@fch.vutbr.cz (M. Pekař).

http://dx.doi.org/10.1016/j.colsurfa.2015.06.058
0927-7757/

## 1. Introduction

Cationic surfactants are known for their cytotoxic properties [1–4] but due to their interactions with negatively charged substances – some kinds of drugs, nucleic acids, cellular surfaces, etc. – they can serve as an interesting tool in drug or gene cell delivery, for the study of cell trafficking processes, or in other cell structure visualisation techniques. The ability to form micelles is another positive property of surfactants and a benefit which is used in drug carriers [5]. Cetyltrimethylammonium bromide (CTAB), in particular, is commonly used as a compound in drug delivery systems; for example, it is an ideal "shape-inducing" agent [6]. In general, it is known that cationic surfactants exhibit the highest cytotoxicity in comparison to anionic and non-ionic ones [7]. In spite of this, several studies have shown the anticancer effect of CTAB or other molecules containing the quaternary ammonium group [8–11]. Additionally, it was showed that these surfactants can behave as cytotoxic agents in dependence on the target cell type – surfactants were substantially cytotoxic to non-polarized cells in contrast to polarized cells [12]. Interestingly, it was shown that CTAB cytotoxicity can be depressed by polymers: Alkilany et al. reduced the CTAB-induced cytotoxicity of a CTAB-capped nanorods solution by PAA (polyacrylic acid) polymer over-coating [13].

The ideal polymer for our study, aimed at surfactant cytotoxicity modulation by forming complexes with oppositely charged biopolymer, appeared to be hyaluronan (HyA), because in our previous study, the reduction of the cytotoxic effects of CTAB on specific cell types in the presence of free sodium hyaluronate (HyA) was described [14]. Hyaluronan is a naturally occurring glycosaminoglycan composed of repeating β-1,4-D-glucuronic acid and β-1,3-*N*-acetyl-D-glucosamine disaccharide subunits [15]. HyA exhibits a wide spectrum of functions at various organism levels [16] and due to its favourable properties – biocompatibility, biodegradability, unique biomechanical features, and modifiability (functional groups) – HyA is called a biomaterial of the near future. Many HyA functions are conditioned by interactions with HyA-binding proteins, which are specific to the place of concrete HyA action [17–20].

As mentioned above, surfactants cytotoxicity could be regulated when complexed with hyaluronan. However, HyA in these complexes can play more roles, not only cell protecting but also it can also help the complex to bind onto the cell surface (via its receptors) and subsequently to move within the cell. Thus, the surfactant-HyA complex can serve as a carrier of non-polar drugs solubilized within the cores of surfactant micelles. HyA is degraded by hyaluronidases (Hyals), especially Hyal1 and Hyal2. Extracellular HyA is attached to Hyal2 anchored in the cell membrane and then cleaved [21]. It seems that this process is in cooperation with the HyA receptor CD44. HyA is then transferred into the cell by endocytosis. In lysosomal vesicles, HyA is cleaved again, but by HyAl1 and then by exoglycosidases into monomers [16,22,23]. This pathway alone could be a way for the delivery of complexes to cells. The effects of HyA on cells have been well described, mostly thanks to its wide medical applications and the needs of regenerative medicine [24–31].

In this work, CTAB–HyA and Septonex–HyA complexes were prepared and their cytotoxicity was determined in comparison to native surfactants. In contrast to the previous study [14], in which the surfactant and hyaluronan were added to cells separately one at a time, the pre-prepared surfactant–HyA complexes were applied on cells. Further, Septonex, a structural analogue of CTAB, was also investigated. In addition, we were interested in the role of fetal bovine serum (FBS) in the ability of cells to overcome stress conditions (i.e. the presence of native surfactants or surfactants–HyA complexes). FBS (the blood fraction after clotting, free of blood cell elements) is a crucial component of the cell growth medium because it provides supplements important for cell cultivation in vitro (for adhesion, division, survival etc.). However, the major compound of FBS, bovine serum albumin, is known to interact with various molecules (it provides a variety of binding sites for both hydrophobic and negatively charged hydrophilic moieties), and the behaviour of surfactants in complexes could be affected by this protein [33,34]. Moreover, it has already been demonstrated that cell behaviour and morphology can be substantially influenced by the presence or absence of FBS in general [14,35].

Surfactants with regulated cytotoxicity might play a role in drug, gene, or diagnostic dye carriers (thanks to the use of the natural HyA-transport system) and could exhibit only a moderate and controllable antiseptic activity (thanks to HyA's protective activity). The results could help to raise the profile of surfactant–HyA complexes with respect to their use in practical cell biology and clinical applications.

**Table 1**
Composition of hyaluronan–surfactant complexes and their zeta potential (values in parentheses represent the standard deviation).

| CTAB (mM) | HyA (mg/l) | Zeta potential (mV) |
|---|---|---|
| 0.04 | 5 | −14(2) |
| 0.05 | 5 | −8(2) |
| 0.05 | 30 | −15(2) |
| 0.05 | 50 | −34(5) |
| 0.08 | 30 | −29(1) |
| 0.08 | 50 | −19(5) |
| 0.10 | 30 | −26(1) |
| 0.10 | 50 | −28(4) |
| **Septonex (mM)** | **HyA (g/l)** | **Zeta potential (mV)** |
| 0.03 | 1 | −70(1) |
| 0.06 | 1 | −72(2) |
| 0.08 | 1 | −68(3) |

## 2. Materials and methods

### 2.1. Surfactants and hyaluronan

Cetyltrimethylammonium bromide (CTAB) was purchased from Sigma–Aldrich (Czech Republic) and carbethoxypendecinium bromide (Septonex) from GNB chem (Czech Republic), both used as received. Hyaluronan was purchased from Contipro Biotech (Czech Republic); two batches were acquired—one with a weight-average molecular weight of 1000 kDa was used in the preparation of complexes with CTAB, while the other with a weight-average molecular weight of 936 kDa was used in complexes with Septonex.

Solutions of complexes were prepared by mixing hyaluronan and surfactant stock solutions, prepared in deionized water, to obtain the desired final concentration. The surfactant solution was always added dropwise to the hyaluronan solution. In the case of CTAB–hyaluronan complexes, the hyaluronan concentration had to be sufficiently low in order to prevent precipitation and prepare homogeneous solutions of complexes. The concentrations of CTAB in complex solutions were 40, 50, 80 and 100 μM; three hyaluronan concentrations were tested: 5, 30 and 50 mg/l. In the case of Septonex–hyaluronan complexes, only one hyaluronan concentration was used (1 g/l) at three different surfactant concentrations: 30, 60 and 80 μM. Eleven different samples of complexes were thus prepared and used in experiments; their exact composition is given in Table 1.

The prepared complexes were characterized by their particle size distribution (measured by dynamic light scattering) and their zeta potential (measured by laser Doppler micro-electrophoresis) using a Zetasizer Nano ZS (Malvern Instruments, UK).

### 2.2. Cell culture

Human osteoblasts were used because they are a well-established and reproducible cell line suitable for this type of primary testing. The cells were incubated under different conditions for 24 h, when the treated cells were observed using light microscopy. This time period was found to be reasonable to obtain reproducible data and before all cells were destroyed in the presence of surfactants only. SAOS-2 cells (a human osteoblast-like cell line derived from osteosarcoma, obtained from Deutsche Sammlung von Mikroorganismen und Zellkulturen (GmbH) in Germany) were cultured at 37 °C in a 5% $CO_2$ atmosphere and in McCoy's 5A medium without phenol red (PromoCell, Germany) supplemented with 15% heat inactivated FBS (PAA, Austria), penicillin (20 U/ml, Sigma–Aldrich, USA) and streptomycin (20 μg/ml Sigma–Aldrich, USA).

### 2.3. Cell treatment with surfactant–HyA complexes

SAOS-2 cells were suspended using trypsin/EDTA and plated at a concentration of 20,000 cells/cm$^2$ onto a 96-well plate in the above mentioned culture medium and under the abovementioned conditions for 24 h. After 24 h, the cells were treated with complexes diluted 1:9 in fresh medium, with "only HyA", or with "only surfactant" with or without FBS. In the latter, after 4 h of incubation without FBS, FBS was added to a final concentration of 15% (non-standard conditions).

### 2.4. Light microscopy

Phase contrast images of the cells were obtained using an Eclipse Ti-S microscope (Nikon, Japan) and a DS-Qi1Mc DigitalCamera (Nikon). Images were acquired with a 10× lens and adjusted by ImageJ (Rasband, W.S., ImageJ, US National Institutes of Health, Bethesda, Maryland, USA, http://imagej.nih.gov/ij/, 1997–2015) and Cell Profiler (Broad Institute, USA) software. Fig. 1 shows typical examples of obtained images.

### 2.5. Measurement of cell metabolic activity

A metabolic activity test (Cell Titer 96 AQueous One Solution Cell Proliferation Assay, MTS, Promega, USA) was performed according to the standard protocol (the reduction of MTS reagent to a coloured formazan product was induced by viable cells). 24 h after the addition of surfactant, the absorbance was measured in a 96-well plate using a multi-detection micro-plate reader (Synergy™ 2, BioTek, USA). The measured results were expressed relative to the control ("only cells").

### 2.6. Statistical analysis

Results from MTS tests were obtained from two independent experiments performed in four parallels. Data were statistically analysed by the Wilcoxon rang test; the obtained values were tested for statistically significant differences at an alpha level of 0.05. The statistical evaluation was performed using Statistica (StatSoft CR, s.r.o.) and Microsoft Excel software.

## 3. Results and discussion

Our previous study [14] revealed that osteoblasts treated with low CTAB concentrations did not show significantly reduced cell viability; however, their metabolic activity decreased with increasing CTAB concentrations. A 1 mM or higher CTAB concentration caused a dramatic reduction in cell metabolic activity. Adding HyA to the medium CTAB cytotoxicity was moderated, but only at the low CTAB concentration (not exceeding 0.2 mM). Consequently, low surfactant concentrations were used in the present work. These low concentrations were also dictated by the effort to avoid the precipitation of hyaluronan–surfactant aggregates which occurs at elevated surfactant concentrations [36,37] and to obtain clear colloidal solutions of hyaluronan–surfactant complexes.

In contrast to the previous study [14], the surfactant and hyaluronan were added to cells just in the form of the pre-prepared complexes. The formation of complexes between oppositely charged surfactants and polyelectrolytes, mainly on the basis of their electrostatic interactions, is a well-known fact [32,36,37]. The complexes were characterized by the two parameters relevant for their supposed interactions with cells—the size and charge. Measurements of particle sizes showed no clear dependence on concentration; all complexes were polydisperse with a main peak around 30 nm and a minor peak around 250 nm. A typical example of the measured size distribution is given in Fig. S1 in Supplementary material. Because the surfactant concentrations were well below their standard critical micellar concentrations, the polydispersity is believed to have been caused essentially by the presence of hyaluronan chains containing different numbers of attached induced micelles or even by the presence of structures formed by several biopolymer chains attached to the same induced micellar structure. The induced micelles are the micellar structures which are formed in solutions containing a polyelectrolyte and an oppositely charged surfactant at a concentration lower than their critical micellar concentration [32]. Zeta potential values are given in Table 1. They had negative values in all cases, indicating the prevailing negative charge of the complexes. This is an indication of the "elimination" of the surfactant's positive charges by interactions with hyaluronan. Complexes prepared from Septonex had significantly lower values due to the higher concentration of anionic hyaluronan. In the case of CTAB-based complexes, a lower hyaluronan concentration usually resulted in increased values of zeta potential. A typical example of the measured zeta potential distribution is shown in Fig. S2 in Supplementary material.

Fig. 2 shows that under standard conditions, the metabolic activity of cells treated with all of the used "only CTAB" concentrations was significantly decreased in comparison to the "only cells" control. Levels of cell metabolic activity after 4 μM or 5 μM CTAB treatments reached 75% or 80%, respectively. This is on the edge of cytotoxicity. Cytotoxicity is often defined by a drop in cell metabolic activity to under 75% [38], thus 8 μM or 10 μM CTAB concentrations (cf. Fig. 2) were already determined to be cytotoxic (inducing cell viabilities of 72% or 59%, respectively). The lowest HyA concentration (0.5 mg/l) was able to reduce the negative effect of "only CTAB" at its lowest concentration (4 μM). Higher HyA concentrations (3 mg/l and 5 mg/l) were able to significantly reduce the negative effects of all higher CTAB concentrations (5 μM, 8 μM and 10 μM). The contrast between the protective effects of the lowest and higher HyA concentrations is clearly apparent at the 5 μM concentration of CTAB and its complexes (see Fig. 2). As shown in the graph, the regenerative ability of HyA increased proportionally with the increase in CTAB concentration. All "only HyA" concentrations exhibited a positive effect on cell viability. Taken together, statistically significant differences between "only CTAB" and their complex analogues with higher HyA concentrations (3 mg/l and 5 mg/l) were observed in all cases. Thus, HyA in CTAB complexes is able to moderate the cytotoxicity induced by CTAB in general. Our results are more or less analogous to a reduction in CTAB cytotoxicity achieved by coating particles with polymers (specifically PAA) [13]. The moderation of cytotoxicity by HyA could be used for CTAB applications in which this surfactant plays the role of an effective disinfectant [4]. Thus, HyA could be used to regulate surfactant antiseptic effects.

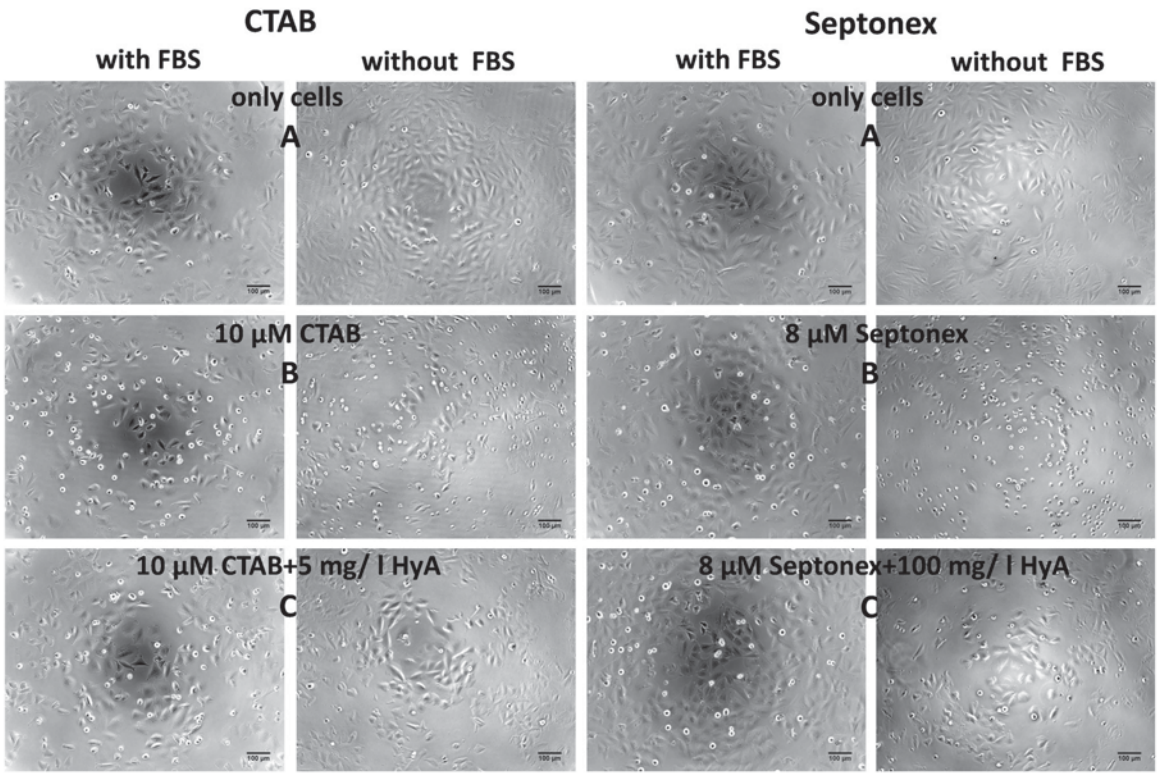


**Fig. 1.** Phase contrast images (10× magnification) of human osteoblasts (SAOS-2) after 24 h treatment with surfactants (CTAB or Septonex (B)) or with complexes of surfactants and HyA (C) in the presence of FBS (with FBS) or in the absence of FBS (without FBS) during first 4 h of cultivation. (A)—untreated cells (only cells).

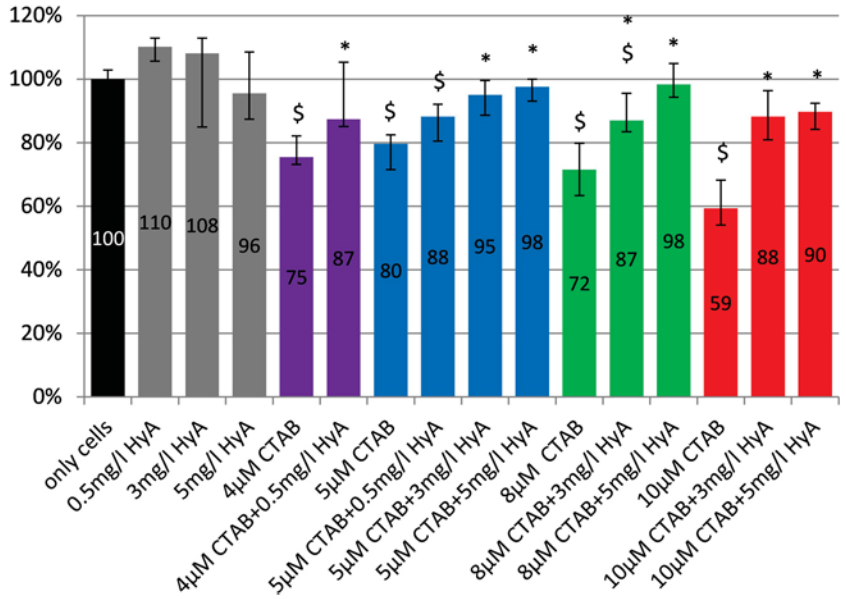


**Fig. 2.** Human osteoblast metabolic activity after 24 h treatment with CTAB or CTAB–HyA complexes. FBS was present during the whole period of treatment (standard conditions). $—significance at alpha level 0.05 compared to control (only cells); *—significance at alpha level 0.05 compared to surfactant alone at the corresponding concentration based on the Wilcoxon rang test.

Results obtained under non-standard conditions with CTAB are shown in Fig. 3. A significant decrease in cell viability in most of the "only CTAB" samples (but not at the 4 µM CTAB concentration) compared to the "only cells" control was observed. Surprisingly, cells under non-standard conditions withstood the presence of 4 µM CTAB better than those under standard conditions, which could be explained by mild stress inducing higher mitochondrial activity (and, hence, the detection of higher metabolic activity). On the other hand, higher CTAB concentrations (5 µM and above) were tolerated by cells under non-standard conditions substantially worse than under standard conditions. This indicates higher cell sensitivity to higher CTAB concentrations under non-standard conditions compared to standard conditions. The differences between "only CTAB" and its complex analogues were statistically significant in all cases. Moreover, the differences were more marked when compared to standard conditions. In contrast to standard

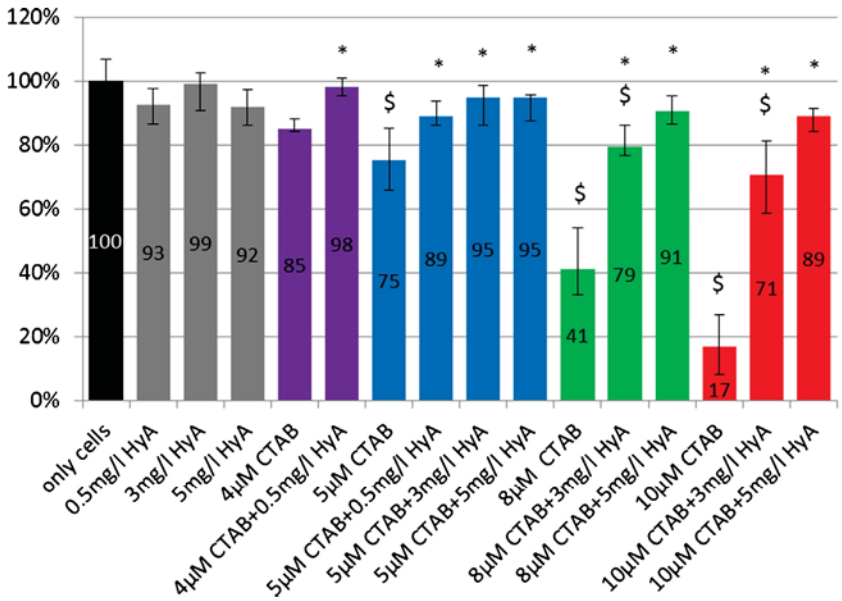


**Fig. 3.** Human osteoblast metabolic activity after 24 h treatment with CTAB or CTAB–HyA complexes. FBS was added after the first 4 h of treatment (non-standard conditions). $—significance at alpha level 0.05 compared to control (only cells); *—significance at alpha level 0.05 compared to surfactant alone at the corresponding concentration based on the Wilcoxon rang test.

conditions, even the lowest HyA concentration (0.5 mg/l) statistically significantly reduced the negative effects caused by the 5 μM CTAB concentration. Higher HyA concentrations (3 mg/l and 5 mg/l) in complexes with CTAB exhibited a highly positive effect on cell metabolic activity—this effect again rose proportionally with increasing CTAB concentration.

Generally, our results obtained with CTAB suggest that (i) cells are more sensitive to CTAB cytotoxicity (at concentrations above 5 μM) in the absence of FBS (non-standard conditions) compared to the setup with FBS present (standard conditions), (ii) FBS plays a positive role under the stress conditions induced by the presence of surfactant, and (iii) the cell protection offered by HyA is greater in the temporary absence of FBS (non-standard conditions). These results are in agreement with those from our previous study [14], in which free HyA was added to CTAB treated cells under standard and non-standard conditions. Furthermore, the protective effect of serum was also previously observed on keratinocytes [39]. FBS positive role could be ascribed to its binding on the cell surface and/or formation of aggregates between the Hya–surfactant complexes and proteinaceous components of serum [14].

Cells under standard conditions treated by Septonex showed a significant decrease in metabolic activity when treated with "only Septonex" and also with all of the Septonex complexes with HyA in comparison to the "only cells" control (see Fig. 4). However, cytotoxicity was observed only at higher concentrations (6 μM and 8 μM). Statistically significantly higher levels of cell viability were observed in all Septonex complexes with HyA compared to "only Septonex". Although these differences were not as apparent as in the case of CTAB, the positive effect of HyA rose proportionally with increasing Septonex concentration. Thus, HyA in complexes was again able to reduce cytotoxicity—in this case, the cytotoxicity induced by Septonex. In addition, the use of a comparable concentration of Septonex and CTAB (8 μM) indicated that Septonex was more cytotoxic. This could point to differences in CTAB and Septonex binding to cell membrane due to their structural differences.

Fig. 5 shows that under non-standard conditions, the data revealed a significant drop in cell metabolic activity under the "only Septonex" treatment and also under all of the Septonex/complex treatments in comparison to the "only cells" control (similarly to standard conditions). Cytotoxicity was observed when Septonex at concentrations of 6 μM and above was used (see Fig. 5). This cytotoxicity was higher under non-standard conditions compared to standard conditions. Nevertheless, significantly higher cell metabolic activities were detected when Septonex complexes were added to cells in comparison to "only Septonex", the one exception being Septonex at a concentration of 3 μM. Interestingly, the cell metabolic activities corresponding to 3 μM Septonex and the 3 μM Septonex–HyA complex were comparable. It seems that 3 μM Septonex under non-standard conditions acted as a mitochondrial activator. It is possible that very low Septonex concentrations could provoke cells to increase their metabolic activity. A similar effect was also observed in a previous study, when low concentrations of detergents caused increases in proliferative activity and mitochondrial metabolism in keratinocytes [39]. The cytotoxicity induced by higher Septonex concentrations (6 μM and 8 μM) was substantially reduced by the presence of HyA—this effect again rose proportionally with increasing Septonex concentration. The trend of metabolic activity in the presence and absence of FBS was similar, but cell viability under non-standard conditions was reduced overall. Thus, similarly to the results obtained for CTAB, a positive effect of FBS on cells treated by Septonex was observed. More significant HyA protection under non-standard conditions compared to standard conditions was also detected. In general, surfactant cytotoxicity reduction induced by HyA under higher surfactant concentrations could be due to the formation of stable micellar structures anchored on the biopolymer chain under these concentration conditions, preventing surfactant molecules from interactions with cell membranes.

Direct comparison with previous results, in which HyA and surfactants were not in the form of complexes, is very difficult due to the differences in concentrations which can be used in the preparation of complexes. The differences in cytotoxicity between plain surfactant and surfactant combined with hyaluronan were found to be more profound if hyualuronan was present in the form of a complex with surfactant. Therefore, it can be generally concluded that the protective effect of hyaluronan is greater when complexed with surfactant.

Taken together, all the presented results indicate the potential of HyA as a useful modulator of CTAB or Septonex induced cytotoxicity.

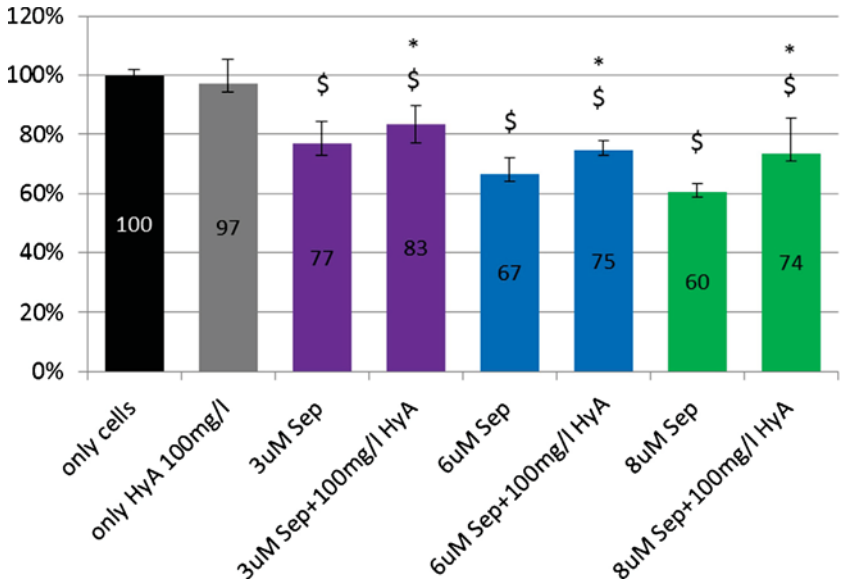


**Fig. 4.** Human osteoblast metabolic activity after 24 h treatment with Septonex or Septonex–HyA complexes. FBS was present during the whole period of treatment (standard conditions). $—significance at alpha level 0.05 compared to control (only cells); *—significance at alpha level 0.05 compared to surfactant alone at the corresponding concentration based on the Wilcoxon rang test.

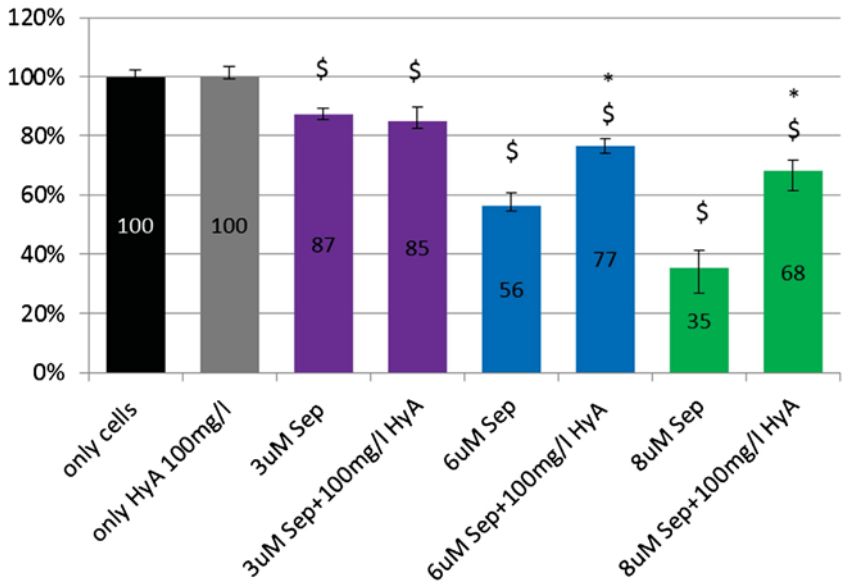


**Fig. 5.** Human osteoblast metabolic activity after 24 h treatment with Septonex or Septonex–HyA complexes. FBS was added after the first 4 h of treatment (non-standard conditions). $—significance at alpha level 0.05 compared to control (only cells); *—significance at alpha level 0.05 compared to surfactant alone at the corresponding concentration based on the Wilcoxon rang test.

## 4. Conclusion

In our study, HyA demonstrated the ability to protect cells against toxic cationic surfactants (CTAB and Septonex) when present in the form of a pre-prepared surfactant–HyA complex. The results also confirm and emphasize the role of FBS in cell response to stress conditions. Cells were more sensitive to surfactant toxicity in the absence of FBS. At the same time, cell protection by HyA was more efficient during the temporary absence of FBS. The combination of HyA and FBS thus provides the most efficient form of cell protection.

## Acknowledgements

This work was supported by COST action CM1101 and projects No. LO1211 funded by the National Sustainability Programme I and LD12068 (Ministry of Education, Czech Republic). The Faculty of Medicine in Pilsen was supported by projects CZ.1.05/2.1.00/03.0076 (European Regional Development Fund) and grant SVV-2015 No. 260170, the 1st Faculty of Medicine by the project PRVOUK-P24/LF1/3, and the Faculty of Science by the project SVV-2015-260209. Special thanks go to Blanka Bílková for technical assistance.

## Appendix A. Supplementary data

Supplementary data associated with this article can be found, in the online version, at http://dx.doi.org/10.1016/j.colsurfa.2015.06.058

## References


[1] Â.S. Inácio, G.N. Costa, N.S. Domingues, M.S. Santos, A.J.M. Moreno, W.L.C. Vaz, O.V. Vieira, Mitochondrial dysfunction is the focus of quaternary ammonium surfactant toxicity to mammalian epithelial cells, Antimicrob. Agents Chemother. 57 (2013) 2631–2639, http://dx.doi.org/10.1128/AAC.02437-12

[2] L. Strakova, Z. Strosova, E. Sevcikova, Septonex color spray—a new disinfectant for the treatment of umbilical stubs (in Czech), Veterinarstvi 34 (1984) 69–70.

[3] K. Nakata, T. Tsuchido, Y. Matsumura, Antimicrobial cationic surfactant, cetyltrimethylammonium bromide, induces superoxide stress in *Escherichiacoli* cells, J. Appl. Microbiol. 110 (2011) 568–579, http://dx.doi.org/10.1111/j.1365-2672.2010.04912.x

[4] O.V. Vieira, D.O. Hartmann, C.M.P. Cardoso, D. Oberdoerfer, M. Baptista, M.A.S. Santos, L. Almeida, J. Ramalho-Santos, W.L.C. Vaz, Y.-S. Bahn, Surfactants as microbicides and contraceptive agents: a systematic in vitro study, PLoS One 3 (2008) e2913, http://dx.doi.org/10.1371/journal.pone.0002913

[5] V.P. Torchilin, Structure and design of polymeric surfactant-based drug delivery systems, J. Control. Release 73 (2001) 137–172, http://dx.doi.org/10.1016/S0168-3659(01)00299-1

[6] I. Pastoriza-Santos, J. Pérez-Juste, L.M. Liz-Marzán, Silica-coating and hydrophobation of CTAB-stabilized gold nanorods, Chem. Mater. 18 (2006) 2465–2467, http://dx.doi.org/10.1021/cm060293g

[7] R.L. Grant, C. Yao, D. Gabaldon, D. Acosta, Evaluation of surfactant cytotoxicity potential by primary cultures of ocular tissues: I. Characterization of rabbit corneal epithelial cells and initial injury and delayed toxicity studies, Toxicology 76 (1992) 153–176, http://dx.doi.org/10.1016/0300-483X(92)90162-8

[8] Q. He, J. Shi, F. Chen, M. Zhu, L. Zhang, An anticancer drug delivery system based on surfactant-templated mesoporous silica nanoparticles, Biomaterials 31 (2010) 3335–3346, http://dx.doi.org/10.1016/j.biomaterials.2010.01.015

[9] I. Giraud, M. Rapp, J.-C. Maurizis, J.-C. Madelmont, Synthesis and in vitro evaluation of quaternary ammonium derivatives of chlorambucil and melphalan, anticancer drugs designed for the chemotherapy of chondrosarcoma, J. Med. Chem. 45 (2002) 2116–2119, http://dx.doi.org/10.1021/jm010926x

[10] E. Ito, K.W. Yip, D. Katz, S.B. Fonseca, D.W. Hedley, S. Chow, G.W. Xu, T.E. Wood, C. Bastianutto, A.D. Schimmer, S.O. Kelley, F.-F. Liu, Potential use of cetrimonium bromide as an apoptosis-promoting anticancer agent for head and neck cancer, Mol. Pharmacol. 76 (2009) 969–983, http://dx.doi.org/10.1124/mol.109.055277

[11] M.J. Weiss, J.R. Wong, C.S. Ha, R. Bleday, R.R. Salem, G.D. Steele, L.B. Chen, Dequalinium, a topical antimicrobial agent, displays anticarcinoma activity based on selective mitochondrial accumulation, Proc. Natl. Acad. Sci. U. S. A. 84 (1987) 5444–5448.

[12] Â.S. Inácio, K.A. Mesquita, M. Baptista, W.L.C. Ramalho-Santos, O.V. Vieira, D.T. Covas, In vitro surfactant structure–toxicity relationships: implications for surfactant use in sexually transmitted infection prophylaxis and contraception, PLoS One 6 (2011) e19850, http://dx.doi.org/10.1371/journal.pone.0019850

[13] A.M. Alkilany, P.K. Nagaria, C.R. Hexel, T.J. Shaw, C.J. Murphy, M.D. Wyatt, Cellular uptake and cytotoxicity of gold nanorods: molecular origin of cytotoxicity and surface effects, Small 5 (2009) 701–708, http://dx.doi.org/10.1002/smll.200801546

[14] M. Kalbáčová, M. Verdánová, F. Mravec, T. Halasová, M. Pekař, Effect of CTAB and CTAB in the presence of hyaluronan on selected human cell types, Colloids Surf. A: Physicochem. Eng. Aspects 460 (2014) 204–208, http://dx.doi.org/10.1016/j.colsurfa.2013.12.048

[15] K. Meyer, Chemical structure of hyaluronic acid, Fed. Proc. 17 (1958) 1075–1077.

[16] K.T. Dicker, L.A. Gurski, S. Pradhan-Bhatt, R.L. Witt, M.C. Farach-Carson, X. Jia, Hyaluronan: a simple polysaccharide with diverse biological functions, Acta Biomater. 10 (2014) 1558–1570, http://dx.doi.org/10.1016/j.actbio.2013.12.019

[17] A. Aruffo, I. Stamenkovic, M. Melnick, C.B. Underhill, B. Seed, CD44 is the principal cell surface receptor for hyaluronate, Cell 61 (1990) 1303–1313, http://dx.doi.org/10.1016/0092-8674(90)90694-A

[18] C.B. Knudson, Hyaluronan and CD44: strategic players for cell–matrix interactions during chondrogenesis and matrix assembly, Birth Defects Res. Part C: Embryo Today: Rev. 69 (2003) 174–196, http://dx.doi.org/10.1002/bdrc.10013

[19] H. Ponta, L. Sherman, P.A. Herrlich, CD4: from adhesion molecules to signalling regulators, Nat. Rev. Mol. Cell Biol. 4 (2003) 33–45, http://dx.doi.org/10.1038/nrm1004

[20] W.F. Cheung, T.F. Cruz, E.A. Turley, Receptor for hyaluronan-mediated motility (RHAMM), a hyaladherin that regulates cell responses to growth factors, Biochem. Soc. Trans. 27 (1999) 8.

[21] G. Lepperdinger, J. Müllegger, G. Kreil, Hyal2—less active, but more versatile? Matrix Biol. 20 (2001) 509–514, http://dx.doi.org/10.1016/S0945-053X(01)00170-6

[22] H. Harada, M. Takahashi, CD44-dependent intracellular and extracellular catabolism of hyaluronic acid by hyaluronidase-1 and -2, J. Biol. Chem. 282 (2007) 5597–5607, http://dx.doi.org/10.1074/jbc.M608358200

[23] E.S.A. Hofinger, J. Hoechstetter, M. Oettl, G. Bernhardt, A. Buschauer, Isoenzyme-specific differences in the degradation of hyaluronic acid by mammalian-type hyaluronidases, Glycoconj. J. 25 (2008) 101–109, http://dx.doi.org/10.1007/s10719-007-9058-8

[24] G.D. Prestwich, Hyaluronic acid-based clinical biomaterials derived for cell and molecule delivery in regenerative medicine, J. Control. Release 155 (2011) 193–199, http://dx.doi.org/10.1016/j.jconrel.2011.04.007

[25] B.P. Toole, Hyaluronan: from extracellular glue to pericellular cue, Nat. Rev. Cancer 4 (2004) 528–539, http://dx.doi.org/10.1038/nrc1391

[26] B.P. Toole, T.N. Wight, M.I. Tammi, Hyaluronan–cell interactions in cancer and vascular disease, J. Biol. Chem. 277 (2002) 4593–4596, http://dx.doi.org/10.1074/jbc.R100039200

[27] J. Lam, W.E. Lowry, S.T. Carmichael, T. Segura, Delivery of iPS-NPCs to the stroke cavity within a hyaluronic acid matrix promotes the differentiation of transplanted cells, Adv. Funct. Mater. 24 (2014) 7053–7062, http://dx.doi.org/10.1002/adfm.201401483

[28] S.K. Seidlits, Z.Z. Khaing, R.R. Petersen, J.D. Nickels, J.E. Vanscoy, J.B. Shear, C.E. Schmidt, The effects of hyaluronic acid hydrogels with tunable mechanical properties on neural progenitor cell differentiation, Biomaterials 31 (2010) 3930–3940, http://dx.doi.org/10.1016/j.biomaterials.2010.01.125

[29] J. Lam, N.F. Truong, T. Segura, Design of cell–matrix interactions in hyaluronic acid hydrogel scaffolds, Acta Biomater. 10 (2014) 1571–1580, http://dx.doi.org/10.1016/j.actbio.2013.07.025

[30] M.J. Wilson, S.J. Liliensiek, C.J. Murphy, W.L. Murphy, P.F. Nealey, Hydrogels with well-defined peptide-hydrogel spacing and concentration: impact on epithelial cell behavior, Soft Matter 8 (2012) 390–398, http://dx.doi.org/10.1039/C1SM06589K

[31] Y. Lee, H. Lee, Y.B. Kim, J. Kim, T. Hyeon, H. Park, P.B. Messersmith, T.G. Park, Bioinspired surface immobilization of hyaluronic acid on monodisperse magnetite nanocrystals for targeted cancer imaging, Adv. Mater. 20 (2008) 4154–4157, http://dx.doi.org/10.1002/adma.200800756

[32] K. Holmberg, B. Jönsson, B. Kronberg, B. Lindman, Surfactants and Polymers in Aqueous Solution, Wiley, Chichester, 2007.

[33] M. Fasano, S. Curry, E. Terreno, M. Galliano, G. Fanali, P. Narciso, S. Notari, P. Ascenzi, The extraordinary ligand binding properties of human serum albumin, IUBMB Life 57 (2005) 787–796, http://dx.doi.org/10.1080/15216540500404093

[34] W.C. Little, R. Schwartlander, M.L. Smith, D. Gourdon, V. Vogel, Stretched extracellular matrix proteins turn fouling and are functionally rescued by the chaperones albumin and casein, Nano Lett. 9 (2009) 4158–4167, http://dx.doi.org/10.1021/nl902365z

[35] M. Verdanova, A. Broz, M. Kalbac, M. Kalbacova, Influence of oxygen and hydrogen treated graphene on cell adhesion in the presence or absence of fetal bovine serum, Phys. Status Solidi (b) 249 (2012) 2503–2506, http://dx.doi.org/10.1002/pssb.201200099

[36] K. Thalberg, B. Lindman, Interaction between hyaluronan and cationic surfactants, J. Phys. Chem. 93 (1989) 1478–1483.

[37] A. Kargerová, M. Pekař, High-resolution ultrasonic spectroscopy study of interactions between hyaluronan and cationic surfactants, Langmuir 30 (2014) 11866–11872.

[38] E. Flahaut, M.C. Durrieu, M. Remy-Zolghadri, R. Bareille, C. Baquey, Investigation of the cytotoxicity of CCVD carbon nanotubes towards human umbilical vein endothelial cells, Carbon 44 (2006) 1093–1099, http://dx.doi.org/10.1016/j.carbon.2005.11.007

[39] P.L. Bigliardi, M.J. Herron, R.D. Nelson, M.V. Dahl, Effects of detergents on proliferation and metabolism of human keratinocytes, Exp. Dermatol. 3 (1994) 89–94, http://dx.doi.org/10.1111/j.1600-0625.1994.tb00053.x.

**B. Pavla Sauerová,** Tereza Pilgrová, Miloslav Pekař and Marie Hubálek Kalbáčová (2017): **Hyaluronic Acid in Complexes with Surfactants: The Efficient Tool for Reduction of the Cytotoxic Effect of Surfactants on Human Cell Types.** Journal of Biological Macromolecules – accepted for publication. IF = 3.138

# Accepted Manuscript

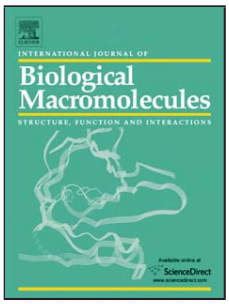


Title: Hyaluronic acid in complexes with surfactants: the efficient tool for reduction of the cytotoxic effect of surfactants on human cell types

Authors: Pavla Sauerová, Tereza Pilgrová, Miloslav Pekař, Marie Hubálek Kalbáčová

PII: S0141-8130(17)31317-X
DOI: http://dx.doi.org/doi:10.1016/j.ijbiomac.2017.05.173
Reference: BIOMAC 7662

To appear in: *International Journal of Biological Macromolecules*

Received date: 12-4-2017
Revised date: 22-5-2017
Accepted date: 30-5-2017

Please cite this article as: Pavla Sauerová, Tereza Pilgrová, Miloslav Pekař, Marie Hubálek Kalbáčová, Hyaluronic acid in complexes with surfactants: the efficient tool for reduction of the cytotoxic effect of surfactants on human cell types, International Journal of Biological Macromoleculeshttp://dx.doi.org/10.1016/j.ijbiomac.2017.05.173

# Hyaluronic acid in complexes with surfactants: the efficient tool for reduction of the cytotoxic effect of surfactants on human cell types

Pavla Sauerová[a,b], Tereza Pilgrová[c], Miloslav Pekař[c] and Marie Hubálek Kalbáčová[a,b*]

[a] Biomedical Centre, Faculty of Medicine in Pilsen, Charles University in Prague, alej Svobody 1655/76, Pilsen, 323 00 Czech Republic

[b] Institute of Inherited Metabolic Disorders, 1st Faculty of Medicine, Charles University in Prague, Ke Karlovu 2, Prague 2, 128 08, Czech Republic

[c] Materials Research Centre, Faculty of Chemistry, Brno University of Technology, Purkyňova 464/118, 612 00, Brno, Czech Republic

*corresponding author: Marie Hubalek Kalbacova, marie.kalbacova@lf1.cuni.cz, +420224967155

Graphical abstract

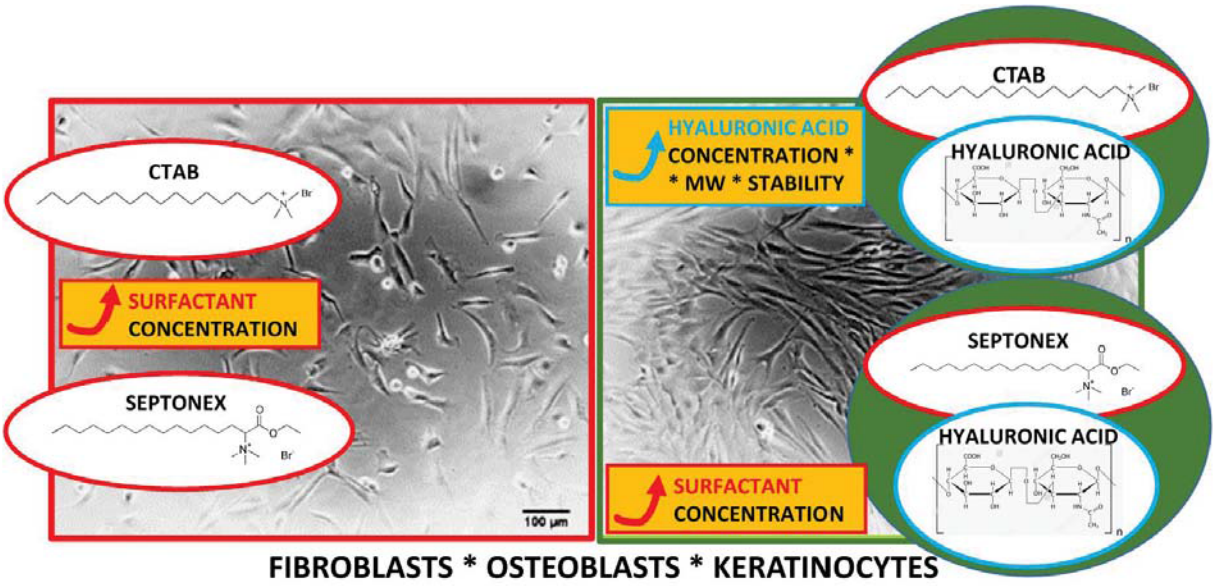

Highlights

- Hyaluronic acid in complex with surfactants (CTAB and Septonex) can reduce surfactant-induced cytotoxicity.
- Human keratinocytes are more sensitive to CTAB, however, osteoblasts and fibroblasts are more sensitive to Septonex.
- Hyaluronic acid protection of cells is limited.
- Surfactants in complex with hyaluronic acid have potential of universal delivery system.

**Abstract**

The cationic surfactants carbethoxypendecinium bromide (Septonex) and cetyltrimethylammonium bromide (CTAB) are known to be harmful for certain cell types (bacteria, fungi, mammal cells, etc.). Colloidal complexes of these surfactants with negatively-charged hyaluronic acid (HyA) were prepared for potential drug and/or universal delivery applications. The complexes were tested for their cytotoxic effect on different human cell types – osteoblasts, keratinocytes and fibroblasts. Both the CTAB-HyA and Septonex-HyA complexes were found to reduce the cytotoxicity induced by surfactants alone concerning all the tested concentrations. Moreover, we suggested the limits of HyA protection provided by the surfactant-HyA complexes, e.g. the importance of the amount of HyA applied. We also determined the specific sensitivity of different cell types to surfactant treatment. Keratinocytes were more sensitive to CTAB, while osteoblasts and fibroblasts were more sensitive to Septonex. Moreover, it was indirectly shown that CTAB combines lethal toxicity with cell metabolism induction, while Septonex predominantly causes lethal toxicity concerning fibroblasts. This comprehensive study of the effect of surfactant-HyA complexes on various human cell types revealed that HyA represents a useful CTAB or Septonex cytotoxic effect modulator at diverse levels. Potential applications for these complexes include drug and/or nucleic acid delivery systems, diagnostic dye carriers and cosmetics production.

**Keywords**

cytotoxicity, osteoblasts, keratinocytes, fibroblasts, hyaluronan, surfactants

# 1 INTRODUCTION

Cationic surfactants make up commonly used agents for a range of molecular biology methods and are known for their antiseptic qualities, which makes them ideal for use in the field of medicine. Furthermore, such surfactants also make up attractive substances for use in a variety of new therapeutic and molecular biology applications due to their micellar behaviour, antiseptic properties, wide availability and affordability. The two surfactants employed in this study - CTAB (cetyltrimethylammonium bromide) and Septonex (carbethoxypendecinium bromide) - belong to this group of materials. Their potential application in the medical and molecular biology fields includes that of drug or universal (nuclei acid, diagnostic dye etc.) delivery systems based on the positive charge of both surfactants and as one of the components that make up antiseptic-hydration agents employed in the pharmaceutical industry. Generally, both CTAB and Septonex are widely used and are well-known cationic surfactant agents, with the latter particularly being used in a number of pharmaceutical preparations in the Czech Republic. While the two surfactants are structurally closely related, the hydrocarbon chain in Septonex is one carbon atom shorter than in CTAB and its polar head, in contrast to CTAB, contains the carbethoxy group. Despite their relatively common use, however, the natural cytotoxicity of both surfactants may present a fundamental complication with respect to certain advanced applications in organisms; indeed, in addition to their positive antimicrobial effects [1], a number of undesirable side-effects have been observed on mammalian cells, i.e. cationic surfactants have been proved to be inducers of apoptosis in low concentrations and necrotic cell death inducers in higher concentrations [2] [3]. However, it is possible to minimise such negative side-effects so as to allow for the advanced application of surfactants. Interestingly, the issue of the reduction of undesirable cytotoxicity is closely connected to research on nanoparticles with respect to their drug delivery potential. CTAB is often used for nanoparticle synthesis purposes; however, this surfactant remains bound to particles even following preparation thus inducing cytotoxicity, which substantially complicates cell application in general [4].

Polymer application provides an interesting method via which to reduce surfactant cytotoxicity [4]. A good example of surfactant toxicity and the polymer reduction effect was provided by an experiment in which gold nanorods were separately covered with either CTAB or commonly used PEG (polyethylene glycol) [3]. More recently, further evidence was presented concerning the high degree of efficiency of synthetic polymers in the reduction of cytotoxicity induced by surfactants [5], [6]. However, with respect to biomaterial applications, polymers naturally occurring in organisms appear to provide the best candidate in terms of

clinical applications. Moreover, in addition to reducing the level of cytotoxicity, natural polymers are more likely to be tolerated by the immune system, are universally biocompatible and degrade naturally within organisms. At the same time, with respect to the natural occurrence of polymers (and their receptors) and the rarity of such occurrences in tissue, such polymers may also serve as a tool for the targeting of specific tissue.

Hyaluronic acid (HyA), a naturally-occurring glycosaminoglycan composed of repeating β-1,4-D-glucuronic acid and β-1,3-N-acetyl-D-glucosamine disaccharide subunits, appears to provide the ideal natural polymer. HyA participates in the maintenance of tissue homeostasis and hydration and is an essential component of the extracellular matrix. It plays a role in cell migration, proliferation and general signalisation. Moreover, it is a commonly occurring substance within organisms and has an abundant number of receptors on cells (CD44, RAMM). Furthermore, it is also well-known for its biocompatibility and high level of modifiability [7], [8]. The attractiveness of HyA for many researchers is further enhanced simply by its omnipresence within organisms [9] which allows it to serve as a carrier of universality under specific conditions. On the other hand, the high modifiability of HyA and proved overexpression of CD44 in certain types of tumour cells may allow this polymer to become a carrier with high specificity. Furthermore, cell-extracellular matrix interactions and migration are generally directly connected to the main HyA receptors, i.e. CD44 and RHAMM (a receptor for HyA-mediated motility which triggers cellular signalisation via its interaction with HyA and CD44) [10], [11]. It appears that these receptors are crucial for the interaction of extracellular HyA with cells and thus also for new potential delivery systems based on HyA. As mentioned previously, HyA-CD44 interactions make up potential drug carriers and, moreover, provide for the possibility of selective targeting based solely on CD44 interactions [12]. In general, the potential of HyA with respect to clinical applications and the development of new materials has been supported by a range of observations connected with the positive effects of HyA on cells [13], [14]. A good example of the positive effects of HyA on cells and its generally high level of efficiency was provided by the simple substitution of the frequently used polymer PEG with HyA for the coating of nanoparticles [15]. Interestingly, a number of effects of the molecular weight of HyA on its functioning have been observed. Indeed, molecular weight appears to be critical in terms of the interaction of HyA with cells (low/intermediate HyA molecular weights are usually defined as < 800 kDa and high molecular weights as >800 kDa [16]). While low molecular weight HyA has a low affinity to CD44 (the dominant cell receptor for HyA) and thus has the potential for passive transport to cells, high molecular weight HyA has the potential for active transport as a consequence of delivery via

CD44. The CD44 preference for high molecular weight HyA could be used for targeting to cells with an overexpression of CD44, e.g. tumour cells [15], a fact which enhances both the overall potential of HyA and its applicability with respect to delivery systems based on HyA [17].

This contribution provides a comprehensive study of the effect of surfactants and complexes thereof with HyA on different human cell types with a focus on the reduction of surfactant cytotoxicity when combined with HyA in a pre-mixed complex, as well as an indication of the limits related to the protection provided. It is hoped that the study will serve as a base for the development of a transfer system based on complexes consisting of surfactants and HyA for the purposes of a range of clinical and molecular biology applications. Clearly, surfactants may assume the role of hydrophobic cargo transporters (due to their positive charge) or that of "killers" due to their cytotoxicity in such a transfer system. On the other hand, the addition of HyA should reduce the degree of toxicity of the surfactants through the coating of their surfaces and, at the same time, provide support for their binding to the cell membrane via HyA-specific receptors. Following cell entry, the transferred cargo may be released or the surfactants may assume the role of endogenous cell destroyers.

## 2 MATERIALS AND METHODS

### 2.1 Surfactants and hyaluronan

Hyaluronan (sodium salt of hyaluronic acid – HyA) with a weight averaged molecular weight of 639 and 903 kDa (determined by the producer using the SEC-MALLS technique), was purchased from Contipro Ltd, Czech Republic. CTAB was purchased from Sigma-Aldrich, Czech Republic and Septonex from GBNchem, Czech Republic. The surfactants were of the best quality available and were used as received without further purification. Stock solutions of the various components were prepared in deionised water, while surfactant-HyA complex solutions were prepared by means of the gradual dropping of the surfactant stock solutions into the biopolymer stock solutions until the desired concentrations were obtained. Due to subsequent dilution in the cell studies, the complexes were prepared at ten times higher concentrations than the final concentrations given in Table 1.

The concentrations of the surfactants and HyA were selected on the basis of a previous study conducted by the authors [18], [17] and aimed at exerting a reasonable effect on the cells. Further, the concentrations were selected bearing in mind the various colloidal aspects. While the surfactant concentrations were well below their standard critical micelle concentration, they were in the region in which the formation of micelles upon the HyA added was detected

(generally, the formation of micelles was induced by the presence of oppositely-charged polyelectrolyte) and no phase separation of the surfactant-HyA complexes was observed. The formation of induced micelles was confirmed by using pyrene as a fluorescence probe and measuring the pyrene polarity index [19]. The polarity index decreased steeply in the selected concentration region indicating the formation of hydrophobic domains and the solubilisation of pyrene within them (data not shown). Increased surfactant concentration can lead to the precipitation of surfactant-HyA complexes. The lower HyA concentration was selected as the lowest concentration exerting a sufficient degree of protective effect as determined in preliminary experiments with CTAB. In the case of preliminary experiments with Septonex, it appeared that the concentration had to be significantly higher; therefore, a higher HyA concentration was also tested (on both surfactants).

### 2.2 Cell culture

Human primary fibroblasts derived from skin (obtained from FN Lochotin, Pilsen, Czech Republic) were cultured at 37°C in a 5% $CO_2$ atmosphere and in DMEM medium (Sigma–Aldrich, USA) supplemented with 10% heat inactivated FBS (PAA, Austria), 1% l-glutamine (Sigma–Aldrich, USA), 1% glucose and 1% penicillin (20 U/ml, Sigma-Aldrich, USA) and streptomycin (20 µg/ml Sigma-Aldrich, USA). Spontaneously immortalised human keratinocyte cell line HaCaT (obtained from ATCC – LGC Standards, Poland) was cultured at 37°C in a 5% $CO_2$ atmosphere and in DMEM medium (Sigma–Aldrich, USA) supplemented with 10% heat inactivated FBS (PAA, Austria), 1% l-glutamine (Sigma–Aldrich, USA) and 0.1% gentamicin (Sigma–Aldrich, USA). Human osteoblasts (SAOS-2; a human osteoblast-like cell line derived from osteosarcoma, obtained from Deutsche Sammlung von Mikroorganismen und Zellkulturen (GmbH) in Germany) were cultured at 37°C in a 5% $CO_2$ atmosphere and in McCoy's 5A medium without phenol red (PromoCell, Germany) supplemented with 15% heat inactivated FBS (PAA, Austria), 1% penicillin (20 U/ml, Sigma-Aldrich, USA) and streptomycin (20 µg/ml Sigma-Aldrich, USA).

### 2.3 Cell treatment with surfactant-HyA complexes

The fibroblasts, osteoblasts and keratinocytes were suspended using trypsin/EDTA and plated at a concentration of 20 000 cells/cm$^2$ onto a 96-well plate in the above-mentioned culture medium and under the above-mentioned conditions for 24 h after which the cells were treated with the complexes, free HyA or free surfactant diluted at a ratio of 1:9 in fresh medium with FBS (standard cultivation conditions) or without FBS (non-standard cultivation – stress conditions); the concentrations finally used are shown in Table 1. Under non-standard

cultivation conditions, applied to the osteoblasts only, FBS was added (to a final concentration of 15%) to cells the incubated in the FBS-free medium following 4 h of incubation.

### 2.4 Light microscopy

Phase contrast images of the cells were obtained using an Eclipse Ti- S microscope (Nikon, Japan) and a DS-Qi1Mc digital camera (Nikon). Images were acquired with a 10× lens and adjusted by means of ImageJ software (Rasband, W.S., ImageJ, US National Institutes of Health, Bethesda, Maryland, USA, http://imagej.nih.gov/ij/, 1997–2015).

### 2.5 Determination of cell metabolic activity

A metabolic activity test (Cell Titer 96 AQueous One Solution Cell Proliferation Assay, MTS, Promega, USA) was performed according to the standard protocol (the reduction of MTS reagent to a coloured formazan product was induced by viable cells). 24 h following the addition of the surfactant, absorbance was measured in a 96-well plate using a multi-detection micro-plate reader (Synergy$^{TM}$ 2, BioTek, USA). The measured results were expressed relative to the control ("only cells"; untreated cells).

### 2.6 Imaging of fluorescently stained cells

The cells were fixed by means of 4% paraformaldehyde in PBS at room temperature (RT) for 15 min following the end of cell metabolic activity measurement. They were then permeabilised in 0.1% Triton X-100 in PBS (Sigma-Aldrich, USA) at RT for 20 min and stained using DAPI - fluorescent dye for cell nuclei - at RT for 45 min (1:1000; Sigma-Aldrich, USA).

The wide field nuclei images for the purpose of the determination of nuclei number were obtained using an Eclipse Ti-S microscope and DS-U2 digital camera (Nikon, Japan). Images were acquired using a 4× lens and adjusted by means of ImageJ software (Rasband, W.S., ImageJ, US National Institutes of Health, Bethesda, Maryland, USA, http://imagej.nih.gov/ij/, 1997–2015) and Cell Profiler (Broad Institute, USA) software.

### 2.7 Statistical analysis

MTS test results were obtained from at least two independent experiments performed in four to six parallels. The data was statistically analysed by means of non-parametric Kruskal-Wallis ANOVA with a subsequent post-hoc Multiple Comparison test; the values obtained were tested for statistically significant differences at an alpha level of 0.05. The statistical evaluation was performed using Statistica (StatSoft CR, s.r.o.) and Microsoft Excel software.

# 3 RESULTS AND DISCUSSION

## 3.1 Determination of the effect of surfactants and HyA complexes thereof on cell morphology

The complexes, modified according to the authors' previous results [17], were composed of various concentrations of CTAB and HyA or Septonex and HyA (Table 1). The charge ratio provided in Table 1 was calculated on the basis of the occurrence of one charge on each surfactant molecule and one charge per each HyA disaccharide repeating unit with a molar weight of 401.299 g/mol. The negative charge originating from the HyA prevailed with respect to all the compositions. Dynamic light scattering revealed the bimodal distribution of particle sizes with peaks of around 20-30 nm and 250-350 nm with no unambiguous correlation with composition or surfactant type. It was supposed that the smaller particles were formed by free HyA chains or HyA chains interacting with individual surfactant molecules, whereas the larger particles were formed by micellar aggregates covered with HyA. So as to enhance the level of comparability, identical concentrations of HyA with CTAB or Septonex were employed.

Three differing cell types - human primary cells: fibroblasts, human immortalised cell lines: osteoblasts, and keratinocytes - were pre-seeded and then exposed to CTAB-HyA and Septonex-HyA complexes or their corresponding controls for 24 h (Fig.1). Cell morphological changes indicating cytotoxicity, and the rate or intensity of cell reaction to the complexes or free surfactant treatment were studied throughout the period of exposure. Light microscopy provided a brief but sufficient live mode observation with the minimisation of cell stress induction during imaging. With respect to all the cell types tested, we observed a linear dependence with increased CTAB or Septonex concentration (both free and integrated within the complexes) and a cumulative damage effect at the cell morphological change level (Fig.1). This phenomenon intensified proportionally over time (0 - 24h). At the same time, as the microscope images show, there was a clear difference between the free surfactant and surfactant-HyA complexes in these respects. Furthermore, the morphological differences between the two complex analogues (which differed only in terms of HyA concentration) and the highest surfactant concentrations of CTAB and Septonex were well distinguished (Fig.1). Similar free surfactant and surfactant complex effects had already been observed with respect to osteoblasts in the authors' previous publication [17]. However, the present study revealed a somewhat surprising phenomenon with concern to all the tested cell types, i.e. a minimum indication of CTAB or Septonex cytotoxicity was recorded only in the presence of complexes

with lower HyA concentration (5 mg/l). The complexes with a higher HyA concentration (500 mg/l) were characterised by a level of cytotoxicity approaching that induced by free surfactant - non-attached/dead cells.

### 3.2 Determination of the effect of surfactants and surfactant-HyA complexes on cell metabolic activity

A detailed characterisation was performed employing cell metabolic activity analysis. As shown in figure 2, changes in cell metabolic activity induced by treatment with surfactants or surfactant-HyA complexes exhibited a similar trend in all the three cell types tested. We observed a clear relationship between cytotoxicity and higher surfactant concentrations, which is in agreement with both the presented microscope observation, the authors' previous results and results obtained by others in the past [17], [18] [20]. The degree of cell viability diminished with increasing concentrations of free surfactants and, at the same time, we noted an increase in viability in cases in which the same amount of surfactant was incorporated into surfactant-HyA complexes. Following on from previously observed differences between the cytotoxicity induced by free and bound surfactants [20] [21], the clear differences determined between free surfactants and their complex analogues appear to verify good interaction between the surfactants and HyA resulting in good complex formation and compactness. As figure 2 also shows, a concentration of 6 μM (and above) of both free surfactants led to cytotoxicity in all the cell types tested – cell viability was reduced to below 75-80% of the control value (untreated cells) [22]. Further, an increase in viability and thus in the level of HyA protection was more apparent in cases of higher surfactant concentrations; however, a more marked difference was evident in this respect between the free surfactants (both CTAB and Septonex) and both their complex analogues containing HyA. The results thus correspond to the authors' previous results according to which the protective effect of HyA was more pronounced under higher stress conditions (a higher amount of surfactant). However, unlike in previous experiments, the modification of complexes to include different HyA concentration (5 or 500 mg/l) employed in this study allowed us to more accurately define the degree of HyA protection. As predicted by the microscopy results, metabolic activity confirmed that the distinct protective effect of HyA in complexes is limited – protection was defined only in complexes with a lower HyA concentration (5 mg/l), whereas a higher HyA concentration (500 mg/l) caused either a markedly lower degree of protection or had no protective effect when compared to treatment with free surfactants. The existence of limits to this protective phenomenon is supported by the

authors' previous results involving the testing of prepared "CTAB-HyA" and "Septonex-HyA" complexes with various CTAB- and Septonex-HyA concentrations [17]. HyA protection was confirmed with respect to all three of the tested HyA concentrations contained in the complexes (0.5, 3 and 5 mg/l of HyA) combined with surfactants, including in the presence of the highest levels of concentration of CTAB (10 μM) and Septonex (8 μM) applied. It follows that HyA protection is limited on the one hand by the concentration thereof in the complex and, on the other, by surfactant concentration in the complex.

In general, it is reasonable to suggest that excessive concentrations of HyA in the complex lead to a loss of HyA protection ability. Nevertheless, this reduction was observed only with respect to HyA with surfactants; free HyA in both concentrations (5 and 500 mg/l) exerted a comparable or positive effect on cell viability in a similar way to the non-treated control cells (fig. 6). Taken together, this observation provides evidence that a reduction in HyA protection is directly connected with surfactant presence. Moreover, this finding is supported by an interesting observation [15], according to which the quality of HyA and its ability to interact with cells may be altered significantly if it is not free and interacts with other components (e.g. particles). In addition, this alteration is fundamentally influenced by the molecular weight of the HyA, which may substantially contribute towards cell interaction via the degree of binding capacity of the HyA molecule. A further explanation for the observed decrease in HyA protection under high HyA concentration conditions may lie in the difference in complex conformation induced solely by the amount of HyA molecules. During the formation of complexes, the surfactant binds to the HyA and divides itself between the HyA molecules in the solution. From the macroscopic point of view, there are no significant differences between complexes located in the polymer-bound surfactant area though they are of different concentrations [23], [24]. However, interactions with cells occur at the microscopic level, with respect to which the differences in molecular arrangement may be significant. The principal interaction force consists of the electrostatic attraction between the oppositely charged groups, which most probably results in an altered HyA conformation compared to non-interaction chains. In addition, the presence of an attached hydrophobic tail or even micellar structures undoubtedly contribute to conformation changes. At higher concentrations, the polyelectrolyte binds more surfactant molecules than at lower concentrations (with the same surfactant concentration; [23]). The resulting conformation of HyA in the complexes formed with higher concentrations thereof may hinder its cell protective effect. It can also be hypothesised that at high HyA concentrations, almost all the surfactant molecules are well

covered by biopolymer chains, i.e. are wrapped within them in micellar form; surfactant-free biopolymer chains exist and subsequently HyA serves as an effective transporter into the cells and only here, following HyA degradation, the toxic effect of the surfactant molecules is manifested. At lower HyA concentrations, but with a charge ratio still higher than one, surfactant molecules bind themselves to almost all the HyA macromolecules present, which thus lose their ability to interact with cells effectively which, in turn, leads to more effective cell protection.

An analysis of metabolic activity changes at different cell type levels revealed that the fibroblasts (Fig.2A) and osteoblasts (Fig.2B) behaved in a more similar manner than either did with the keratinocytes (Fig.2C) following general surfactant treatment. While the osteoblasts and fibroblasts reacted mildly to increased concentrations of both surfactants and their analogous complexes, the keratinocytes reacted mildly only to Septonex treatment, while they reacted dramatically to CTAB treatment. The sensitivity of the fibroblasts to both the surfactants altered markedly and was more distinguishable with respect only to the highest surfactant concentration (8 uM). Moreover, a higher sensitivity to Septonex than to CTAB was evident. Unlike the fibroblasts, the osteoblasts exhibited a higher degree of sensitivity to Septonex than to CTAB with concern to all the concentrations tested. In contrast to the fibroblasts and osteoblasts, the keratinocytes appeared to be extremely sensitive to CTAB. As figure 2 shows, overall, the keratinocytes proved to be the most sensitive cell type of all the tested cell types to surfactant treatment. While the keratinocyte metabolism decreased rapidly to below cytotoxic level (around 75%) [22], as early as in the presence of the lowest (3 μM ) CTAB concentration, the metabolism of the fibroblasts and osteoblasts markedly decreased to below this level only in the presence of higher CTAB concentrations (6 μM and more). Indeed, this development is supported by the authors' previous finding which revealed that the surfactant sensitivity of keratinocytes was more similar than that of osteoblasts [18]. Taken together, the results clearly show that cell reactions to free surfactants or complexes thereof with HyA are determined by a combination of cell origin and cell sensitivity to the structure of the surfactant. The dependence of toxicity only on the structure of the surfactant and its subsequent impact on different cell types has already been well described in the past by other authors [20] [25] [26] [27]. The Inácio team demonstrated significant differences in the toxicity of surfactants in polarised and non-polarised epithelial cells. These differences were based solely on the chemical nature of the polar head group of surfactants. Based on this evidence, our results indicate that, in addition to elevated concentration, the sensitivity of keratinocyte is given by its ability to distinguish between the chemical structures of CTAB and Septonex. In

comparison, fibroblasts and osteoblasts react only to increasing concentrations of both surfactants. It is proposed that one reason for the selective sensitivity of keratinocytes may consist of their origin; in general, keratinocytes make up the predominant cell type in the epidermis (the outer layer of the skin), thus they are the first cells to come into contact with external chemical substances and, thus, are required to be selectively sensitive. Fibroblasts, in contrast, make up extracellular matrix producers and form tissue stroma, and osteoblasts synthesise bone tissue. Thus, both cell types perform a more structural function which may well be linked to a higher level of mechanical resistance. Further, the impact of the size of the different cell types on the cytotoxicity phenomenon can be disregarded due to the similarity in this respect of fibroblasts and keratinocytes (HaCaT), which is in contrast to the significant difference in surfactant treatment observed between these cell types.

### 3.3 Determination of the effect of surfactants and HyA-complexes thereof on fibroblast cell number

The analysis of the effect of surfactants and HyA-complexes thereof on cells was expanded to include the determination of nuclei number (cell number), the aim of which was to assist in distinguishing between lethal cytotoxicity that results in cell death and sub-lethal cytotoxicity that leads merely to cell metabolism inhibition [28].

Generally, the cell number results (Fig.3) corresponded with the trend of the MTS results thus indicating that the MTS results reflect both cytotoxicity and cell number. Despite the significant deviations in the cell number results, more detailed analysis revealed an interesting tendency which differed with respect to the two surfactants, i.e. a certain percentage difference was noticeable between the nuclei number and metabolic activity results (Fig.2). CTAB exerted a more marked influence in terms of reducing the number of cells than it did with concern to affecting metabolic activity, which did not decline with the same degree of intensity. This appears to suggest the higher lethal toxicity of CTAB and, at the same time, an increase in the cell metabolism of the surviving cells. This is supported by the study presented by Inácio's team which described levels of cytotoxicity induced by ammonium surfactants which can play role only in mitochondrial respiratory inhibition, which, in turn, is induced by their sub-lethal concentrations; on the other hand, mitochondrial fragmentation and cell death, however, are induced by their higher concentrations [28]. Further, Enomoto's team detected an increase in apoptotic features following CTAB treatment under below-critical micellar concentrations [2]. Similarly, a "switch" between surfactant- (CTAB) induced toxicity and its ability to activate the mitochondrial metabolism of cells based on surfactant concentration has

been described previously [27]. Low concentrations of surfactants are able to elevate the rate of cell mitochondrial metabolism. However, a different situation from that of CTAB was observed with respect to Septonex treatment concerning which, in general, a higher level of similarity of cell number and metabolic activity was observed. Higher Septonex concentrations appeared to lead to a mild elevation in both lethality and cell metabolism, which is somewhat in contrast to the theory suggesting that only low surfactant concentrations exert an activating effect on cells [27]. However, this apparent contradiction may be due to the chemical dissimilarity between Septonex and the other surfactant tested, which may have caused the above-mentioned alteration in terms of cell activation. Taken together, it appears that Septonex (and its analogue HyA complexes) induces lower lethal toxicity than does CTAB and does not have such a marked effect on the elevation of cell metabolism. From the viewpoint of fibroblasts as a cell type, this observation provides evidence of a higher degree of cell tenderness with respect to Septonex than to CTAB. At the same time, it seems that CTAB induced cell metabolism in addition to lethal toxicity. Based on the previous observation that antibacterial cationic surfactants make up apoptosis inducers [2], we are able to predict that the observed lethality of both surfactants is connected to the apoptosis phenomenon.

### 3.4 Determination of the stability of surfactants and HyA-complexes thereof over time tested with respect to osteoblasts

Due to the known instability of similar complexes over time [29], the study included an investigation of possible changes affecting free surfactants and their complex analogues over time (testing of the same complex batches over time). The metabolic activity was determined of cells treated with freshly prepared, 4-week old and 10-week old solutions of free surfactants and their corresponding complex analogues. In order to ensure the highest degree of reproducibility of the obtained results, a well-defined immortalised osteoblast cell line was used for this purpose. No significant changes in cell metabolic activity were identified following the treatment of the cells using the same, but varying in age, CTAB (Fig.4A) and Septonex (Fig.4B) surfactants and their HyA-complexes. We suggest that only very moderate changes (if any) were evident with respect to the surfactant and complex solutions over time which resulted in no noticeable changes in the level of HyA protection or cytotoxicity of the free surfactants employed. Indeed, this finding is supported by the good colloidal stability of the prepared complexes during storage – no opacity or phase separation development was observed, nor was there a shift in particle size distribution to higher dimensions (data not shown).

### 3.5 Determination of the effect of surfactants and HyA-complexes thereof on osteoblasts under standard and non-standard conditions

Further, the well-defined osteoblast cell line was used for the verification of the effect of complexes on cells under standard (foetal bovine serum (FBS) present in the cultivation medium during whole of the incubation period) and non-standard conditions (FBS added only 4 h following cell seeding). While FBS makes up a typical representative standard cultivation component, it cannot be used for clinical applications due its many potential health risks [30]; nor should it be used due to requirements concerning certain cell types and molecular-biological methods [31]. Figure 5 demonstrates the positive role of FBS under stress conditions under which the cells were treated with the surfactant (CTAB). This positive serum effect has already been observed in previous studies [25] [27] [32] [17]. The trend of cell viability under non-standard conditions was similar to the standard trend, although it was reduced in general. Despite a certain degree of viability reduction under non-standard conditions, the results confirmed the applicability of complexes under such conditions. These findings suggest the potential for broader application in practice, e.g. the use of such complexes for nuclei acid delivery purposes, which is usually performed under serum-free conditions.

### 3.6 The effect of HyA molecular weight in a complex with CTAB on osteoblast metabolic activity

Finally, potential differences between complexes made up of HyA of differing molecular weights were determined. As mentioned in the introduction, it is known that the biological function of HyA depends on its molecular weight. Thus, complexes of CTAB with high molecular weight HyA (ca 900 kDa) and a CTAB complex with lower molecular weight HyA (ca 600 kDa) were studied on osteoblasts under standard conditions. In addition, CTAB complexes composed of the highest surfactant concentration (8 μM) and a lower HyA concentration (5 mg/l) were tested since the protective role of HyA in this CTAB-HyA complex was found to be the most extensive and significant in comparison to free CTAB (see Fig.1 and Fig.2). Figure 6 reveals no significant change in osteoblast metabolic activity following treatment with complexes of differing HyA molecular weight. Thus, HyA protection in relation to complexes with surfactants is determined solely by its concentration (5 or 500 mg/l) and not by its molecular weight in the range tested. This presumption is supported by Mizrahy et al. [15], who demonstrated a linear relationship between the molecular weight of HyA and its affinity to the CD44 receptor (the dominant HyA receptor). This means that the molecular weight of HyA directs “HyA-cell” interactions and thus the means of transport to the cell.

Furthermore, evidence was found of an alteration with respect to general HyA affinity to CD44 induced by HyA molecular weight where the HyA was coated with nanoparticles (NPs), i.e. not free. While the binding of free HyA of different molecular weights (132 kDa, 700 kDa and 1500 kDa) to CD44 was very similar, 132 kDa HyA-coated NPs bound less to cells than 700kDa or 1500kDa HyA-coated NPs. It seems that potential reaction sites on lower-molecular-weight-HyA easily become unavailable to CD44 since they are depleted in terms of interaction with NPs as compared to higher-molecular-weight-HyA where enough potential reaction sites exist for both interactions – both CD44 and NP. Thus, there appears to be no significant difference in terms of HyA protection between 600 kDa and 900 kDa HyA, which the research concluded could be caused by the similarity of both molecular weight ranges – it seems that a molecular weight of 600 kDa provides enough potential reaction sites for surfactant binding (and thus a reduction in its cytotoxicity) and for potential cell interaction, which leads to a comparable level of protection as provided by 900 kDa HyA.

## 4 CONCLUSION

The research study confirmed HyA protection ability with respect to cationic surfactant-(CTAB and Septonex) induced cytotoxicity and provided a detailed definition of the limits, conditions and factors concerning the protection phenomenon. In addition, the results obtained from the study of various cell types and differently modified complexes enhanced present knowledge of the ways in which surfactant-induced cytotoxicity occurs and the reduction thereof following the addition of HyA. Keratinocytes indicated extreme sensitivity to the CTAB surfactant in general and relatively low sensitivity to Septonex which suggests that surfactant sensitivity is influenced by both surfactant concentration and by distinguishing between the structures of the two surfactants. Fibroblasts and osteoblasts indicated a comparable level of sensitivity to both surfactants depending solely on the surfactant concentration applied. All these cytotoxic effects were diminished by the presence of HyA in the surfactant complexes. Moreover, only low concentration HyA (5 mg/l) caused a considerable protective effect, whereas the same HyA at the higher concentration (500 mg/l) failed to protect cells from negative effects induced by the surfactants. No significant effect was observed with respect to surfactant complexes with HyA of differing molecular weight (600 kDa or 900 kDa) or differing age (fresh, 4-week old, 10-week old). We also revealed the positive effect of FBS on cells under stress conditions (surfactant presence) and the cell protective function of HyA in complexes containing surfactants under non-standard conditions. In addition, we confirmed the potential use of the complexes studied in serum-free systems. Further, we demonstrated HyA protection

ability and the limits thereof in relation to different cell types. Our results strongly indicate that cationic surfactant-HyA complex systems can be employed for “delivery system” purposes in various biomedical applications.

**Acknowledgement**

This study was supported by National Sustainability Programme I projects No. LO1503 and No. LO1211 and by project SVV 260 390.

## 5 REFERENCES


[1] K. Nakata, T. Tsuchido, and Y. Matsumura, "Antimicrobial cationic surfactant, cetyltrimethylammonium bromide, induces superoxide stress in Escherichia coli cells," *J. Appl. Microbiol.*, vol. 110, no. 2, pp. 568–579, 2011.

[2] R. Enomoto *et al.*, "Cationic Surfactants Induce Apoptosis in Normal and Cancer Cells," *Ann. N. Y. Acad. Sci.*, vol. 1095, no. 1, pp. 1–6, 2007.

[3] K. Lun Cheung *et al.*, "CTAB-coated gold nanorods elicit allergic response through degranulation and cell death in human basophils," *Nanoscale*, vol. 4, no. 15, pp. 4447–4449, 2012.

[4] A. M. Alkilany, P. K. Nagaria, C. R. Hexel, T. J. Shaw, C. J. Murphy, and M. D. Wyatt, "Cellular Uptake and Cytotoxicity of Gold Nanorods: Molecular Origin of Cytotoxicity and Surface Effects," *Small*, vol. 5, no. 6, pp. 701–708, 2009.

[5] Y. Zhang, D. Xu, W. Li, J. Yu, and Y. Chen, "Effect of Size, shape, and surface modification on cytotoxicity of gold nanoparticles to human HEp-2 and canine MDCK cells," *J. Nanomater.*, vol. 2012, p. 7, 2012.

[6] J. Wan, J.-H. Wang, T. Liu, Z. Xie, X.-F. Yu, and W. Li, "Surface chemistry but not aspect ratio mediates the biological toxicity of gold nanorods in vitro and in vivo," *Sci. Rep.*, vol. 5, p. 11398, 2015.

[7] G. D. Prestwich, "Hyaluronic acid-based clinical biomaterials derived for cell and molecule delivery in regenerative medicine," *J. Controlled Release*, vol. 155, no. 2, pp. 193–199, 2011.

[8] K. T. Dicker, L. A. Gurski, S. Pradhan-Bhatt, R. L. Witt, M. C. Farach-Carson, and X. Jia, "Hyaluronan: A simple polysaccharide with diverse biological functions," *Acta Biomater.*, vol. 10, no. 4, pp. 1558–1570, 2014.

[9] R. Stern, "Hyaluronidases in cancer biology," *Semin. Cancer Biol.*, vol. 18, no. 4, pp. 275–280, 2008.

[10] A. Aruffo, I. Stamenkovic, M. Melnick, C. B. Underhill, and B. Seed, "CD44 is the principal cell surface receptor for hyaluronate," *Cell*, vol. 61, no. 7, pp. 1303–1313, 1990.

[11] W.-F. Cheung, T. F. Cruz, and E. A. Turley, "Receptor for hyaluronan-mediated motility (RHAMM), a hyaladherin that regulates cell responses to growth factors," *Biochem. Soc. Trans.*, vol. 27, no. 2, pp. 135–142, 1999.

[12] R. E. Eliaz, S. Nir, and F. C. Szoka, "Interactions of Hyaluronan-targeted liposomes with cultured cells: Modeling of binding and endocytosis," *Methods Enzymol.*, vol. 387, pp. 16–33, 2004.

[13] J. Lam, N. F. Truong, and T. Segura, "Design of cell–matrix interactions in hyaluronic acid hydrogel scaffolds," *Acta Biomater.*, vol. 10, no. 4, pp. 1571–1580, 2014.

[14] S. K. Seidlits *et al.*, "The effects of hyaluronic acid hydrogels with tunable mechanical properties on neural progenitor cell differentiation," *Biomaterials*, vol. 31, no. 14, pp. 3930–3940, 2010.

[15] S. Mizrahy *et al.*, "Hyaluronan-coated nanoparticles: The influence of the molecular weight on CD44-hyaluronan interactions and on the immune response," *J. Controlled Release*, vol. 156, no. 2, pp. 231–238, 2011.

[16] J. E. Rayahin, J. S. Buhrman, Y. Zhang, T. J. Koh, and R. A. Gemeinhart, "High and low molecular weight hyaluronic acid differentially influence macrophage activation," *ACS Biomater. Sci. Eng.*, vol. 1, no. 7, pp. 481–493, 2015.

[17] P. Sauerová *et al.*, "Hyaluronic acid as a modulator of the cytotoxic effects of cationic surfactants," *Colloids Surf. Physicochem. Eng. Asp.*, vol. 483, pp. 155–161, 2015.

[18] M. Kalbáčová, M. Verdánová, F. Mravec, T. Halasová, and M. Pekař, "Effect of CTAB and CTAB in the presence of hyaluronan on selected human cell types," *Colloids Surf. Physicochem. Eng. Asp.*, vol. 460, pp. 204–208, 2014.

[19] T. Halasová, F. Mravec, and M. Pekař, "The effect of hyaluronan on the aggregation of hydrophobized amino acids—A fluorescence study," *Carbohydr. Polym.*, vol. 97, no. 1, pp. 34–37, 2013.

[20] Â. S. Inácio, K. A. Mesquita, M. Baptista, J. Ramalho-Santos, W. L. C. Vaz, and O. V. Vieira, "In vitro surfactant structure-toxicity relationships: implications for surfactant use in sexually transmitted infection prophylaxis and contraception," *PloS One*, vol. 6, no. 5, p. e19850, 2011.

[21] T. S. Hauck, A. A. Ghazani, and W. C. W. Chan, "Assessing the Effect of Surface Chemistry on Gold Nanorod Uptake, Toxicity, and Gene Expression in Mammalian Cells," *Small*, vol. 4, no. 1, pp. 153–159, 2008.

[22] E. Flahaut, M. C. Durrieu, M. Remy-Zolghadri, R. Bareille, and C. Baquey, "Investigation of the cytotoxicity of CCVD carbon nanotubes towards human umbilical vein endothelial cells," *Carbon*, vol. 44, no. 6, pp. 1093–1099, 2006.

[23] K. Holmberg, B. Jönsson, B. Kronberg, and B. Lindman, "Surfactant Micellization," in *Surfactants and Polymers in Aqueous Solution*, John Wiley & Sons, Ltd, 2002, pp. 39–66.

[24] K. Thalberg, B. Lindman, and G. Karlstrom, "Phase diagram of a system of cationic surfactant and anionic polyelectrolyte : tetradecyltrimethylammonium bromide-hyaluronan-water," *J. Phys. Chem.*, vol. 94, no. 10, pp. 4289–4295, 1990.

[25] M. Cornelis, C. Dupont, and J. Wepierre, "Prediction of eye irritancy potential of surfactants by cytotoxicity tests in vitro on cultures of human skin fibroblasts and keratinocytes," *Toxicol. In Vitro*, vol. 6, no. 2, pp. 119–128, 1992.

[26] J. K. Lee, D. B. Kim, J. I. Kim, and P. Y. Kim, "In vitro cytotoxicity tests on cultured human skin fibroblasts to predict skin irritation potential of surfactants," *Toxicol. In Vitro*, vol. 14, no. 4, pp. 345–349, 2000.

[27] P. L. Bigliardi, M. J. Herron, R. D. Nelson, and M. V. Dahl, "Effects of detergents on proliferation and metabolism of human keratinocytes," *Exp. Dermatol.*, vol. 3, no. 2, pp. 89–94, 1994.

[28] Â. S. Inácio *et al.*, "Mitochondrial Dysfunction Is the Focus of Quaternary Ammonium Surfactant Toxicity to Mammalian Epithelial Cells," *Antimicrob. Agents Chemother.*, vol. 57, no. 6, pp. 2631–2639, 2013.

[29] D. Li, M. S. Kelkar, and N. J. Wagner, "Phase Behavior and Molecular Thermodynamics of Coacervation in Oppositely Charged Polyelectrolyte/Surfactant Systems: A Cationic Polymer JR 400 and Anionic Surfactant SDS Mixture," *Langmuir*, vol. 28, no. 28, pp. 10348–10362, 2012.

[30] M. Sundin, O. Ringdén, B. Sundberg, S. Nava, C. Götherström, and K. L. Blanc, "No alloantibodies against mesenchymal stromal cells, but presence of anti-fetal calf serum antibodies, after transplantation in allogeneic hematopoietic stem cell recipients," *Haematologica*, vol. 92, no. 9, pp. 1208–1215, 2007.

[31] G. Gstraunthaler, "Alternatives to the use of fetal bovine serum: serum-free cell culture," *Altex*, vol. 20, no. 4, pp. 275–281, 2003.

[32] M. Verdanova, A. Broz, M. Kalbac, and M. Kalbacova, "Influence of oxygen and hydrogen treated graphene on cell adhesion in the presence or absence of fetal bovine serum," *Phys. Status Solidi B*, vol. 249, no. 12, pp. 2503–2506, 2012.

Figure 1: Phase contrast images of human osteoblasts (SAOS-2), human keratinocytes (HaCaT) and human fibroblasts after 24 h treatment with free surfactants (CTAB or Septonex) or by complexes composed of surfactants and HyA under standard conditions; only cells are untreated control cells.

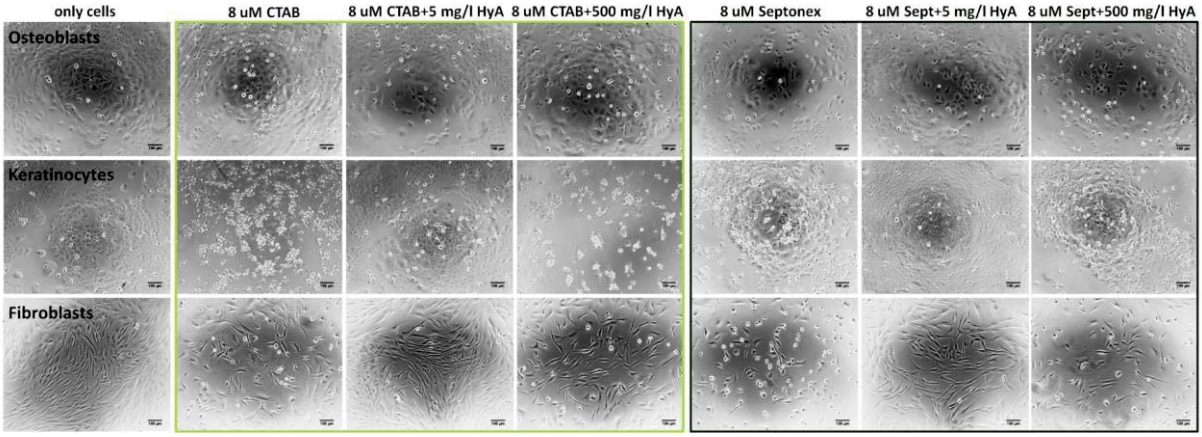

Figure 2: Metabolic activity of human fibroblasts (A), osteoblasts (B) and keratinocytes (C) 24 h after treatment with CTAB or Septonex and CTAB-HyA or Septonex-HyA complexes under standard conditions expressed as a percentage of the untreated cells. $ - significance at alpha level 0.05 compared to control (untreated cells); * - significance at alpha level 0.05 between surfactant and its complex analogue; # - significance at alpha level 0.05 between different Hya concentrations with the same surfactant concentration in the complex – based on non-parametric Kruskal-Wallis ANOVA with subsequent post-hoc Multiple comparison test.

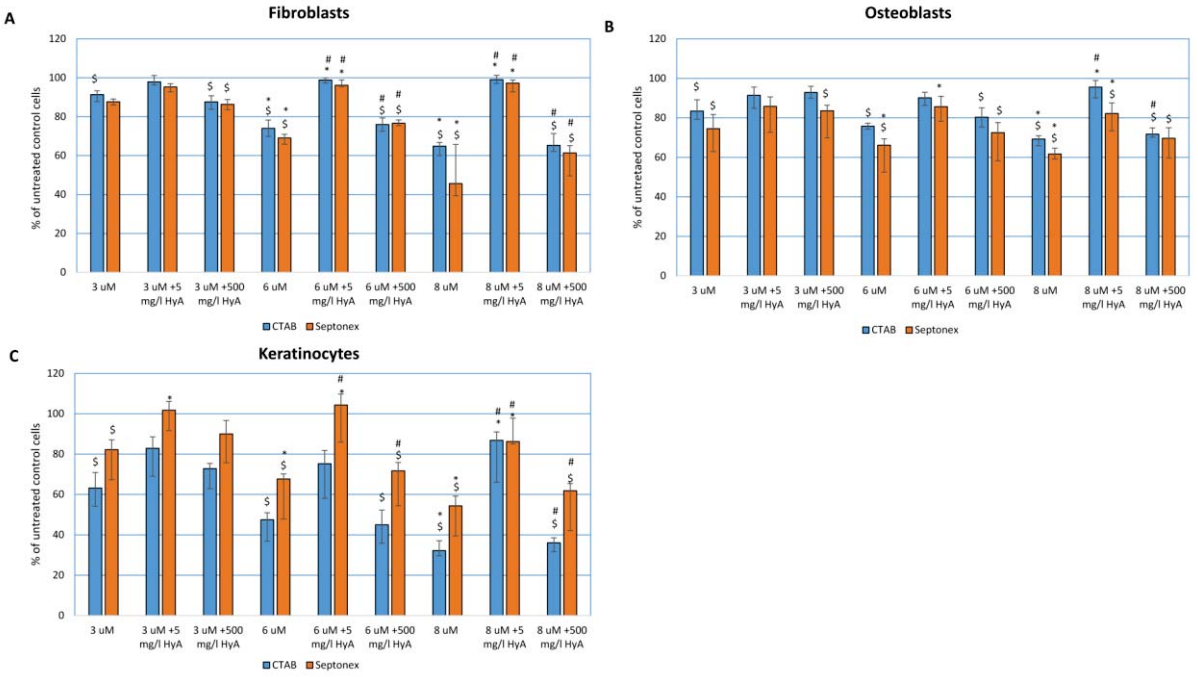

Figure 3: Cell number determination in human fibroblasts 24 h after treatment with CTAB or Septonex and CTAB-HyA or Septonex-HyA complexes under standard conditions expressed as a percentage of the untreated cells. $ - significance at alpha level 0.05 compared to control (untreated cells); * - significance at alpha level 0.05 between surfactant and its complex analogue; # - significance at alpha level 0.05 between different Hya concentrations with the same surfactant concentration in the complex – based on non-parametric Kruskal-Wallis ANOVA with subsequent post-hoc Multiple comparison test.

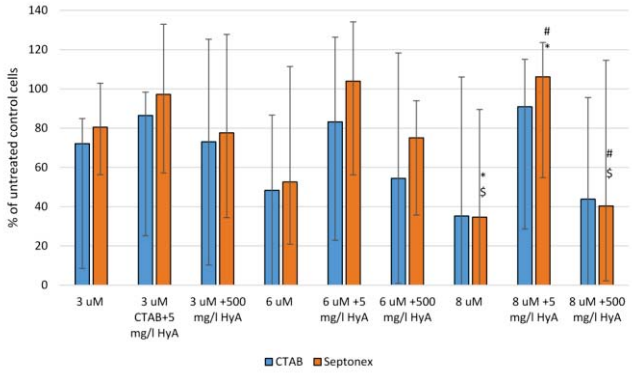

Figure 4: Determination of complex stability – metabolic activity of human osteoblasts treated with fresh, 4-weeks old and 10-weeks old CTAB complex(A) and Septonex complex (B) 24 h after the treatment under standard conditions. $ - significance at alpha level 0.05 compared to control (untreated cells); * - significance at alpha level 0.05 between surfactant and its complex analogue; # - significance at alpha level 0.05 between different Hya concentrations with the same surfactant concentration in the complex; ## - significance at alpha level 0.05 between different times with the same surfactants or complexes – based on non-parametric Kruskal-Wallis ANOVA with subsequent post-hoc Multiple comparison test.

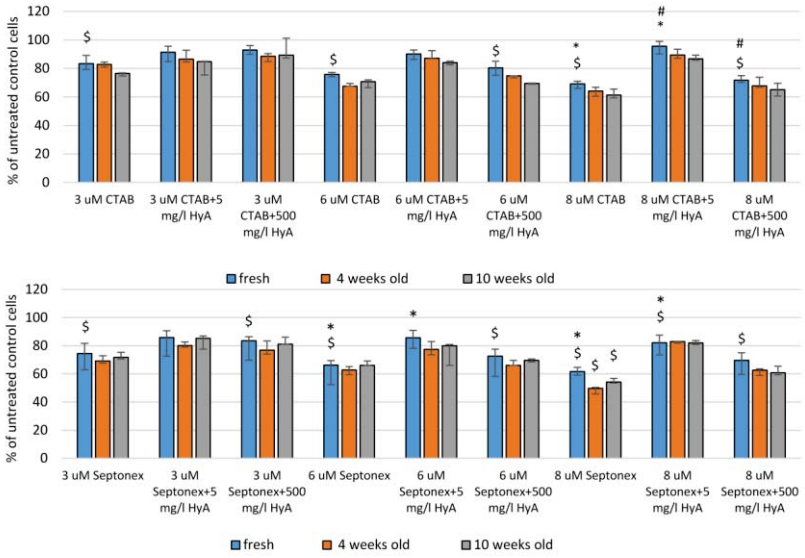

Figure 5: Metabolic activity of human osteoblasts cultivated under standard (FBS present for whole time of treatment) and non-standard cultivation condition (FBS was added after first 4 h of treatment) 24 h after treatment by CTAB or Septonex and CTAB-HyA or Septonex-HyA complexes expressed as a percentage of the untreated cells. $ - significance at alpha level 0.05 compared to control (untreated cells); * - significance at alpha level 0.05 between surfactant and its complexe analogue; # - significance at alpha level 0.05 between different Hya concentrations with the same surfactant concentration in the complex; ## - significance at alpha level 0.05 between different conditions with the same surfactants or the complexes – based on non-parametric Kruskal-Wallis ANOVA with subsequent post-hoc Multiple comparison test.

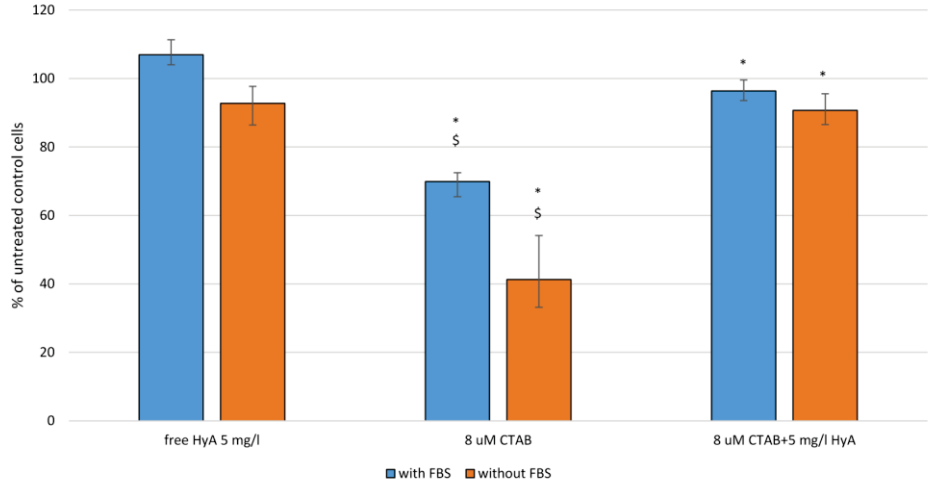

Figure 6: Metabolic actitivy of human osteoblasts treated with complexes o different molecular weight size of HyA (cca 600 kDa and 900 kDa) 24 h after the treatment with CTAB or Septonex and CTAB-HyA or Septonex-HyA complexes expressed as a percentage of the untreated cells. $ - significance at alpha level 0.05 compared to control (untreated cells); * - significance at alpha level 0.05 between surfactant and its complex analogue; # - significance at alpha level 0.05 between different Hya concentrations with the same surfactant concentration in the complex; ## - significance at alpha level 0.05 between different weight size of HyA in the same complexes – based on non-parametric Kruskal-Wallis ANOVA with subsequent post-hoc Multiple comparison test.

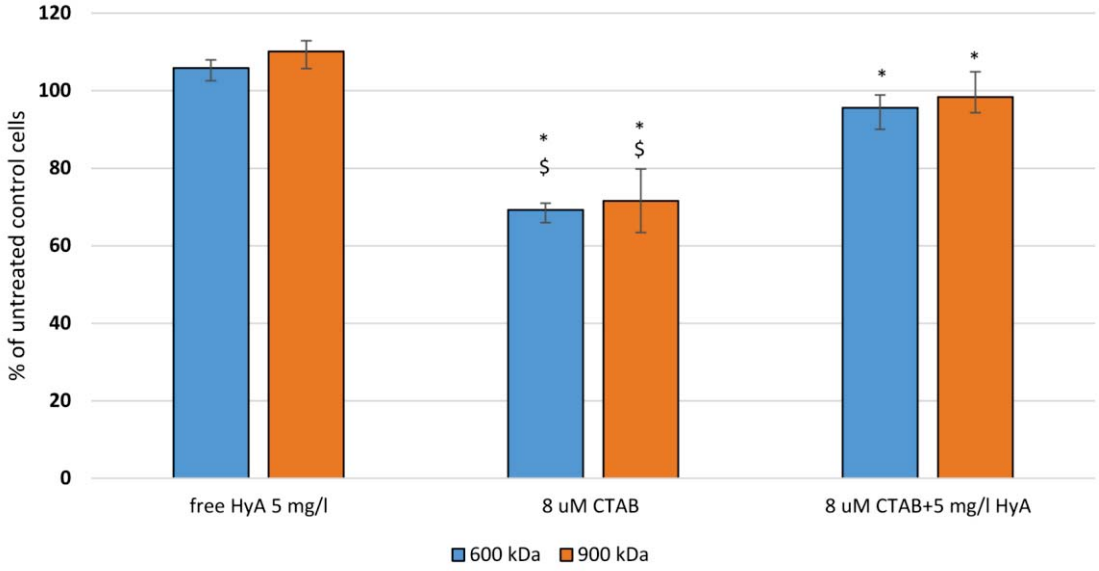

Table 1: The composition and the charge ratio of individual CTAB-HyA and Septonex-HyA complexes. Final working concentrations are indicated. * HyA - 5 mg/l and 500 mg/l concentrations are indicated in the text as lower and higher HyA concentration, respectively.

| CTAB (µM) | HyA (mg/l)* | charge ratio Hya:surfactant |
|---|---|---|
| 3 | 5 | 4,2 |
| | 500 | 415 |
| 6 | 5 | 2,1 |
| | 500 | 208 |
| 8 | 5 | 1,6 |
| | 500 | 156 |
| **Septonex (µM)** | **HyA (mg/l)** | **charge ratio Hya:surfactant** |
| 3 | 5 | 4,2 |
| | 500 | 415 |
| 6 | 5 | 2,1 |
| | 500 | 208 |
| 8 | 5 | 1,6 |
| | 500 | 156 |

**C.** Tomáš Suchý, Monika Šupová, **Pavla Sauerová**, Martina Verdánová, Zbyněk Sucharda, Šárka Rýglová, Margit Žaloudková, Radek Sedláček and Marie Hubálek Kalbáčová (2015): **The Effects of Different Cross-Linking Conditions on Collagen-Based Nanocomposite Scaffolds - An in Vitro Evaluation Using Mesenchymal Stem Cells.** Biomed Mater. 10, 065008. IF = 3.697

Biomedical Materials

PAPER

# The effects of different cross-linking conditions on collagen-based nanocomposite scaffolds—an *in vitro* evaluation using mesenchymal stem cells

RECEIVED
22 June 2015

REVISED
23 October 2015

ACCEPTED FOR PUBLICATION
29 October 2015

PUBLISHED
20 November 2015

**Tomáš Suchý[1,2], Monika Šupová[1], Pavla Sauerová[3,4], Martina Verdánová[4,5], Zbyněk Sucharda[1], Šárka Rýglová[1], Margit Žaloudková[1], Radek Sedláček[2] and Marie Hubálek Kalbáčová[3,4]**

[1] Department of Composites and Carbon Materials, Institute of Rock Structure and Mechanics, Academy of Sciences of the Czech Republic, V Holesovickach 41, Prague 8, 182 09, Czech Republic
[2] Laboratory of Biomechanics, Department of Mechanics, Biomechanics and Mechatronics, Faculty of Mechanical Engineering, Czech Technical University in Prague, Technicka 4, Prague 6, 166 07, Czech Republic
[3] Biomedical Centre, Faculty of Medicine in Pilsen, Charles University in Prague, Alej Svobody 1655/76, Pilsen—Severni Predmesti, 323 00, Czech Republic
[4] Institute of Inherited Metabolic Disorders, 1st Faculty of Medicine, Charles University in Prague, Ke Karlovu 2, Prague 2, 128 08, Czech Republic
[5] Department of Genetics and Microbiology, Faculty of Science, Charles University in Prague, Albertov 6, Prague 2, 128 43, Czech Republic

E-mail: suchyt@irsm.cas.cz

**Keywords:** cross-linking agents, nano-composite scaffolds, human mesenchymal stem cells, EDC/NHS, genipin

## Abstract

Nanocomposite scaffolds which aimed to imitate a bone extracellular matrix were prepared for bone surgery applications. The scaffolds consisted of polylactide electrospun nano/sub-micron fibres, a natural collagen matrix supplemented with sodium hyaluronate and natural calcium phosphate nano-particles (bioapatite). The mechanical properties of the scaffolds were improved by means of three different cross-linking agents: N-(3-dimethylamino propyl)-N'-ethylcarbodiimide hydrochloride and N-hydroxysuccinimide in an ethanol solution (EDC/NHS/EtOH), EDC/NHS in a phosphate buffer saline solution (EDC/NHS/PBS) and genipin. The effect of the various cross-linking conditions on the pore size, structure and mechanical properties of the scaffolds were subsequently studied. In addition, the mass loss, the swelling ratio and the pH of the scaffolds were determined following their immersion in a cell culture medium. Furthermore, the metabolic activity of human mesenchymal stem cells (hMSCs) cultivated in scaffold infusions for 2 and 7 days was assessed. Finally, studies were conducted of cell adhesion, proliferation and penetration into the scaffolds. With regard to the structural stability of the tested scaffolds, it was determined that EDC/NHS/PBS and genipin formed the most effectively cross-linked materials. Moreover, it was discovered that the genipin cross-linked scaffold also provided the best conditions for hMSC cultivation. In addition, the infusions from all the scaffolds were found to be non-cytotoxic. Thus, the genipin and EDC/NHS/PBS cross-linked scaffolds can be considered to be promising biomaterials for further *in vivo* testing and bone surgery applications.

## 1. Introduction

Bone tissue engineering is important in terms of the treatment of bone defects arising from bone damage associated with a range of diseases, trauma, inflammation, tumour surgery and non-union bone repair following fracturing [1]. In general, ideal bone replacement materials should be biodegradable, featuring non-toxic degradation products, compatible with the host immune system, supportive with concern to cell attachment, growth and differentiation so as to allow new bone tissue formation and, finally, should be remodellable by local cells.

One of a number of methods employed for the preparation of optimal bone replacement materials consists of the imitation of real bone composition and structure. Such composite materials combine the advantages of synthetic and natural biodegradable

polymers and bioactive inorganic components. The project described herein resulted in the design and construction of a new composite material the composition of which combines the advantages of biodegradable polylactide electrospun nano-fibres or submicron fibres, a natural collagen matrix supplemented with sodium hyaluronate, and natural calcium phosphate nano-particles (bioapatite). The combination of the nanofibre material, its extensive specific surface and fibre orientation provide for cell adhesion regulation, proliferation, movement, differentiation and cell behaviour in general [2–4]. Conversely, since their surfaces are hydrophobic, polylactide polymers display an insufficient degree of cell adhesion—an adverse effect which might be diminished via the incorporation of basic salts within the polymer. Moreover, the addition of calcium phosphate could serve to both buffer the associated degradation products [5] and to provide effective support for the adhesion, growth, and osteogenic differentiation of human osteoblast-like cells [6]. Indeed, polylactide materials are often applied as bonding agents for bioceramics and decalcified bone grafts as well as carriers for factors supporting the growth of bone tissue. In a similar way to collagen, these materials can also be combined with hydroxyapatite for bone tissue engineering purposes. A further analogy to the amorphous component of the bone extracellular matrix, applicable in the field of bone tissue engineering, consists of hyaluronic acid, i.e. unbranched high-molecular-weight glycosaminoglycan which is widely distributed within the connective tissues of the human body and is also active in the mineralisation process. In addition, hyaluronic acid is employed extensively in biomedical applications such as wound healing and tissue engineering scaffolds, the treatment of arthritis and as an implant material component [7, 8].

Collagen-based scaffolds are being widely studied as potential tissue engineering materials due to the positive effect of collagen on a large number of cell types, its lattice-like organisation ability and for reasons of biocompatibility [9]. However, the application of collagen in terms of tissue engineering is limited due to its poor mechanical properties, high swelling rate in aqueous environment, low structural stability and low level of resistivity to the enzymatic degradation of its untreated form [10].

Therefore, a large part of the research work focused on improving the physico-chemical properties of collagen so as to enhance its applicability to tissue engineering. Thus, cross-linking methods, e.g. physical cross-linking (combined riboflavin/ultraviolet A and rose bengal/white-light irradiation [11–13]) and chemical cross-linking are being developed aimed at both improving the material's mechanical properties and at slowing down the biodegradation rate of collagen-based biomaterials.

Chemical cross-linking is accomplished principally by means of covalent amine/imine linkage [13]. The use of aldehydes, such as glutaraldehyde or glyceraldehyde, improves the mechanical properties and reduces immunogenicity but, on the other hand, the level of long-term stability is low. However, e.g. glutaraldehyde it is known to be highly cytotoxic. A further widely used covalent cross-linking method is that using N-(3 dimethylaminopropyl)-N-ethylcarbodiimide hydrochloride (EDC)/N-hydroxysuccinimide (NHS) [14] in aqueous or ethanol solutions [15–17]. Genipin, an iridoid glycoside, is one of the main components of gardenia fruit (*Gardenia jasminoides ELLIS*) and generates cross-links spontaneously with protein, collagen, gelatin, chitosan, etc. A large number of studies have noted the remarkably low cytotoxicity and genotoxicity of genipin compared to aldehydes [18–20].

Generally, biocomposites contain several heterogeneous components which may potentially react with a cross-linking agent as well as collagen component reacts. The use of a cross-linking reagent is specific for an existing composite system and, therefore, the testing and comparison of individual cross-linking agents are necessary for each case. Following the preparation and characterisation of biomaterials, the biological *in vitro* evaluation thereof is necessary as is the verification of the handling of the biomaterial under cell cultivation conditions, its cytotoxicity and its interactions with cells. Subsequently, the *in vivo* assessment of the proven biomaterial can be conducted. Such steps are fundamental in terms of the application of any biomaterial at the clinical practice level.

Human mesenchymal stem cells (hMSCs) are attractive for bone tissue engineering purposes due to their ability to differentiate into a range of specialised cell types including osteoblasts (bone forming cells). Moreover, the use of autologous hMSCs should eliminate the risk of an undesirable immune response. Extracellular matrix composition and structure are essential in terms of MSC survival and differentiation ability. Thus, the modification of the biochemical and physical features of artificial extracellular matrices substantially influence MSC survival and differentiation [21].

The purpose of this study was to determine effective cross-linking conditions for scaffolds based on a collagen matrix reinforced with polylactide sub-micron fibres and supplemented by bioapatite nano-particles and hyaluronic acid. With this aim in view, we investigated scaffolds cross-linked in various ways commonly described in literature as relatively standard methods for collagen cross-linking and compared their influence on the structural and mechanical properties, swelling ratio and mass loss of the cross-linked scaffolds; in addition, hMSC adhesion and proliferation within the scaffolds were also investigated.

## 2. Materials and methods

### 2.1. Collagen extraction

Collagen type I was isolated from freshwater fish skin (*Cyprinus Carpio*, *Třeboň carp*, Třeboň fishery, Czech Republic, controlled breeding); all the procedures were

performed at a temperature of 20 °C. The skin was degreased for 48 h using diethylether and subsequently washed using distilled water. Preliminary extraction in a phosphate buffer (pH 7.4, 24 h, repeated three times) and a citrate buffer (pH 3.7, 24 h, repeated three times) was conducted so as to remove non-collagenous proteins and pigments. Collagen extraction was carried out by soaking the treated skin in 0.5 M acetic acid for 24 h followed by centrifugation (9 000 rpm). The liquid portion was dialysed against 0.1 M acetic acid in dialysis tubing (Spectra/Por, USA) for 2 × 24 h. The final solution was frozen at a temperature of −15 °C and lyophilised at −105 °C and at a pressure of approximately 1.3 Pa (BenchTop 4KZL, VirTis).

### 2.2. Poly(DL-lactide) fibres

PDLLA (poly(DL-lactide), PURASORB PDL05, Purac, NE) sub-micron fibre (275–300 nm, lower—upper quartile) mats were prepared by means of electrospinning from a 10 wt% chloroform solution (Nanospider NS LAB 500, Elmarco, Czech Republic). Prior to the preparation of the scaffolds, PDLLA fibres were homogenised using a disintegrator for 5 min at 14 000 rpm (DI 18, IKA) in distilled water, frozen at −15 °C for 24 h and subsequently lyophilised at −105 °C and at a pressure of approximately 1.3 Pa.

### 2.3. Bovine bone bioapatite isolation

Bioapatite (bCaP) was obtained from chemically- and thermally-treated bovine bone inspired by Murugan *et al* [22]. The cortical bovine bone was sliced into pieces of the required size. Macroscopic soft tissue and marrow impurities were removed by means of heating with a 2% NaCl solution at 150 °C and a pressure of 0.2 MPa in autoclave followed by degreasing in acetone–ether mixture (ratio 3 : 2) for 24 h. The bone samples were then treated with 4% NaOH solution at 70 °C for 24 h. The product was washed with deionised water until neutral reaction. The chemically-treated bone samples were calcined overnight at 600 °C under atmospheric pressure and ambient humidity. The product was finally washed with deionised water and dried in a vacuum oven.

### 2.4. Preparation of composite scaffolds

Composite scaffolds based on a collagen matrix (50.5 wt%), PDLLA fibres (47 wt%), bCaP (2 wt%) and 0.5 wt% of sodium hyaluronate (HA) powder (HySilk, Contipro Biotech, Czech Republic) were prepared employing the following procedure: An aqueous collagen dispersion (5 wt%) was prepared by the swelling of collagen in deionised water, homogenised using a disintegrator (10 000 rpm, 10 min) and left for 60 min at a temperature of 20 °C. Collagen dispersion was further modified by means of PDLLA fibres, bCaP particles and HA powder; final homogenisation was performed using the disintegrator (6 500 rpm, 10 min). The resulting dispersion was placed in separate cylindrical containers with an inner diameter of 10 mm, frozen at −70 °C for 3 h and then lyophilised. The final stage involved the cutting of the cylindrical specimens into 1.5 mm thick samples.

### 2.5. Chemical cross-linking of the scaffolds

The collagen part of the scaffolds was cross-linked employing three different chemical treatments commonly published in literature as the PBS or ethanol solution of EDC/NHS (e.g. [15–17]) and a PBS solution of genipin (e.g. [18–20]). The first group of samples (*EDC/NHS/EtOH*) was cross-linked with an ethanol solution containing EDC and NHS at a weight ratio of 4:1 (EDC: 4.08 mg ml$^{-1}$ and NHS: 1.02 mg ml$^{-1}$). EDC and NHS (Sigma Aldrich, Germany) were used as received. The second group (*EDC/NHS/PBS*) was cross-linked by means of a phosphate buffer saline solution (0.0027 M potassium chloride and 0.137 M sodium chloride, pH 7.4 at 25 °C) (PBS, Sigma Aldrich, Germany) containing EDC/NHS (weight ratio 4 : 1, EDC: 4.08 mg ml$^{-1}$ and NHS: 1.02 mg ml$^{-1}$). The third group (*GENIPIN*) was cross-linked using a PBS containing genipin (Sigma Aldrich, Germany) at a concentration of 1.34 mg ml$^{-1}$. Following a reaction period of 24 h at room temperature (orbital shaker, 180 rpm), all the scaffolds were washed in the 0.1 M $Na_2HPO_4$ (2 × 45 min), followed by rinsing using deionised water (30 min), frozen at −15 °C for 5 h and lyophilised.

### 2.6. Scaffold characterisation

The structure of the scaffolds was evaluated by means of attenuated total reflection infrared spectrometry (FTIR) using a Protégé 460 E.S.P. infrared spectrometer (Thermo Nicolet Instruments, USA) equipped with an ATR device (GladiATR, PIKE Technologies, USA) with a diamond crystal. All the spectra were recorded in absorption mode at a resolution of 4 cm$^{-1}$ and 128 scans. The areas of the bands (integral absorbencies) were determined using OMNIC 7 software.

### 2.7. Characterisation of the mechanical properties of the scaffolds

In general, the behaviour of porous materials under deformation is somewhat different from the behaviour of common compact materials and the testing methods for standard non-porous materials or materials with low porosity cannot be easily adopted. In order to describe the mechanical behaviour of the scaffolds prior to cross-linking and following the application of different cross-linking conditions, compression tests were performed by means of the adaptation of the ISO 13314 standard [23] which refers to the mechanical testing of porous and cellular metals. The mechanical properties of the scaffolds were measured on dry samples before and after cross-linking. Five cylindrical samples with a diameter of 10.2 mm and a length of 12 mm were tested in each group (i.e. a sample length to diameter ratio of approximately 1.2). Plateau stress, elastic gradient, compressive proof stress and energy absorption were determined using an MTS Mini

Bionix 858.02 system (MTS, USA) equipped with 100 N and 250 N load cells. The measurements were carried out at a constant crosshead speed of 2.0 mm $min^{-1}$ (deformation rate approx. 0.003 $s^{-1}$, i.e. in the range of $10^{-3}$ and $10^{-2}$). The stress-strain curves obtained were used to determine the mechanical properties as follows: Plateau stress ($\sigma_{pl}$) was defined as the arithmetical mean of the stresses between 20% and 30% compressive strain. The elastic gradient ($E_{\sigma 20-\sigma 70}$) was calculated as the gradient of the elastic straight lines determined by elastic loading and unloading between stresses of 70% and 20% of the $\sigma_{pl}$. Compressive proof strength ($\sigma_{ps}$) was determined as compressive stress at a plastic compressive strain of 1.0%. Energy absorption ($W$) was calculated as the area under the stress-strain curve up to 50% strain. Finally, energy absorption efficiency ($W_e$) was calculated as energy absorption divided by the product of the maximum compressive stress within the strain range and the magnitude of the strain range. Plateau stress and elastic gradient represent the closest concepts to that of yield stress and Young's modulus respectively which are employed for solid materials [24]. In order to simplify the comparison of our results and the results of other studies, we assumed that plateau stress represents compression strength and that elastic gradient represents the modulus of elasticity under compression [24–26].

### 2.8. Scaffold degradation

The *in vitro* degradation of the scaffolds was evaluated by means of the determination of mass loss, the swelling ratio and the pH (IKATRON, electrode THETA 90). The experiment aimed to simulate *in vitro* test conditions—the samples were immersed in a fully supplemented $\alpha$ MEM medium (Life Technologies, USA) and incubated in conical flasks at 37 °C and a 5 % $CO_2$ atmosphere (DH $CO_2$ incubator, Thermo Scientific) for 1, 3 and 8 d. The extent of *in vitro* degradation was calculated according to the following equation: $D = \frac{W_0 - W_t}{W_0} 100$ [%], where $D$ is mass loss, $W_o$ is the initial dried weight of the sample and $W_t$ is the dried weight of the sample after degradation ($n = 5$). The swelling ratio ($E_{sw}$) was calculated using the following equation: $E_{sw} = \frac{W_{sw} - W_0}{W_0} 100$ [%], where $W_o$ is the initial dried weight of the sample and $W_{sw}$ is the weight of the swollen sample ($n = 5$). The weight of the swollen samples was measured following the removal of each sample from the medium and after a 1 min delay and the removal of the excessive medium surrounding the sample. The dried weight of the samples was measured after lyophilisation.

### 2.9. Cells and culture conditions

Human mesenchymal stem cells (hMSCs) were obtained from healthy donors after they had provided fully-informed written consent. Bone marrow blood was aspirated from the posterior iliac crest and the mono-nuclear fraction was isolated by means of gradient centrifugation. The adherent cells were cultivated in 75 $cm^2$ flasks (TPP, Switzerland) in an $\alpha$-MEM medium (Life Technologies, USA) with 10% heat-inactivated fetal bovine serum (PAA, Austria), penicillin (20 mg $ml^{-1}$; Sigma-Aldrich, USA) and streptomycin (20 mg $ml^{-1}$; Sigma-Aldrich, USA). The medium was changed once per week. The experiments were performed using hMSCs taken from three healthy donors in a passage number two to five. The cells were cultivated at a temperature of 37 °C and in a 5% $CO_2$ atmosphere. This research conforms to general ethical principles and standards—all the procedures involving living human participants were approved by the Ethics Committee.

### 2.10. Scaffold infusions

The scaffolds—in 48-well plate (Thermo Scientific, USA)—were fixed in wells using CellCrown™ inserts (Sigma-Aldrich, USA). The scaffolds were then sterilised in 70% ethanol (10 min) and subsequently rinsed in sterile deionised water three times for 3 min. A fully-supplemented $\alpha$ MEM medium (800 $\mu$l) was added to each scaffold which were then incubated at 37 °C and in a 5% $CO_2$ atmosphere for 1 d in order to obtain scaffold infusions which were then transferred (500 $\mu$l) to the pre-seeded cells in 48-well plate (these '1 d infusions' can also be termed degradation products of the individual scaffolds).

The cells were seeded 1 d before the addition of the infusion at a concentration of 10 000 cells $cm^{-2}$ for 2 d cultivation and 5 000 cells $cm^{-2}$ for 7 d cultivation. Cell metabolic activity (described below) was measured after 2 d and 7 d of cell cultivation within the scaffold infusions.

### 2.11. Cell seeding onto scaffolds

The 1 d infused scaffolds were subsequently used for cell cultivation. The cells were seeded onto the scaffolds at a concentration of 10 000 cells $cm^{-2}$ for 2 d cultivation (these scaffolds were immersed for 3 d in total) and 5 000 cells $cm^{-2}$ for 7 d cultivation (these scaffolds were immersed for 8 d in total) following which cell metabolic activity was measured and the number of cells on the scaffolds determined.

### 2.12. Determination of cell metabolic activity

The cell metabolic activity test (Cell Titer 96 AQueous One Solution Cell Proliferation Assay, MTS, Promega, USA) was performed according to the standard protocol: the absorbance (at 490 nm and at 655 nm as a reference value) of soluble formazan accomplished by means of metabolically-active cellular dehydrogenases was determined after 2 d or 7 d of cell cultivation in either the scaffold infusions or the scaffolds themselves. Absorbance was measured using a multi-detection micro-plate reader (Synergy™ 2, BioTek, USA). The results were normalised (in percentage terms) with respect to the cells with no scaffold infusions and those cells cultivated on control polystyrene

(positive controls). Polystyrene was used as the *in vitro* cultivation standard.

### 2.13. Determination of cell number

The cell number on the scaffolds was determined indirectly according to a calibration curve based on the cell metabolic activity of a defined amount of cells, i.e. the cells intended for cell number determination were seeded in concentrations of (5, 10, 15, 20, 25, 30 and 35) $\times$ $10^3$ cells $cm^{-2}$ on 48-well plate. Following 14–16 h of cell cultivation, the cell metabolic activity test was performed. The calibration curve was then created based on the measured values, and the cell number on the scaffolds was determined from MTS values using a regression equation.

### 2.14. Cell fluorescence staining

The cells on the scaffolds were fixed in 4% paraformaldehyde in PBS at room temperature for 15 min subsequently after the measurement of cell metabolic activity. Cells were permeabilised with 0.1% Triton X-100 in PBS (Sigma-Aldrich, USA) at room temperature for 20 min and stained with fluorescence dyes: the cell nuclei were stained with DAPI at room temperature for 45 min (1 : 1 000; Sigma-Aldrich, USA) and the actin filaments with Phalloidin-Alexa Fluor 488 also at room temperature and for 45 min (1 : 500; Life Technologies, USA). Cells cultivated on control polystyrene were stained in the same way; in addition, they served as an essential control for the cultivation conditions and staining procedure.

### 2.15. Imaging of fluorescently stained cells

Wide field images of the cells on the scaffolds were obtained using an Eclipse Ti-S, lens S Plan Fluor 40x (N.A. 0.6) microscope and DS-U2 Digital Camera (Nikon, Japan). 3D images of the cells on the scaffolds were acquired using a Nikon TE2000E microscope equipped with a confocal scanning head (C1si), Plan Fluor 10x lens (N.A. 0.3) and 405 and 488 nm excitation lasers (Nikon, Japan). The emission of individual fluorophores was detected using 450/30 nm and 515/30 nm band-pass filters. Image sampling density was corrected according to the Nyquist criterion. The images were deconvoluted via the use of the classic maximum likelihood restoration algorithm in Huygens Professional Software (SVI, Netherlands). The Z-stack images were rendered in NIS elements software (LIM, Czech Republic).

### 2.16. Statistical analysis

The data gathered from the biological evaluation was derived from three independent experiments performed in two biological parallels. The non-parametric Kruskal-Wallis ANOVA with subsequent post-hoc test based on pair-wise comparisons with the Bonferroni correction was used for determining significant differences between the datasets. STATISTICA Software (StatSoft, Czech Republic) was used for these statistical analyses. With regard to the non-biological tests, statistically significant differences were investigated using non-parametric methods (STATGRAPHICS Centurion XV, StatPoint, USA) due to the problematical nature of the verification of the normality of the assessed data; the Kruskal-Wallis test was used for this purpose. The Mann-Whitney test was used as a post hoc test. *P* values of less than 0.05 were considered to be statistically significant.

## 3. Results

### 3.1. Scaffold characterisation

It was observed that the inner pores were interconnected in irregular patterns and the pore size varied over a relatively small range under different cross-linking conditions (see figure 1). The average pore size of the scaffolds prior to cross-linking was 252–373 $\mu$m (lower and upper quartiles) (figure 1). The application of the cross-linking agents led to a statistically significant decrease in pore size except in the case of genipin (6% increase). This decrease in average pore size (median) varied from approximately 16% for EDC/NHS/EtOH to approximately 32% for EDC/NHS/PBS.

Potential changes in scaffold structure after cross-linking were also analysed using FTIR spectroscopy (figure 2, table 1). The FTIR spectra of non-cross-linked (original) and cross-linked composite scaffolds contain bands typical for collagen such as N–H stretching at ~3 303 $cm^{-1}$ for amide A and C–H stretching at ~3 080 $cm^{-1}$ for amide B. Generally, amide I bands (~1 650 $cm^{-1}$) originate from $C = O$ stretching vibrations coupled with N–H bending vibration. Amide II bands (~1 548 $cm^{-1}$) arise from N–H bending vibrations coupled with C–N stretching vibrations. The observed spectra bands consist of PDLLA as well as bands of PDLLA shared with collagen (figure 2).

### 3.2. Scaffolds mechanical properties

The mechanical properties of the scaffolds obtained in the study are provided in table 2. Both the compressive strength (represented by plateau stress and compressive proof strength) and elastic modulus (represented by the elastic gradient) increased following the application of all the cross-linking conditions. The statistically significant (Mann-Whitney, 0.05) highest compressive strength and elastic modulus values were evinced by samples cross-linked with genipin. As for a comparison of the three cross-linking conditions applied, the lowest increase in mechanical properties (Mann-Whitney, 0.05) was evinced by the EDC/NHS/EtOH samples. The improvement in resistance to deformation of the scaffolds following cross-linking is illustrated by an increase in calculated energy absorption. Here again, the highest values (Mann-Whitney, 0.05) were obtained for samples cross-linked with genipin. The same values (Mann-Whitney, 0.05) of calculated energy absorption efficiency illustrate the similar character of the stress-strain curves of all the tested materials. This indicates minimal changes in the inner structure of the scaffolds following cross-linking.

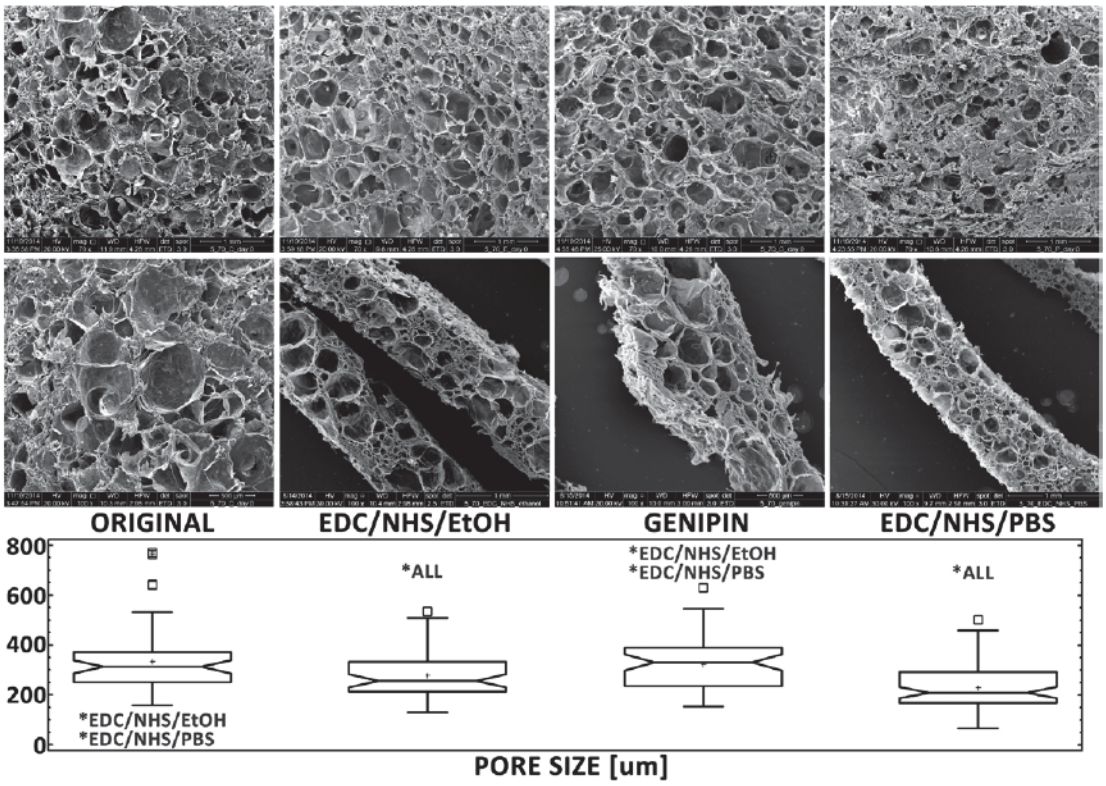


**Figure 1.** Representative SEM images of scaffold surfaces (above) and their cross-sections (middle) prior to cross-linking (ORIGINAL) and following chemical cross-linking employing chemical agents. Box plots of pore size before and after cross-linking, * denotes statistically significant differences (Mann-Whitney, 0.05).

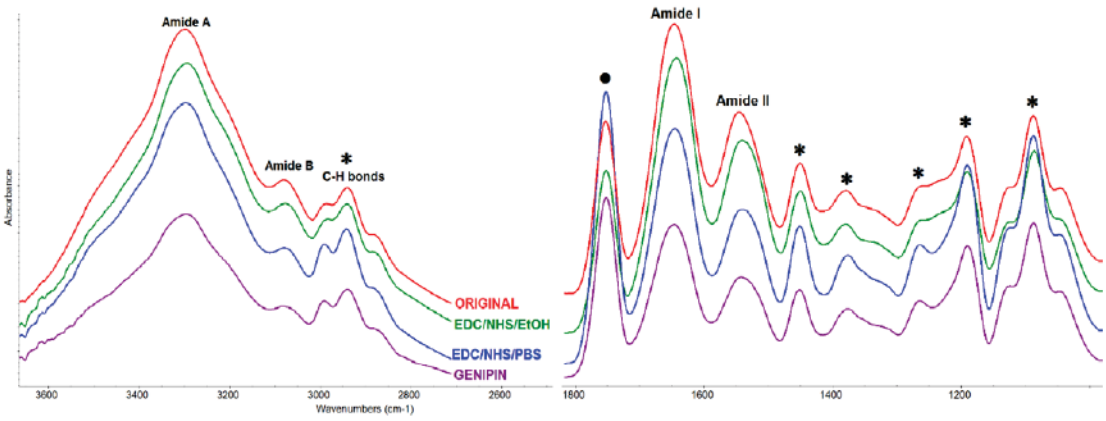


**Figure 2.** The FTIR spectra of non-cross-linked and cross-linked composite scaffolds. ● = PDLLA bands, * = collagen and PDLLA shared bands.

**Table 1.** The area containing amide bands and their positions within the FTIR spectra of collagen before and after chemical cross-linking.

| | Amide A | | Amide B | | Amide I | | Amide II | |
|---|---|---|---|---|---|---|---|---|
| Amidic band | Peak position | Area | Peak position | Area | Peak position | Area | Peak position | Area |
| ORIGINAL | 3298 | 10.40 | 3081 | 0.20 | 1646 | 4.51 | 1545 | 1.86 |
| EDC/NHS/EtOH | 3294 | 9.90 | 3077 | 0.19 | 1643 | 4.71 | 1541 | 2.06 |
| GENIPIN | 3297 | 5.90 | 3081 | 0.09 | 1645 | 2.48 | 1542 | 1.14 |
| EDC/NHS/PBS | 3297 | 9.50 | 3079 | 0.15 | 1645 | 3.87 | 1541 | 1.68 |

**Table 2.** Summary of the mechanical properties of the composite scaffolds measured via the performance of compression tests. Both mean and standard deviation are presented ($n = 5$).

| | | $\sigma_{pl}$ [MPa] | $E_{\sigma 20-\sigma 70}$ [MPa] | $\sigma_{ps}$ [MPa] | W [MJm$^{-3}$] | $W_e$ [%] |
|---|---|---|---|---|---|---|
| ORIGINAL | mean | 0.51 | 11.20 | 0.50 | 0.26 | 61.0 |
| | SD | 0.10 | 4.01 | 0.02 | 0.03 | 2.9 |
| EDC/NHS/ETOH | mean | 0.86[a] | 24.70[a] | 0.67[a] | 0.42[a] | 61.8 |
| | SD | 0.26 | 9.97 | 0.09 | 0.13 | 2.6 |
| GENIPIN | mean | 1.98[a] | 57.30[a] | 1.50[a] | 0.91[a] | 62.1 |
| | SD | 0.32 | 7.21 | 0.10 | 0.11 | 3.4 |
| EDC/NHS/PBS | mean | 1.01[a] | 29.9[a] | 0.83[a] | 0.50[a] | 60.0 |
| | SD | 0.17 | 5.08 | 0.08 | 0.06 | 2.7 |

[a] Statistically significant differences in comparison with the non-cross-linked (original) samples (Mann-Whitney, 0.05).

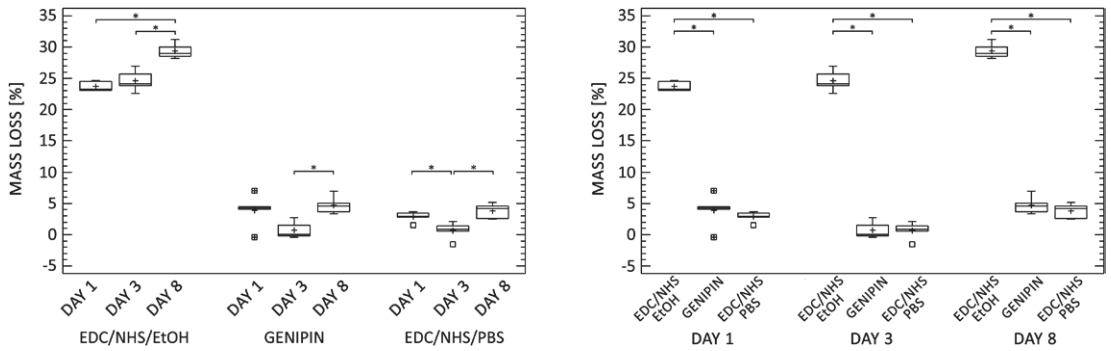


**Figure 3.** The mass loss of cross-linked scaffolds. The sign '*' denotes statistically significant differences (Mann-Whitney, 0.05).

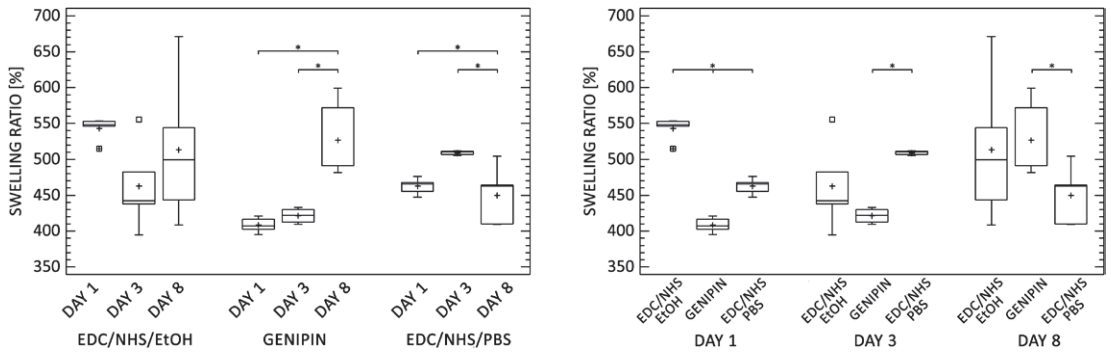


**Figure 4.** The swelling ratios of cross-linked scaffolds. The sign '*' denotes statistically significant differences (Mann-Whitney, 0.05).

### 3.3. Scaffold degradation

The degradation experiment aimed both to verify changes to the physical and structural properties of cross-linked scaffolds during *in vitro* cultivation and to provide support for the findings of the biological evaluation. Due to the extensive disintegration of the non-cross-linked (original) samples under degradation test conditions, it was not possible to use them as control samples. The mass losses of cross-linked scaffolds are summarised in figure 3. Accelerated mass loss was observed in the case of the EDC/NHS/EtOH cross-linked sample (23–29%); the mass loss of this sample increased markedly as early as on the first day of the experiment and continued to increase up to day 8 (up to a further 5%). In contrast, in the case of cross-linking with EDC/NHS/PBS and genipin, the mass loss did not change significantly from day 1 to day 8. The accelerated mass loss in the case of the EDC/NHS/EtOH cross-linked samples may indicate an insufficient rate of collagen matrix cross-linking.

The swelling ratio, determined by the immersion of scaffolds in an α MEM medium is summarised in figure 4. On the first day those scaffolds cross-linked with EDC/NHS/EtOH show the highest swelling ratio rate (548%); conversely, those scaffolds cross-linked with genipin show the lowest rate (407%). The swelling ratio of scaffolds cross-linked with EDC/NHS/PBS was found to be somewhere between that of the aforementioned two scaffolds. However, the swelling ratio of EDC/NHS/EtOH samples remained unchanged over

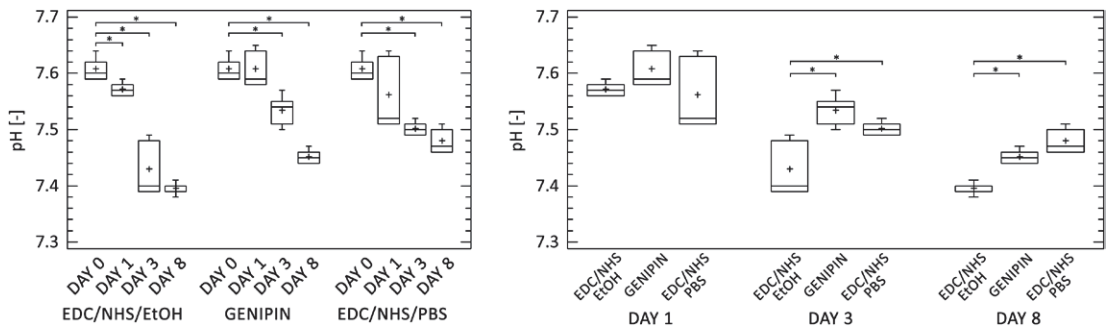


**Figure 5.** Values of pH of the α MEM medium at the beginning of the experiment (DAY 0) and after 1, 3 and 8 d of cross-linked scaffold immersion. The sign '*' denotes statistically significant differences (Mann-Whitney, 0.05).

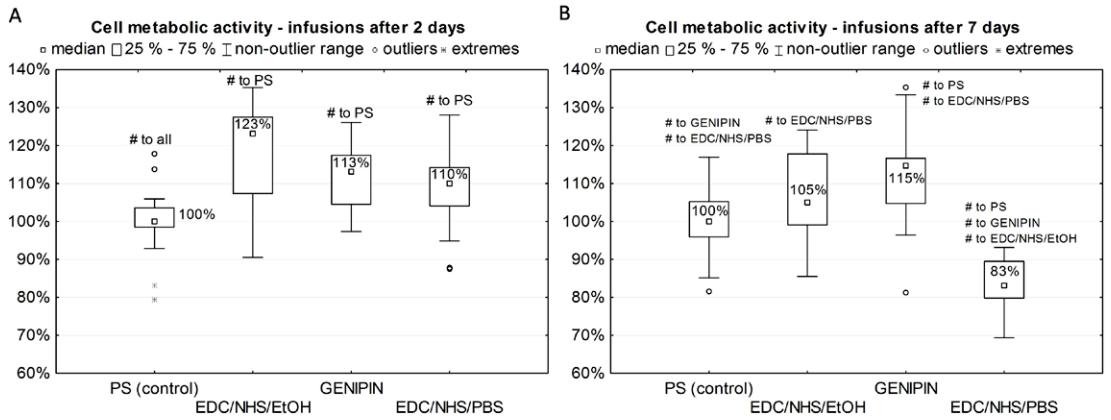


**Figure 6.** Metabolic activity of hMSCs cultivated in 1 d infusions (degradation products of the individual scaffolds) of control polystyrene (PS) and the tested scaffolds cross-linked with EDC/NHS/EtOH, genipin and EDC/NHS/PBS for 2 d (A) and 7 d (B). #—significant difference at $p > 0.05$.

the 8 d incubation period. Figure 4 (left) shows the data variance between swelling ratios, especially in the case of day 8. The assessed swelling ratio values may have been influenced by the degradation processes occurring within each sample. The accelerated mass loss of the EDC/NHS/EtOH samples influenced the high rate of variability of the swelling ratio data due to the gradual disintegration of the samples. Interestingly, the mass loss of the EDC/NHS/PBS and genipin cross-linked samples were found not to be statistically significantly different over time; however, a differing trend was observed in terms of the swelling ratio from day 8.

The pH values of the α MEM medium during the experiment are summarised in figure 5. The data provided in figure 5 (left) clearly reveals a statistically significant decrease in the pH values of the medium for all types of scaffolds over time. However, in the case of EDC/NHS/EtOH only, pH decreases immediately after the first day. In other cases at least 3 d of soaking were necessary in order to produce a significant drop in pH. When comparing different cross-linking agents in individual periods (figure 5, right), it is clear both that the pH of the medium containing the EDC/NHS/EtOH cross-linked scaffold reached the lowest level of all the compared scaffolds and that the drop was significant after 3 and 8 d.

### 3.4. hMSCs cultivation in the scaffold infusions

Initially, hMSCs were cultivated in the infusions of the cross-linked scaffolds (i.e. the degradation products of the individual scaffolds) in order to check for the release of cytotoxic agents from the individual scaffolds into the cultivation medium. Cell metabolic activity was determined following 2 and 7 d of infusion treatment. After 2 d of cultivation (figure 6(A)) the cell metabolic activity in all the infusions was found to be mutually comparable. After 7 d (figure 6(B)) the situation had changed markedly except for those cells in the genipin cross-linked scaffold infusion which maintained a similar level of metabolic activity as after 2 d of cultivation. The metabolic activity of the cells in the EDC/NHS/EtOH cross-linked scaffold infusion decreased at the same rate as that of the positive control cells. Conversely, the metabolic activity of the cells in the EDC/NHS/PBS cross-linked scaffold infusion decreased significantly, i.e. from 110% to 83% of that of the positive control cells.

### 3.5. hMSCs cultivation on the scaffolds

The cells were seeded directly on the infused scaffolds and cultivated for 2 and 7 d whereupon the number of adhered cells on the scaffolds was determined. The amounts of cells adhered to the scaffolds were

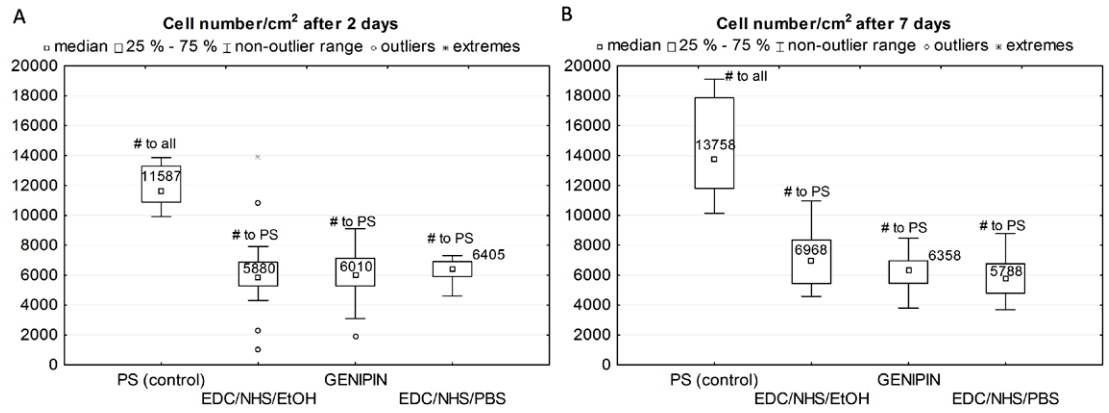


**Figure 7.** Number of hMSCs (per cm$^2$) cultivated on control polystyrene (PS) and the tested scaffolds cross-linked with EDC/NHS/EtOH, genipin and EDC/NHS/PBS for 2 d (A) and 7 d (B). #—significant difference at $p > 0.05$.

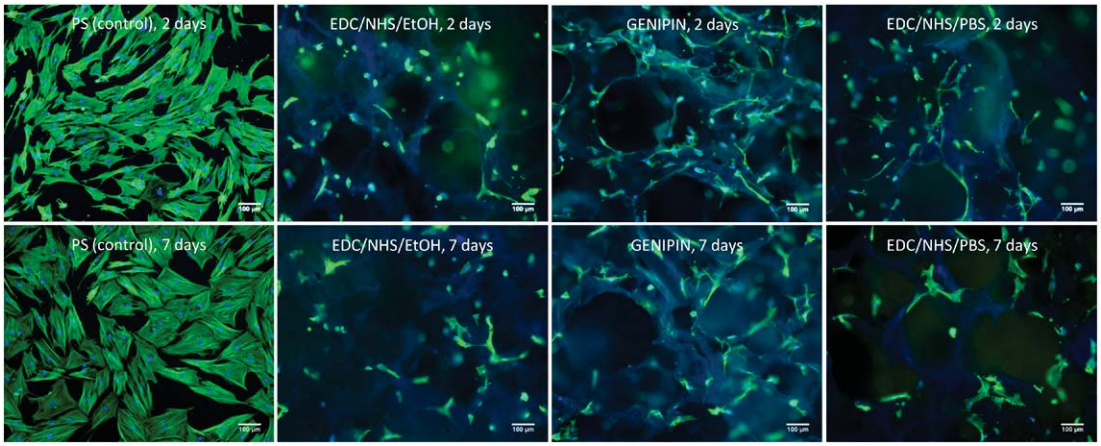


**Figure 8.** Fluorescence images of hMSCs cultivated on the control polystyrene (PS) and the tested scaffolds cross-linked with EDC/NHS/EtOH, genipin and EDC/NHS/PBS for 2 d (upper line) and 7 d (lower line). Actin filaments representing cell morphology are stained in green, the cell nuclei in blue.

comparable for all three scaffolds at both time points (figure 7).

The cells which adhered to the scaffolds were visualised using wide-field microscopy (figure 8) in order to determine cell morphology and distribution on the samples. The ability of cells to adhere was observed with regard to all the tested samples. After 2 d a visible morphology difference was evident between the donor cells (not shown). However, the cells of all three donors evinced the best appearance and homogenous distribution on the genipin cross-linked scaffold. The cells on the EDC/NHS/EtOH and EDC/NHS/PBS cross-linked scaffolds were smaller and had a lower extent of spreading. Interestingly, after 7 d, the cells on all the scaffolds were similarly organised and displayed a comparable appearance—the differences in cell morphology and distribution were markedly less pronounced. This could have been caused by the fact that the scaffolds cross-linked with EDC/NHS/EtOH and EDC/NHS/PBS experienced a higher swelling ratio than that cross-linked with genipin during the first 3 d of scaffold immersion in the medium (figure 4).

The cells adhered to the scaffolds were also visualised three-dimensionally. The use of confocal microscopy (figure 9) facilitated the visualisation of cell ability to penetrate through the scaffold. However, only the first 300 $\mu$m of the depth of the scaffolds could be scanned because of the limits of the confocal method. Interestingly, there was no difference in penetration level between the scaffolds as well as between both incubation times. The majority of adhered cells were observed on the surface of the scaffolds and up to a depth of 200 $\mu$m (i.e. 10–15% of scaffold depth); this analysis was performed with regard to representative cells from one donor.

## 4. Discussion

### 4.1. Scaffold characterisation

The structure of the pores, their size and interconnectivity represent essential scaffold parameters with respect to tissue engineering. The inner structure of a successful scaffold must allow cell growth, migration and nutrient flow throughout the whole of the

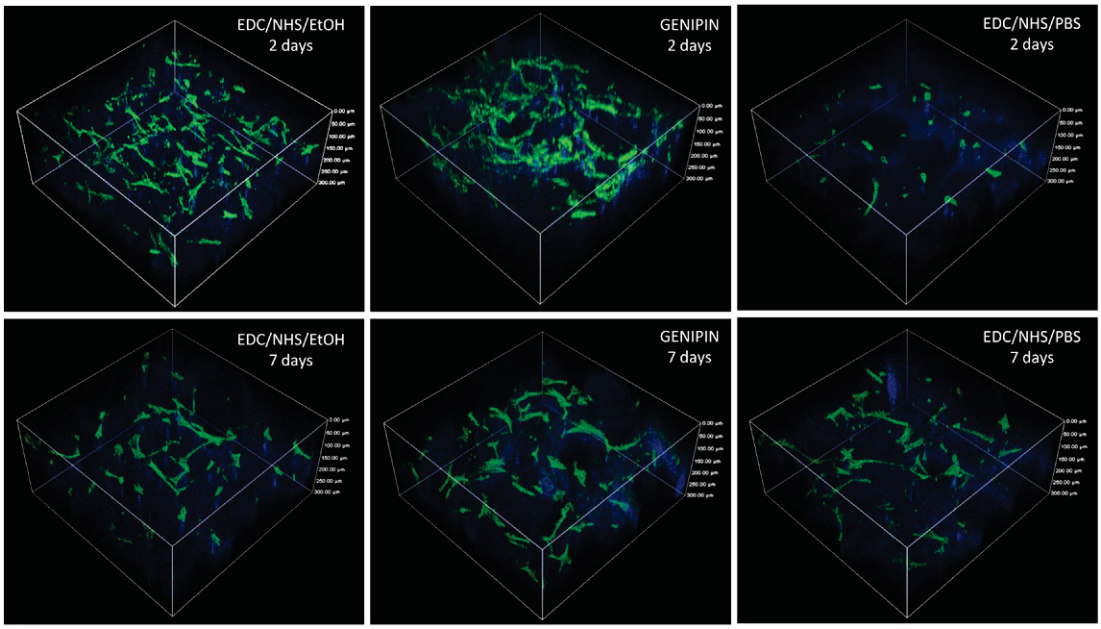


**Figure 9.** Fluorescence images (3D reconstruction of confocal microscope images) of hMSCs cultivated on tested scaffolds cross-linked with EDC/NHS/EtOH, genipin and EDC/NHS/PBS for 2 d (upper line) and 7 d (lower line). Actin filaments representing cell morphology are stained in green, the cell nuclei in blue. The fluorescent background of the scaffolds is visible in blue.

scaffold. Scaffolds with mean pore sizes in the range of 20–1500 $\mu$m have been investigated in various studies [27] many of which suggest that the optimal mean pore size for bone formation and vascularisation within the scaffold is greater than ~300 $\mu$m, while upper pore size limits may comprise the mechanical properties of the scaffolds [27–30]. The pore sizes achieved are in accordance with theoretical assumptions pertaining to the optimal structure which allows cell ingrowth.

Following chemical cross-linking the position of the FTIR bands remained practically unchanged which may suggest that the secondary structure of collagen was not destroyed (table 1). However, individual spectra differ in terms of the integral absorbance of amidic bands. As can clearly be seen in figure 2 and table 1, those scaffolds cross-linked with EDC/NHS/EtOH, with EDC/NHS/PBS and with genipin embody smaller areas of amide A and amide B as compared to non-cross-linked scaffolds. The amide A and OH bands (from water bonded to collagen) are located within the same range (3 700–3 100 $cm^{-1}$) of the FTIR spectrum. The reduced integral absorbance is caused by the loss of water bonded to collagen during the cross-linking reaction. The same trend was observed by Sionkowska *et al* [31]. It can be expected that the intensity of the amide I and amide II bands will increase with the level of polymer cross-linking due to the increasing strength of $C = O$ and N-H vibrations in the new covalent bonds [32]. However, this cannot be taken as a certainty; according to Wang *et al* [33], due to the transformation of $–NH_2$ into N-H groups in cross-linked collagen, the intensity of the amide II band may decrease since the intensity of the $–NH_2$ band is stronger than that of N-H. It was observed by Chaubaroux *et al* [34] that during rinsing following the cross-linking procedure some of the non-cross-linked collagen elements in the sample were washed away. Consequently, there is a lower number of $C = O$ vibrations and thus a smaller amide I peak area. It would also appear that the presence of PDLLA does not negatively influence the cross-linking of collagen; however, PDLLA was found to share bands with collagen (figure 2). A region from 1 410 to 1 500 $cm^{-1}$ which demonstrates the formation of conjugated alkene and which confirms cross-linking by genipin is overlapped by a PDLLA band and, consequently, it is difficult to assess the effectiveness of cross-linking in genipin cross-linked scaffolds. It can, however, be confirmed that scaffolds cross-linked with EDC/NHS/EtOH show similar integral absorbencies of amidic bands as non-cross-linked scaffolds. On the basis of FTIR analysis, the application of EDC/NHS/PBS and genipin cross-linkers appears to be the most effective in this respect.

Since bone tissue formation is known to be influenced by mechanical loading, it is important to match the mechanical properties of the scaffolds with those of the tissue they replace. In the case of scaffolds to be applied in bone tissue engineering it is important that their mechanical properties be designed so as to be similar to trabecular or cortical bone tissue. The published compression strength and elastic modulus under compression for trabecular bone vary between 0.7–15 MPa and 0.05–22.2 GPa respectively [35–37]. This scatter in terms of material properties is caused by differences between the methods applied, differences in sample preparation and conditions and further obvious facts such as age, porosity etc. The determined properties of the cross-linked scaffolds studied herein are in the range of the mechanical properties determined for trabecular bone found in literature, i.e. compression

strength 0.86–1.98 MPa and modulus of elasticity under compression 24.7–57.3 MPa. The mechanical properties of the scaffolds described herein are also comparable with those determined by other authors. Prosecka *et al* [15] designed composite scaffolds with similar compositions (collagen, hydroxyapatite, polycaprolactone nanofibers) and with a three orders lower initial modulus of elasticity of 8.5 kPa. Their scaffolds, i.e. an enriched thrombocyte-rich solution and autologous MSCs were successfully biologically evaluated *in vivo* (rabbit model). Other authors (e.g. [38–41]) designed and successfully evaluated polymer composite scaffolds with a compression strength of 0.12–4.5 MPa and a modulus of elasticity under compression of approximately 0.3–13 MPa.

### 4.2. Scaffold degradation

Mass loss and swelling ratio provide effective indices for the evaluation of the scaffold cross-linking rate; indeed, they are also useful in terms of the interpretation of the biological evaluation findings. The highest mass losses were related to samples cross-linked with EDC/NHS/EtOH: weight loss occurred immediately following 24 h of immersion. Assuming that the collagen part of the scaffold (50.5 wt%) is the only component susceptible to rapid degradation within such a short time period, then the mass loss of the collagen part of the EDC/NHS/EtOH would be equal to half of its complete amount within the scaffold (up to 29%). This behaviour, as well as the considerable variance in the swelling ratios after the third and eighth days of incubation, indicates the lowest stability level of the collagen part and thus the whole of the scaffold structure. It is possible to hypothesise that the structural stability of the scaffold is related to the degree of cross-linking [42]. In contrast to the scaffolds cross-linked in an ethanol solution, the mass loss of samples cross-linked with EDC/NHS/PBS and genipin show the same low level of mass defects, i.e. the highest stability levels and, most probably, the highest degree of cross-linking. Nevertheless, their structural stability evaluated in terms of swelling behaviour evinces a different tendency following the early stages of incubation. In both cases the swelling ratios on day 1 and day 3 are equal, however, 8 d subsequent to incubation the swelling ratio of the genipin cross-linked samples increased; conversely, the swelling ratio of the EDC/NHS/PBS cross-linked samples decreased. The decrease in swelling ratio was not reflected in mass loss which might have indicated the disintegration of the internal structure.

From the cell behaviour point of view, the difference between the observed pH values of all the tested scaffolds at all the time points was negligible (pH 7.4–7.6). The decrease in the pH values of all the tested scaffolds from day 0 to day 8 is interesting when compared to the lack of a change in the pH of the medium with no scaffolds under the same conditions. Thus, it would appear that the decrease in pH may have been caused by one of the components of the scaffolds; nevertheless, it is also affected by the cross-linking agent employed. It has already been shown that neither cell viability nor the population doubling time of mammalian cells were affected under a pH range of 7.4 to 6.7 (7.4 to 7.0 [43]). So, taken as a whole, it can be expected that the lowest measured pH value (7.4) should not fundamentally affect cell behaviour.

### 4.3. hMSCs cultivation in the scaffold infusions

Cytotoxicity is often determined by a decrease in cell metabolic activity under 75% [44]. Thus, all the infusions would seem to have been non-cytotoxic after both 2 and 7 d. Based on such infusion results, it is reasonable to speculate that a substance (or substances) can be released from the scaffolds which is, subsequently, able to support or even induce cell metabolism. However, its form and amount vary depending on the cross-linking agent employed and the duration of cultivation. In addition, this substance could be utilised by cells in different ways (substance turnover). On the other hand, any cytotoxic agent manifested or created (any degradation product) after a longer incubation period might be released from the scaffolds (especially from the EDC/NHS/PBS cross-linked scaffold for which infusion led to a dramatic decrease in cell metabolic activity after 7 d). Taken together, the infusion results revealed that cross-linking agents can influence cell viability and scaffold behaviour. Moreover, these findings confirm the necessity of the *in vitro* biological evaluation of the resulting biomaterials.

### 4.4. hMSCs cultivation on the scaffolds

The observed substantial reduction in cell adhesion and the differing cell morphology on the scaffolds compared to the control cells on the polystyrene (non-porous, solid and specially developed for cell cultivation) could be reasonably predicted due to their significantly differing properties [45]. Nevertheless, polystyrene is very important as a cultivation standard and serves as both a control and a criterion for comparison with other studies. However, from the application point of view, it is relevant merely to compare the scaffolds to each other.

The scaffold porosity level, pore size and the heterogeneity of the pores all play a significant role in terms of cell adhesion [46]. Specifically, hMSC behaviour can be significantly influenced by pore size [47]. In addition, cell adhesion to the scaffolds might also be affected by the accessibility of specific motifs within the collagen triple-helix [48] and/or other scaffold components; in addition, motif accessibility could be influenced by cross-linking. Moreover, motif nano-spacing can affect hMSC adhesion, shape and differentiation as was demonstrated on an RGD motif (sequence motif for cell adhesion) [49]. Notably, a recent study [50] revealed a relationship between collagen concentration in collagen-grafted PLGA/chitosan scaffolds and cell behaviour; the increase in collagen concentration

within the scaffolds enhanced cell adhesion and the viability of bone marrow stromal cells.

The swelling stability of the genipin cross-linked scaffold during the initial days of cultivation could have been more favourable for 'early' cell adhesion and subsequent cell spreading than scaffolds which swelled over time. Indeed, this corresponds to published results concerning osteoblast cultivation on collagen-glycosaminoglycan scaffolds. The higher the detected scaffold stiffness, the higher was the cell number and enhanced cellular distribution observed [51]. Moreover, it has been shown previously that scaffold stiffness alone is able to affect the fate of MSCs without the addition of differentiation supplements in which case stiffer scaffolds direct MSCs towards osteogenic differentiation [52]. Thus, it is reasonable to predict that the stability and non-swelling nature of the genipin cross-linked scaffold during early incubation is more suitable for the osteogenic differentiation of hMSCs. A further advantage of the genipin cross-linked scaffold lies in pore size stability following cross-linking (pore size: approximately 300 $\mu$m). Conversely, a reduction in pore size was observed with reference to the scaffolds cross-linked with other agents (pore size: 200–250 $\mu$m). From this point of view, and based on our observations, hMSCs may prefer a larger (300 $\mu$m) pore size for 'early' cell adhesion and distribution (up to 2 d). A similar effect was observed with regard to collagen–glycosaminoglycan scaffolds embedded with osteoblasts: the specific surface area of the scaffolds was important in terms of initial adhesion (2 d). Moreover, improved cell migration was observed with reference to scaffolds with a pore size of greater than 300 $\mu$m. It would appear that larger pore size represents a positive factor for cells in the early as well as later phases of cultivation. Furthermore, a recent study revealed that larger pore size reduced the formation of undesirable cell aggregates [27]. These results are in accordance with the uniform distribution of the cells observed on the genipin cross-linked scaffolds from the very beginning of the cultivation process.

The observed disinclination of the cells to penetrate into the scaffolds could have been due to the inner structure of the scaffolds—the unevenness of the cross-linking and the afore-mentioned pore size variability [46]. In addition, penetration may have been influenced by specific collagen sequence/motif accessibility (as mentioned above), changes thereof [48] and by the nano-spacing of cell-attractive motifs in general [49]. Furthermore, cells have a relatively low level of motivation to enter more deeply into the scaffold if similar conditions are available on the surface of the scaffold; indeed, the availability of nutrients may be higher on the scaffold surface than at depth. Consequently, new daughter cells may be forced to migrate more deeply into the scaffold due to a lack of space on the scaffold's surface after longer periods of cultivation. It should also be noted that the cells were seeded on the surfaces of the scaffolds only and that no dynamic cultivation or injection into the scaffolds was performed. Dynamic cell cultivation might well induce an improvement in the occupation of inner scaffold structures. Moreover, enhanced penetration might be supported by the application of cell attractants to the scaffolds should it be deemed necessary.

## 5. Conclusions

With regard to the structural stability of the tested scaffolds, the most effective cross-linking agents were found to be EDC/NHS/PBS and genipin. The scaffolds cross-linked with EDC/NHS/PBS embodied a low degradation together with a low swelling ratio. Genipin cross-linked scaffolds provided the best conditions for human mesenchymal stem cells following both 2 d and 7 d of cultivation. In addition, genipin scaffolds maintained constant mechanical properties without any change in contrast to the EDC/NHS/EtOH scaffolds the mechanical properties of which changed negatively following a longer incubation time. The EDC/NHS/EtOH scaffolds revealed the highest mass loss together with a high swelling ratio after 1 to 8 d of incubation in the $\alpha$-MEM medium. The cells on EDC/NHS/EtOH and EDC/NHS/PBS cross-linked scaffolds were found to be less spread out which may have been connected with a reduction in pore size during incubation in the cell culture medium. Based on *in vitro* testing, the genipin cross-linked scaffold was selected as having provided the best results and it is strongly recommended for further advanced *in vitro* (3D cultivation) and *in vivo* testing.

## Acknowledgments

This study was supported by a grant project provided by the Ministry of Health of the Czech Republic (NV 15-25813A)by the National Sustainability Program I (NPU I) Nr. LO1503 provided by the Ministry of Education Youth and Sports of the Czech Republic and by grants provided by the Charles University in Prague; grant SVV–2015 No.260 170 and SVV-2015–260209, the GAUK 400215 grant and the PRVOUK-P24/LF1/3 project. We gratefully acknowledge the financial support provided for our work by the long-term conceptual development research organisation under project no. RVO: 67985891. Special thanks go to Blanka Bilkova and Martina Krizkova for their technical assistance and to Darren Ireland for the language revision of the English manuscript.

## References

[1] Lee K W, Wang S, Yaszemski M J and Lichun L 2010 Enhanced cell ingrowth and proliferation through 3D nanocomposite scaffolds with controlled pore structures *Biomacromolecules* **11** 682–9

[2] Venugopal J and Ramakrishna S 2005 Applications of polymer nanofibres in biomedicine and biotechnology *Appl. Biochem. Biotechnol.* **125** 147–57
[3] Rampichová M *et al* 2013 Elastic 3D poly (ε-caprolactone) nanofibre scaffold enhances migration, proliferation and osteogenic differentiation of mesenchymal stem cells *Cell Prolifer.* **46** 23–37
[4] Manning C N, Schwartz A G, Liu W, Xie J, Havlioglu N, Sakiyama-Elbert S E, Silva M J, Xia Y, Gelberman R H and Thomopoulos S 2013 Controlled delivery of mesenchymal stem cells and growth factors using a nanofiber scaffold for tendon repair *Acta Biomater.* **9** 6905–14
[5] Hu H-T, Shin T-C, Lee S-Y, Chen C-C and Yang J-C 2011 Influence of hydrolytic degradation on the surface properties of poly -5D/95L-lactide resorbable bone plates *Polym. Degtrad. Stabil.* **96** 1522–9
[6] Novotna K *et al* 2014 Polylactide nanofibers with hydroxyapatite as growth substrates for osteoblast-like cells *J. Biomed. Mater. Res.* A **102** 3918–30
[7] Tokita Y and Okamoto A 1995 Hydrolytic degradation of hyaluronic acid *Polym. Degtrad. Stabil.* **48** 269–73
[8] Yoshikawa M, Tsuji N, Toda T and Ohgushi H 2007 Osteogenic effect of hyaluronic acid sodium salt in the pores of a hydroxyapatite scaffold *Mater. Sci. Eng.* C **27** 220–6
[9] Glowacki J and Mizuno S 2008 Collagen scaffolds for tissue engineering *Biopolymers* **89** 338–44
[10] Chan B P and So K-F 2005 Photochemical crosslinking improves the physicochemical properties of collagen scaffolds *J. Biomed. Mater. Res.* A **75** 689–701
[11] Wollensak G and Spoerl E 2004 Collagen crosslinking of human and porcine sclera *J. Cataract Refract. Surg.* **30** 689–95
[12] Raiskup F and Spoerl E 2013 Corneal crosslinking with riboflavin and ultraviolet A. I. principles *Ocul. Surf.* **11** 65–74
[13] Walters B D and Stegemann J P 2014 Strategies for directing the structure and function of 3D collagen biomaterials across length scales *Acta Biomater.* **10** 1488–501
[14] McDade J K, Brennan-Pierce E P, Ariganello M B, Labow R S and Lee J M 2013 Interactions of U937 macrophage-like cells with decellularized pericardial matrix materials: Influence of crosslinking treatment *Acta Biomater.* **9** 7191–9
[15] Prosecká E *et al* 2015 Collagen/hydroxyapatite scaffold enriched with polycaprolactone nanofibers, thrombocyte-rich solution and mesenchymal stem cells promotes regeneration in large bone defect *in vivo J. Biomed. Mater. Res.* A **103** 671–82
[16] Sell S A, Francis M P, Garg K, McClure M J, Simpson D G and Bowlin G L 2008 Cross-linking methods of electrospun fibrinogen scaffolds for tissue engineering applications *Biomed. Mater.* **3** 1–11
[17] Park S N, Park J C, Kim H O, Song M J and Suh H 2002 Characterization of porous collagen/hyaluronic acid scaffolds modified by 1-ethyl-3-(3 dimethylaminopropyl) carbodiimide cross-linking *Biomaterials* **23** 1205–12
[18] Tsai C C, Huang R N, Sung H W and Liang H C 2000 *In vitro* evaluation of the genotoxicity of a naturally occurring crosslinking agent (genipin) for biologic tissue fixation *J. Biomed. Mater. Res.* **52** 58–65
[19] Chang Y, Hsu C K, Wei H J, Chen S C, Liang H C, Lai P H and Sung H W 2005 Cell-free xenogenic vascular grafts fixed with glutaraldehyde or genipin: *in vitro* and *in vivo* studies *J. Biotechnol.* **120** 207–19
[20] Zhang X, Chen X, Yang T, Zhang N, Dong L, Ma S, Liu X, Zhou M and Li B 2014 The effects of different crossing-linking conditions of genipin on type I collagen scaffolds: an *in vitro* evaluation *Cell Tissue Bank.* **15** 531–41
[21] Battista S, Guarnieri D, Borselli C, Zeppetelli S, Borzacchiello A, Mayol L, Gerbasio D, Keene D R, Ambroso L and Netti P A 2005 The effect of matrix composition of 3D constructs on embryonic stem cell differentiation *Biomaterials* **26** 6194–207
[22] Murugan R, Ramakrishna S and Panduranga Rao K 2006 Nanoporous hydroxy-carbonate apatite scaffold made of natural bone *Mater. Lett.* **60** 2844–7
[23] ISO, ISO13314: 2011 Mechanical testing of metals—ductility testing—compression test for porous and cellular metals, 2011
[24] Amin S *et al* 2013 Fatigue behaviour of porous biomaterials manufactured using selective laser melting *Mater. Sci. Eng.* C **33** 4849–58
[25] Ahmadi S M, Campoli G, Yavari S A, Sajadi B, Wauthlé R, Schrooten J, Weinans H and Zadpoor A 2014 Mechanical behavior of regular open-cell porous biomaterials made of diamond lattice unit cells *J. Mech. Behav. Biomed.* **34** 106–15
[26] Bobe K, Willbold E, Morgenthal I, Andersen O, Studnitzky T, Nellesen J, Tillmann W, Vogt C, Vano K and Witte F 2013 *In vitro* and *in vivo* evaluation of biodegradable, open-porous scaffolds made of sintered magnesium W4 short fibres *Acta Biomater.* **9** 8611–23
[27] Murphy C M, Haugh M G and O'Brien F J 2010 The effect of mean pore size on cell attachment, proliferation and migration in collagen–glycosaminoglycan scaffolds for bone tissue engineering *Biomaterials* **31** 461–6
[28] Kuboki Y, Jin Q and Takita H 2001 Geometry of carriers controlling phenotypic expression in BMP-induced osteogenesis and chondrogenesis *J. Bone Joint Surg. Am.* **83** S105–15
[29] Roosa S M, Kemppainen J M, Moffitt E N, Krebsbach P H and Hollister S J 2010 The pore size of polycaprolactone scaffolds has limited influence on bone regeneration in an *in vivo* model *J. Biomed. Mater. Res.* A **92** 359–68
[30] McCoy R J, Jungreuthmayer C and O'Brien F J 2012 Influence of flow rate and scaffold pore size on cell behavior during mechanical stimulation in a flow perfusion bioreactor *Biotechnol. Bioeng.* **109** 1583–94
[31] Sionkowska S A, Skopinska-Wisniewska J, Gawron M, Kozlowska J and Planecka A 2010 Chemical and thermal cross-linking of collagen and elastin hydrolysates *Int. J. Biol. Macromol.* **47** 570–7
[32] Staroszcyk H, Sztuka K, Wolska J, Wojtasz-Pajak A and Kolodziejska I 2014 Interactions of fish gelatin and chitosan in uncrosslinked and crosslinked with EDC films, FT-IR study *Spectrochim. Acta* A **117** 707–12
[33] Wang X H, Li D P, Wang W J, Feng Q L, Cui F Z, Xu Y X, Song X H and van der Werf M 2003 Crosslinked collagen/chitosan matrix for artificial livers *Biomaterials* **24** 3213–20
[34] Chaubaroux C *et al* 2012 Collagen-based fibrillar multilayer films cross-linked by a natural agent *Biomacromolecules* **13** 2128–35
[35] Woodard J R, Hilldore A J, Lan S K, Park C J, Morgan A W, Eurell J A C, Clark S G, Wheeler M B, Jamison R D and Wagoner Johnson A J 2005 The mechanical properties and osteoconductivity of hydroxyapatite bone scaffolds with multi-scale porosity *Biomaterials* **28** 45–54
[36] Murugan R and Ramakrishna S 2005 Development of nanocomposites for bone grafting *Compo. Sci. Technol.* **65** 2385–406
[37] Kopperdahl D L and Keaveny T M 1998 Yield strain behavior of trabecular bone *J Biomech.* **31** 601–8
[38] Gorna K and Gogolewski S 2006 Biodegradable porous polyurethane scaffolds for tissue repair and regeneration *J. Biomed. Mater. Res.* **79A** 128–38
[39] Serra I R, Fradique R, Vallejo M C S, Correia T R, Miguel S P and Correia I J 2015 Production and characterization of chitosan/gelatin/β-TCP scaffolds for improved bone tissue regeneration *Mater Sci. Eng.* C **55** 592–604
[40] Andric T, Wright L D, Taylor B L and Freeman J W 2012 Fabrication and characterization of 3D electrospun scaffolds for bone tissue engineering *J. Biomed. Mater. Res.* A **100A** 2097–105
[41] Kim S S, Ahn K M, Park M S, Lee J H, Choi C Y and Kim B S 2007 A poly(lactide-co-glycolide)/hydroxyapatite composite scaffold with enhanced osteoconductivity *J. Biomed. Mater. Res.* A **80A** 206–15
[42] Bi L, Cao Z, Hu Y, Song Y, Yu L, Yang B, Mu J, Huang Z and Han Y 2011 Effects of different cross-linking conditions on the properties of genipin-cross-linked chitosan/collagen scaffolds

AQ4

for cartilage tissue engineering *J. Mater. Sci. Mater. Med.* **22** 51–62
[43] Gerweck L and Rottinger E 1976 Enhancement of mammalian cell sensitivity to hyperthermia by pH alteration *Radiat. Res.* **67** 508–11
[44] Flahaut E, Durrieu M C, Remy-Zolghadri M, Bareille R and Baquey C 2006 Investigation of the cytotoxicity of CCVD carbon nanotubes towards human umbilical vein endothelial cells *Carbon* **44** 1093–9
[45] Walters N J and Gentleman E 2015 Evolving insights in cell–matrix interactions: Elucidating how non-soluble properties of the extracellular niche direct stem cell fate *Acta Biomater.* **11** 3–16
[46] O'Brien F J, Harley B A, Yannas I V and Gibson L J 2005 The effect of pore size on cell adhesion in collagen-GAG scaffolds *Biomaterials* **26** 433–41
[47] Kasten P, Beyen I, Niemeyer P, Luginbühl R, Bohner M and Richter W 2008 Porosity and pore size of $\beta$-tricalcium phosphate scaffold can influence protein production and osteogenic differentiation of human mesenchymal stem cells: an *in vitro* and *in vivo* study *Acta Biomater.* **4** 1904–15
[48] Xu H, Bihan D, Chang F, Huang P H, Farndale R W and Leitinger B 2012 Discoidin domain receptors promote $\alpha1\beta1$- and $\alpha2\beta1$-integrin mediated cell adhesion to collagen by enhancing integrin activation *PLoS ONE* **7** e52209
[49] Wang X, Yan C, Ye K, He Y, Li Z and Ding J 2013 Effect of RGD nanospacing on differentiation of stem cells *Biomaterials* **34** 2865–74
[50] Kuo Y-C and Yeh C-F 2011 Effect of surface-modified collagen on the adhesion, biocompatibility and differentiation of bone marrow stromal cells in poly(lactide-co-glycolide)/chitosan scaffolds *Colloid Surf.* B **82** 624–31
[51] Haugh M G, Murphy C M, McKiernan R C, Altenbuchner C and O'Brien F J 2010 Crosslinking and mechanical properties significantly influence cell attachment, proliferation, and migration within collagen glycosaminoglycan scaffolds *Tissue Eng.* A **17** 1201–8
[52] Murphy C M, Matsiko A, Haugh M G, Gleeson J P and O'Brien F J 2012 Mesenchymal stem cell fate is regulated by the composition and mechanical properties of collagen–glycosaminoglycan scaffolds *J. Mech. Behav. Biomed. Mater.* **11** 53–62

**E.** Tomáš Suchý, Monika Šupová, Eva Klapková, Václava Adámková, Jan Závora, Margit Žaloudková, Šárka Rýglová, Rastislav Ballay, František Denk, Marek Pokorný, **Pavla Sauerová**, Marie Hubálek Kalbáčová, Lukáš Horný, Jan Veselý, Tereza Voňavková, Richard Průša (2017): **The Release Kinetics, Antimicrobial Activity and Cytocompatibility of Differently Prepared Collagen/Hydroxyapatite/Vancomycin Layers: Microstructure vs. Nanostructure.** European Journal of Pharmaceutical Sciences 100, 219-229. IF = 3.77

European Journal of Pharmaceutical Sciences 100 (2017) 219–229

Contents lists available at ScienceDirect

European Journal of Pharmaceutical Sciences

journal homepage: www.elsevier.com/locate/ejps

# The release kinetics, antimicrobial activity and cytocompatibility of differently prepared collagen/hydroxyapatite/vancomycin layers: Microstructure vs. nanostructure

Tomáš Suchý [a,b,*], Monika Šupová [a], Eva Klapková [c], Václava Adamková [d], Jan Závora [d], Margit Žaloudková [a], Šárka Rýglová [a], Rastislav Ballay [e], František Denk [a,b], Marek Pokorný [f], Pavla Sauerová [g,h], Marie Hubálek Kalbáčová [g,h], Lukáš Horný [b], Jan Veselý [b], Tereza Voňavková [b], Richard Průša [c]

[a] Department of Composites and Carbon Materials, Institute of Rock Structure and Mechanics, Academy of Sciences of the Czech Republic, Prague 8, Czech Republic
[b] Faculty of Mechanical Engineering, Czech Technical University in Prague, Prague 6, Czech Republic
[c] Department of Medical Chemistry and Clinical Biochemistry, Charles University, 2nd Medical School and University Hospital Motol, Prague 5, Czech Republic
[d] Clinical Microbiology and ATB Centre, Institute of Medical Biochemistry and Laboratory Diagnostics, 1st Faculty of Medicine, Charles University in Prague and Motol University Hospital, Prague 2, Czech Republic
[e] 1st Department of Orthopaedics, 1st Faculty of Medicine, Charles University in Prague and Motol University Hospital, Prague 5, Czech Republic
[f] Contipro a.s., R&D Department, Dolni Dobrouc, Czech Republic
[g] Institute of Inherited Metabolic Disorders, 1st Faculty of Medicine, Charles University in Prague, Ke Karlovu 2, Prague 2, Czech Republic
[h] Biomedical Centre, Faculty of Medicine in Pilsen, Charles University in Prague, Alej Svobody 76, Pilsen, Czech Republic

ARTICLE INFO

*Article history:*
Received 28 November 2016
Received in revised form 16 January 2017
Accepted 25 January 2017
Available online 27 January 2017

*Keywords:*
Coating
Controlled release
Drug delivery system
Nanoparticle
Pharmacokinetics
Polymeric drug delivery system

ABSTRACT

The aim of this study was to develop an osteo-inductive resorbable layer allowing the controlled elution of antibiotics to be used as a bone/implant bioactive interface particularly in the case of prosthetic joint infections, or as a preventative procedure with respect to primary joint replacement at a potentially infected site. An evaluation was performed of the vancomycin release kinetics, antimicrobial efficiency and cytocompatibility of collagen/hydroxyapatite layers containing vancomycin prepared employing different hydroxyapatite concentrations. Collagen layers with various levels of porosity and structure were prepared using three different methods: by means of the lyophilisation and electrospinning of dispersions with 0, 5 and 15 wt% of hydroxyapatite and 10 wt% of vancomycin, and by means of the electrospinning of dispersions with 0, 5 and 15 wt% of hydroxyapatite followed by impregnation with 10 wt% of vancomycin.

The maximum concentration of the released active form of vancomycin characterised by means of HPLC was achieved via the vancomycin impregnation of the electrospun layers, whereas the lowest concentration was determined for those layers electrospun directly from a collagen solution containing vancomycin. Agar diffusion testing revealed that the electrospun impregnated layers exhibited the highest level of activity. It was determined that modification using hydroxyapatite exerts no strong effect on vancomycin evolution. All the tested samples exhibited sufficient cytocompatibility with no indication of cytotoxic effects using human osteoblastic cells in direct contact with the layers or in 24-hour infusions thereof. The results herein suggest that nano-structured collagen-hydroxyapatite layers impregnated with vancomycin following cross-linking provide suitable candidates for use as local drug delivery carriers.



## 1. Introduction

The infection of implanted endoprostheses represents a serious problem (Bauer & Zhang, 2016; Brown et al., 2016) with respect to orthopaedic and trauma surgery and one of the ways in which to increase the efficacy of therapy consists of the application of a local antibiotic delivery system (Nair et al., 2011; Simchi et al., 2011; Rahaman et al., 2014). The local delivery of antibiotics maximises target tissue concentration while minimising the risk of systemic toxicity.

Glycopeptide (Li & Starkey, 2016) vancomycin is one of the most commonly used local delivery antibiotic vehicles (Kirst et al., 1998). Since the 1950s vancomycin has been used to treat severe infections caused by gram-positive bacteria. Vancomycin-resistant *Staphylococcus aureus* (VRSA) (Gardete & Tomasz, 2014; Sfaciotte et al., 2015) is most common in elderly patients, especially those patients with a history of

* Corresponding author at: Department of Composites and Carbon Materials, Institute of Rock Structure and Mechanics, Academy of Sciences of the Czech Republic, v.v.i. V Holešovičkách 41, Prague 8 182 09, Czech Republic.
*E-mail address:* suchyt@irsm.cas.cz (T. Suchý).

http://dx.doi.org/10.1016/j.ejps.2017.01.032
0928-0987/

vancomycin-resistant enterococci. One possible explanation as to why infections caused by VRSA are becoming more commonly reported is that vancomycin breaks down over time to form crystalline degradation products (CDP-1s) (Somerville et al., 1999; Suchý et al., 2016) which are antimicrobially ineffective. During in vitro exposure at a temperature of 20–25 °C, up to 50% of vancomycin is converted to CDP-1s within 16 h and 90% of vancomycin is converted to CDP-1s within 40 h. In addition, an acidic pH of 4.1 to 4.2 contributes towards the formation of the two conformational isomers of CDP-1s: CDP-1M (major) and CDP-1m (minor).

The most extensively studied and earliest commercially available device designed for the controlled release of antibiotics was developed in the 1970s according to Buchholz and Engelbrecht"s (Buchholz & Engelbrecht, 1970) innovative idea of releasing antibiotics from polymethylmethacrylate (PMMA) bone cement. This device is still widely used; however, it enables only a small fraction of the loaded drug to diffuse through the polymer pores and provides an initial burst release of antibiotics with the larger part of the loaded antibiotic remaining within the cement. Since PMMA is not biodegradable, secondary surgery is subsequently necessary to remove the PMMA before new bone can regenerate. Thus, with a view to overcoming these disadvantages, various biodegradable devices made from both natural and synthetic polymers have been produced by means of various processes in recent years (Inzana et al., 2016). Biodegradable polymers can be modified by means of calcium phosphate nanoparticles and tailored for a specific application (ter Boo et al., 2015; Zilberman & Elsner, 2008; Alt et al., 2015) and local antibiotic delivery systems can be prepared in a number of final forms. Over the past decade, researchers have developed biodegradable polymeric scaffolds (Garvin & Feschuk, 2005; Gursel et al., 2001; Kankilic et al., 2011), degradation beads (Liu et al., 2002), sheets (Hirose et al., 2006) and membranes (Chen et al., 2012a) for use in the treatment of bone infections. A further alternative method with respect to the treatment of osteomyelitis involves the use of a hydrogel structure that is easily administered (injectable) (Posadowska et al., 2016; Hong et al., 2013; Adams et al., 2009) and, moreover, is not particularly invasive. Antibiotic-loaded implant coatings provide a straightforward approach to the prevention of implant-associated infections (Ordikhani et al., 2015; Ordikhani et al., 2014; Yang et al., 2013; Kong et al., 2013; Raphel et al., 2016). This "soft matter on hard matter" method provides an immediate response to the threat of implant contamination and, moreover, does not require the use of any other carrier than the orthopaedic implant itself.

The loading of drugs can be conducted via the use of a number of different techniques, the most simple of which consists of the straightforward mixing of the polymer and antibiotics in the form of a dry powder (Liu et al., 2002) or solution (Kankilic et al., 2011; Hirose et al., 2006; Posadowska et al., 2016; Makarov et al., 2010; Fang et al., 2012). Although all the approaches employed are generally successful in terms of providing for the long-lasting release of therapeutic antibiotic concentrations, drug loading is often conducted by means of the mixing of the drug with polymers sometimes dissolved in harsh solvents. A further method involves the soaking of the antibiotics by means of immersion in a drug-containing solution (Adams et al., 2009; Kluin et al., 2009; Harth et al., 2010; Yao et al., 2013; Noel et al., 2010; Ruiz et al., 2008; Leprêtre et al., 2009; Jean-Baptiste et al., 2012). Electrospinning, a promising processing technique that utilises electrical forces to produce ultrafine polymeric fibres from polymer solutions is seen as having great potential in terms of the development of nano-structured biomedical materials. Nanofibers are particularly efficient drug delivery agents due to their high surface-area-to-volume ratios, high porosities and 3D open porous structures (Rogina, 2014). The resulting electrospun fibres have been successfully investigated with respect to their use as matrices containing antibiotics (Waeiss et al., 2014), sandwich structures for the repair of infected wounds (Chen et al., 2012a; Chen et al., 2012b; Jang et al., 2015) and the electrospun vancomycin-loaded coating for titanium implants (Hsu et al., 2014; Zhang et al., 2014). Ying-Chao Chou et al. (Chou et al., 2016) have used electrospinning for the preparation of an artificial periosteum that incorporates biodegradable drug-embedded nanofibers so as to provide an adequate level of drug release capacity as well as biodegradable stents for the mimicking of the mechanical properties of the periosteum in connection with the management of open fractures. A further promising technique concerning the bioactive modification of the surface of titanium implants consists of electromechanically-assisted deposition by means of which collagenous or chitosan interfaces can be created (Ordikhani et al., 2015; Ordikhani et al., 2014; Yang et al., 2013; Kong et al., 2013; Tu et al., 2012).

The technology and conditions concerning composite preparation are of particular importance since they are able to significantly affect the final microstructure of the composite and, consequently, the vancomycin release profile. The fact that vancomycin can be washed out during the rinsing and cross-linking processes is often not taken into consideration (Makarov et al., 2010). In addition, the fact that the temperature applied during the preparation of the composite (Liu et al., 2002) may lead to the transformation of vancomycin into its microbiologically inactive products is very often neglected; indeed, the monitoring of the antibiotically inactive forms of vancomycin is a very important issue which is, unfortunately, often ignored (Chen et al., 2012a; Zhang et al., 2014). The analysis of vancomycin concentrations continues to be performed by means of UV/VIS assay (Ordikhani et al., 2015; Jang et al., 2015; Tu et al., 2012); however, this method is incapable of determining the inactive degradation products of vancomycin. Only the high performance liquid chromatography (HPLC) method is able to provide an effective tool for the quantitative and qualitative analysis of such products (Suchý et al., 2016; Melichercik et al., 2014).

The aim of this study is to compare biodegradable composite layers prepared using three different techniques, the main requirement of which is that they are capable of releasing the active form of vancomycin with an initial burst release which eliminates the development of a biofilm and, for at least 3 weeks at concentrations exceeding the minimum inhibitory concentration for VRSA, ensure that such vancomycin release rates are not toxic for the participating cells. Nano- and micro-structured layers based on collagen (type I, isolated from calf skin) and 0, 5 and 15 wt% of hydroxyapatite nanoparticles were prepared employing either the lyophilisation or electrospinning of the dispersions with or without the presence of 10 wt% vancomycin hydrochloride and were subsequently cross-linked with N-(3-dimethylaminopropyl)-N-ethylcarbodiimide hydrochloride (EDC)/N-hydroxysuccinimide (NHS) (McDade et al., 2013), a commonly used cross-linking agent. The pure cross-linked collagen/hydroxyapatite electrospun mats obtained were subsequently impregnated with 10 wt% vancomycin. The in vitro release rates of the vancomycin and its inactive degradation products were characterised by means of the HPLC method. The antimicrobial effects of the layers were determined using the agar diffusion testing technique against four different clinical isolates. The in vitro biological evaluation was conducted using SAOS-2 cells in direct contact with the layers or their 24-hour infusions. The multidisciplinary results of the comparison of the three different techniques concerning the preparation of a collagen/hydroxyapatite/antibiotic drug delivery system suggest that the electrospinning of collagen/hydroxyapatite in combination with antibiotic impregnation provides a promising method with respect to creating a drug delivery system for use in orthopaedic surgery which exhibits a higher level of effectiveness than does the direct electrospinning of antibiotic solutions.

## 2. Materials and Methods

### 2.1. Materials, Preparation and Characterisation

Nano- and micro-structured layers were prepared based on collagen (type I, VUP Medical, Czech Republic), 0 wt%, 5 wt% or 15 wt% of hydroxyapatite nanoparticles (avg. 150 nm, Sigma Aldrich, Germany)

and vancomycin (VANCO, vancomycin hydrochloride, Mylan S.A.S, France) in the amount of 10 wt% of the total weight of collagen (COL) with hydroxyapatite (HA). The micro-structured layers (L0, L5 and L15) were prepared by means of the lyophilisation of a COL/HA/VANCO dispersion in a phosphate buffer (PBS)/ethanol solution (the preparation process has been described elsewhere (Suchý et al., 2016)). The nano-structured layers were prepared via the electrospinning of an 8 wt% collagen PBS/ethanol solution modified by 8 wt% (to COL) polyethylene oxide (PEO; $M_r$ 900,000, Sigma Aldrich, Germany) with dispersed HA particles. The vancomycin was applied using two different procedures, i.e. direct introduction to the COL solution prior to electrospinning (E0, E5 and E15) or the subsequent impregnation of the electrospun COL/HA cross-linked layers (EI0, EI5 and EI15). Both types of electrospun mats were prepared using a high voltage level of 45 kV and the feeding rate was set at 130 μl·min$^{-1}$, the temperature at 24 °C and the relative humidity at 20–25% (4SPIN, Contipro, Czech Republic). The production rate of the nanofibrous collagen mats was increased via the application of electroblowing (Pokorný et al., 2016); the flow rate of the preheated air (25 °C) was set at 30 l·min$^{-1}$. All the electrospun mats were collected on a static continual collector (22 × 29 cm) and then cut to the appropriate sizes using a scalpel following cross-linking. The stability of all the collagen layers was enhanced by means of cross-linking with a 95% ethanol solution containing EDC and NHS at a weight ratio of 4:1; the EDC and NHS (Sigma Aldrich, Germany) were used as received. Following a reaction period of 24 h at 37 °C, all the layers were washed in 0.1 M $Na_2HPO_4$ (2 × 45 min), followed by rinsing using deionised water (30 min). They were then frozen at −15 °C for 5 h and lyophilised at −105 °C at a pressure level of approximately 1.3 Pa (BenchTop 4KZL, VirTis, U.S.A.). Following cross-linking, the PEO and NaCl were fully leached out. The electrospun COL/HA cross-linked layers were impregnated with a vancomycin ethanol solution and dried at room temperature in a laminar box until a constant weight was achieved (up to 2 h).

The structure of the prepared samples was evaluated by means of attenuated total reflection infrared spectrometry (FTIR) using a Protégé 460 E.S.P. infrared spectrometer (Thermo Nicolet Instruments, USA) equipped with an ATR device (GladiATR, PIKE Technologies, USA) with a diamond crystal. All the spectra were recorded in absorption mode at a resolution of 4 cm$^{-1}$ and 128 scans. The areas of the bands (integral absorbencies) were determined using OMNIC 7 software. The samples were also characterised using scanning electron microscopy (SEM) (QUANTA 450, FEI, USA).

### 2.2. Preliminary Evaluation of Antimicrobial Susceptibility and Vancomycin Release

An investigation was conducted of the in vitro release of vancomycin from COL/HA/VANCO layers prepared by means of three different methods. Six samples of each type of layer were placed on a sterile gauze pad and firmly caulked prior to being transferred to separate test tubes containing a weight/volume ratio of 200 mg/20 ml of PBS (pH 7.4) which were placed in an incubator at a temperature of 37 °C. The solid phase extraction method and HPLC analysis (HPLC on an Agilent 1200 series system equipped with a DAD diode array detector - Agilent Technologies) were then employed in order to characterise the in vitro release rates of the vancomycin and its crystalline degradation antibiotically inactive products over a 21-day period. Details of the HPLC analysis are described in an article written by Melicherčík et al. (Melichercik et al., 2014).

A methiciline-resistant *Staphylococcus aureus* (MRSA) isolate was used for the preliminary selection of the optimal COL/HA/VANCO layer preparation method. Model isolates were retrieved by means of the examination of hospital (General University Hospital, Prague, Czech Republic) patient specimens. The disc diffusion test was performed as described below.

### 2.3. Comprehensive Evaluation of Antimicrobial Susceptibility

Following the selection of a suitable method for the preparation of the COL/HA/VANCO layers, the evaluation of the antimicrobial susceptibility of the EI0, EI5 and EI15 samples was conducted by means of the use of four types of isolate retrieved from the hospital patient specimens mentioned above. The group consisted of one MRSA isolate, one *Staphylococcus epidermidis* isolate (gentamicin-resistant) and two *Enterococcus faecalis* isolates, one of which consisted of an *E. faecalis* gentamicin-resistant isolate and the other of *E. faecalis* acquired as a result of the analysis of an infected joint replacement. Each inoculum was produced from an 18–24 h pure culture of the test isolates via a Mueller-Hinton agar medium. Suspensions were prepared from 1 to 4 colonies of the test isolates (only well-isolated, morphologically similar colonies grown on a non-selective medium) in 2 ml of sterile saline solution and the turbidity was adjusted (using a Densi 2, Erba Lachema densitometer, Brno, Czech Republic) to 0.5 of the McFarland turbidity standard (approximately 1–2 × $10^8$ CFU/ml). Disc diffusion was performed using a Mueller-Hinton agar medium (Oxoid Ltd., Hampshire, UK; batch LOT1381672) with the test samples. Sterile cotton swabs were used to spread the inoculum evenly over the agar plates in three directions. Discs with a diameter of 6 mm ($n = 7$) were firmly applied to the dried surface of the inoculum agar plates using a sterile needle within a 15-minute time period and further incubated at 37 °C for 24 h. It was expected that the careful application of the inoculum and the streaking of the plates would result in even growth without the occurrence of separate colonies. The inhibition zones were read off using a ruler while holding each agar plate approximately 30 cm from the eye. Standard 6 mm antibiotic discs were used for positive control (PC) purposes, i.e. vancomycin 30 μg for *S. aureus* and *S. epidermis*, and vancomycin 5 μg for both *Enterococci*, and discs made up of electrospun mats without vancomycin impregnation served for negative control purposes (analogically with 0, 5 and 15 wt% HA).

### 2.4. Evaluation of Vancomycin Release in Blood Plasma

In addition, samples prepared by means of electrospinning followed by impregnation with vancomycin (EI0, EI5, and EI15) were subjected to an investigation of the in vitro release of vancomycin in human blood plasma. The samples ($n = 6$) were placed in separate test tubes with a weight/volume ratio of 200 mg/20 ml of human blood plasma (16 donors of different blood group, sex and age) and incubated at 37 °C in a 5% $CO_2$ atmosphere (DH $CO_2$ incubator, Thermo Scientific) with antibiotics (penicillin and streptomycin) for 6 h and for 1, 3, 10, 15 and 30 days. Solid phase extraction and HPLC analysis were conducted as described above.

### 2.5. Evaluation of Structural and Mechanical Stability

Structural and mechanical stability were further analysed with respect to the electrospun impregnated layers (EI0, EI5 and EI15) by means of the testing of degradation in blood plasma under the conditions described above (at 37 °C, 5% $CO_2$ atmosphere, penicillin/streptomycin, for 6 h and for 1, 3, 10, 15 and 30 days). The volume of the medium was maintained at a weight/volume ratio of 30 mg/15 ml. The extent of in vitro degradation was calculated according to the following equation: $D = \frac{W_0 - W_t}{W_0} 100$ [%], where $D$ is the mass loss, $W_o$ is the initial dried weight of the sample and $W_t$ is the dried weight of the sample after degradation ($n = 6$). The swelling ratio ($E_{sw}$) was calculated using the following equation: $E_{sw} = \frac{W_{sw} - W_0}{W_0} 100$ [%], where $W_o$ is the initial dried weight of the sample and $W_{sw}$ is the weight of the swollen sample ($n = 6$). The weight of the swollen samples was measured following the removal of each sample from the medium and after a 1-minute delay and the removal of any excessive medium surrounding the

sample; the dried weight of the samples was measured following lyophilisation.

The mechanical properties prior to and following immersion in blood plasma were evaluated by means of the uniaxial tensile testing of rectangular strips of the layers (the average width and length of the samples was approximately 10 mm and 40 mm respectively). During the test procedure the value of strain at failure (the maximum strain sustained by the material before breaking, where strain is defined as the ratio of the elongation of the sample to reference length), the ultimate tensile strength (the maximum nominal stress sustained by the material; nominal stress is defined as the ratio of applied force to the reference cross-section of a sample) and the modulus of elasticity (the slope of the tangent made to a stress-strain relationship on the initial linear part) were determined. Tensile tests were conducted using a Zwick/Roell multipurpose testing machine equipped with a built-in video extensometer. By using contrasting marks on the surface of samples, the video extensometer automatically determined the reference length and elongation of the samples. Tensile experiments were conducted at a constant clamp velocity of 0.1 mm/s. The loading force was measured by a U9B (±250 N, HBM, Germany) force transducer.

Degradation tests under physiological conditions were used as an alternative way in which to assess the stability of the collagenous layers, and ultraviolet-visible spectrophotometry was employed for the quantification of the free amino groups released during the degradation of the samples of 50 mg ($n = 3$) immersed in the PBS (37 °C, pH 7.4). PBS was collected after 2, 6, 96, 240, 360, 528, 720, 1536 and 2400 h. The PBS collected (2.5 ml) was mixed with 2 ml of 0.1 M $NaHCO_3$ and 1 ml of 0.01% aqueous solution of 2,4,6-trinitrobenzenesulphonic acid (TNBS, Sigma-Aldrich). The mixture was incubated at 40 °C for 2 h. Subsequently, 1 ml of a 10% solution of sodium dodecyl sulphate (Sigma-Aldrich) and 0.5 ml of 1 M HCl were added. Absorbance at 340 nm was measured using a Unicam UV 500 spectrophotometer and correlated to the concentration of free amino groups using a calibration curve obtained with L-lysine (Sigma-Aldrich) and L-α-amino-n-butyric acid (Lachema, Czech Republic).

### 2.6. Biological Evaluation of Cytotoxicity and Cytocompatibility

The biological evaluation of the electrospun impregnated layers (EI0, EI5 and EI15) was conducted under in vitro conditions. The aim of the in vitro tests was to verify whether eluted doses of vancomycin exert a negative effect on bone-like cell behaviour. In addition to the effect of antibiotics on bone cells, the influence of the composition of the COL/HA/VANCO layers (EI0, EI5, EI15) and layers containing no vancomycin (N0, N5, N15) on cell behaviour was investigated.

#### 2.6.1. Cells Culture Conditions

SAOS-2 cells (a human osteoblast-like cell line derived from osteosarcoma, obtained from Deutsche Sammlung von Mikroorganismen und Zellkulturen (GmbH), Germany) were cultured at 37 °C in a 5% $CO_2$ atmosphere and in McCoy's 5A medium without phenol red (PromoCell, Germany) supplemented with 15% heat-inactivated FBS (PAA, Austria), penicillin (20 U/ml, Sigma-Aldrich, USA) and streptomycin (20 μg/ml Sigma-Aldrich, USA).

#### 2.6.2. Layer Infusions

The nano-structured layers (EI0, EI5 and EI15) on a 48-well plate (Thermo Scientific, USA) were fixed in wells using CellCrown™ inserts (Sigma-Aldrich, USA) following which fully supplemented McCoy's 5A medium (800 ul) was added to each layer type and incubated at 37 °C and in a 5% $CO_2$ atmosphere for 24 h in order to obtain layer infusions. The resulting infusions were transferred (400 μl) to pre-seeded cells on a 48-well plate; the cells had been seeded 20 h prior to the addition of the infusions at a concentration of 20,000 cells/$cm^2$. Cell metabolic activity (described below) was measured following 24 h of cell cultivation with the layer infusions.

#### 2.6.3. Cell Cultivation on Layers

The nano-structured layers (EI0, EI5, EI15 and N0, N5, N15) used for cell cultivation purposes were fixed in the wells of a 48-well plate (Thermo Scientific, USA) by means of CellCrown™ inserts (Sigma-Aldrich, USA). The cells were seeded onto structured layers at a concentration of 15,000 cells/$cm^2$ for 2-day and 8-day (after 4 days, fresh medium was added to the cells) cultivation periods, following which both cell metabolic activity and the number of cells on the structured layers were determined.

#### 2.6.4. Determination of Cell Metabolic Activity

The cell metabolic activity test (Cell Titer 96 AQueous One Solution Cell Proliferation Assay, MTS, Promega, USA) was performed according to the standard protocol: the absorbance (490 nm and 655 nm as reference values) of soluble formazan obtained by means of metabolically active cellular dehydrogenases was determined after 24 h (layer infusions) and 2 and 8 days (directly on the layers) of cell cultivation with respect to both the layer infusions and directly on the layers. Absorbance was determined using a multi-detection micro-plate reader (Synergy™ 2, BioTek, USA). The results were normalised (in percentage) with respect to the control cells with no layer infusions and cells cultivated on control tissue culture polystyrene.

#### 2.6.5. Fluorescence Staining of the Cells

Those cells incubated for 2 and 8 days on structured layers were fixed in 4% paraformaldehyde in PBS at room temperature (RT) for 15 min following the measurement of cell metabolic activity. The cells were permeabilised using 0.1% Triton X-100 in PBS (Sigma-Aldrich, USA) at RT for 20 min and stained using fluorescence dyes: the cell nuclei were stained with DAPI at RT for 45 min (1:1000; Sigma-Aldrich, USA) and the actin filaments with Phalloidin-Alexa Fluor 488 also at RT for 45 min (1:500; Life Technologies, USA).

#### 2.6.6. Imaging of Fluorescently Stained Cells

Wide-field images of the cells on the structured layers were obtained using an Eclipse Ti-S microscope and a DS-U2 Digital Camera (Nikon, Japan). The images were acquired using 10× and 40× lenses and adjusted by means of ImageJ software (Rasband, W.S., ImageJ, US National Institutes of Health, Bethesda, Maryland, USA, http://imagej.nih.gov/ij/, 1997–2015) and Cell Profiler (Broad Institute, USA) software.

### 2.7. Statistical Evaluation

The subsequent statistical analysis was performed using statistical software (STATGRAPHICS Centurion XV, StatPoint, USA). The normality of the data was verified primarily by means of the Shapiro-Wilk's and Chi-Squared tests; outliers were identified via either the Grubbs' or Dixon's tests. The mean values and variability of normally distributed numerical data were expressed as the arithmetical mean and the standard deviation (SD) while non-normally distributed numerical data was expressed as the median and interquartile range (IQR). Homoscedasticity was verified by means of the Levene's and Bartlett's tests. Non-parametric analysis was employed since either the assumption of normality or homoscedasticity were violated and, consequently, the Kruskal-Wallis test for multiple comparison or the Mann-Whitney W test (as a post hoc test) was performed. Statistical significance was accepted at $p \leq 0.05$.

## 3. Results and Discussion

### 3.1. Characterisation of the COL/HA/VANCO Layers

Representative SEM images of micro and nanostructured COL/HA/VANCO samples prepared using different techniques are shown in the Supplement (Supplement 1). FTIR spectroscopy was employed in order to characterise the composition of the samples and so as to verify

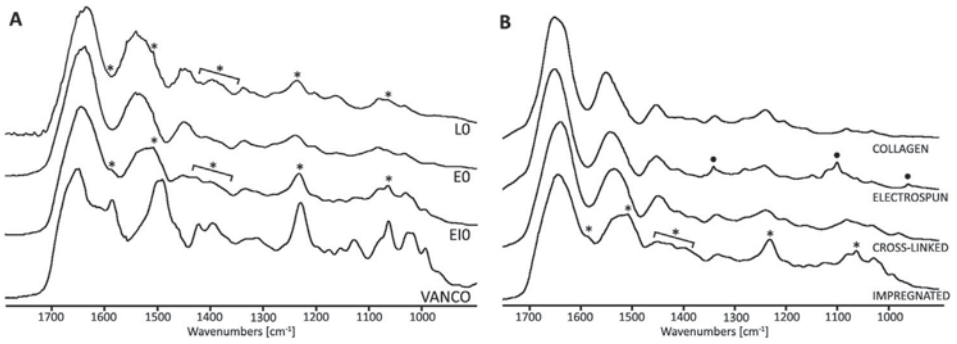


**Fig. 1.** Illustration of the presence of vancomycin in layers prepared in different ways. (A): The FTIR spectra of pure vancomycin (VANCO) lyophilised (L0), electrospun (E0) and electrospun impregnated (EI0) layers without HA. (B): The FTIR spectra of E0 samples in each of the preparation stages from pure collagen, following electrospinning, following cross-linking and following impregnation. * denotes typical vancomycin bands, ● denotes PEO bands.

the theoretical presence of HA and vancomycin following the application of the three different preparation procedures. The electrospun impregnated layers clearly exhibited vancomycin peaks in the collagen spectra (Fig. 1A, B), which remained visible even in the presence of HA (data not shown). Vancomycin peaks following impregnation were easily identifiable with respect to all the electrospun impregnated samples (EI0, EI5, EI15) principally in the 1585, 1420 to 1425, 1227 and 1060 $cm^{-1}$ positions. The IR spectra of the electrospun (E0) samples illustrate the effect of the cross-linking procedure on the presence of vancomycin (Fig. 1A). From a comparison of the spectra of pure collagen and the E0 samples prior to and following cross-linking (data not shown) it follows that during the 24-hour cross-linking procedure in an ethanol solution, a considerable amount of vancomycin is probably simply washed out - principally in the case of the electrospun samples. Further, the advantageous high surface-area-to-volume ratios of the nanostructured samples exert a negative role at this stage of preparation. It can be concluded, therefore, that the addition of vancomycin in the final stage of layer preparation presents an effective way in which to deposit antibiotics in detectable amounts. The FTIR spectra in Fig. 1B illustrate the steps involved in the preparation of the electrospun impregnated layers, from pure collagen lyophilisate through electrospinning and cross-linking to the final stage, i.e. vancomycin impregnation. The PEO is fully leached out following the cross-linking procedure. The FTIR spectra further illustrate the presence of vancomycin following impregnation.

### *3.2. Preliminary Evaluation of Antimicrobial Susceptibility and Vancomycin Release*

The effect of the preparation and structural properties of COL/HA/VANCO on the kinetics of vancomycin release was further analysed by means of the HPLC method (Fig. 2). Initial measurements after 3 h revealed average concentrations of up to 18 ± 1 mg/l (mean ± SD) for the lyophilised (L0) samples (Suchý et al., 2016), up to 48 ± 13 mg/l for the electrospun samples (E15) and up to 696 ± 208 mg/l for the electrospun impregnated (EI0) samples (Fig. 2). The highest average concentration of vancomycin was achieved with respect to the lyophilised samples after 8 days (approximately 250 mg/l), the electrospun samples after 24 h (approximately 60 mg/l) and the electrospun impregnated samples after just 3 h (approximately 700 mg/l). The average concentration of CDP-1M (a major degradation product) was found to be similar to that of the active form of vancomycin with respect to the lyophilised samples after 14 days (~180 mg/l), the electrospun samples after 10 days (~30 mg/l) and the electrospun impregnated samples after 12 days (~310 mg/l) of incubation, data not shown. In all cases, the vancomycin was converted into its degradation products (CD-1M, CD-1m) at a much slower rate than that reported by Melicherčík et al. (6 days) (Melichercik et al., 2014). Despite the considerable tendency of vancomycin degradation towards crystalline thermal degradation products, levels of the released active form of vancomycin remained above the MIC for VRSA (16 mg/l) for >3 weeks, with the exception of the E15 samples (15.85 mg/l, 21st day). Wachol-Drewek (Wachol-Drewek et al., 1996) determined that vancomycin release from collagen was characterised by a rapid bolus release; at least 90% of the antibiotic was released within the first day with complete elution occurring within 4 days. Similar results were obtained by Tu et al. (Tu et al., 2012) who studied vancomycin release from mineralised collagen coatings (dense and porous). They found that 80% of the vancomycin was released in the first 10 h and the remaining 20% over a period of up to 4 days. A burst release was evident with concern to both the dense and porous collagen coatings involving the release of >85% of the antibiotic over 16 h. The maximum concentration of the released active form of vancomycin exceeded the MIC by up to 17 times (lyophilised samples), 4 times (electrospun samples) and up to 44 times (electrospun impregnated samples). By the end of the experiment, the MIC had been exceeded by up to 6 times (lyophilised), up to 12 times (electrospun impregnated) and was approximately equal in the case of the electrospun samples. The addition of hydroxyapatite exerted only a minor effect on vancomycin release.

The results of the preliminary evaluation of antimicrobial susceptibility are in agreement with the results of vancomycin release chromatography analysis (Fig. 3). The highest rates of antimicrobial activity

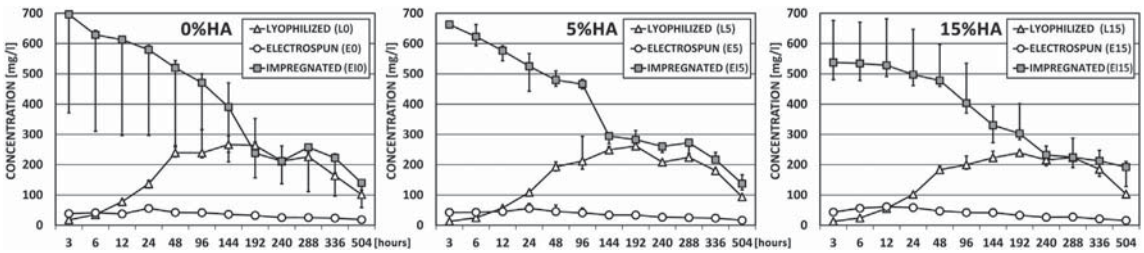


**Fig. 2.** The concentration of the released active form of vancomycin (median, IQR) with respect to samples with 0, 5 and 15 wt% of HA prepared using different methods (Suchý et al., 2016).

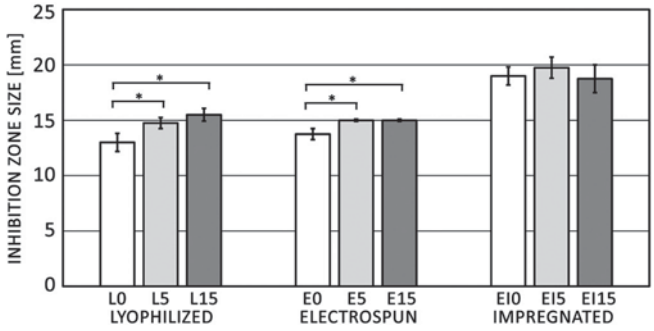


**Fig. 3.** Inhibition zone sizes of vancomycin loaded lyophilised, electrospun and electrospun impregnated samples with different amounts of hydroxyapatite in contact with MRSA isolates. * denotes statistically significant differences (mean, SD, Mann-Whitney, 0.05).

were determined with respect to the electrospun impregnated samples (EI0, EI5, and EI15). Similar to previous results, no statistically significant differences were detected between the electrospun impregnated samples containing different amounts of hydroxyapatite. The electrospun impregnated COL/HA/VANCO layers were subsequently selected for the comprehensive evaluation of antimicrobial susceptibility and vancomycin release as well as for the evaluation of structural and mechanical stability.

### 3.3. Evaluation of Vancomycin Release in Human Blood Plasma

PBS contains only inorganic ions and solely the hydrolytic degradation of the material can be expected compared to blood plasma, with respect to which other types of degradation are enabled, e.g. enzymatic. A comparison of vancomycin release and its degradation in such differing environments consisting of a complex of inorganic and organic components might be beneficial. Therefore, an investigation was conducted of the in vitro release of vancomycin from EI0, EI5 and EI15 layers immersed in human blood plasma for up to 30 days (Fig. 4). Initial measurements after 6 h revealed average vancomycin concentrations (mean ± SD) of up to 655 ± 46 mg/l (EI0), 497 ± 22 mg/l (EI5) and 609 ± 62 mg/l (EI15). The average concentration of vancomycin peaked after 24 h in the case of all the samples, i.e. 703 ± 108 mg/l (EI0), 872 ± 225 mg/l (EI5) and 863 ± 146 mg/l (EI15). The average concentration of CDP-1M was found to be higher than that of the active form of vancomycin after 30 days (EI0: 280 ± 119 mg/l, EI5: 360 ± 223 mg/l, EI15: 260 ± 173 mg/l). The vancomycin concentrations in blood plasma exhibits higher variances than concentrations in PBS (comparison of release kinetics in PBS and blood plasma is illustrated in Supplement (Supplement 2). This can be caused by the potential interaction of vancomycin with various blood plasma components. Generally, the vancomycin release profiles of both plasma and PBS are similar and in both cases the vancomycin released remained above MIC for a period of at least 3 weeks. With respect to immersion in human blood plasma, vancomycin was converted into its degradation products at a relatively slow rate: levels of the released active form of vancomycin remained above the MIC for VRSA for as long as 4 weeks. The maximum concentration of the released active form of vancomycin exceeded the MIC by up to 60 (EI0), 46 (EI5) and 75 (EI15) times.

### 3.4. Comprehensive Evaluation of Antimicrobial Susceptibility

The antimicrobial activity of the EI0, EI5 and EI15 samples against the four bacteria strains were assessed by means of the presence or absence of inhibition zones (disc diffusion test, Fig. 5). All the materials examined exhibited potential antibacterial activity with respect to both *Staphylococci* isolates and gentamicin-resistant isolates, while the vancomycin-free samples (negative control) exhibited no activity at all with respect to any of the bacteria species tested. The sizes of the inhibition zones surrounding the samples investigated were comparable to those of standard antibiotic discs (PC), i.e. no statistically significant differences ($p = 0.05$) in the case of *S. aureus* and *S. epidermis*, and statistically significantly higher in the case of both of the *Enterococci* species. The size of the inhibition zones around the discs containing different amounts of hydroxyapatite, as a possible vancomycin binder, appeared to have no antibacterial influence.

### 3.5. Evaluation of Structural Stability

The degradation rates expressed as mass loss and the swelling ratios of the cross-linked collagen samples with various HA concentrations are depicted in Fig. 6. Negative values of degradation indicate a weight increase which can be explained by the adsorption of various components (proteins, saccharides and vitamins) of the blood plasma immediately following exposure (within 6 h). Conversely, the microstructured lyophilised samples with the same composition studied in (Liu et al., 2002) exhibited weight losses. The difference in behaviour between the nanofibrous layers and the lyophilised samples can be explained by the high specific surface area of the nanofibers. This phenomenon

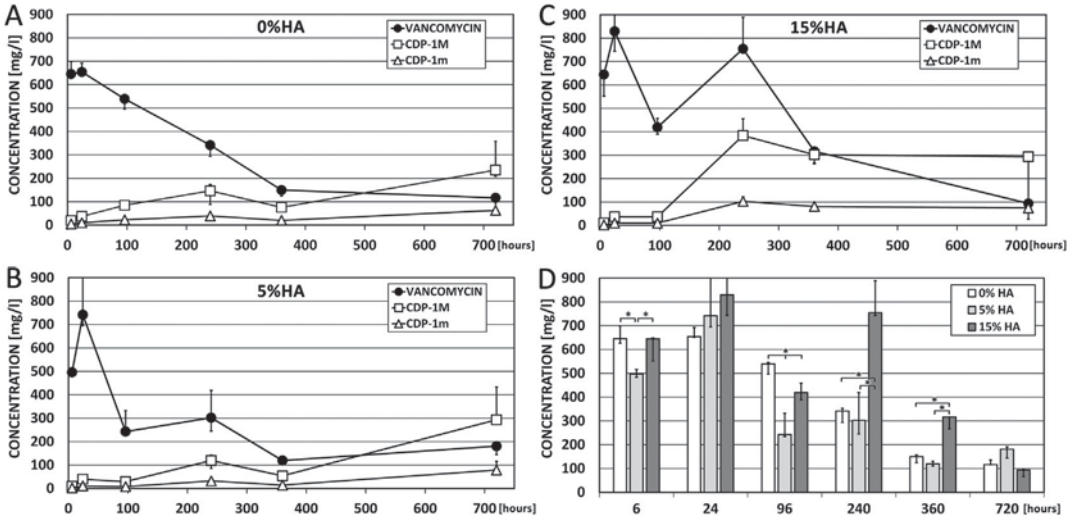


**Fig. 4.** Evaluation of vancomycin release from electrospun impregnated samples immersed in human blood plasma. (A, B, C): The concentration of the released active form of vancomycin and its degradation products CDP-1M and CDP-1m (median, IQR). (D): The concentration of the released active form of vancomycin (median, IQR). * denotes statistically significant differences (Mann-Whitney, 0.05).

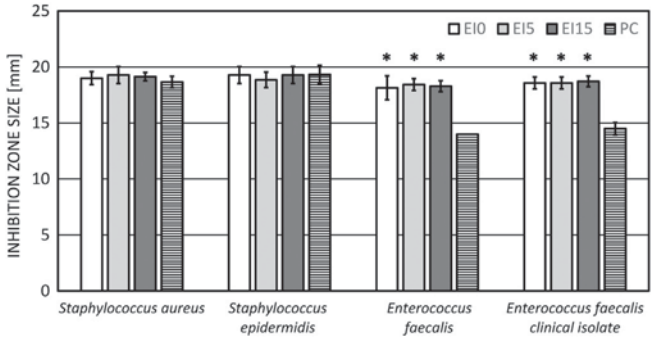


**Fig. 5.** Inhibition zone sizes of the electrospun impregnated samples with different amounts of hydroxyapatite, and the positive controls. The vancomycin-free negative controls evinced zero inhibition zones (data not shown). * denotes statistically significant differences (mean, SD, Mann-Whitney, 0.05) in comparison with the PC for each of the examined isolate species.

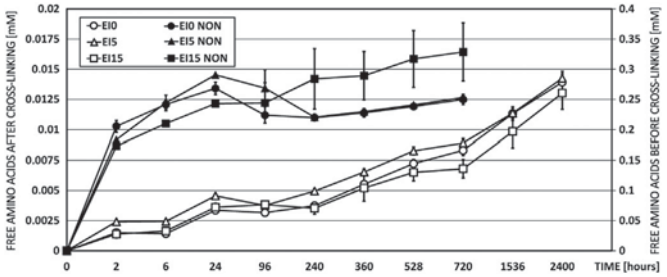


**Fig. 7.** The concentration of amino acids released from the electrospun impregnated samples (EI0, EI5, EI15) and identical samples prior to cross-linking (NON); note that the opposite axis has a different scale.

is also apparent in the swelling behaviour (Fig. 6B). No obvious dependence was detected of increment size on the type of sample or time period (M–W 0.05). It can be concluded from the results of studies on behaviour in physiological environments and from a comparison with samples studied by Suchý et al. (Suchý et al., 2016) that all the electrospun impregnated layers (EI0, EI5, and EI15) achieved the appropriate degree of cross-linking so as to create stable layers. The application of FTIR spectroscopy (Fig. 6C) proved the occurrence of only minor local changes within the samples during leaching in plasma. HA content was detected in both the EI5 and EI15 layers after 30 days; however, the vancomycin had been completely released from all the samples. In addition, the collagen as such was found to remain stable within the electrospun impregnated samples during the whole immersion period (up to 100 days) as documented by the very low (approximately 0.014 mM) free amino acid concentration at the end of the experiment (Fig. 7).

### 3.6. Evaluation of Mechanical Stability

The results obtained from the mechanical tests are shown in Fig. 8. All the HA concentrations exhibit an increase in tensile strength after 6 h of exposure to human blood plasma. From 6 to 360 h of exposure, the ultimate tensile stress stagnates and after 360 h a slightly decreasing trend in 0 and 5% of HA can be observed, whereas the tensile strength of the 15% HA samples slightly increases. After 720 h, the ultimate tensile strength did not decrease to values less than the initial value in either case. In contrast to tensile stress, strain at failure was seen to decrease immediately (6 h) following plasma exposure (Fig. 8A). During the whole experiment (24–720 h), ultimate tensile strain practically stagnated. The elastic modulus may, albeit roughly, be considered to be a ratio of tensile stress to strain as confirmed by Fig. 8C. The elastic modulus of all the samples increased during 720 h of blood plasma exposure analogically compared to samples in the dry state (0 h). The results of the mechanical tests, in accordance with those provided by other stability investigation methods, revealed that the EI0, EI5, and EI15 layers remained stable following leaching in plasma. Comparison of the uniaxial tensile responses of the layers before and after 30 days of plasma incubation as well as representative images of tested samples can be found in Supplements (Supplement 3, Supplement 4).

### 3.7. In vitro Evaluation of Cytotoxicity

#### 3.7.1. Evaluation of the Effect of Layer Infusions on Human Cells

The vancomycin impregnated electrospun layers (EI0, EI5 and EI15) and their respective controls without the presence of vancomycin (N0, N5 and N15) were soaked in a cultivation medium for 24 h. The infusions thus obtained were then transferred to pre-cultivated cells on tissue-culture polystyrene (PS) and incubated together. After 24 h, the cell metabolic activity was determined (Fig. 9A). The resulting data shows a significant decrease in cell metabolic activity in those cells incubated in infusions obtained from the COL/HA layers with 0 wt% and 5 wt% of hydroxyapatite (N0 and N5) and from COL/HA/VANCO with 0 wt% of hydroxyapatite (EI0) compared to the control infusion from PS. That said, the observed effect was weak (approximately a 10% decrease) and thus cannot be stated to be cytotoxic (Flahaut et al., 2006). Moreover, the effect was no stronger with respect to the vancomycin sample infusions, which suggests an effect of a different character. The metabolic activity of the other infusions was comparable to the control sample, thus it can be concluded that the compounds released from the electrospun layers (active vancomycin, the degradation forms thereof and substances issuing from the COL/HA layer) do not have a cytotoxic effect on the human osteoblastic cell line. Interestingly, those samples with no HA presence were found to be “the most” toxic, independent of the presence of vancomycin; therefore, it might be suggested that certain other compounds are released from this type of layer which negatively influence cell metabolic activity. On the other hand, infusions containing samples with the highest HA concentration (15 wt%) were seen to have a significantly more positive effect on cell metabolic activity (again irrespective of the presence of vancomycin). According to the results presented in Fig. 2, the amount of vancomycin released after 24 h was in the range of 500–600 mg/l; thus, it can be concluded that this concentration has no negative effect on osteoblast growth, which is in agreement with data concerning the local administration of

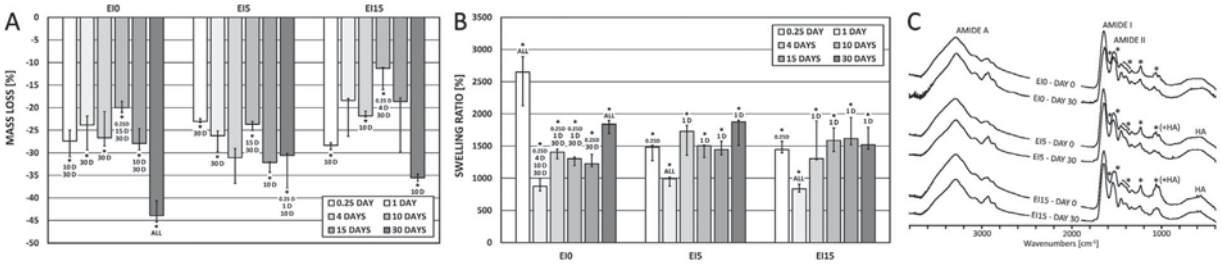


**Fig. 6.** Evaluation of the structural stability of the electrospun impregnated samples in human blood plasma. (A): Degradation rates are expressed as mass loss (median, IQR), (B): swelling ratios (median, IQR), (C): FTIR spectra before and after exposure to human blood plasma. * denotes statistically significant differences (median, IQR, Mann-Whitney, 0.05).

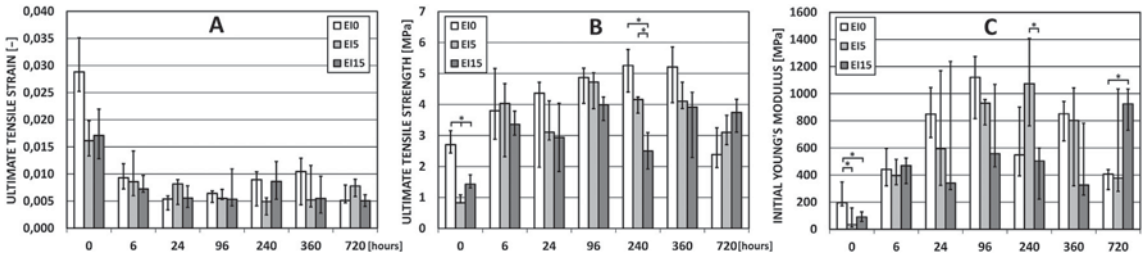


**Fig. 8.** Mechanical stability of the electrospun impregnated layers. (A): ultimate tensile strain, (B): ultimate tensile strength, (C): initial Young's modulus during 720 h of exposure in human blood plasma. * denotes statistically significant differences (median, IQR, Mann-Whitney, 0.05).

vancomycin to osteoblastic cells (MG-63) with respect to which concentrations of 1 g/l and less had no negative effect on these cells (Edin et al., 1996). However, the concentrations employed in the study described herein led to the creation of the largest inhibition zones with respect to the bacterial strains subjected to testing (as is apparent in Fig. 5).

*3.7.2. Evaluation of the Effect of the Cultivation of Osteoblasts on Layers*

Osteoblasts were seeded on the nanostructured vancomycin impregnated electrospun layers (EI0, EI5 and EI15) as well as on their respective controls without the presence of vancomycin (N0, N5 and N15) for 2 and 8 days following which their metabolic activity was determined. Fig. 9(B, C) shows that after 2 days of incubation, the cells on those layers containing 0 and 5 wt% of HA (EI0 and EI5) were strongly inhibited by the presence of vancomycin; however, those cells on the layer containing 15 wt% of HA (EI15) behaved in a comparable way to the control without the presence of vancomycin. Moreover, most of the cells inhibited by vancomycin were found on layers with 0 wt% of hydroxyapatite and the degree of inhibition was seen to decrease with increased amounts of HA in the sample. Following further incubation (8 days), the tendency towards the inhibitory effect of vancomycin on cells deposited on layers with different amounts of HA persisted; nevertheless, the inhibitory effect of vancomycin was not so dramatic. Moreover, the cells cultivated on the COL/HA/VANCO layer with the highest content of hydroxyapatite (15 wt%) manifested significantly increased metabolic activity compared to those cells in the control without the presence of the antibiotic.

The data presented in Fig. 9 (B, C) is supported by the fluorescence images of those cells (the staining of the actin cytoskeleton – green and nuclei – blue) cultivated on nanostructured vancomycin impregnated electrospun layers for 2 and 8 days (Fig. 10). After 2 days, the osteoblasts on all the layers tested were seen to be rather round and poorly dispersed: however, they adhered to the layers in reasonable amounts. Fewer cells were apparent with respect to those samples with vancomycin thus confirming the inhibitory effect of vancomycin (Fig. 10). After 8 days, the osteoblasts were mostly well dispersed and exhibited a polygonal-like morphology, thus once more confirming the inhibitory effect of vancomycin on cells cultivated on layers with 0 wt% and 5 wt% of hydroxyapatite despite the greater number of cells found on these samples. The osteoblasts cultivated on a vancomycin impregnated layer with 15 wt% of hydroxyapatite were present in a higher amount thus supporting the results concerning the increased metabolic activity of cells on this sample. The inhibitory effect of vancomycin on cell growth was apparent with respect to all the samples tested; moreover, the effect was more pronounced following a short period of incubation (2 days) and declined (EI0 and EI5) or completely disappeared (EI15) following a longer incubation period (8 days). Importantly, the cells were seen to react not only to vancomycin but also to the properties of the scaffold (differing amount of HA).

With respect to the 2-day period, a small number of cells was also visible on the sample without the presence of HA (N0) (Fig. 10); thus, the scaffold itself and the presence of vancomycin were jointly responsible for the lowest cell count provided by the EI0 sample. It might be speculated that cells of an osteoblastic nature which are known to prefer hard substrates for their growth (Engler et al., 2006) were initially inhibited in terms of growth on the scaffold, which had no content of HA. Moreover, according to the data obtained, this sample exhibited the greatest degree of swelling (Fig. 6B) and the 24 h-infusion created from this layer also exerted a slight but negative effect on the cells (Fig. 9A). Thus, the various properties of the EI0 layer may have had a cumulative negative effect on cell behaviour. The observed inhibitory effect of vancomycin in the layers is dependent on and may be modulated by the respective amounts of HA. HA makes up the fundamental component of the bone matrix, thus the observed phenomenon could be the result of the character of the adhesion surface (e.g. HA) and the potential for adhesion (Deligianni et al., 2001). Furthermore, it is important to bear in mind that cell adhesion is mediated by FBS proteins and the interaction of these proteins with the tested layers (Wilson et al., 2005). The potential for improved adhesion means that the cells are in better condition, which results in increased cell resistance to stress conditions. In addition, the inhibitory effect might be caused by the direct interaction of vancomycin with HA particles in the layer – antibiotic conformation as well as the general level of activity may be altered and HA behaviour (in particular its release) in the layer during incubation may also be critical. As the results herein indicate, the highest level of vancomycin release was observed with respect to EI15 when compared to the rest of the samples with a maximum incubation period of 24 h (Fig. 4). At the same time, this layer appears to exert the lowest inhibitory influence on cell metabolic activity after 2 days (as well as 8 days) (Fig. 9B, C).

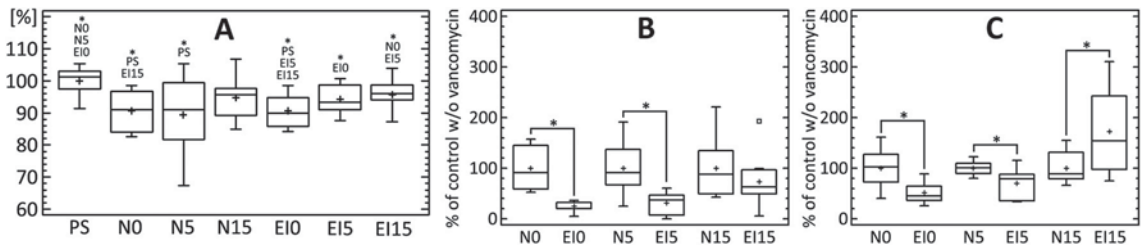


**Fig. 9.** Metabolic activity of SAOS cells incubated in 24-hour infusions expressed as a percentage of the positive control (PS) (A). Metabolic activity of osteoblasts incubated on scaffolds for 2 (B) and 8 (C) days. * denotes statistically significant differences (Mann-Whitney, 0.05).

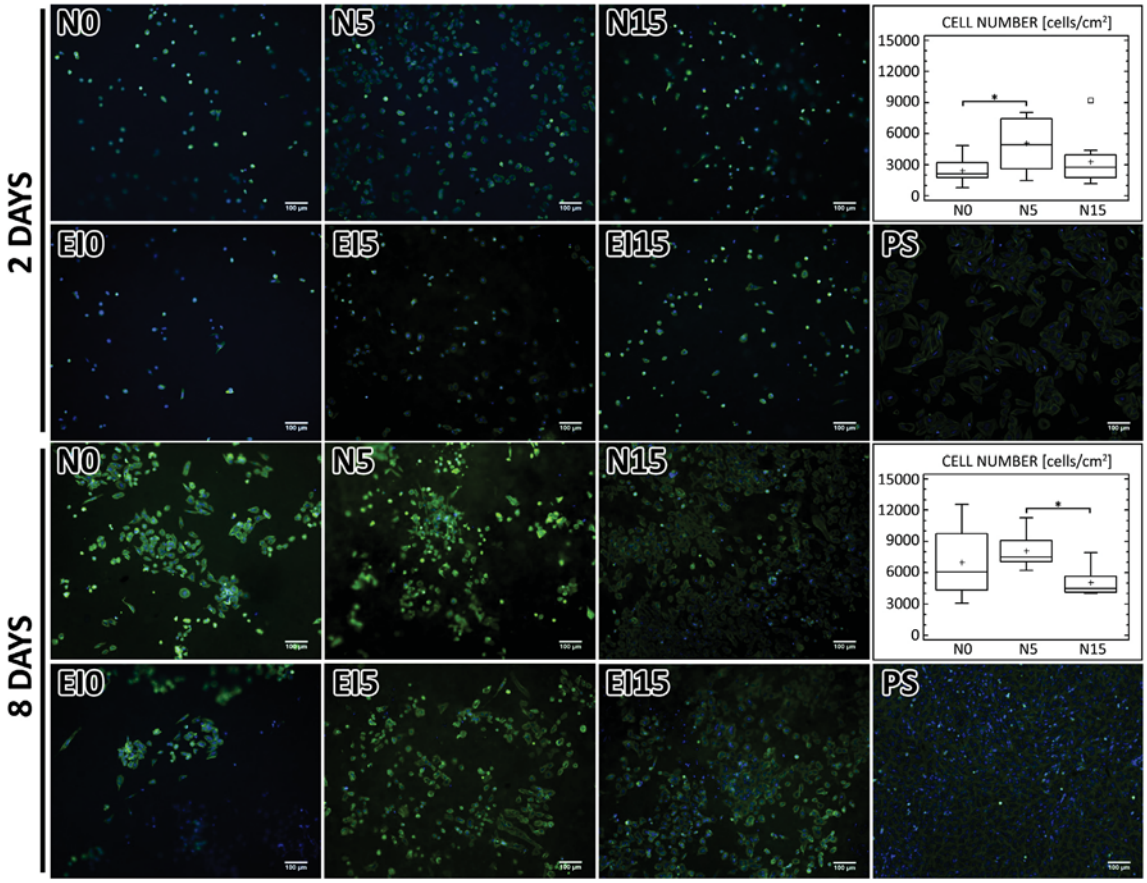


**Fig. 10.** Fluorescence images of osteoblasts cultivated (for 2 and 8 days) on electrospun impregnated vancomycin-free layers (N0, N5, N15) and identical samples impregnated with vancomycin (EI0, EI5, EI15), with the corresponding cell numbers of the vancomycin-free samples. * denotes statistically significant differences (Mann-Whitney, 0.05).

Despite the initial strongly negative effect of the properties of the layers and the presence of vancomycin on the cells, once the osteoblasts had overcome these issues, growth proceeded well. It seems that COL/HA layers become stabilised over time and vancomycin is released at similar levels from all the samples tested; hence, it appears that the cells are very well capable of overcoming stress conditions. Moreover, those cells cultivated on the EI15 layer were seen to grow better than on the same layer without the presence of vancomycin.

## 4. Conclusion

The most critical element of contemporary implant technology and design consists not of the bulk material from which an implant is produced, but rather its surface, which is required to provide an interface which is suitable for the purposes of post-implantation integration between the bone and the replacement. Inflammatory reactions to both local and systemic infection represent the greatest threat to successful osteo-integration and may lead to the formation of a biofilm which creates a barrier to the binding of the implant. This process may, in turn, result in the loosening and thus suboptimal functioning of the implant and even an indication to re-implantation.

The main goal of the research described herein was to develop a new structured layer based on a collagen-hydroxyapatite composite which can be used (1) as a pro-osteo-integration interface and which, simultaneously, will serve (2) as a local drug delivery system. Three preparation methods were investigated, two of which involved the direct addition of vancomycin to a dispersion from which (A) micro-structured COL/HA layers were obtained by means of lyophilisation and (B) nanostructured layers were obtained via electrospinning. The electrospinning method, which provides a high surface-to-volume ratio to the internal structure of the resulting material, was also utilised for the production of layers without the presence of vancomycin in the source dispersion, but with the addition of the antibiotic to the electrospun material via impregnation. This paper demonstrated that the third method provides layers with the highest concentrations of released antibiotics over the longest time period. The highest average concentration of vancomycin in PBS was achieved with respect to these electrospun impregnated samples after just 3 h (approximately 700 mg/l). The minimum inhibitory concentration was exceeded up to 44 times and the vancomycin released remained above MIC for a period of at least 3 weeks compared to an initial burst release with complete elution occurring within 4 days as described by previous studies. The average concentration of CDP-1M (a major degradation product) was found to be similar to that of the active form of vancomycin with respect to the electrospun impregnated samples after 12 days (~310 mg/l) of incubation. The addition of hydroxyapatite exerted only a minor effect on vancomycin release. The results of the preliminary evaluation of antimicrobial susceptibility were in agreement with the results of vancomycin release chromatography analysis. The highest rates of antimicrobial activity were determined with respect to the electrospun impregnated samples. The in vitro release of vancomycin from the electrospun impregnated COL/HA/VANCO layers immersed in human blood plasma for up to 30 days revealed that levels of the released active form of vancomycin remained above the MIC for VRSA for as long as 4 weeks. In vitro testing against populations of *S. aureus*, *S. epidermis*, and *E. faecalis* confirmed the inhibitory effect of vancomycin released from COL/HA/VANCO layers (EI0, EI5, and EI15). On the other hand, cytocompatibility testing, which employed osteoblasts cells, revealed that these bone-producing cells survive on the layers and that their metabolic activity increases as the degree of mineralisation of the layer increases. This suggests that COL/HA/VANCO layers prepared by means of electrospinning with subsequent impregnation with vancomycin cannot be considered to be cytotoxic for newly-formed bone.

Finally, the evaluations of structural and mechanical stability conducted in blood plasma for up to 30 days and in a simulated body environment for up to 100 days revealed that our material retains structural consistency, as proved by the very low free amino acid concentration at the end of the experiment (approximately 0.014 mM). Structural stability makes up a necessary precondition for providing a solid scaffold for cell migration and, hence, for the formation of new bone.

We are able to conclude, therefore, that nanostructured layers prepared by means of electrospinning from a COL/HA dispersion, subsequently cross-linked with EDC/NHS and finally impregnated with vancomycin provide eminently suitable candidates for the preparation of bioactive and pro-osteo-integrating bone-implant interfaces and that they are capable of providing for local drug delivery. It is intended that the next phase of development will be based on the experimental implantation of EI0–15 covered implants in rodents.

Supplementary data to this article can be found online at http://dx.doi.org/10.1016/j.ejps.2017.01.032.

## Acknowledgements

This study was supported by a grant provided by the Technology Agency of the Czech Republic under project no. TA04010330. In addition, the research team gratefully acknowledges the financial support provided for their work by the long-term conceptual development of research organisation's project no. RVO: 67985891, the National Sustainability Programme I (NPU I) no. LO1503 provided by the Ministry of Education Youth and Sports of the Czech Republic and the Faculty of Medicine in Pilsen: project SVV–2016 no. 260 279 and GAUK 400215 and by the Ministry of Education, Youth and Sport of the Czech Republic, program NPU1, project No LO1207.

## References

Adams, S.B., Shamji, M.F., Nettles, D.L., Hwang, P., Setton, L.A., 2009. Sustained release of antibiotics from injectable and thermally responsive polypeptide depots. J. Biomed. Mater. Res. B 90, 67–74.

Alt, V., Jörg, F., Schnettler, R., 2015. Local delivery of antibiotics in the surgical treatment of bone infections. Tech. Orthop. 30, 230–235.

Bauer, T.W., Zhang, Y., 2016. Implants and implant reactions. Diagn. Histopathol. 22, 384–396.

Brown, J.M., Mistry, J.B., Cherian, J.J., Elmallah, R.K., Chughtai, M., Harwin, S.F., Mont, M.A., 2016. Femoral component revision of total hip arthroplasty. Orthopedics 39, 1129–1139.

Buchholz, H.W., Engelbrecht, H., 1970. Uber die Depotwirkung einiger Antibiotica bei Vermischung mit dem Kunstharz Palacos. Chirurg 41, 511–515.

Chen, D.W., Hsu, Y.H., Liao, J.Y., Liu, S.J., Chen, J.K., Neng Ueng, S.W., 2012a. Sustainable release of vancomycin, gentamicin and lidocaine from novel electrospun sandwich-structured PLGA/collagen nanofibrous membranes. Int. J. Pharm. 430, 335–341.

Chen, D.W.C., Liao, J.Y., Liu, S.J., Chan, E.C., 2012b. Novel biodegradable sandwich-structured nanofibrous drug-eluting membranes for repair of infected wounds: an *in vitro* and *in vivo* study. Int. J. Nanomedicine 7, 763–771.

Chou, Y.C., Cheng, Y.S., Hsu, Y.H., Yu, Y.H., Liu, S.J., 2016. A bio-artificial poly([d,l]-lactide-co-glycolide) drug-eluting nanofibrous periosteum for segmental long bone open fractures with significant periosteal stripping injuries. Int. J. Nanomedicine 11, 941–953.

Deligianni, D.D., Katsala, N.D., Koutsoukos, P.G., Missirlis, Y.F., 2001. Effect of surface roughness of hydroxyapatite on human bone marrow cell adhesion, proliferation, differentiation and detachment strength. Biomaterials 22, 87–96.

Edin, M.L., Miclau, T., Lester, G.E., et al., 1996. Effect of cefazolin and vancomycin on osteoblasts in vitro. Clin. Orthop. Relat. Res. 333, 245–251.

Engler, A.J., Sen, S.S., Sweeney, H.L., Discher, D.E., 2006. Matrix elasticity directs stem cell lineage specification. Cell 126, 677–689.

Fang, T., Wen, J., Zhou, J., Shao, Z., Dong, J., 2012. Poly (ε-caprolactone) coating delays vancomycin delivery from porous chitosan/β-tricalcium phosphate composites. J. Biomed. Mater. Res. B 110, 1803–1811.

Flahaut, E., Durrieu, M.C., Remy-Zolghadri, M., Bareille, R., Baquey, C., 2006. Investigation of the cytotoxicity of CCVD carbon nanotubes towards human umbilical vein endothelial cells. Carbon 44, 1093–1099.

Gardete, S., Tomasz, A., 2014. Mechanisms of vancomycin resistance in *Staphylococcus aureus*. J. Clin. Invest. 124, 2836–2840.

Garvin, K., Feschuk, C., 2005. Polylactide-polyglycolide antibiotic implants. Clin. Orthop. 437, 105–110.

Gursel, I., Korkusuz, F., Turesin, F., Alaeddinoglu, N.G., Hasirci, V., 2001. *In vivo* application of biodegradable controlled antibiotic release systems for the treatment of implant-related osteomyelitis. Biomaterials 22, 73–80.

Harth, K.C., Rosen, M.J., Thatiparti, T.R., Jacobs, M.R., Halaweish, I., Bajaksouzian, S., Furlan, J., von Recum, H.A., 2010. Antibiotic-releasing mesh coating to reduce prosthetic sepsis: an *in vivo* study. J. Surg. Res. 163, 337–343.

Hirose, K., Marui, A., Arai, Y., Nomura, T., Inoue, S., Kaneda, K., Kamitani, T., Fujita, M., Mitsuyama, M., Tabata, Y., Komeda, M., 2006. Sustained-release vancomycin sheet may help to prevent prosthetic graft methicillin-resistant *Staphylococcus aureus* infection J. Vasc. Surg. 44, 377–382.

Hong, D.W., Lai, P.L., Ku, K.L., Lai, Z.T., Ming Chu, I., 2013. Biodegradable in situ gel-forming controlled vancomycin delivery system based on a thermosensitive mPEG-PLCPPA hydrogel. Polym. Degrad. Stab. 98, 1578–1585.

Hsu, Y.H., Chih Chen, D.W., Tai, C.D., Chou, Y.C., Liu, S.J., Ueng, S.W.N., Chan, E.C., 2014. Biodegradable drug-eluting nanofiber-enveloped implants for sustained release of high bactericidal concentrations of vancomycin and ceftazidime: *in vitro* and *in vivo* studies international. J. Nanomed. 9, 4347–4355.

Inzana, J.A., Schwarz, E.M., Kates, S.L., Awad, H.A., 2016. Biomaterials approaches to treating implant-associated osteomyelitis. Biomaterials 81, 58–71.

Jang, C.H., Cho, Y.B., Jang, Y.S., Kim, M.S., Kim, G.H., 2015. Antibacterial effect of electrospun polycaprolactone/polyethylene oxide/vancomycin nanofiber mat for prevention of periprosthetic infection and biofilm formation. Int. J. Pediatr. Otorhinolaryngol. 79, 1299–1305.

Jean-Baptiste, E., Blanchemain, N., Martel, B., Neuta, C., Hildebrand, H.F., Haulon, S., 2012. Safety, healing, and efficacy of vascular prostheses coated with hydroxypropyl-β-cyclodextrin polymer: experimental *in vitro* and animal studies. Eur. J. Vasc. Endovasc. Surg. 43, 188–197.

Kankilic, B., Bayramli, E., Kilic, E., Dağdeviren, S., Korkusuz, F., 2011. Vancomycin containing PLLA/β-TCP controls MRSA *in vitro*. Clin. Orthop. Relat. Res. 469, 3222–3228.

Kirst, H.A., Thompson, D.G., Nicas, T.I., 1998. Historical yearly usage of vancomycin. Antimicrob. Agents Chemother. 42, 1303–1304.

Kluin, O.S., van der Mei, H.C., Busscher, H.J., Neut, D., 2009. A surface-eroding antibiotic delivery system based on poly-(trimethylene carbonate). Biomaterials 30, 4738–4742.

Kong, Z., Yu, M., Cheng, K., Weng, W., Wang, H., Lin, J., Du, P., Han, G., 2013. Incorporation of chitosan nanospheres into thin mineralized collagen coatings for improving the antibacterial effect. Colloid Surf. B Biointerfaces 111, 536–541.

Leprêtre, S., Chai, F., Hornez, J.C., Verme, G., Neut, C., Descamps, M., Hildebrand, H.F., Marte, B., 2009. Prolonged local antibiotics delivery from hydroxyapatite functionalised with cyclodextrin polymers. Biomaterials 30, 6086–6093.

Li, S., Starkey, E.S., 2016. What do I need to know about glycopeptide antibiotics? Arch. Dis. Child. Educ. Pract. Ed. 101, 323–326.

Liu, S.J., Neng Ueng, S.W., Lin, S.S., Chan, E.C., 2002. *In vivo* release of vancomycin from biodegradable beads. J. Biomed. Mater. Res. Part B 63, 807–813.

Makarov, C., Gotman, I., Radin, S., Ducheyne, P., Gutmanas, E.Y., 2010. Vancomycin release from bioresorbable calcium phosphate–polymer composites with high ceramic volume fractions. J. Mater. Sci. 45, 6320–6324.

McDade, J.K., Brennan-Pierce, E.P., Ariganello, M.B., Labow, R.S., Lee, J.M., 2013. Interactions of U937 macrophage-like cells with decellularized pericardial matrix materials: influence of crosslinking treatment. Acta Biomater. 9, 7191–7199.

Melichercik, P., Klapkova, E., Landor, I., Judl, T., Sibek, M., Jahoda, D., 2014. The effect of vancomycin degradation products in the topical treatment of osteomyelitis. Bratisl. Lek. Listy 115, 796–799.

Nair, M.B., Kretlow, J.D., Mikos, A.G., Kasper, F.K., 2011. Infection and tissue engineering in segmental bone defects — a mini review. Curr. Opin. Biotechnol. 22, 721–725.

Noel, S.P., Courtney, H.S., Bumgardner, J.D., Haggard, W.O., 2010. Chitosan sponges to locally deliver amikacin and vancomycin a pilot *in vitro* evaluation. Clin. Orthop. Relat. Res. 468, 2074–2080.

Ordikhani, F., Tamjid, E., Simchi, A., 2014. Characterization and antibacterial performance of electrodeposited chitosan–vancomycin composite coatings for prevention of implant-associated infections. Mater. Sci. Eng. C-Mater. Biol. Appl. 41, 240–248.

Ordikhani, F., Dehghani, M., Simchi, A., 2015. Antibiotic-loaded chitosan–laponite films for local drug delivery by titanium implants: cell proliferation and drug release studies. J. Mater. Sci.-Mater. Med. 26–29.

Pokorný, M., Rassushin, V., Wolfová, L., Velebný, V., 2016. Increased Production of Nanofibrous Materials by Electroblowing from Blends of Hyaluronic Acid and Polyethylene Oxide. Polym. Eng, Sci http://dx.doi.org/10.1002/pen.

Posadowska, U., Brzychczy-Wloch, M., Pamula, E., 2016. Injectable gellan gum-based nanoparticles-loaded system for the local delivery of vancomycin in osteomyelitis treatment. J. Mater. Sci.-Mater. Med. 27, 9.

Rahaman, M.N., Bal, B.S., Huang, W., 2014. Review: emerging developments in the use of bioactive glasses for treating infected prosthetic joints. Mater. Sci. Eng. C 41, 224–231.

Raphel, J., Holodniy, M., Goodman, S.B., Heilshorn, S.C., 2016. Multifunctional coatings to simultaneously promote osseointegration and prevent infection of orthopaedic implants. Biomaterials 84, 301–314.

Rogina, A., 2014. Electrospinning process: versatile preparation method for biodegradable and natural polymers and biocomposite systems applied in tissue engineering and drug delivery. Appl. Surf. Sci. 296, 221–230.

Ruiz, J.C., Alvarez-Lorenzo, C., Taboada, P., Burillo, G., Bucio, E., De Prijck, K., Nelis, H.J., Coenye, T., Concheiro, A., 2008. Polypropylene grafted with smart polymers (PNIPAAm/PAAc) for loading and controlled release of vancomycin. Eur. J. Pharm. Biopharm. 70, 467–477.

Sfaciotte, R.A.P., Coronel, L.G., Osaki, S.C., Wosiacki, S.R., 2015. Gram-positive bacterial resistant strains of interest in animal and public health. Semina Cienc. Agrar. 36, 2693–2712.

Simchi, A., Tamjid, E., Pishbin, F., Boccaccini, A.R., 2011. Recent progress in inorganic and composite coatings with bactericidal capability for orthopaedic applications. Nanomed. Nanotechnol. Biol. Med. 7, 22–39.

Somerville, A.L., Wright, D.H., Rotschafer, J.C., 1999. Implications of vancomycin degradation products on therapeutic drug monitoring in patients with end-stage renal disease. Pharmacotherapy 19, 702–707.

Suchý, T., Šupová, M., Klapková, E., Horný, L., Rýglová, Š., Žaloudková, M., Braun, M., Sucharda, Z., Ballay, R., Veselý, J., Chlup, H., Denk, F., 2016. The sustainable release of vancomycin and its degradation products from nanostructured collagen/hydroxyapatite composite layers. J. Pharm. Sci. 105, 1288–1294.

ter Boo, G.J.A., Grijpma, D.W., Moriarty, T.F., Richards, R.G., Eglin, D., 2015. Antimicrobial delivery systems for local infection prophylaxis in orthopedic- and trauma surgery. Biomaterials 52, 113–125.

Tu, J., Yu, M., Lu, Y., Cheng, K., Weng, W., Lin, J., Wang, H., Du, P., Han, G., 2012. Preparation and antibiotic drug release of mineralized collagen coatings on titanium. J. Mater. Sci.-Mater. Med. 23, 2413–2423.

Wachol-Drewek, Z., Pfeiffer, M., Scholl, E., 1996. Comparative investigation of drug delivery of collagen implants saturated in antibiotic solutions and a sponge containing gentamicin. Biomaterials 17, 1733–1738.

Waeiss, R.A., Negrini, T.C., Arthur, R.A., Bottino, M.C., 2014. Antimicrobial effects of drug-containing electrospun matrices on osteomyelitis-associated pathogens. J. Oral Maxillofac. Surg. 72, 1310–1319.

Wilson, C.J., Clegg, R.E., Leavesley, D.I., Pearcy, M.J., 2005. Mediation of biomaterial–cell interactions by adsorbed proteins: a review. Tissue Eng. 11, 1–18.

Yang, C.C., Lin, C.C., Liao, J.W., Yen, S.K., 2013. Vancomycin–chitosan composite deposited on post porous hydroxyapatite coated Ti6Al4V implant for drug controlled release. Materials Science & Engineering, C: Materials for Biological Applications 33, 2203–2212.

Yao, Q., Nooeaid, P., Roether, J.A., Dong, Y., Zhang, Q., Boccaccini, A.R., 2013. Bioglass®-based scaffolds in corporating polycaprolactone and chitosan coatings for controlled vancomycin delivery. Ceram. Int. 39, 7517–7522.

Zhang, L., Yan, J., Yin, Z., Tang, C., Guo, Y., Li, D., Xu, B.W.Y., Gu, Q., Wang, L., 2014. Electrospun vancomycin-loaded coating on titanium implants for the prevention of implant-associated infections. Int. J. Nanomedicine 9, 3027–3036.

Zilberman, M., Elsner, J.J., 2008. Antibiotic-eluting medical devices for various applications. J. Control. Release 130, 202–215.

**G.** Martina Verdánová, **Pavla Sauerová**, Ute Hempel, Marie Hubálek Kalbáčová (2017): **Initial Cell Adhesion of Three Cell Types in the Presence and Absence of Serum Proteins.** Histochemistry and Cell biology 147 (5), published online. IF = 2.78

Histochem Cell Biol
DOI 10.1007/s00418-017-1571-7

ORIGINAL PAPER

# Initial cell adhesion of three cell types in the presence and absence of serum proteins

**Martina Verdanova[1,2] · Pavla Sauerova[1,3] · Ute Hempel[4] · Marie Hubalek Kalbacova[1,3]**

Accepted: 11 April 2017


**Abstract** With the development of a wide range of new biomaterials for the sensing of different cell behaviour, it is important to consider whether the cells tested in vitro are in direct contact with the material or whether cell–biomaterial contact is mediated by an interfacial layer of proteins originating from the culture medium or from the cells themselves. Thus, this study describes the differences between the cell adhesion mediated by proteins originating from foetal bovine serum and without the presence of such proteins 2 h following cell seeding exemplarily with different cell types (an osteoblastic cell line, primary fibroblasts, and mesenchymal stem cells). Three of the examined cell types were found to react differently to differing conditions in terms of cell shape, area, and number. Nevertheless, the expression and localization of the various proteins involved in cell adhesion and signalling (CD44, vinculin, talin, actin, focal adhesion kinase, Rho-GTPases and extracellular signal-regulated kinases 1 and 2) were, in general, similar with respect to all the cell types tested, albeit varying according to the presence or absence of serum. Moreover, no classical focal adhesions were formed during cell adhesion without serum proteins, while different signalling pathways were involved in this process. The study systematically describes and discusses the cell adhesion of three different human cell types to a well-known substrate without the presence of external proteins and it is hoped that this knowledge will be subsequently applied in biomaterial applications in which the presence of external proteins is undesirable (e.g. for biosensing purposes).

**Keywords** Cell adhesion · Foetal bovine serum · Fluorescence microscopy · Protein expression · Cell signalling

✉ Martina Verdanova
martinka.verdan@seznam.cz

[1] Institute of Inherited Metabolic Disorders, 1st Faculty of Medicine, Charles University in Prague, Ke Karlovu 2, 128 08 Prague 2, Czech Republic

[2] Department of Genetics and Microbiology, Faculty of Science, Charles University in Prague, Albertov 6, 128 43 Prague 2, Czech Republic

[3] Biomedical Center, Faculty of Medicine in Pilsen, Charles University in Prague, alej Svobody 1655/76, 323 00 Pilsen, Czech Republic

[4] Institute of Physiological Chemistry, Faculty of Medicine Carl Gustav Carus, Technical University Dresden, Fiedlerstraße 42, 01307 Dresden, Germany

## Introduction

The contact of cells with each other and with the extracellular matrix (ECM) is fundamental in terms of the performance of the appropriate cell functions and for the formation of tissue and organs. Proper cell adhesion is crucial for anchorage-dependent cells such as mesenchymal, epithelial or endothelial cells; if they do not receive adhesion-specific signals for survival, they die through apoptotic cell death, which in this specific case is known as anoikis (Frisch and Francis 1994; Chiarugi and Giannoni 2008).

The interaction of cells with a surface involves several hierarchical steps. First, proteins from body fluids or a culture medium adsorb on the surface. Second, the initial contact of cells with the adsorbed protein layer occurs within seconds. Third, the cells spread slightly and integrin receptors bind the ligands within the ECM and subsequently cluster together; this phase lasts a matter of minutes. Fourth, both cytoskeleton reorganization and active cell spreading occur within several hours. Finally, the cells

Published online: 21 April 2017

synthesize their own ECM within a number of hours to days (Anselme et al. 2010; Zaidel-Bar et al. 2004).

The connection between the cells and the ECM is mediated via focal adhesions (FAs) which consist of large macromolecular complexes consisting of a large number of proteins (Geiger and Yamada 2011). It is possible to classify the FA architecture in terms of several functional layers (Kanchanawong et al. 2010). The integrin extracellular domain makes up the first layer leading from the outside of the cell. Integrins are transmembrane heterodimeric receptors and their external parts bind to various ECM ligands such as fibronectin (FN) and vitronectin (VN). The second component of FAs is made up of the integrin signalling layer located beneath the cell membrane consisting of integrin intracellular domains, paxillin, α-actinin and focal adhesion kinase (FAK) and many other proteins that mediate cell signalling. This component is followed by the force transduction layer which is composed of proteins such as talin and vinculin that link the integrins to actin filaments (Calderwood et al. 2013; Critchley 2009; Humphries et al. 2007). Talin and vinculin are often employed as FA markers. The last FA layer consists of the actin regulatory layer which is composed of specialized proteins applied with respect to FA strengthening; this layer is followed by actin stress fibres (Kanchanawong et al. 2010). Thus, FAs act to couple integrins to the actin cytoskeleton to transduce information from the ECM to the cell nucleus in which changes in gene expression may occur. The mechanical link between cell surface and nucleus (through FAs and across the nuclear envelope) mediates LINC complex (a linker of nucleoskeleton and cytoskeleton). This complex includes nesprin and Sun proteins (Crisp et al. 2006).

In vitro cells are cultivated in a culture medium supplemented with serum in the standard way, most frequently with foetal bovine serum (FBS). FBS proteins rapidly adsorb fast onto the substrate and, subsequently, cells adhere to this adsorbed protein layer (Wilson et al. 2005). Thus, cell adhesion in vitro to any material is strongly influenced by FBS proteins. FBS contains various proteins and factors which are important in terms of cell adhesion, proliferation and survival including adhesion-mediating proteins (e.g. FN, VN, laminin), growth factors, vitamins, hormones, cofactors, transport factors (e.g. albumin, transferrin), electrolytes and nutrients (Krebs 1950). The use of FBS involves a number of disadvantages primarily with respect to medical applications, i.e. it presents high batch-to-batch variability, is able to transmit fungi, bacteria, and virus and prion infections and can induce the production of anti-FBS antibodies (Sundin et al. 2007).

FN and VN make up the two primary FBS proteins that mediate cell adhesion. Both FN and VN are glycoproteins which contain the RGD sequence which is recognized and subsequently bound by a large number of integrins (Ruoslahti 1996). However, FBS is composed primarily of bovine serum albumin (BSA) (more than 50% of FBS protein content). Negative effects of BSA on cell adhesion have been described in most cases (Wei et al. 2009); nevertheless, the positive effect has also been observed of BSA at high concentrations together with adhesion-promoting proteins in low concentration on a plastic substrate (Koblinski et al. 2005). Generally, it is believed that FBS proteins compete for adsorption to a surface and that cell adhesion is influenced by the balance between adhesion-promoting (e.g. FN) and adhesion-inhibiting (e.g. BSA) proteins (Carre and Lacarriere 2010).

Moreover, cell membrane proteins (other than the integrins mentioned previously) are extremely important in terms of cell adhesion, particularly during the initial phases. The CD44 membrane glycoprotein is prominent as a receptor for hyaluronan that is also able to interact with FN, fibrin, osteopontin and selectins (Ponta et al. 2003).

Induced by ECM–integrin interactions, various intracellular signalling proteins become activated. Three representatives of such signalling proteins were investigated in this study: focal adhesion kinase (FAK), Rho-GTPase proteins and extracellular signal-regulated kinases 1 and 2 (ERK1/2). FAK is a non-receptor protein tyrosine kinase that is activated by the autophosphorylation of tyrosine 397 residue (pFAK-Y397) in response to integrin clustering and growth factor stimulation. Phosphorylation leads to subsequent signal transduction within the cell, resulting in changes in focal adhesion dynamics (Schlaepfer et al. 1999). Rho-GTPases act as molecular switches from the active GTP state to an inactive GDP state and are involved in the regulation of cell shape, polarity, migration and cell cycle cytokinesis. ERK1 and ERK2 are also known as MAPK3 and MAPK1 (mitogen-activated protein kinases); these two serine/threonine kinases are activated by phosphorylation at two sites (T202/Y204 and T185/Y187, respectively) following growth factor binding or as a consequence of adhesion. Active ERK1/2 kinases phosphorylate a large number of cytoplasmic and nuclear proteins including transcription factors (Roskoski 2012; Yoon and Seger 2006).

Since cell adhesion is cell-type specific, three different cell types (osteosarcoma cell line SAOS-2, primary fibroblasts and mesenchymal stem cells) were employed in this study. SAOS-2 is a well-established osteoblastic cell line derived from primary osteosarcoma and represents the tumour and permanent cell line in this study (Rodan et al. 1987). Human primary fibroblasts are versatile cells which are widespread in connective tissue and are widely used in vitro as a classic cell model. Human mesenchymal stem cells (hMSCs) are progenitor cells that are able to differentiate into various cell types such as osteoblasts, adipocytes or chondrocytes (Abumaree et al. 2013).

To the best of our knowledge, no detailed comparison of different cell adhesion of various cell types in the presence and absence of FBS proteins on TCPS (a material generally used as a control material for comparative biomaterial studies and as a standard substrate for culture of cells in vitro) has been compiled to date. This paper, therefore, aims to contribute towards filling this gap in scientific knowledge.

## Materials and methods

### Cells and culture conditions

*Osteoblasts SAOS-2*

The human osteoblast-like cell line SAOS-2 derived from osteosarcoma was obtained from DSMZ, Germany (Deutsche Sammlung von Mikroorganismen und Zellkulturen, GmbH). The long-term cultivation of the SAOS-2 was performed in McCoy's 5A medium without phenol red (PromoCell, Germany) supplemented with 15% heat-inactivated FBS (Gibco®, Life Technologies, USA), penicillin (20 U/ml, Sigma–Aldrich, USA) and streptomycin (20 µg/ml, Sigma–Aldrich, USA). The cells were cultivated at 37 °C in a 5% $CO_2$ atmosphere. The experimental procedures involved the cells being cultivated in the above-mentioned medium supplemented with 0, 1, 5 and 15% FBS.

*Primary human fibroblasts*

Normal human dermal fibroblasts (NHDF) were isolated from facial skin removed during cosmetic plastic surgery from donors after they had provided informed, written consent, in collaboration with the Lochotín hospital, Czech Republic. NHDF were obtained from the dermis by means of the digestion method (Ruszova et al. 2013). The fibroblasts were cultivated in Dulbecco's modified Eagle's medium–low glucose (DMEM) medium (Thermo Fisher Scientific, USA) supplemented with 10% heat inactivated FBS (PAA, Austria), penicillin (20 U/ml; Sigma-Aldrich, USA), streptomycin (20 mg/ml; Sigma-Aldrich, USA), D-glucose (2 g/l; Thermo Fisher Scientific, USA) and L-glutamine (2 mM; Thermo Fisher Scientific, USA) at 37 °C and in a 5% $CO_2$ atmosphere. NHDF in the 3rd–4th passage were used for experimental purposes.

*Human mesenchymal stem cells*

Human mesenchymal stem cells were obtained from healthy donors after they had provided informed, written consent. Bone marrow blood was aspirated from the posterior iliac crest and the mononuclear fraction was isolated by means of gradient centrifugation. The adherent cells were cultivated in a-MEM medium (Thermo Fisher Scientific, USA) with 10% heat inactivated FBS (PAA, Austria), penicillin (20U/mL; Sigma-Aldrich) and streptomycin (20 mg/mL; Sigma-Aldrich). The experiments were performed with hMSCs taken from two donors in the 1st passage.

### Cell seeding

Cells were collected at 50–90% confluence using trypsin washed in an FBS-free medium and seeded onto tissue culture polystyrene (TCPS) plates (TPP, Switzerland) at a density of $1.5 \times 10^4$ cells/cm$^2$ and cultivated in media as specified above (FBS: 0, 1, 5, 10 and 15%) for 2 h unless otherwise indicated.

### Protein pre-adsorption on glass surfaces

Fibronectin taken from bovine plasma (40 µg/ml, Sigma-Aldrich, USA) and vitronectin also from bovine plasma (2 µg/ml, Sigma-Aldrich, USA) and FBS (15%) diluted in a medium without FBS were applied (100 µl/well) to 4-well glass slides (Nunc™ Lab-Tek™ II Chamber Slide™, Thermo Scientific, USA) and incubated at 37 °C in a 5% $CO_2$ atmosphere for 2 h. Following protein pre-adsorption, SAOS-2 cells ($2 \times 10^4$ cells/cm$^2$) were seeded in wells in a medium without FBS and incubated for 2 and 20 h.

### Fluorescence staining of the cells

The cells were fixed in 4% paraformaldehyde (Sigma-Aldrich, USA) in phosphate-buffered saline (PBS) at room temperature (RT) for 15 min and permeabilized by means of 0.1% Triton X-100 in PBS (Sigma-Aldrich, USA) at RT for 20 min. Non-specific binding sites were reduced by means of incubation in a blocking solution (1% FBS + 0.05% Tween® 20 in PBS, Sigma-Aldrich, USA) at RT for 1 h. The primary antibodies were diluted in the blocking solution and incubated with the cells at 37 °C for 1 h or at 4 °C overnight: mouse monoclonal anti-CD44 antibody (1:100; Abcam, United Kingdom), mouse monoclonal anti-vinculin antibody (1:500; Sigma-Aldrich, USA), mouse monoclonal anti-talin (clone 8d4) antibody (1:250; Sigma-Aldrich, USA), rabbit monoclonal anti-pFAK-Y397 antibody (1:100; BioSource International, USA), rabbit monoclonal anti-Rho (Y486) antibody (1:100; Abcam, United Kingdom) and rabbit monoclonal anti-pERK1/2 (clone 269434) antibody (1:20; R&D Systems, USA). The following secondary antibodies were diluted in the blocking solution and incubated with the cells at 37 °C for 45 min: donkey polyclonal anti-rabbit antibody conjugated with Alexa Fluor 488 (1:1 000; Life Technologies,

USA) and donkey polyclonal anti-mouse antibody conjugated with Alexa Fluor 488 (1:1 000; Life Technologies, USA). The actin filaments were stained by means of phalloidin conjugated with Alexa Fluor 488 (1:500; Life Technologies, USA) which was diluted in PBS and incubated with the cells at RT for 45 min. The cell nuclei were stained by means of DAPI (4′,6-diamidino-2-phenylindole, 1:1 000; Sigma-Aldrich, USA) which was diluted in PBS and incubated with the cells at RT for 15 min.

### Cell imaging

Phase contrast and wide-field fluorescence images of the cells were acquired using an Eclipse Ti-S microscope (Nikon, Japan) with a Plan Fluor 10× (N.A. 0.30) objective, S Plan Fluor 20× (N.A. 0.45) objective, S Plan Fluor 40× (N.A. 0.60) objective and S Plan Fluor 60× (N.A. 0.70) objective and a DS-U2 digital camera (Nikon, Japan).

### Cell number and cell area determination

The cell number (nuclei staining, 10× objective) and the cell area (actin filament staining, 20× objective) were counted automatically from the fluorescence images using ImageJ software (Rasband, W.S., ImageJ, U. S. National Institutes of Health, Bethesda, Maryland, USA, http://imagej.nih.gov/ij/, 1997–2016) and CellProfiler (Broad Institute, USA).

### Cell adhesion strength determination

The SAOS-2 cells were seeded in media with or without FBS (see the "Cell seeding" section) and incubated at 37 °C in a 5% $CO_2$ atmosphere for 2 h. One plate containing cells was shaken using a PMS-1000 shaker (Grant Instruments, United Kingdom) at 1000 rpm for 10 min. Following shaking, the cells were washed three times using PBS. A second (control) plate was not shaken and was left at RT also for 10 min., following which the cells were similarly washed using PBS. The cells were fixed in 4% paraformaldehyde in PBS at RT for 15 min and permeabilized using 0.1% Triton X-100 in PBS at RT for 20 min. The cell nuclei were stained using DAPI diluted in PBS (1:1000) and incubated at RT for 15 min. The number of cells was assessed according to the procedure described in the "Cell number and cell area determination" section.

### Measurement of fluorescence intensity

The fluorescence intensity of the ERK1/2 signal was measured with respect to 230 SAOS-2 cells from grey-scale images taken by a 60× objective using CellProfiler software. The imaging conditions were constant for all images and no binning of data was performed.

### Detection of pERK1/2 by means of Western blot

SAOS-2 cells ($2 \times 10^6$) were plated in media with or without FBS in 60 $cm^2$ Petri dishes for 2 h, washed using PBS and incubated on ice in a lysis buffer (50 mM Tris–HCl [pH 6.8], 50 mM dithiothreitol and 2% sodium dodecyl sulphate [SDS]) for 15 min. The lysates were collected, sonicated, heated at 100 °C for 5 min and then separated on a 13% SDS–polyacrylamide gel. Subsequently, the proteins were blotted onto polyvinylidene difluoride membranes (Millipore, Immobilon, Germany). The membranes were incubated in a blocking solution (5% non-fat dry milk [Laktino - Promil, Czech Republic] in PBS containing 0.05% Tween-20) at 4 °C overnight to block non-specific binding. The membranes were incubated with primary antibodies diluted in 5% BSA/PBS containing 0.05% Tween-20 at RT for 1 h (rabbit monoclonal anti-phosphoERK1/ERK2 antibody, clone 269434, 1:1 000; R&D Systems, USA and mouse monoclonal anti-GAPDH antibody, 1:5 000; Sigma-Aldrich, USA). Subsequently, the membranes were incubated with secondary antibodies, i.e. goat anti-rabbit horseradish peroxidase-conjugated antibody (1:10 000; Thermo Scientific-Pierce, USA) and goat anti-mouse horseradish peroxidase-conjugated antibody (1:20 000; Thermo Scientific-Pierce, USA), diluted in the blocking solution and incubated at RT for 45 min. Protein signals were detected using an immunodetection kit with Super-Signal West Femto Chemiluminescent Substrate (Thermo Scientific-Pierce, USA).

### Determination of the amount of pERK1/2 by means of enzyme-linked immunosorbent assay (ELISA)

SAOS-2 cells ($1 \times 10^5$) were plated in media with or without FBS in 9 $cm^2$ Petri dishes. 2 h following plating, the cells were placed on ice, washed carefully in PBS and lysed using a phospho-ERK1/2 ELISA kit (Phospho-ERK1(T202/Y204)/ERK2(T185/Y187) DuoSet IC; R&D Systems, Germany) according to the manufacturer's instructions. Protein concentration was determined by Roti-Quant protein assay (Carl Roth GmbH, Germany) and calculated from a linear calibration curve ($r < 0.99$) obtained with a BSA standard.

### Statistical analysis

The nonparametric Mann–Whitney *U* test was used to determine the significant differences between the datasets,

and p values of less than 0.01 were considered statistically significant; STATISTICA Software (StatSoft, Czech Republic) was employed for the statistical analysis.

## Results

This study aimed to compare the early adhesion process of a human osteoblast-like cell line (SAOS-2), primary human fibroblasts and human mesenchymal stem cells (hMSCs) in the presence or absence of serum proteins. The primary focus of the study concerns differences between cell adhesion to a substrate mediated by proteins originating from FBS (defined by the authors as "indirect" adhesion) and cell adhesion to a substrate with no preformed protein layer between the cells and the surface (referred to as "direct" adhesion). This study is the first to compare the "indirect" and "direct" adhesion of three different human cell types on TCPS.

### Cell morphology of the osteoblasts, fibroblasts and mesenchymal stem cells in the presence and absence of FBS

The cell morphology of human osteoblasts, fibroblasts and hMSCs is presented in Fig. 1. The osteoblasts and hMSCs that adhered on FBS proteins exhibited a round shape in contrast to the fibroblasts that exhibited an elongated and ragged shape. Conversely, the osteoblasts and hMSCs that adhered on TCPS without FBS proteins displayed a ragged shape and the fibroblasts primarily a round shape.

### The effect of FBS on cell area and cell number of the osteoblasts, fibroblasts and mesenchymal stem cells

This observation correlates with the measured cell area (Fig. 2a). Osteoblasts that adhered on FBS had a statistically significantly smaller cell area (605 $\mu m^2$) than those that adhered on TCPS without FBS proteins (859 $\mu m^2$), whereas the opposite was determined with respect to the fibroblasts (cell area 2107 $\mu m^2$ with FBS vs. 1434 $\mu m^2$ without FBS). Due to the large variations in cell area detected with concern to the hMSCs, a similar cell area was observed for these cells under both conditions (2984 $\mu m^2$ with FBS vs. 2808 $\mu m^2$ without FBS).

With regard to cell number, a statistically significantly lower number of osteoblasts was observed when the cells adhered on TCPS in the presence of FBS (7617 cells/$cm^2$) than when FBS was absent (9284 cells/$cm^2$), whereas the opposite situation was detected with respect to the fibroblasts (10,051 cells/$cm^2$ with FBS vs. 7842 cells/$cm^2$ without FBS) and hMSCs (13,476 cells/$cm^2$ with FBS vs. 7211 cells/$cm^2$ without FBS) with regard to which more cells were detected in the presence of FBS during cell seeding (Fig. 2b).

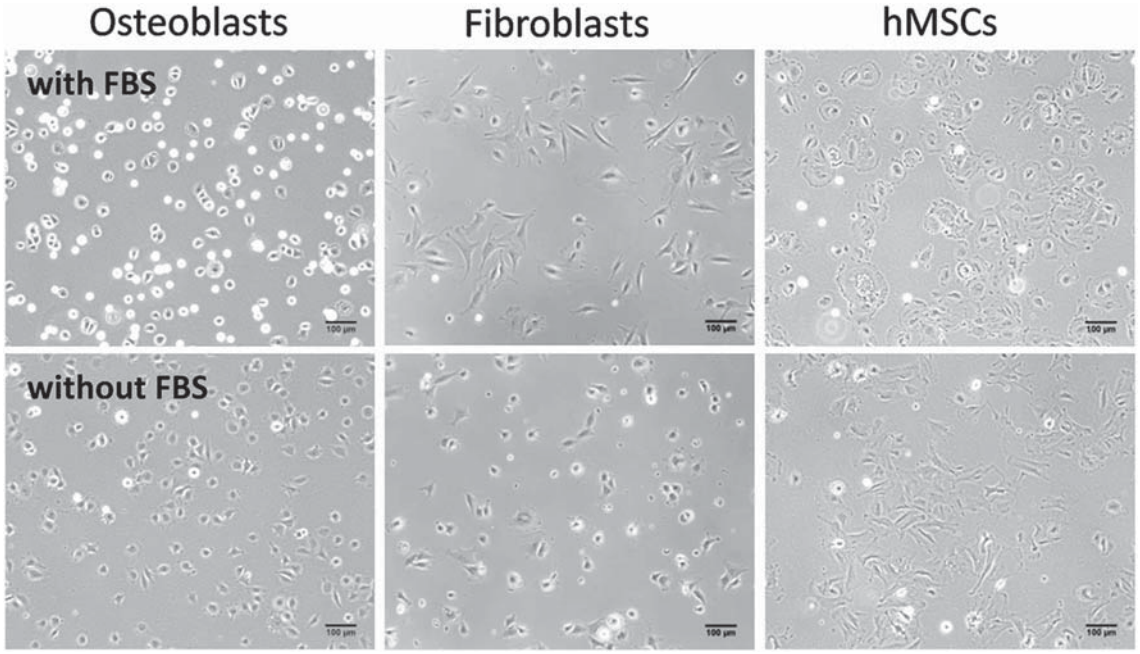


**Fig. 1** Phase contrast images of osteoblasts, fibroblasts and human mesenchymal stem cells (hMSCs). These cells were cultivated in FBS presence (with FBS) or in FBS absence (without FBS) on tissue culture polystyrene for 2 h

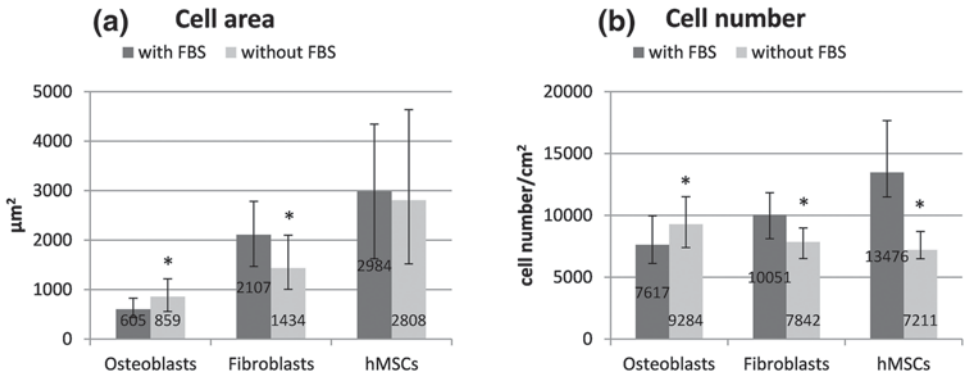


**Fig. 2** Effect of FBS on cell area and cell number. Osteoblasts, fibroblasts and human mesenchymal stem cells (hMSCs) were cultivated in FBS presence (with FBS) or absence (without FBS) on tissue culture polystyrene for 2 h. Cell area (**a**) (osteoblasts: $N = 2000$ cells, fibroblasts: $N = 450$ cells, hMSCs: $N = 250$ cells), cell number (**b**) (osteoblasts: $N = 400$ fields of view, fibroblasts: $N = 140$ fields of view, hMSCs: $N = 40$ fields of view) were determined as described in "Materials and methods" section. Median and interquartile range are expressed. * indicates significant difference at $p < 0.01$ (Mann–Whitney $U$ test) between with and without FBS in the same cell type

### The effect of FBS on the expression of various structural, membrane and signalling proteins in the osteoblasts, fibroblasts and mesenchymal stem cells

In order to characterize the quality of cell adhesion, the expression of proteins such as actin, vinculin, talin, CD44, pFAK, Rho and pERK1/2 in those osteoblasts, fibroblasts and hMSCs that were cultivated in both the presence and absence of FBS for 2 h was studied by means of fluorescence microscopy (Fig. 3).

Actin cytoskeleton distribution was affected by the shape and morphology of the cells. With respect to well-spread cells, the actin signal revealed a filamentous character (e.g. fibroblasts in the presence of FBS). On the other hand, concerning the roundish cells (e.g. osteoblasts in the presence of FBS) an actin ring on the cell perimeter accompanied by a more diffused signal was observed.

Focal adhesion structural proteins—vinculin and talin—were localized in FAs on the perimeter of all three cell types that adhered in the presence of FBS in contrast to those cells that were seeded in the absence of FBS. The vinculin and talin signals in these cells were spread diffusely throughout the whole cell with very occasional intensification at the cell edges.

In contrast to all the previous intracellular proteins, the CD44 membrane protein revealed a diffuse signal with occasional aggregates irrespective of cell type and FBS presence.

The activation of the FAK-Y397 protein kinase, which is located in the FAs, was investigated to evaluate the consequences of a particular type of cell adhesion in terms of cell signalling downstream from the cell membrane. Activated, i.e. phosphorylated, FAK exhibited the same expression pattern as vinculin and talin. pFAK was localized in the FAs in all those cells that adhered on TCPS in the presence of FBS and a diffuse pFAK signal throughout the whole of the cells with sporadic intensification at the cell edges was detected in all the cells that adhered in the absence of FBS.

Varying Rho-GTPases (A, B, and C) were studied as important regulators of actin dynamics. The Rho GTPase signal was diffuse throughout the whole of the cells with occasional intensification at the cell edges in the osteoblasts and hMSCs that adhered on FBS proteins in contrast to the fibroblasts, with concern to which this expression pattern was observed more with respect to cells which adhered in the absence of FBS. Conversely, a diffuse Rho protein signal only was observed in those osteoblasts and hMSCs that were seeded without FBS proteins and the fibroblasts that adhered on FBS proteins.

pERK1/2 signalling proteins were localized at the cell edges in those osteoblasts and hMSCs that adhered on FBS proteins. Conversely, a sporadic pERK1/2 signal at the cell edges with a somewhat diffuse signal throughout the whole of the cells was observed in those osteoblasts and hMSCs that were seeded without FBS. The pERK1/2 signal in the fibroblasts was distributed equally throughout the whole of the cells with occasional intensification in the middle of the cells and sometimes at the cell edges regardless of the presence of FBS.

Western blot analysis and ELISA assay were performed with concern to the deeper characterization of pERK1/2 expression in the osteoblasts and the quantification of the pERK1/2 fluorescence signal. The quantification of the fluorescence signal from microscopic images revealed an increased signal of pERK1/2 kinases in those osteoblasts adhered in the presence of FBS compared to those that adhered in the absence of FBS (Fig. 4; 100 vs. 84%). The higher expression level of pERK1/2 proteins in the osteoblasts that adhered to FBS proteins was supported by Western blot analysis (Fig. 4) and by ELISA assay (Fig. 4).

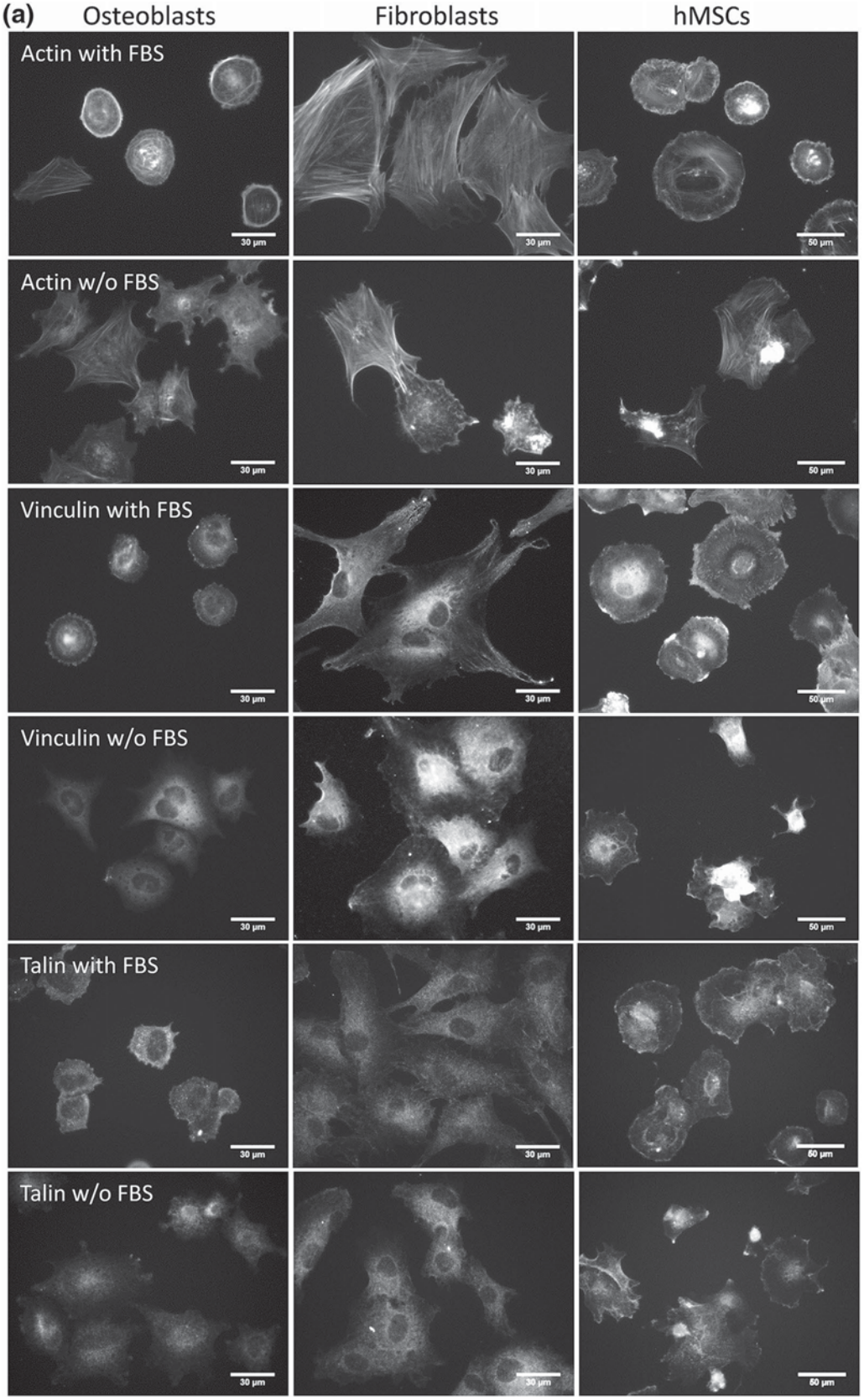


**Fig. 3** Effect of FBS on expression and localization of structural, membrane and signalling proteins. Osteoblasts, fibroblasts and human mesenchymal stem cells (hMSCs) were cultivated in FBS presence (with FBS) or absence (w/o FBS) on tissue culture polystyrene for 2 h. Immunofluorescently stained proteins are depicted in the images: **a** actin, vinculin, talin; **b** CD44, pFAK; **c** Rho, pERK1/2

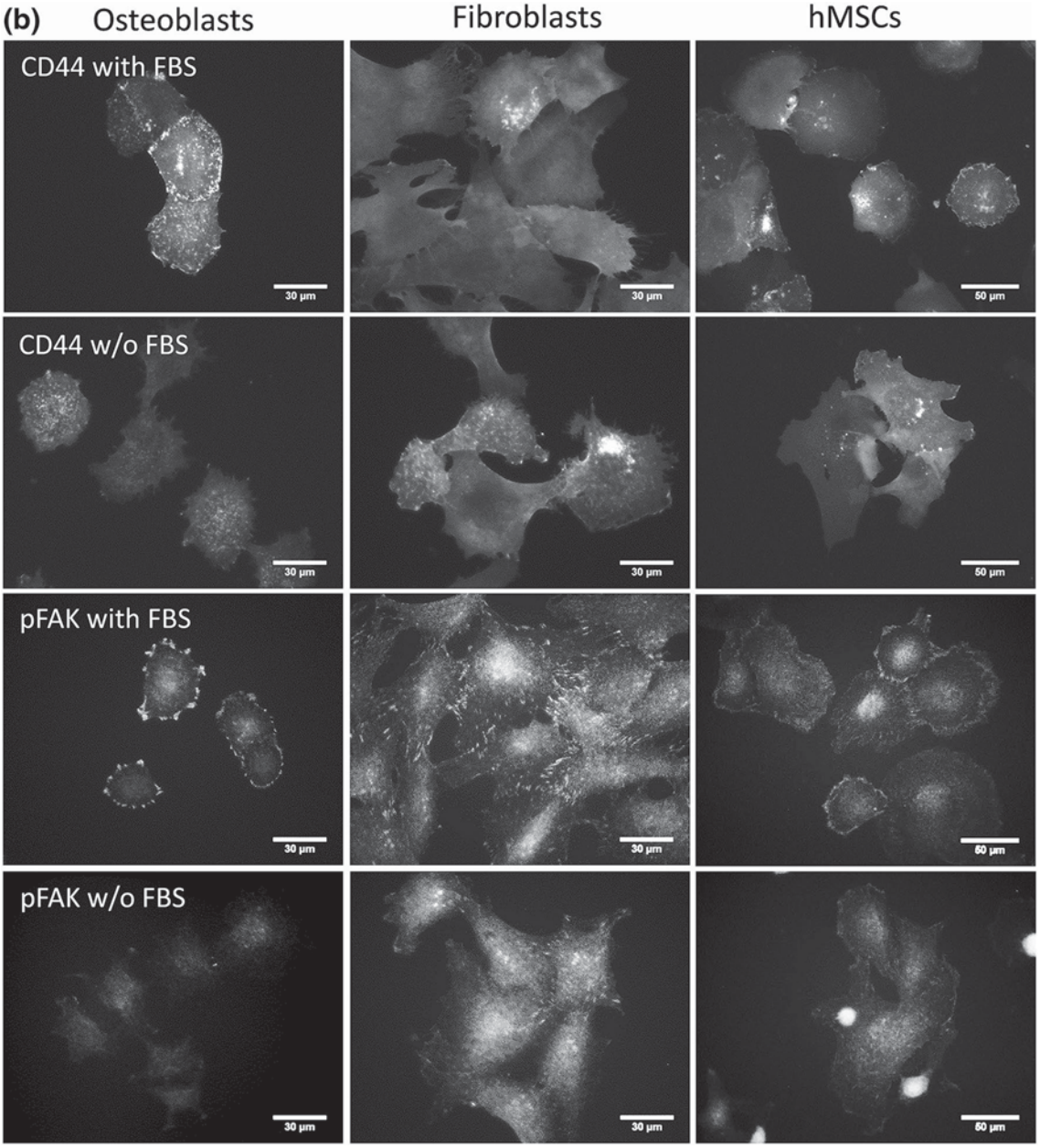


**Fig. 3** continued

Taken together, the osteoblasts and hMSCs demonstrated a similar cell shape with respect to the presence/absence of FBS (a round shape in the presence of FBS vs. a star-like shape in the absence of FBS). On the other hand, the fibroblasts and hMSCs exhibited a similar trend in cell number with regard to the presence/absence of FBS (a higher number of cells in the presence of FBS compared to the absence thereof). Concerning the cell adhesion mechanism, in the presence of FBS on the TCPS surface all three cell types developed classical FAs with the expression of vinculin, talin and pFAK in the FAs. In contrast, these classical FAs were not observed in any of the tested cell types in the absence of FBS. The osteoblasts and hMSCs differed from the fibroblasts in terms of the localization of Rho and pERK1/2 proteins dependent on the presence/absence of FBS which goes hand-in-hand with cell shape and area (Figs. 1, 2). It can be stated, therefore, that certain features (especially cell shape, area and number) of cell adhesion in the presence of FBS are cell type-specific; however, the formation of focal adhesion (detected by FA structural proteins) is similar with respect to all the tested cell types.

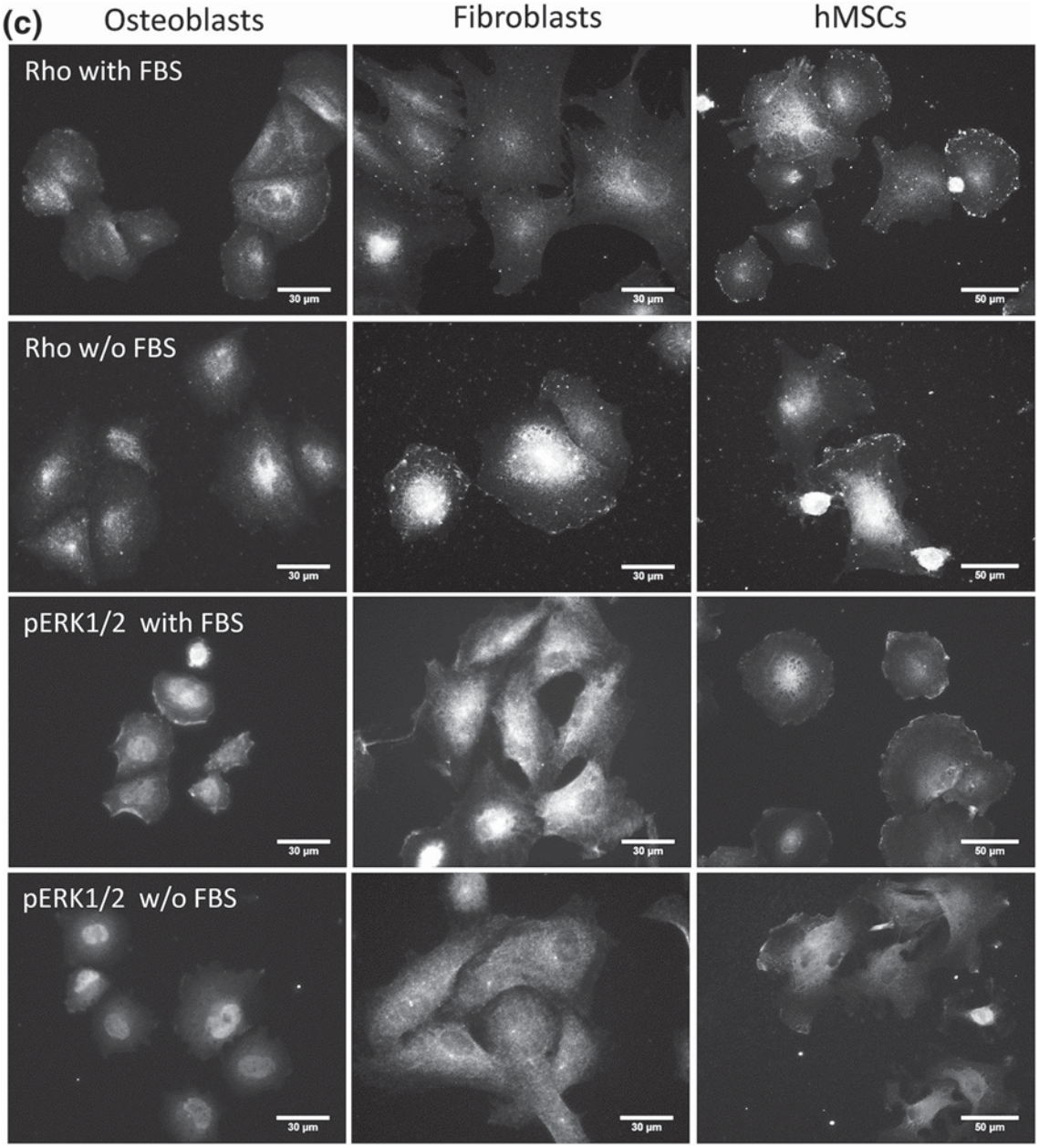


**Fig. 3** continued

### Osteoblast adhesion in the presence of various concentrations of FBS

Since SAOS-2 represents a well-established stable osteoblastic line, it has been used in a large number of publications focusing on biomaterials and the authors of this study have a great deal of experience with it (Kalbacova et al. 2011; Ostrovska et al. 2016; Verdanova et al. 2016), a deeper characterization of cell adhesion in both the presence and absence of FBS was performed with concern to these particular osteoblasts.

According to the supplier's recommendations, SAOS-2 cell cultivation requires the supplementation of a culture medium with a 15% FBS content; nevertheless, it was decided that it would be advantageous to perform a study of the influence of different FBS concentrations, i.e. 0, 1, 5 and 15% on the adhesion process. The images provided in Fig. 5 reveal that the FA structural protein vinculin was expressed to a similar extent in the presence of FBS regardless of FBS concentration. Moreover, those osteoblasts cultivated in the absence of FBS were also found to produce the vinculin protein; however, in this case the protein was

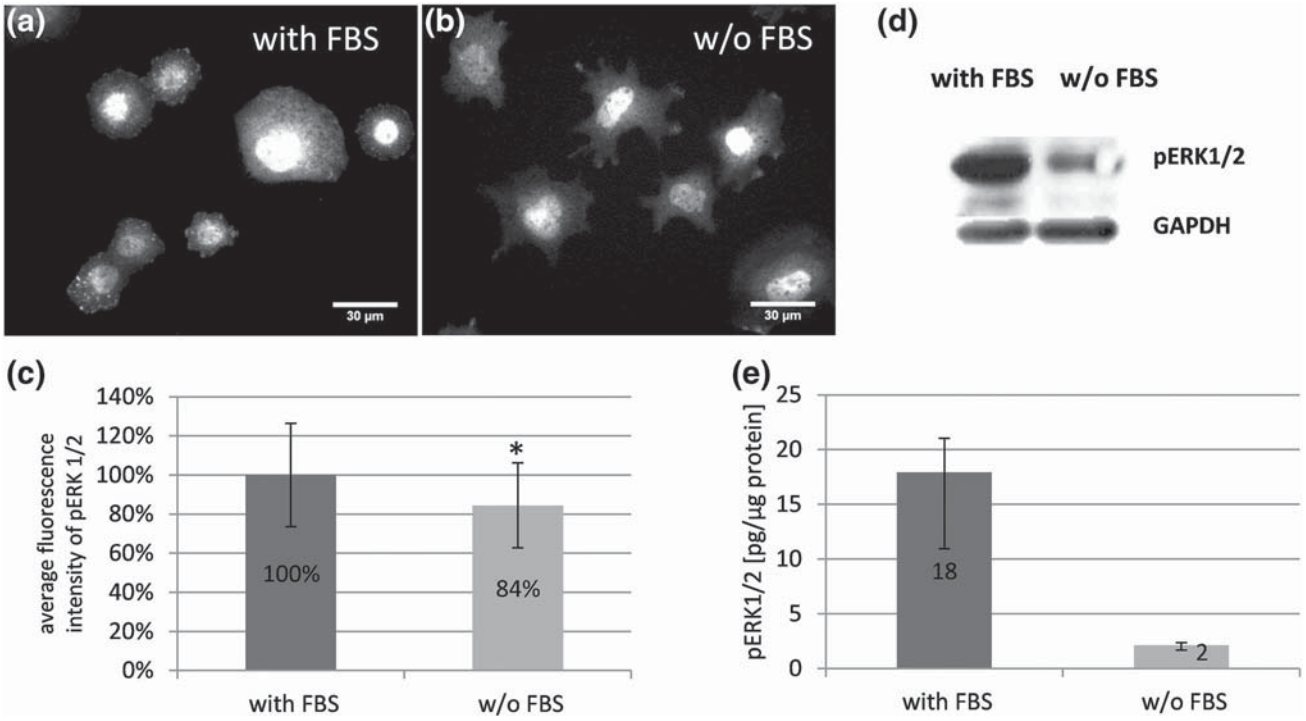


**Fig. 4** Effect of FBS on ERK1/2 activation in osteoblasts. SAOS-2 cells were cultivated in FBS presence (with FBS) or absence (w/o FBS) on tissue culture polystyrene for 2 h. The cells were immunofluorescently stained for pERK1/2 (**a**, **b**). The histogram (**c**) shows the quantification of the fluorescence signal of pERK1/2 from the images. Mean and standard deviation are expressed; * indicates significant difference at $p < 0.01$ (Mann–Whitney $U$ test); $N = 230$. In addition, cell lysates were separated by SDS-PAGE and analysed after western blotting for pERK1/2 and GAPDH as a reference protein/internal standard (**d**). The lysates were further applied in an intracellular pERK1/2 ELISA (**e**); medians with interquartile range as deviations are expressed, $N = 3$

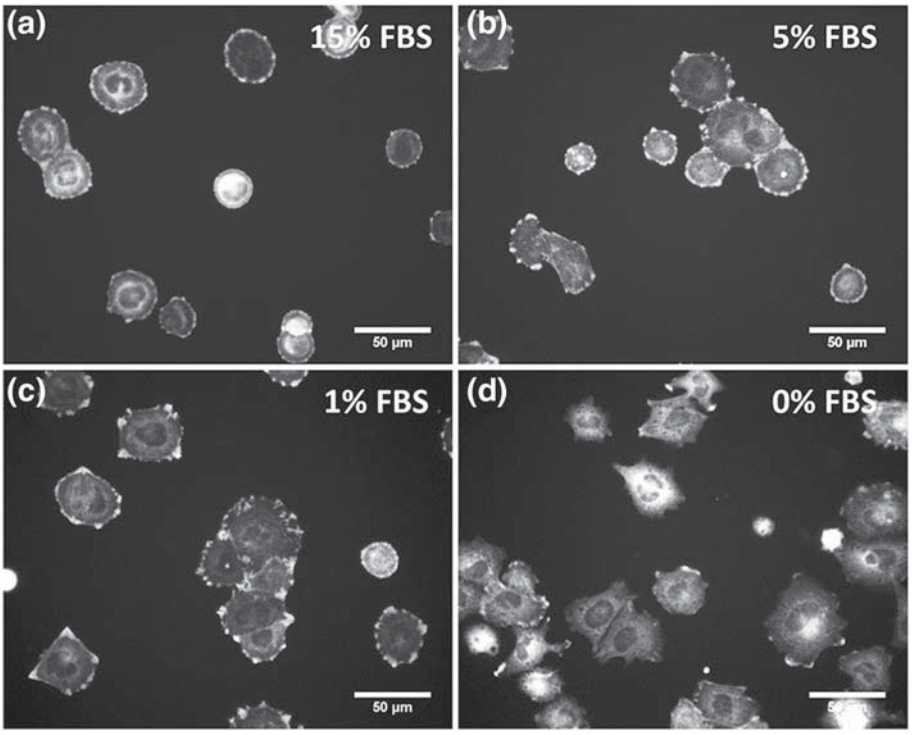


**Fig. 5** Immunofluorescence staining of vinculin. Osteoblasts (SAOS-2) were cultivated in the presence of 15% FBS (**a**), 5% FBS (**b**), 1% FBS (**c**) or without FBS (0% FBS; **d**) on tissue culture polystyrene for 2 h

located diffusely within the cytoplasm rather than localized in individual FAs. The vinculin signal was restricted to a few large clusters on the edges of the cells.

### The effect of FBS on the adhesion strength of osteoblasts

Osteoblast adhesion without FBS was stronger than with FBS as evaluated by means of the application of shaking strength on the cells (Fig. 6). After 10 min of shaking, the number of cells that adhered without the presence of FBS was found to be three times higher (approximately 11,500 cells/cm$^2$) than the number of cells that adhered to FBS proteins (approximately 4000 cells/cm$^2$). Those osteoblasts that attached to proteins were found to be strongly washed out. As expected, a significantly lower number of cells was detected following shaking (approximately 4000 cells/cm$^2$) compared to those detected without being subjected to shaking (approximately 6000 cells/cm$^2$) in the presence of FBS. However, surprisingly, those osteoblasts that adhered directly to the surface of the TCPS were mechanically (as the result of shaking) stimulated into accelerated adhesion; thus, significantly more cells were found to be present following shaking (approximately 11,500 cells/cm$^2$) than without the application of shaking (approximately 10,000 cells/cm$^2$).

### The effect of individual FBS proteins on osteoblast adhesion

The response of osteoblasts on FN and VN (from bovine plasma) was studied so as to allow for the evaluation of the effect of the individual selected proteins originating from FBS on osteoblast adhesion. Both proteins were

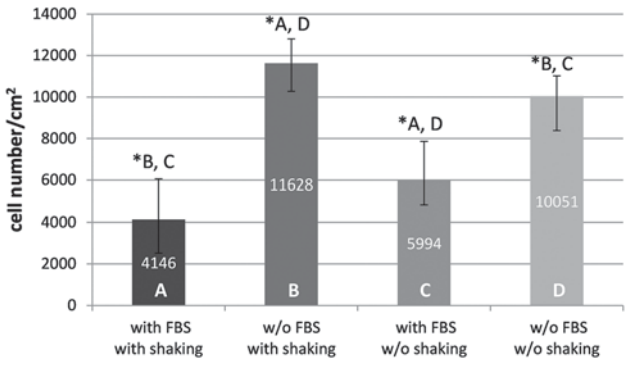


**Fig. 6** Effect of FBS on adhesion strength of osteoblasts. SAOS-2 cells were cultivated in FBS presence (with FBS) or absence (w/o FBS) on tissue culture polystyrene for 2 h. Cell adhesion strength ($N = 120$) was determined as described in "Materials and methods" section. Median and interquartile range are expressed. * and *letters* (*A–D*) indicate significant difference at $p < 0.01$ (Mann–Whitney *U* test) among the particular columns

immobilized on glass by means of adsorption. Osteoblast adhesion (vinculin expression, FA distribution patterns and morphology) was studied after 2 and 20 h and compared to adsorptively immobilized complete FBS or a "naked" surface. After 2 h of cultivation, the morphology of the osteoblasts that were cultivated on FN, VN and FBS was comparable but differed significantly from the morphology of those osteoblasts that were cultivated without the presence of proteins. In this case, the osteoblasts exhibited a more star-like than round shape. In addition, the FAs (visualized by means of vinculin staining) of the osteoblasts that were cultivated on FN, VN and FBS were all found to have a similar appearance. The FAs were relatively well developed and that predominantly on the edges of the cells in contrast to those cells that were cultivated without proteins regarding which only a few or no FAs were seen to be developed (Fig. 7a–d).

However, after 20 h of cultivation, the distribution of the FAs in the cells differed according to the protein on which they were cultivated. The FAs in those osteoblasts that were cultivated on FN were large, well separated from one another and evenly distributed over the whole of the cell (Fig. 7e). In contrast, those osteoblasts that were cultivated on VN had larger and primarily peripherally distributed FAs (Fig. 7f). The osteoblasts cultivated on FBS were smaller; however, their FAs formed large aggregates around the cells (Fig. 7g). Completely different FA characteristics were observed in those osteoblasts that were cultivated directly on glass (with no protein). Only a few cells survived under such repressive conditions, and those few that did developed FAs in large clusters at the ends of cellular projections (filopodia) (Fig. 7h).

An overall picture of osteoblast distribution and morphology following 20 h of cultivation on differently covered glass surfaces is provided in Fig. 8. The osteoblasts that were cultivated on FN were the most spread out and exhibited an elongated shape (Fig. 8a). The osteoblasts that were cultivated on VN were also well spread out but were not as elongated as the osteoblasts cultivated on FN (Fig. 8b). In contrast, the osteoblasts that were cultivated on FBS were also spread out but smaller and more round-shaped than their FN and VN counterparts (Fig. 8c). Finally, very few spread out osteoblasts were detected directly on glass and these were found to be extremely elongated (Fig. 8d). Most of the osteoblasts were badly adhered and were spherical in shape.

In conclusion, those osteoblasts that were cultivated on FN, VN and FBS exhibited comparable morphologies and FA patterns following a short period of incubation; however, this similarity lessened after longer periods of incubation. In contrast, the osteoblasts that were seeded and cultivated directly on the surface exhibited a morphology that differed significantly from the outset from those osteoblasts exposed to particular proteins.

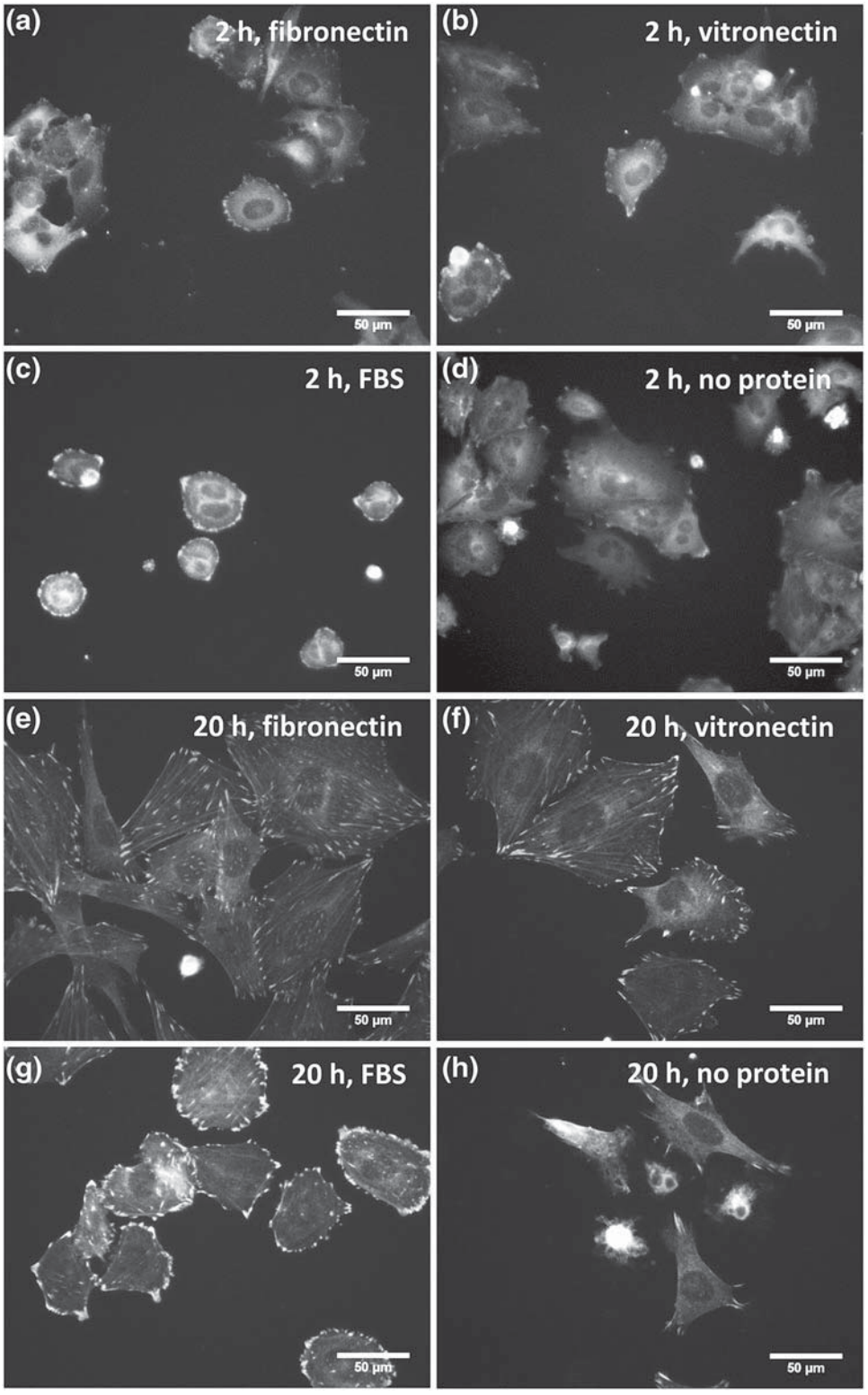


**Fig. 7** Effect of immobilized fibronectin, vitronectin, and FBS proteins on formation of focal adhesions in osteoblasts. SAOS-2 cells were cultivated on glass with immobilized fibronectin (**a**, **e**), vitronectin (**b**, **f**), FBS proteins (**c**, **g**) and bare glass (no protein; **d**, **h**) for 2 h (**a–d**) and 20 h (**e**–**h**). The cells were immunofluorescently stained for vinculin

## Discussion

This study describes cell adhesion mediated by FBS proteins in comparison to cell adhesion with no FBS proteins in the system. The SAOS-2 human osteoblast cell line, human primary fibroblasts and human mesenchymal stem cells were used in the experiments. It was discovered that the various cells reacted differently to the presence

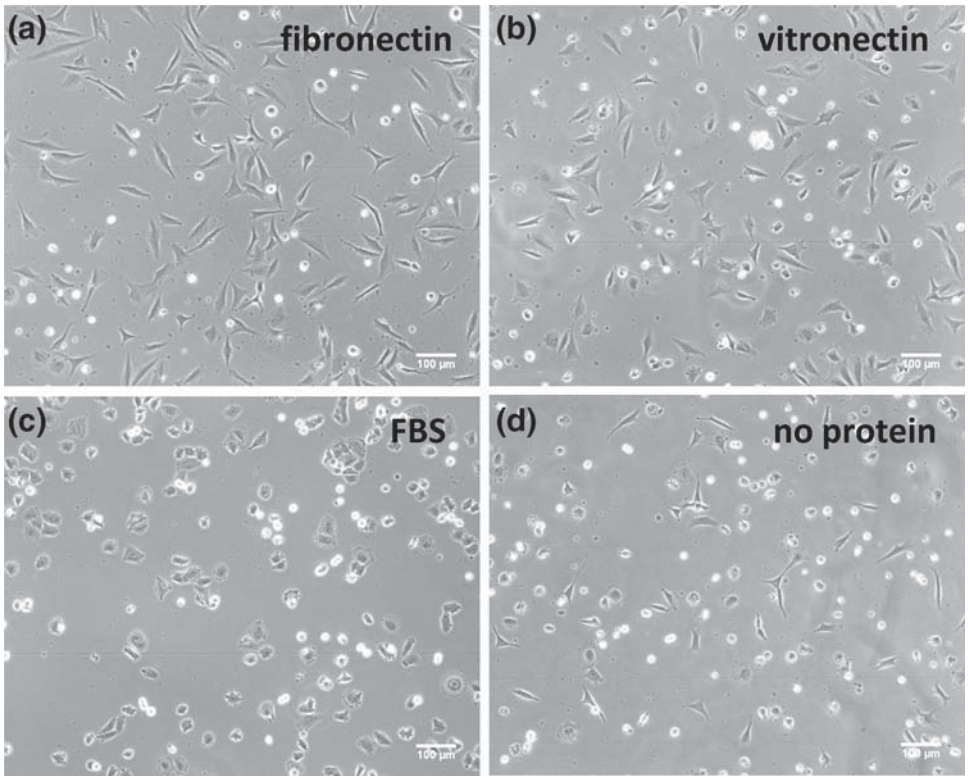


**Fig. 8** Effect of immobilized fibronectin, vitronectin and FBS proteins on morphology of osteoblasts. SAOS-2 cells were cultivated on glass with immobilized fibronectin (**a**), vitronectin (**b**), FBS proteins (**c**) and bare glass (no protein; **d**) for 20 h. The phase contrast images were taken with a light microscope from living cells in culture

or absence of FBS with respect to cell shape, area and number; it was concluded that the differing cell reactions were probably connected to the origin of the cells. SAOS-2 cells are osteosarcoma cell line that is generally used in the form of a permanent line of human osteoblast-like cells (Rodan et al. 1987). The osteoblast cancer cell line possesses certain characteristic features (Pautke et al. 2004) that may differ from those of primary and healthy cells such as primary human dermal fibroblasts and hMSCs. Literature has described the differing adhesion of fibroblastic and melanoma cells to fibronectin (Humphries et al. 1986). It has been shown that a particular cell type is able to bind only to certain specific adhesion motifs due to the exclusivity of interaction between cell surface adhesion receptors and particular adhesion motifs in proteins (Mager et al. 2011). Generally, tumour cells are characterized by changes in intercellular adhesion selectivity as well as adhesion selectivity to ECM. Shifts in cell–cell and cell–ECM interactions (e.g. the down- or up-regulation of integrin genes) are oncogene- and cell type-specific. However, cell adhesiveness is generally lower in cancer cells (Khalili and Ahmad 2015) which may explain the lower level of adhesiveness of the osteosarcoma cell line in the presence of FBS in contrast to primary fibroblasts and hMSCs from healthy donors, since FBS mimics the situation in the body in the presence of proteins.

The expression and especially localization of the cell structural and signalling proteins investigated varied significantly with respect to those cells that adhered on FBS proteins and those that adhered directly on the surface without the presence of FBS proteins; however, these differences were similar in all three of the cell types studied—the expression of Rho proteins only was found to be an exception. Generally, the expression of particular proteins was more affected by cell morphology than by the specific cell type.

The most distinct feature was found to be the lack of formation of classical FAs in cells that adhered in the absence of FBS. It is probable that the cells that adhered without the presence of external proteins use a different mechanism to anchor themselves to the surface; moreover, this contact is most likely mediated by non-specific physical interactions such as van der Waals bonding, hydrogen bonding or charged interactions between polar groups (e.g., hydroxyl) on the substrate and integrins on the surface of the cells (Audiffred et al. 2010). The differences between cell morphology in the presence and absence of FBS could be caused also by the differences in the kinetics of adhesion (Ryzhkov et al. 2010).

FAs are formed following integrin clustering. Since no classical FAs were detected in the case of those cells that were in direct contact with the surface of the TCPS, it was decided that an investigation of the integrins would not be

practical. Therefore, the study focused on another membrane protein involved in cell adhesion—the CD44 hyaluronan receptor. Clearly visible CD44 spots in those cells cultivated in the presence of FBS indicated that CD44 is involved in classical cell adhesion as demonstrated by FA formation. It was revealed that growth factors (present in FBS) lead to the formation of a growth-promoting complex that includes CD44 molecules (Ponta et al. 2003). The clustering of these complexes could be seen as the granular signal of CD44 in those cells which adhered to FBS in contrast to the markedly diffused CD44 signal in the directly adhered cells in which no growth factors originating from FBS were present. In addition, FN present in FBS is known to be a binding partner for CD44 (Jalkanen and Jalkanen 1992) and thus may lead to the clustering of these receptor molecules.

The opposite expression of the Rho proteins in the fibroblasts in the presence/absence of FBS compared to the osteoblasts and hMSCs was probably related to the shape of the cells. Generally, the more Rho proteins are activated the smaller the cells are with rounder shape (Kolyada et al. 2003; Sailem et al. 2014). Indeed, this correlated with the findings of this study, i.e. that those fibroblasts that adhered in the absence of FBS expressed a greater number of Rho proteins and, at the same time, were smaller and rounder than the fibroblasts that adhered in the presence of FBS. The opposite situation was observed with respect to the osteoblasts and hMSCs; the difference could be related to the differing character of the cells studied. Since the hMSC culture consists of a heterogeneous mix of cells at a different level of differentiation, some of these cells may in fact be predetermined osteoblasts. Therefore, hMSCs and osteoblasts may respond to certain stimuli in a similar way, whereas fibroblasts may react in a completely different way.

On the basis of the expression and localization of signalLing proteins such as pFAK and ERK1/2, it can be stated that cell signalLing in the absence of FBS is transduced by a different signalling pathway to that of standard cell signalling initiated by FBS proteins (Saoncella et al. 1999). Since a cell environment without FBS is poor in terms of growth factors, a lower level of activated, i.e. phosphorylated ERK1/2 was found in those cells that adhered in the absence of FBS than in those cells that adhered on FBS proteins. Indeed, this correlates with a study by Chen et al. which determined that the addition of growth factors to serum-deprived cells led to the increased phosphorylation of ERK proteins (Chen et al. 1992).

Enhanced osteoblast adhesion (number of adherent cells) was observed following mechanical stimulation performed by means of shaking experiments in the absence of FBS. Not only were more osteoblasts found on the surface without FBS but also more osteoblasts were detected following shaking than under static conditions on this particular surface. This finding correlates with a study by Ashida et al. which determined that vortex-mediated mechanical stress induced the adhesion of monocytic cells (Ashida et al. 2003).

Although no FA formation in the directly adhering osteoblasts was detected after 2 h, FAs were produced after 20 h in the surviving osteoblasts, which would tend to indicate that FAs can be formed over time. Their appearance may be linked to the formation of a new cell-derived ECM. However, the exact time at which ECM production begins is unknown; the only information found in literature refers to a period of a few days (Anselme et al. 2010). Thus, the exact reason for FA development in the surviving osteoblasts that were cultivated without FBS is pure speculation. However, most of the osteoblasts (anchorage-dependent) cultivated on glass with no protein for 20 h died, the cause of which was most likely insufficient cell adhesion (a special type of programmed cell death—anoikis) rather than a lack of the nutrients present in FBS. This hypothesis is supported by the results obtained from osteoblasts that were cultivated on FN- or VN-coated surfaces, but without the presence of FBS. The osteoblasts were found to be alive after 20 h of cultivation under these non-standard conditions indicating that adhesion mediated by FAs is clearly required for osteoblast survival under FBS-free conditions.

The few osteoblasts that survived 20 h of cultivation without FBS presented a very long and thin morphology and they developed FAs on their protrusions. Thus, the osteoblasts that survived FBS-free conditions and that were not exposed to any anchorage-mediating proteins somehow adapted to this condition.

## Conclusions

Generally, cell adhesion mediated by FBS proteins differs greatly from “direct” cell adhesion without FBS protein contribution. The osteosarcoma cell line, primary fibroblasts and primary mesenchymal stem cells reacted differently to the presence and absence of FBS with respect to cell shape, area and number. However, the expression and localization of the various proteins involved in cell adhesion and signalling were, generally, similar in all the tested cell types, but varied with concern to the presence or absence of FBS.

It was determined that no classical FAs were formed during cell adhesion in the absence of FBS proteins. Furthermore, signalling within these cells proceeded in an uncommon manner. Since the use of FBS may prove problematic, the characterization of cell adhesion without the presence of FBS proteins is necessary with regard to a large number of biological and medical applications including,

e.g. the evaluation of biomaterials and scaffolds for wound healing and tissue engineering approaches, as well as the development of new laboratory and diagnostic techniques such as sensors.

**Acknowledgements** This study was supported by: Charles University in Prague, First Faculty of Medicine: project PROGRES Q26, Faculty of Medicine in Pilsen: project SVV 260 390 and GAUK 400215; further by the National Sustainability Program I (NPU I) Nr. LO1503 provided by the Ministry of Education, Youth and Sports of the Czech Republic and project 15-25813A-AZV CR. Special thanks go to Blanka Bilkova for her technical assistance.

**Compliance with ethical standards**

**Conflicts of interest** The authors declare that they have no conflict of interest.

## References

Abumaree MH, Al Jumah MA, Kalionis B, Jawdat D, Al Khaldi A, AlTalabani AA, Knawy BA (2013) Phenotypic and functional characterization of mesenchymal stem cells from chorionic villi of human term placenta. Stem Cell Rev Rep 9:16–31

Anselme K, Ploux L, Ponche A (2010) Cell/material interfaces: influence of surface chemistry and surface topography on cell adhesion. J Adhes Sci Technol 24:831–852

Ashida N, Takechi H, Kita T, Arai H (2003) Vortex-mediated mechanical stress induces integrin-dependent cell adhesion mediated by inositol 1,4,5-trisphosphate-sensitive Ca2 + release in THP-1 cells. J Biol Chem 278:9327–9331

Audiffred JF, De Leo SE, Brown PK, Hale-Donze H, Monroe WT (2010) Characterization and applications of serum-free induced adhesion in jurkat suspension cells. Biotechnol Bioeng 106:784–793

Calderwood DA, Campbell ID, Critchley DR (2013) Talins and kindlins: partners in integrin-mediated adhesion. Nat Rev Mol Cell Biol 14:503–517

Carre A, Lacarriere V (2010) How substrate properties control cell adhesion. a physical–chemical approach. J Adhes Sci Technol 24:815–830

Chen RH, Sarnecki C, Blenis J (1992) Nuclear localization and regulation of erk- and rsk-encoded protein kinases. Mol Cell Biol 12:915–927

Chiarugi P, Giannoni E (2008) Anoikis: a necessary death program for anchorage-dependent cells. Biochem Pharmacol 76:1352–1364

Crisp M, Liu Q, Roux K, Rattner JB, Shanahan C, Burke B, Stahl PD, Hodzic D (2006) Coupling of the nucleus and cytoplasm: role of the LINC complex. J Cell Biol 172:41–53

Critchley DR (2009) Biochemical and structural properties of the integrin-associated cytoskeletal protein talin. Annu Rev Biophys 38:235–254

Frisch SM, Francis H (1994) Disruption of epithelial cell-matrix interactions induces apoptosis. J Cell Biol 124:619–626

Geiger B, Yamada KM (2011) Molecular architecture and function of matrix adhesions. Csh Perspect Biol 3

Humphries MJ, Akiyama SK, Komoriya A, Olden K, Yamada KM (1986) Identification of an alternatively spliced site in human plasma fibronectin that mediates cell type-specific adhesion. J Cell Biol 103:2637–2647

Humphries JD, Wang P, Streuli C, Geiger B, Humphries MJ, Ballestrem C (2007) Vinculin controls focal adhesion formation by direct interactions with talin and actin. J Cell Biol 179:1043–1057

Jalkanen S, Jalkanen M (1992) Lymphocyte CD44 binds the COOH-terminal heparin-binding domain of fibronectin. J Cell Biol 116:817–825

Kalbacova M, Broz A, Kromka A, Babchenko O, Kalbac M (2011) Controlled oxygen plasma treatment of single-walled carbon nanotube films improves osteoblastic cells attachment and enhances their proliferation. Carbon 49:2926–2934

Kanchanawong P, Shtengel G, Pasapera AM, Ramko EB, Davidson MW, Hess HF, Waterman CM (2010) Nanoscale architecture of integrin-based cell adhesions. Nature 468:580–584

Khalili AA, Ahmad MR (2015) A review of cell adhesion studies for biomedical and biological applications. Int J Mol Sci 16:18149–18184

Koblinski JE, Wu M, Demeler B, Jacob K, Kleinman HK (2005) Matrix cell adhesion activation by non-adhesion proteins. J Cell Sci 118:2965–2974

Kolyada AY, Riley KN, Herman IM (2003) Rho GTPase signaling modulates cell shape and contractile phenotype in an isoactin-specific manner. Am J Physiol-Cell Ph 285:C1116–C1121

Krebs HA (1950) Chemical composition of blood plasma and serum. Annu Rev Biochem 19:409–430

Mager MD, LaPointe V, Stevens MM (2011) Exploring and exploiting chemistry at the cell surface. Nat Chem 3:582–589

Ostrovska L, Broz A, Fucikova A, Belinova T, Sugimoto H, Kanno T, Fujii M, Valenta J, Kalbacova MH (2016) The impact of doped silicon quantum dots on human osteoblasts. Rsc Adv 6:63403–63413

Pautke C, Schieker M, Tischer T, Kolk A, Neth P, Mutschler W, Milz S (2004) Characterization of osteosarcoma cell lines MG-63, Saos-2 and U-2 OS in comparison to human osteoblasts. Anticancer Res 24:3743–3748

Ponta H, Sherman L, Herrlich PA (2003) CD44: from adhesion molecules to signalling regulators. Nat Rev Mol Cell Biol 4:33–45

Rodan SB, Imai Y, Thiede MA, Wesolowski G, Thompson D, Barshavit Z, Shull S, Mann K, Rodan GA (1987) Characterization of a human osteosarcoma cell-line (Saos-2) with osteoblastic properties. Cancer Res 47:4961–4966

Roskoski R Jr (2012) ERK1/2 MAP kinases: structure, function, and regulation. Pharmacol Res Off J Ital Pharmacol Soc 66:105–143

Ruoslahti E (1996) RGD and other recognition sequences for integrins. Annu Rev Cell Dev Biol 12:697–715

Ruszova E, Cheel J, Pavek S, Moravcova M, Hermannova M, Matejkova I, Spilkova J, Velebny V, Kubala L (2013) Epilobium angustifolium extract demonstrates multiple effects on dermal fibroblasts in vitro and skin photo-protection in vivo. Gen Physiol Biophys 32:347–359

Ryzhkov P, Prass M, Gummich M, Kuhn JS, Oettmeier C, Dobereiner HG (2010) Adhesion patterns in early cell spreading. J Phys Condens Matter Inst Phys J 22:194106

Sailem H, Bousgouni V, Cooper S, Bakal C (2014) Cross-talk between Rho and Rac GTPases drives deterministic exploration of cellular shape space and morphological heterogeneity. Open Biol 4

Saoncella S, Echtermeyer F, Denhez F, Nowlen JK, Mosher DF, Robinson SD, Hynes RO, Goetinck PF (1999) Syndecan-4 signals cooperatively with integrins in a Rho-dependent manner in the assembly of focal adhesions and actin stress fibers. Proc Natl Acad Sci USA 96:2805–2810

Schlaepfer DD, Hauck CR, Sieg DJ (1999) Signaling through focal adhesion kinase. Prog Biophys Mol Biol 71:435–478

Sundin M, Ringden O, Sundberg B, Nava S, Gotherstrom C, Le Blanc K (2007) No alloantibodies against mesenchymal stromal cells, but presence of anti-fetal calf serum antibodies, after transplantation in allogeneic hematopoietic stem cell recipients. Haematologica 92:1208–1215

Verdanova M, Rezek B, Broz A, Ukraintsev E, Babchenko O, Artemenko A, Izak T, Kromka A, Kalbac M, Kalbacova MH (2016) Nanocarbon allotropes—graphene and nanocrystalline diamond—promote cell proliferation. Small 12:2499–2509

Wei JH, Igarashi T, Okumori N, Igarashi T, Maetani T, Liu BL, Yoshinari M (2009) Influence of surface wettability on competitive protein adsorption and initial attachment of osteoblasts. Biomed Mater 4

Wilson CJ, Clegg RE, Leavesley DI, Pearcy MJ (2005) Mediation of biomaterial-cell interactions by adsorbed proteins: a review. Tissue Eng 11:1–18

Yoon S, Seger R (2006) The extracellular signal-regulated kinase: multiple substrates regulate diverse cellular functions. Growth Factors 24:21–44

Zaidel-Bar R, Cohen M, Addadi L, Geiger B (2004) Hierarchical assembly of cell-matrix adhesion complexes. Biochem Soc Trans 32:416–420